Aus dem Zentralinstitut für Seelische Gesundheit
Abteilung Neuropsychologie und Psychologische Resilienzforschung

(Seniorprofessorin: Prof. Dr. Dr. h.c. Dr. h.c. Herta Flor)

Cortical Activity to Painful and Non-Painful Stimulation in Amputees: A Functional Near Infrared Spectroscopy Study

Inauguraldissertation
zur Erlangung des Doctor scientiarum humanarum (Dr. sc. hum.)
an der
Medizinischen Fakultät Mannheim
der Ruprecht-Karls-Universität
zu
Heidelberg

vorgelegt von
Jiawen Liao

aus
Zhejiang
2025

Dekan: Prof. Dr. med. Sergij Goerdt

Referentin: Prof. Dr. rer.soc. Dr. h.c. Dr. h.c. Herta Flor

TABLE OF CONTENTS

ABBREVIATIONS

PLP	phantom limb pain
RLP	residual limb pain
fNIRS	functional near-infrared spectroscopy
HbO2	oxygenated hemoglobin
HbR	deoxygenated hemoglobin
fMRI	functional magnetic resonance imaging
DM	diabetes mellitus
PAD	peripheral arterial disease
PDPN	painful diabetic peripheral neuropathy
S1	primary somatosensory cortex
EEG	electroencephalography
PFC	prefrontal cortex
DLPFC	dorsolateral prefrontal cortex
VAS	visual analogue scale
HRF	hemodynamic response function
ANOVA	analysis of variance
FDR	false discovery rate
SE	standard error
MPI	West Haven-Yale Multidimensional Pain Inventory

1 INTRODUCTION

Amputation is a common surgical procedure. Some patients often experience a vivid sensation that the amputated limb remains intact, a phenomenon known as the phantom limb (Weiss, 1956). The earliest documented description of phantom limb dates back to the 16th century, as described by Ambroise Paré (Lafuente, 2002). Many individuals after amputation also report painful sensations such as tingling, burning, or cramping in the phantom limb, known as phantom limb pain (PLP) (Flor, 2002a). Current evidence suggests that the pathophysiology of PLP is associated with amputation-induced changes in both the peripheral and central nervous systems (Kuner & Flor, 2017; Subedi & Grossberg, 2011a); however, the precise mechanisms remain only partially understood. Additionally, pre-amputation pain, as well as preoperative depression and anxiety, have been identified as potential predictors of the incidence and severity of PLP, residual limb pain (RLP), and phantom limb sensations following amputation (Larbig et al., 2019). Most existing research on PLP relies on longitudinal studies and questionnaire-based investigations. In contrast, pre-amputation neuroimaging studies are extremely limited, making it unclear whether cortical activity prior to amputation can predict the development of PLP. Functional near-infrared spectroscopy (fNIRS) is a neuroimaging technique that allows real-time assessment of hemodynamic and metabolic changes associated with brain activity by measuring fluctuations in oxygenated hemoglobin (HbO2) and deoxygenated hemoglobin (HbR) concentrations (Ferrari & Quaresima, 2012). This technique has been widely used to investigate cortical activity in various neurological and mental disorders, including Alzheimer's disease, bipolar disorder, and depression (Ehlis et al., 2014; Husain et al., 2021; R. Li et al., 2018; P.-Y. Lin et al., 2013; Vural Keleş & Yıldırım, 2023). In research on amputees, functional magnetic resonance imaging (fMRI) has been the preferred imaging modality due to its superior spatial resolution and ability to record the activity of deeper brain structures (Afrasiabi & Noroozian, 2015; Boccia et al., 2020; Lotze et al., 2001). However, fMRI is not always suitable for amputees, as some may have metal implants or claustrophobia or the procedure may be too demanding in the case of multimorbidity. By contrast, fNIRS has some advantages that compensate for these parts, including portability and minimal usage restrictions for participants (Chaudhary et al., 2014). In the field of pain research, numerous studies have demonstrated that fNIRS can effectively record the changes in

cortical oxygenation levels in response to external pain stimuli in both healthy individuals and patients with pain-related conditions (Hu et al., 2021; Karunakaran et al., 2021). The present thesis aims at examining cortical responses to painful and non-painful stimulation at different lower limb sites in both healthy individuals and pre-amputation patients. In the following section, basic aspects covering clinical and methodological approaches to pain are presented: (1) an overview of pain before and after lower limb amputation; (2) the introduction on fNIRS methodology and (3) a review of current pain research on the application of fNIRS.

1.1 Pre- and post- amputation pain

Amputation, which involves the complete or partial removal of a limb, is one of the most common and traditional surgical procedures used to treat severe limb ischemia, control pain, and life-savings (Weigel, 2020). Lower limb amputation is typically performed to remove devitalized tissue and prevent further disease progression. Common causes of lower limb amputation include diabetes mellitus (DM), peripheral arterial disease (PAD), peripheral neuropathy, bone and joint infections, trauma, and malignant tumors (Kröger et al., 2017; Marshall & Stansby, 2008). Although the overall number of major amputations has decreased (Behrendt et al., 2018), the incidence of diabetes-related complications continues to rise globally. By 2030, the global prevalence of type 2 diabetes is expected to reach 7,079 per 100,000 population, with all regions around the world projected to experience a continued increase (Khan et al., 2020). As a result, diabetic foot disease remains the leading cause of non-traumatic lower limb amputations (J. H. Lee et al., 2020). Additionally, with the aging population, cases of PAD have been steadily increasing (Fowkes et al., 2013), resulting in a sustained or even rising amputation rate among high-risk subgroups, particularly those with DM and PAD (Walter et al., 2022).

Amputation imposes a significant physiological, economic, and psychological burden on patients. Physiologically, amputation leads to the loss of limb function, requiring patients to adapt to a new lifestyle and often rely on prosthetics or other assistive devices, which complicates daily activities and may lead to other health issues (Canbolat Seyman & Uzar Ozcetin, 2021; Furtado et al., 2015). Economically, patients face substantial treatment costs, rehabilitation expenses, and the purchase of prostheses, while potentially losing their ability to work, which further exacerbates

financial stress (Dillingham et al., 2005). Psychologically, the loss of a limb and mobility issues can trigger emotional problems such as depression, anxiety, and low self-esteem, negatively affecting patients' quality of life and social adaptation (Horgan & MacLachlan, 2004; Pomares et al., 2020). In addition, pain is a significant issue faced by patients. Many patients experience persistent pain before amputation due to severe disease or injury (Jensen et al., 1985a). Similar to pre-amputation pain, post-amputation pain also has high prevalence after limb amputation. Post-amputation pain mainly manifests in two forms: phantom limb pain and residual limb pain (Hsu & Cohen, 2013). Pain can severely affect patients' quality of life, often accompanied by emotional distress, sleep disturbances, and other issues, further exacerbating their suffering (Demet et al., 2003; Serda et al., 2015; Trevelyan et al., 2016).

1.1.1 Pre-amputation pain

Pre-amputation pain is typically defined as persistent or intermittent pain resulting from an underlying pathology or injury that occurs prior to amputation (Devjit Srivastava, 2017). A study of 57 amputees showed that 98% of them reported experiencing pre-amputation pain (Jensen et al., 1985b). Pain prior to amputation affects the involved limb and is present for a significant period before the surgical intervention. In many cases, it serves as an indication for amputation (Marshall & Stansby, 2008).

Pre-amputation pain can arise from various underlying causes, including ischemia, nerve damage, infection, trauma, or tumors. The causes of pain prior to lower limb amputation are mainly related to primary diseases, such as PAD, neuropathic pain caused by diabetes, malignant tumors, etc. The primary mechanism underlying pain in PAD is limb ischemia (Ouriel, 2001a; Rüger et al., 2008a). Arterial stenosis is the main pathological cause of PAD, which leads to reduced blood supply to the distal limbs, causing tissue hypoxia and accumulation of metabolic byproducts, thereby causing pain (Berliner et al., 1995; Muir, 2009). The pain is often as associated to an intermittent claudication, caused by lack of oxygen to the muscles when walking, and relieved by rest when blood flow is partially restored (Meru et al., 2006). As the disease progresses, ischemic rest pain may occur, in which the nerves continue to be deprived of oxygen even in the absence of physical activity, causing severe burning pain or dull pain. If the ischemia is not resolved, tissue necrosis and ulceration may exacerbate the pain and eventually require amputation (Davies, 2012; Rüger et al., 2008b). Painful

diabetic peripheral neuropathy (PDPN) is also a common pre-amputation pain in the lower limbs, which is mainly related to the duration of diabetes (Sloan et al., 2018). Long-term high blood glucose level can lead to nerve fiber degeneration, demyelination, and axonal damage, resulting in burning, paresthesia, or electric shock-like pain (Boulton et al., 2004; Callaghan et al., 2012). Around one third of diabetic patients report such symptoms (Abbott et al., 2011).

Overall, it can be seen that pain before lower limb amputation is closely related to these diseases. Different diseases and pathogenetic mechanisms also directly affect the manifestation and duration of pain before lower limb amputation. It is worth noting that current research suggests a correlation between pre-amputation pain and the development of PLP (D. Srivastava, 2017; Yin et al., 2017). Therefore, for patients undergoing amputation, effective pain management - such as analgesic medications, nerve blocks, and physical therapy - not only enhances quality of life but may also help reduce the risk of postoperative PLP (Limakatso et al., 2024).

1.1.2 Phantom limb pain

PLP refers to pain localized in the missing limb following amputation. It is typically described as painful shooting, squeezing, cutting, burning or cramping and is classified as neuropathic pain (Kaur & Guan, 2018; Nikolajsen & Christensen, 2015; Weeks et al., 2010). The reported incidence of PLP varies, generally ranging from 45% to 85% in patients undergoing major upper and lower limb amputations (Kuffler, 2018). An early study indicated that the incidence of PLP was 72%, 65% and 59% at eight days, six months and two months after the amputation, respectively (Jensen et al., 1985c). In a systematic review study, the point prevalence of PLP was 6.7% - 88.1%, the prevalence measured in a period lasting from 1 to 3 months ranged from 49% to 93.5%, and the lifetime prevalence was as high as 76% - 87% (Stankevicius et al., 2021). These variations may stem from differences in study populations, amputation sites, assessment methods, and the time points for assessing PLP (Schone et al., 2022a). For example, the prevalence of PLP is significantly higher in developed countries compared to developing countries (Limakatso et al., 2020). Another study showed that patients with upper limb amputation have a significantly higher rate of PLP than patients with lower limb amputation, but it is not related to the amputation side (Shukla

et al., 1982). Based on these studies, although the prevalence of PLP is currently inconsistent, a majority of patients after amputation will experience PLP.

The pathogenesis of PLP is complex and is attributed to multiple mechanisms involving abnormal changes in both the central and peripheral nervous systems, as well as psychological factors:

(1) Central mechanisms

Cortical reorganization is one of the most widely discussed central mechanisms of PLP. Numerous studies have demonstrated that PLP is closely associated with plastic changes in the cerebral cortex (Andoh et al., 2020; Chern et al., 1998; Flor et al., 1995, 1998). In healthy individuals, different regions of the primary somatosensory cortex (S1) correspond to sensory inputs from distinct body parts, forming a somatotopic map (Penfield, 1937). Under normal conditions, the topographical organization of the S1 and motor cortex (M1) remains stable. However, following amputation, the cortical area that previously represented the missing limb undergoes functional changes due to the loss of peripheral input (R. Chen et al., 2002; Sparling et al., 2024a). Specifically, this area may become responsive to sensory input from adjacent body regions. For instance, in upper-limb amputees, the cortical representation of the hand in S1 may be taken over by input from the face or shoulder (Bramati et al., 2019; MacIver et al., 2008). This cortical remodeling has been found to correlate positively with the severity of PLP, with more pronounced reorganization associated with greater pain intensity (Flor et al., 1995). This phenomenon is often interpreted as evidence of cortical reorganization. However, some researchers have challenged this hypothesis. Makin and Krakauer (2023) argue that the observed cortical changes do not constitute "reorganization" in the traditional sense but rather reflect the potentiation of pre-existing neural circuits. According to this perspective, functional changes following amputation do not result from a new area assuming a different function but instead arise from the strengthening or readjustment of existing neural pathways (Makin et al., 2013). This adaptive process is constrained by the brain's inherent structural blueprint rather than representing unrestricted plasticity. Despite these differing interpretations, both perspectives acknowledge that the cortex undergoes adaptive modifications following amputation, and neural plasticity plays an important role in the development of PLP. Beyond cortical mechanisms, subcortical structures, including the thalamus,

brainstem, and corpus callosum, have also been implicated in PLP (Collins et al., 2018; Flor et al., 2006; Katayama et al., 2002). For example, one study reported a case in which phantom limb pain after amputation disappeared following a stroke localized to the posterior internal capsule, suggesting that this region may serve as a potential source of PLP (Yarnitsky et al., 1988). Another study using diffusion tensor imaging showed that PLP caused a symmetrical increase in axial diffusivity of white matter in the left and right hemispheres of the brain. Meanwhile, there was an association between white matter radial diffusivity and visual analogue scale scores of PLP and it was mainly reflected in the hemisphere associated with the former representation of the missing hand and the corpus callosum (Seo et al., 2019). Additionally, some studies highlight pain memory as a key contributor to PLP. Prolonged and intense somatosensory input can induce lasting changes in central nervous structures, which, when combined with cognitive evaluation and memory of pre-amputation pain, can evoke past pain experiences associated with the phantom limb (Flor, 2008; Hill et al., 1996; Katz & Melzack, 1990). Overall, the central nervous system mechanisms of PLP have not yet been fully clarified; further research is needed to explore their specific role in the occurrence of PLP.

(2) Peripheral mechanisms

Peripheral mechanisms of PLP are primarily associated with abnormal nerve activity in the residual limb following amputation and the adaptive changes resulting from peripheral nerve injury (Vaso et al., 2014). After amputation, damaged peripheral nerves may undergo regeneration and remodeling; however, during this process, neuronal excitability can become pathologically heightened, leading to spontaneous high-frequency discharges (Flor, 2002a; Navarro et al., 2007). Therefore, the formation of neuromas is considered a key peripheral mechanism underlying PLP (Livingston, 1945). Neuromas are localized, non-neoplastic growths of damaged nerves that typically develop when normal nerve conduction is disrupted due to injury, chronic inflammatory irritation of the nerve fibers, or inadequate surgical repair (Ginanneschi et al., 2023). In the neuroma, enhanced expression of sodium channels, manifested by higher spontaneous firing rates and heightened sensitivity to mechanical or chemical stimulation, may be the source of PLP (Dickinson et al., 2010; Subedi & Grossberg, 2011b). One study also highlighted that changes in severed nerve endings may still be key to causing pain after amputation, with a positive Tinel sign being

significantly more frequent in amputees who experienced pain (Buch et al., 2020). The severity of pain associated with neuroma formation is influenced by various factors, including the type of nerve involved, the location of the injury, local inflammatory responses, blood supply, and alterations in nerve electrical activity (Stokvis, 2010; Ellis and Bennett, 2013; Matsuda, Huh and Ji, 2019). Notably, some studies have reported that PLP can manifest immediately after amputation, even before neuromas have formed (Aboud et al., 2018; Journal et al., 2013). This finding suggests that, beyond neuroma formation, other peripheral factors may contribute to the development and persistence of PLP. The factors may include impaired axonal regeneration, increased dorsal root ganglion excitability, and autonomic nervous system dysfunction (e.g., abnormal sympathetic nerve activity), which may further exacerbate neuropathic pain (Pham et al., 2018; Wulf & Tom, 2023). For example, a study has shown that after complete nerve transection, dorsal root ganglion cells become more active and increasingly sensitive to chemical and mechanical changes (Kajander et al., 1992).

(3) Psychological factors

Beyond the analysis of central and peripheral mechanisms underlying PLP, psychological factors have also been implicated in the occurrence and severity of PLP (Fuchs, Flor & Bekrater-Bodmann, 2018). For instance, a study of 69 lower limb amputees showed that anxiety was associated with the development of PLP and that anxiety may be a risk factor for acute phantom limb pain and residual limb pain after amputation (K. A. Raichle et al., 2015). Additionally, studies indicated that situational stress may be significantly associated with PLP, potentially due to increased sympathetic nervous system activity and heightened muscle tension under stress (Arena et al., 1990; Fuchs et al., 2018b). Additional factors also influence the occurrence of PLP (Flor, 2002b). One such factor is pre-amputation pain, which has been identified as a significant risk factor for the development of PLP. Both pre-amputation pain and acute postoperative pain may contribute to the persistence of chronic PLP (Hanley et al., 2007). Moreover, although existing research highlights the close relationship between these factors and PLP, the precise nature of their interactions remains unclear. Further studies are needed to elucidate the complex interplay between physiological and psychological influences on PLP development and maintenance.

Clarifying the mechanisms underlying PLP may contribute to more effective treatment strategies. Currently, the treatment of PLP remains challenging, with limited efficacy. Existing therapeutic approaches can be broadly categorized into pharmacological, physical, and psychological interventions. Among physical therapies, transcutaneous electrical nerve stimulation (TENS) and repetitive transcranial magnetic stimulation (rTMS) are widely used. In a study using low-frequency, high-intensity TENS at auricular acupoints, it was found that TENS can effectively relieve PLP, and the pain relief is not affected by emotional factors (Katz & Melzack, 1991). Additionally, a systematic review concluded that rTMS has significant therapeutic effects on PLP, potentially through the promotion of beta-endorphin release, which exerts analgesic effects (Nardone et al., 2019a). Among psychological interventions, mirror therapy is one of the most commonly applied techniques. Studies have demonstrated that mirror training significantly reduces pain in amputees by utilizing visual feedback through mirrors, this approach creates the illusion of the missing limb, which can help alleviate PLP (Xie et al., 2022; Yildirim & Kanan, 2016). Recently, with advancements in technology, virtual reality has been explored as a novel approach for PLP treatment. By simulating sensory experiences and creating immersive virtual environments, virtual reality therapy allows patients to visualize and interact with a virtual limb, facilitating relaxation and pain relief. Despite the availability of various treatment modalities, the evidence base for some interventions remains insufficient, and their efficacy requires further validation (Dunn et al., 2017; Osumi et al., 2019). PLP continues to pose significant challenges in clinical management, highlighting the need for further research and improved therapeutic strategies.

1.1.3 Residual limb pain

In addition to PLP, RLP is another common type of post-amputation pain frequently encountered in clinical practice. RLP refers to pain localized in the residual limb proximal to the amputation, affecting approximately 60% of amputees (List et al., 2021). A meta-analysis of 1,347 patients showed that the prevalence of RLP at 1 week, 1 month, 3 months, 6 months, 1 year, and 2 years was 50%, 11%, 23%, 27%, 22%, and 24%, respectively. The severity of residual limb pain varies according to the cause of amputation, with patients with cancer amputation reporting the most severe pain (Evans et al., 2021). The underlying causes of RLP are multifactorial, including nerve injury, neuroma formation, poor blood circulation, and improper prosthetic fitting (List

et al., 2021; Sparling et al., 2024b). During amputation, nerves may be severed or damaged, leading to neuropathic pain, which often emerges within the first week postoperatively. This pain is typically described as throbbing or burning and may either resolve spontaneously or persist for an extended period (Clarke et al., 2013). Additionally, ill-fitting prostheses are a common contributor to RLP, as they may exert excessive pressure on the residual limb, exacerbating pain and discomfort (Pascale & Potter, 2014). Moreover, most studies reported that PLP and RLP are positively correlated, and patients with PLP have a higher risk of RLP (Ahmed et al., 2017; Schone et al., 2022b). Although the precise mechanisms underlying this association remain unclear, one possible explanation is that peripheral nerve damage and persistent noxious input from injured nerves contribute to both pain conditions. Further research is needed to elucidate the complex interplay between PLP and RLP and to develop more effective treatment strategies.

1.2 Functional near-infrared spectroscopy

1.2.1 Principles of fNIRS imaging

In 1977, Jöbsis(1977) first demonstrated that near-infrared light could be utilized to detect human brain activity, successfully capturing changes in cerebral cortical blood oxygenation during deep breathing. FNIRS uses the strong scattering properties of red blood cells in the 650 - 1000 nm near-infrared spectrum to measure changes in HbO2 and HbR associated with brain activity (Chaudhary et al., 2011; Ferrari & Quaresima, 2012). The imaging principle of fNIRS is mainly related to the neurovascular coupling mechanism and the light absorption and scattering:

(1) Neurovascular coupling mechanism

From a physiological perspective, neuronal activity requires energy to maintain and restore the membrane potential, which represents the potential difference between the intracellular and extracellular environments of neurons (McCormick, 2014). This energy is almost entirely supplied by aerobic glucose metabolism. In the absence of external stimulation, HbO2 releases oxygen changing to HbR with a specific ratio, and the released oxygen is absorbed by cells to support basic metabolic processes. However, when external stimulation occurs, the metabolic activity of the brain regions associated with processing of these stimuli increases, providing the necessary energy

for neuronal activity. As a result, metabolic activity initially leads to a decrease in HbO2 and an increase in HbR in the local blood supply. However, to compensate for the oxygen consumption associated with neural activity, the brain engages in a series of regulatory mechanisms, such as local vasodilation, increased cerebral blood flow, and elevated cerebral blood volume, delivering oxygen-rich blood to the concerned region. The oxygen supply provided by increased cerebral blood flow far exceeds the actual consumption by neurons. Consequently, after these regulatory processes, the final observable change is an increase in HbO2 and a decrease in HbR. This secondary hemodynamic response to neural activity is known as the neurovascular coupling process (Phillips et al., 2015). The resulting changes in blood oxygenation typically peak within several seconds and then return to baseline (Hoshi, 2016). In summary, neurovascular coupling translates rapidly occurring neuronal electrical activity into slower hemodynamic changes. fNIRS detects these hemodynamic responses using near-infrared light, indirectly reflecting neuronal activity and its dynamic patterns in localized brain regions. Therefore, similar to fMRI, fNIRS does not measure neuronal activity directly but rather the metabolic changes associated with it (Willems & Cristia, 2017). This is why the recording of this activity is often called neuro-metabolic signal or time-course.

(2) Light absorption and scattering

In addition to the neurovascular coupling mechanism of the brain, fNIRS imaging is also based on the principles of light absorption and scattering. When light passes through biological tissue, it is attenuated due to absorption by the tissue. According to the well-known Beer-Lambert law, the degree of light absorption by a substance is proportional to both the path length of light transmission and the concentration of the absorbing substance (Swinehart, 1962). The near-infrared light used in fNIRS falls within the wavelength range of approximately 650 - 1000 nm (Pinti et al., 2018). Light in this range can penetrate tissues such as the scalp and skull to reach the brain, while the overall absorption coefficient of the absorbing compounds remains low, ensuring that the light is not completely absorbed before reaching the detector (Huppert et al., 2009a). Additionally, the absorption coefficients of HbO2 and HbR differ significantly within this range, allowing for the estimation of their concentration changes based on absorption differences at different wavelengths (Giacometti & Diamond, 2013). In addition to light absorption, scattering is another fundamental physical principle

underlying fNIRS imaging. Since brain tissue is a highly scattering medium, near-infrared light penetrating the brain from the scalp surface undergoes scattering. While most photons are absorbed by the brain tissue, a small portion travels back to the scalp surface near the light source. By placing a detector close to the light source, these photons can be captured, enabling the detection of neural activity in the cortical region. Considering both the absorption and scattering properties of light, researchers have introduced a correction for optical path length to the original Beer-Lambert law, leading to the development and adoption of the modified Beer-Lambert law, which serves as the foundation for fNIRS data analysis and can be written as follows:

$$OD = \varepsilon \cdot C \cdot DPF \cdot L + G \tag{1}$$

where OD represents the optical density, ε and C are the extinction coefficient and the concentration of absorptive substance. The length of the optical path is the physical distance L between a source and a detector corrected by a correction factor, i.e. differential pathlength factor (DPF), accounting for the scattering effect. In addition, a parameter G is introduced to represent the sum of light attenuation due to other effects (Kocsis et al., 2006).

1.2.2 Advantages and limitations of fNIRS

Building on the previously discussed principles of fNIRS technology, its rapid development in recent years is largely attributed to its distinct advantages. As a non-invasive brain imaging technique, the most significant benefit of fNIRS is its ability to expand the range of experimental subjects and paradigms in brain imaging research. For example, compared to fMRI, fNIRS imposes fewer restrictions on participants and can be applied to individuals with metal implants or those unable to undergo fMRI scans due to conditions such as claustrophobia (Cui et al., 2011a; Pereira et al., 2023). Additionally, fNIRS is less sensitive to head and limb movements, making it particularly suitable for populations with increased motion, such as infants, children, and individuals with attention-deficit/hyperactivity disorder, who may have difficulty tolerating equipment-related discomfort (Monden et al., 2012, 2015; T. Wilcox & Biondi, 2015a). Due to its portability and tolerance for head movement, fNIRS also enables the study of motor functions in real-world settings, such as outdoor running and cycling (Huang et al., 2019; P. Lin et al., 2013; B. Liu et al., 2023). This capability enhances

the ecological validity of research by allowing experimental designs that more closely reflect everyday life. Furthermore, the portability of fNIRS offers practical advantages in clinical applications (Chaudhary et al., 2014). For instance, many patients awaiting amputation experience mobility impairments, and fNIRS can be transported to their location for measurements. Compared to fMRI, fNIRS systems are also more cost-effective, reducing the financial burden of experiments. Another advantage of fNIRS is its compatibility with other neuroimaging techniques. Compared to fMRI, fNIRS provides superior temporal resolution, and compared to electroencephalography (EEG), it offers better spatial resolution (Eggebrecht et al., 2014). This allows fNIRS to be used in conjunction with fMRI and EEG for multimodal neuroimaging studies, leveraging the strengths of each method (Z. Liu et al., 2021; Steinbrink et al., 2006). Additionally, existing research has demonstrated that fNIRS can be combined with transcranial magnetic stimulation (TMS) for investigating and developing interventions for certain neurological disorders (Curtin et al., 2019; Kozel et al., 2009).

Despite its advantages, fNIRS is associated with several technical and methodological constraints. First, due to the absorption and scattering properties of light in biological tissues, fNIRS is limited in its ability to measure deep brain structures and is generally restricted to the cortical structures, with an effective penetration depth of approximately 1.5 to 2 cm (Pinti et al., 2020). Second, fNIRS lacks precise anatomical localization capabilities. However, previous studies have demonstrated a reasonable correspondence between the internationally standardized 10 - 10 EEG electrode placement system and cortical anatomy, allowing many fNIRS studies to infer the underlying brain regions based on 10 - 10 EEG electrode placement system (Homan et al., 1987; Jeon et al., 2018; T. Wilcox & Biondi, 2015b). Furthermore, accurate quantification of localized changes in cerebral hemoglobin concentration still remains a technical challenge for fNIRS. This is primarily due to uncertainties in optical path length estimation, differences in the optical properties of various tissue layers, and interference from extra cerebral hemodynamics (Hoshi, 2005). For instance, individual physiological factors such as skull thickness and hair color can significantly affect light penetration and scattering characteristics (Holmes et al., 2024). Compared to fMRI, fNIRS generally exhibits a lower signal-to-noise ratio and is more susceptible to noise introduced by scalp blood flow fluctuations and ambient light interference (Cui et al., 2011b).

In summary, although fNIRS offers advantages such as non-invasiveness and portability, its spatial resolution, quantification accuracy, and noise resistance remain areas that require further technological improvement and refinement.

1.3 Exploring pain through fNIRS studies[1]

The occurrence of pain is a complex and multifaceted psychophysiological process involving multiple psychobiological components. Acute pain can be induced by various stimuli and neuroimaging can aid in unraveling the central nervous system factors related to pain perception (Espinoza & Habas, 2018). Prior neuroimaging studies have demonstrated that painful stimuli elicit responses across a wide array of cortical and subcortical networks (Apkarian et al., 2005). For instance, Freund et al. (2009) observed that when healthy participants were exposed to painful thermal stimulation to the left or right side of the hand, fMRI consistently showed activation in the right anterior insula, the ipsilateral sensorimotor cortex, and the bilateral posterior insula. In another fMRI investigation, the bilateral secondary somatosensory cortex exhibited notable activation when both painful and non-painful electrical stimulation were administered to healthy participants (T. L. Chen et al., 2008). Furthermore, other published brain imaging studies have also provided evidence that structures such as the prefrontal cortex (PFC), dorsolateral PFC (DLPFC), and cingulate cortex are linked to the modulation and perception of pain (Bornhövd et al., 2002; Sandström et al., 2019; Tsuji et al., 2021). Based on the current scientific literature, the brain regions implicated in pain processing encompass the primary (S1) and secondary (S2) somatosensory cortex, the primary motor cortex (M1), DLPFC, the cingulate area, the insula, as well as subcortical structures such as the thalamus and hypothalamus (Ng et al., 2018). Typically, the cingulate cortex, insula, and limbic system areas are implicated in the emotional aspects of pain (Bushnell et al., 2013). S1 and S2 are typically associated with the sensory dimension of pain, while cognitive aspects of pain

[1] *Portions of this section have been published in Scientific Reports (2025): Liao, J., Silvoni, S., Desch, S., Serian, A., Andoh, J., & Flor, H. (2025). Cortical activity during painful and non-painful stimulation over four lower limb body sites: a functional near-infrared spectroscopy study. Scientific Reports, 15(1), 5070.*

are linked to the frontal and parietal regions of the brain (Kulkarni et al., 2005; Vierck et al., 2013).

Currently, numerous studies have demonstrated that fNIRS can effectively detect changes in hemoglobin concentration in the cerebral cortex under painful conditions (Karunakaran et al., 2021). Due to the aforementioned limitations of fNIRS in spatial resolution, most studies have focused on the prefrontal and primary sensory cortices. For instance, Becerra et al. found that PFC and S1 activation was observed bilaterally when painful thermal stimulation was given on the dorsum of the right hand (Becerra et al., 2008). Another fNIRS study reported PFC activation in response to a mechanical painful stimulus applied to the right index finger (C. H. Lee et al., 2013). However, contrasting results emerged in a different study where a painful mechanical stimulus was applied to the gingiva (Sakuma et al., 2014). Additionally, some studies utilizing electrical stimulation found that PFC exhibited deactivation when pain was induced in the thumbs of healthy participants (Aasted et al., 2016; Yücel et al., 2015). These studies suggest that the PFC may be involved in pain processing by modulating attention and other cognitive functions. The S1, as the key cortical region for pain processing, plays a crucial role in assessing the intensity of peripheral sensory stimulation. Furthermore, fNIRS has been used to observe S1 responses to pain in both adults and infants (Donadel et al., 2021; Jones et al., 2022). Additionally, some studies have utilized fNIRS to examine the responses of other brain regions to painful stimulation (Hernández-Román et al., 2023; Oliver et al., 2018; Tachibana et al., 2011). For example, research has shown that high-intensity neuromuscular electrical stimulation activates the supplementary motor area in association with increased pain ratings, suggesting that the resulting cortical responses may partly reflect enhanced pain and attentional processing, as well as increased bilateral sensorimotor integration (Muthalib et al., 2015).

In clinical practice, fNIRS is frequently used to study chronic pain conditions. For example, a study using fNIRS have shown that patients with chronic low back pain exhibit significantly increased oxygenated hemoglobin levels in the prefrontal cortex at rest (Y. Li et al., 2023). In a study of 25 patients with fibromyalgia syndrome, fNIRS data revealed increased bilateral cortical activation in patients with fibromyalgia syndrome compared with healthy controls under unilateral pressure pain stimulation, further demonstrating that central neural processing is altered in patients with

fibromyalgia syndrome (Üçeyler et al., 2015). Regarding clinical intervention studies, one study involving 15 patients with knee osteoarthritis demonstrated that after a six-week exercise intervention, fNIRS detected a significant reduction in DLPFC activation in response to pain stimulation (Öztürk et al., 2021). Additionally, an fNIRS study investigating the effects of repeated peripheral magnetic stimulation combined with core muscle training on chronic nonspecific low back pain found that repeated peripheral magnetic stimulation combined with core muscle training alleviated pain with associated enhancement of left primary motor cortex (M1) activation, showing superior effects compared to the sham stimulation group (Yan et al., 2024). It is worth noting that in recent years, the application of fNIRS in the study of PLP has gradually increased. A recent published study utilized fNIRS to investigate the relationship between PLP, RLP, and the metabolic response of the cortical motor network (Simis et al., 2024). The findings revealed that metabolic activity was predominantly increased in the hemisphere ipsilateral to the amputation. Specifically, PLP was associated with heightened metabolic activity in the ipsilateral primary motor cortex (PMC) and premotor area, whereas RLP was primarily linked to increased metabolic activity in the contralateral PMC. This study further validated the feasibility of using fNIRS to investigate phantom limb pain.

In conclusion, fNIRS has demonstrated considerable potential in acute and chronic pain research and is progressively emerging as a practical tool for exploring pain mechanisms and assessing treatment efficacy.

1.4 Aims and hypotheses

As mentioned above, pain has become a widely studied topic in neuroscience, and through the existing fNIRS studies on pain, it can be confirmed that fNIRS has a certain feasibility in pain research, but the research on PLP still needs further exploration. Therefore, the purpose of this thesis is to further explore the pathogenesis and the predictors of PLP by using fNIRS. However, due to the lack of fNIRS studies on lower limb pain, this thesis is divided into two parts.

(1) The main purpose of the first part of the study was to use fNIRS to monitor the changes in blood oxygen concentration in PFC and S1 when healthy people were subjected to electrical stimulation of different intensities (including painful and non-

painful) and whether these changes would be different when stimulating different parts of the lower limb (bilateral groins and knees). Based on a comprehensive review of previous research results on stimulation of other body parts under external sensory stimulation (Hu et al., 2021), the hypothesis of this study was that stimulation of lower limb parts should cause an increase in the neuro-metabolic activity of S1 to painful stimulation compared with non-painful stimulation. In addition, we expected that the neuro-metabolic activity of the prefrontal region would be reduced during painful stimulation compared with non-painful stimulation. In addition, we did not expect significant differences in the activation patterns of different body parts.

(2) The second study aimed to compare cortical activation patterns between pre-amputation patients and matched healthy controls during painful and non-painful electrical stimulation applied to different regions of the lower limb. In addition, perceptual thresholds, pain thresholds, and pain tolerance levels were assessed and compared between the two groups. Based on postoperative outcomes, patients were further divided into those who developed PLP and those who did not. By comparing these subgroups with healthy controls, the study sought to explore potential neural predictors of PLP in the pre-amputation phase. It was hypothesized that, prior to amputation, patients would exhibit greater cortical activation in both the PFC and the S1 cortex compared to healthy controls. Furthermore, among the patient group, those who experienced PLP were expected to show higher cortical activation in the DLPFC and S1 regions than those who did not, particularly in response to painful stimulation. Patients were also anticipated to demonstrate lower pain threshold and pain tolerance compared to healthy controls.

2 MATERIALS AND METHOD

2.1 Study 1[2]

2.1.1 Participants

Sixteen right-handed healthy persons (8 male) between 21 and 30 years of age (mean = 24, SD = 3.4) participated in the study. They were recruited via flyers posted on the official website of the Central Institute of Mental Health and distributed throughout the university campus. The ethics committee of the Medical Faculty Mannheim, Heidelberg University, Germany, approved the study (ethics approval number: 2014–596 N-MA). All methods were performed in accordance with the relevant guidelines and regulations. Each participant gave written informed consent before the experiments. Exclusion criteria were: prior history of diseases of vital organs, brain tumors or other cerebral disorders or trauma, and history of mental illness).

2.1.2 Experimental design

The study design consisted of the following procedure: (a) assessment of perception and pain thresholds as well as pain tolerance to electrical skin surface stimulation of the left/right groin and left/right knee; (b) determination of painful and non-painful stimulation intensities; (c) delivery of painful and non-painful stimulation using a block-design experimental stimulation modality with pre- and post-assessment of perceived stimulation intensity through a rating using a visual analogue scale (VAS) (Williamson & Hoggart, 2005). Throughout the experiment, fNIRS was utilized to monitor changes in blood oxygen concentration.

For somatosensory stimulation, we applied electrical stimuli, using a copper electrode connected to a Digitimer stimulator (DS7A, Digitimer, Hertfordshire, England) with monophasic square-wave pulses of 0.2 ms at a 5 Hz frequency. Before the experimental stimulation modality, we tested the participants' perception and pain

[2] *All content from Study 1 has been published in Scientific Reports (2025): Liao, J., Silvoni, S., Desch, S., Serian, A., Andoh, J., & Flor, H. (2025). Cortical activity during painful and non-painful stimulation over four lower limb body sites: a functional near-infrared spectroscopy study. Scientific Reports, 15(1), 5070.*

thresholds as well as pain tolerance to find the optimal painful and non-painful stimulation intensities. Similar to previous studies (H. Liu et al., 2020; Löffler et al., 2018), for each threshold, we calculated the average value of the stimulation intensity (mA) of three ascending series. The participants were instructed to press a button when they started to feel the stimulus (perception threshold), when the stimuli started to hurt (pain threshold), and when they could no longer tolerate the stimuli (pain tolerance). We preset the non-painful stimulation intensity at 50% between perception and pain thresholds, and the painful stimulation intensity was preset at 50% between pain threshold and pain tolerance. Next, to ensure the applicability of the obtained stimulus intensities in the experimental stimulation modalities, participants evaluated the provided stimuli, and the stimulation intensities were further calibrated. The painful and non-painful stimulus intensities were adjusted to a perceived stimulation intensity around 75% and 25% of a VAS scale, respectively. The VAS scale was presented as a 600-pixel (16.2 cm) vertical line, with “No sensation” at the bottom, “Pain sensation” in the middle, and “Extreme pain” at the top. Participants were instructed to evaluate the perceived electrical stimulation by marking a point on this line to reflect their experience, which could later be converted into numerical values of 0 to 100. We defined the values between “No sensation” and “Pain sensation” as non-painful stimulation intensity, and the values between “Pain sensation” and “Extreme pain” as painful stimulation intensity. We assessed the response to stimulation in four body sites: left and right groins, and left and right knees. The stimulation site on the groin is at the junction between the trunk and the thigh, while on the knee, it is above the patella, as shown in Fig. A-1 (a). According to a previous study (Yücel et al., 2015) and the aim of our study, a block-design experimental stimulation modality was employed to deliver painful and non-painful stimulation to the participants. Each body site was tested using two stimulation modalities: a painful stimulation and a non-painful stimulation. Each stimulation modality consisted of six 5-second stimulation blocks, interspersed with six rest blocks of pseudo-randomized durations (ranging from 25 to 29 s). This pseudo-randomization was designed to prevent participants’ expectations and mitigate the effects of pain anticipation in the recorded signals, as shown in Fig. A-1 (b). Before and after the stimulation modality, the participants rated the perceived stimulation intensity by a VAS rating. The order of stimulation modalities was counterbalanced across the participants. Before the first stimulation block, we recorded 25 s of baseline neuro-metabolic activity during which the participant was asked to

relax and look at a cross displayed on a screen. During the experiment, the participants kept their eyes open, concentrating on the stimulation, while looking at the screen where instructions were presented.

Figure A-1 (a-b)

Schematic of electrical stimulation and experimental block.

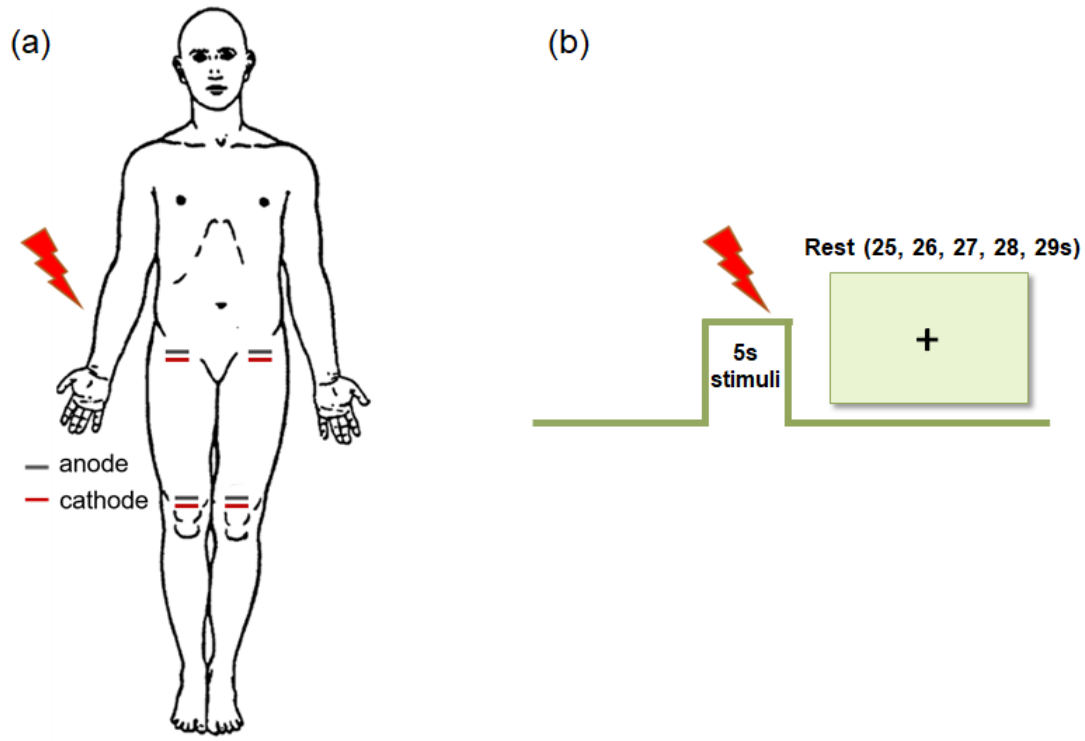

Notes: (a) Schematic illustration of the stimulation at the various body sites. The electrical stimulation was applied at left and right groins and both knees via an anode and cathode at a distance of about one centimeter between them. The blue line represents the anode. The red line represents the cathode. And the lightning bolt represents the electrical stimulation. (b) Representation of one stimulation block and a rest block. Each stimulation modality consisted of 6 stimulation blocks of 5 s, each separated by 6 rest blocks of pseudo-randomised duration (25 to 29 s). The lightning bolt represents the electrical stimulation.

2.1.3 FNIRS data recording

Cerebral hemodynamic activity was recorded using a non-invasive multichannel functional near-infrared spectrometer operating at 760 and 850 nm wavelengths (NIRScout 24*24, NIRx Medical Technologies, Berlin, Germany). NIRStar software was used for data recording (NIRx Medizintechnik GmbH, Berlin, Germany). The signal sampling rate was 3.91 Hz. We employed a MATLAB-based toolbox37 (fOLD—fNIRS optode location decider) to identify the functional brain region of interest for optode-based neuro-metabolic recording. This software accurately estimates spatial brain mapping of the standard electroencephalography (EEG) 10-10 systems on associated

Brodmann areas (Rorden & Brett, 2000). According to this method, we identified the Brodmann areas 1, 2, 3, 9, 10, 11, and 46 as the regions of interest in this study. In fOLD software, specificity is defined as the proportion of photon fluence within the regions of interest relative to the total fluence across all regions covered by the source-detector pair. This metric represents the degree to which the photon distribution is concentrated in the regions of interest, providing anatomical specificity for channels corresponding to these regions. In this study, a specificity threshold of 10% was applied to select channels that received at least 10% of the total fluence from the regions of interest. The channels were further adjusted and visualized using NIRSite software (NIRx Medical Technologies, Glen Head, NY). The probe consisted of sixteen light sources and sixteen detectors. Optodes were placed on the prefrontal and bilateral primary somatosensory areas, forming a 49-channel setup with an inter-probe distance of a maximum of 3 cm. The placement of optodes and channels were shown in Fig. A-2. Detailed information for each channel can be found in Table A-10 of supplementary materials. The infrared light sources and detectors were placed in an EEG cap (EASYCAP GmbH, Germany). The cap size was determined depending on the head circumference of participants (54 cm, 56 cm, 58 cm, and 60 cm).

Figure A-2 (a-b)

FNIRS optode and channel placement.

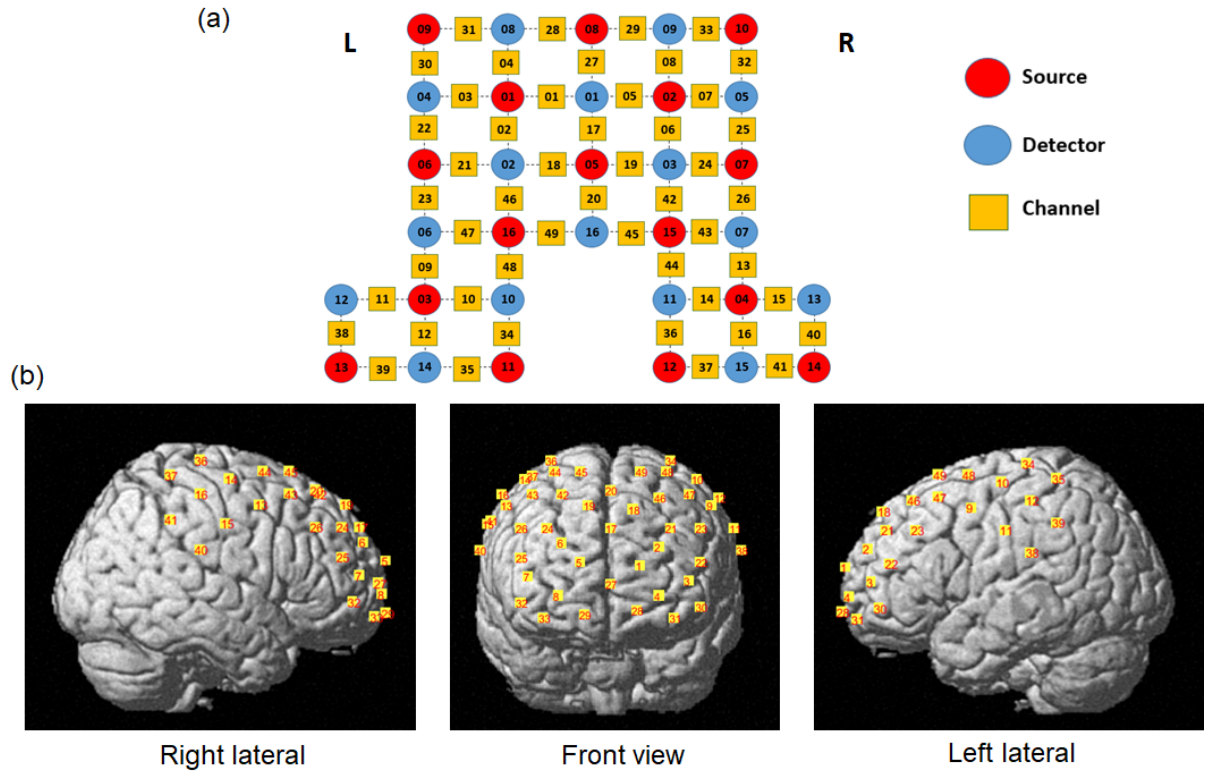

Notes: (a) fNIRS optode and channel placement over the bilateral primary somatosensory cortex and prefrontal cortex within the international 10–10 standard system. The red and blue dots represent the location of light sources and detectors, respectively. The yellow squares represent the location of the channels. Sources 03, 04, and 05 represent C3, C4, and Fz, respectively. (b) The co-registration of the 49 channels on a standard human brain template.

2.1.4 Data processing, analysis and statistics

To ensure the quality of our data, we first examined the results of the VAS rating used in our experiment. We then eliminated any fNIRS data where participants reported feeling pain in response to non-painful stimuli and where non-painful stimuli were reported as painful. After this screening process, the sample size of analyzed data was 13 participants for the left groin, 15 for the right knee, 16 for the right groin, and 16 for the left knee. These data were then processed and analyzed separately for the painful and non-painful stimulation. We computed the coefficient of variation (CV) for each channel by dividing the standard deviation of the channel data by the mean and multiplying by 100. The CV threshold was set at 15% to minimize the impact of physical artifacts and ensure the quality of the fNIRS data (Piper et al., 2014). No channels were excluded during this process. Subsequently, to explore the spatial correlations under different stimulation madalities, the NIRS data were analyzed using the open-source software NIRS-SPM (Ye et al., 2009), implemented in Matlab R2020a. The raw intensity data recorded by NIRStar software were first converted to optical density values using NIRS-SPM's built-in conversion function. We preprocessed the data

using the wavelet-minimum description length (wavelet-MDL) and the low-pass filter of NIRS-SPM. The wavelet-MDL method, using a wavelet filter with a support size of 9, effectively removed various types of noise and artefacts, including cardiac activity, respiration, and vaso-motion, thereby providing a more accurate estimation of the brain signal (Shuvra et al., 2019). In NIRS-SPM, the low-pass filter was applied by selecting the 'hrf' (hemodynamic response function) option, with a 6 dB cut-off frequency of 0.1 Hz to filter out high-frequency noise. We employed a pre-coloring method to estimate the temporal correlation of fNIRS data (Friston et al., 1995). Subsequently, we utilized a general linear model to calculate parameter estimates of the neuro-metabolic activity through convolution with the canonical hemodynamic response function (with time and dispersion derivatives) for each of the two experimental stimulation modalities separately (painful and non-painful stimulation) referred to the neuro-metabolic activity of all intervals without stimulation. We obtained the beta (β) value of each channel representing the magnitude of the task response. Then, according to the regions of interest in this study, we grouped channels into different brain regions to obtain the average β value of each brain region. Channel 9, 10, 11, 12, 34, 35, 38 represent the left S1 cortex. Channel 13, 14, 15, 16, 36, 37, 40 represent the right S1 cortex. And channel 1, 2, 3, 4, 5, 6, 7, 8, 17, 18, 19, 20, 21, 22, 23, 24, 25, 26, 27, 28, 29, 30, 31, 32, 33, 42, 43, 46 and 47 represent the PFC area. The β value calculated by this method represents an increase (activation) or a decrease (deactivation) of the regional neuro-metabolic activity during stimulation with respect to the non-stimulation intervals. On a linear scale, positive β values indicate activation, while negative β values denote deactivation.

Data analysis was conducted using Matlab R2020a. Somatosensory intensities were analyzed using a two-way analysis of variance (ANOVA), while the VAS ratings and β values were examined with repeated-measures ANOVA. For the β values analysis, due to the unbalanced sample size, we handled missing data using three approaches: deleting subjects with missing data, replacing the missing data with the mean, and replacing it with the median. The results were consistent across all three methods. Therefore, the findings of this analysis are primarily based on available data with complete set of β values for each of the four body sites. The effect size for the ANOVA was calculated using partial eta-squared (η^2), and the magnitude of the effect was interpreted based on the criteria: small ($\eta^2 = 0.01$), medium ($\eta^2 = 0.06$), and large ($\eta^2 = 0.14$) (J. Cohen, 1988). The post-hoc tests for stimulation intensities and VAS rating

were controlled for multiple comparisons using the Tukey-Kramer test. The post-hoc tests for the β values were controlled using the false discovery rate (FDR). Cohen's d was used to calculate the effect size for each contrast. Effect sizes were interpreted as small (d = 0.2), medium (d = 0.5), and large (d = 0.8) (J. Cohen, 1988). The normality test was performed using Shapiro-Wilk normality test, see Supplementary Tables A-S1, S3 and S5. Although the normality assumption was not confirmed, a repeated measures ANOVA was used for modeling the data, due to its robustness against violations of normality (R. R. Wilcox, 2011). We also tested data transformation to normalize the data but were not successful. Where appropriate, we used the non-parametric equivalent to ANOVA contrasts. There were no deviations from the parametric versions. BrainNet Viewer (Xia et al., 2013), an open-source toolbox, was used for data visualization. The significance level was set at 0.05. The results section highlights HbO2 concentration changes, which are generally more sensitive to task-related neural activity compared to HbR changes (Hoshi et al., 2001a; Iso et al., 2021; Q. Sun et al., 2020).We however also include findings related to HbR, which are now provided in the supplementary materials (see Supplementary Fig. A-1 and Table A-9).

2.2 Study 2

2.2.1 Participants

Twenty-three persons before lower limb amputation (age: 71.1± 10.8, six females and 17 males), and 10 healthy persons (age: 68.4 ± 7.7, four females and 6 males) participated in this study. The persons before lower limb amputation were recruited at the Diakonissen-Stiftungs-Krankenhaus Speyer, and healthy persons were recruited via flyers on the official website of the Central Institute of Mental Health. The ethics committee of the Medical Faculty Mannheim, Heidelberg University, Germany, approved the study (ethics approval number: 2014-596 N-MA). All procedures were performed in accordance with relevant guidelines and regulations. Each subject signed written informed consent before the experiment. Exclusion criteria were: prior history of diseases of vital organs, brain tumors or other cerebral disorders or trauma, and history of mental illness. All patients and healthy controls were asked to complete the German version of the West Haven-Yale Multidimensional Pain Inventory (MPI-D) to assess the psychosocial impact of pain (Flor et al., 1990). However, due to health issues at the time of assessment, three patients were unable to complete the

questionnaire. At least three months after the scheduled amputation, we recontacted the amputees to inquire about their post-operative pain status. Two participants did not undergo amputation, and five could not be reached. Detailed information on these two groups is provided in Table B-1.

2.2.2 Experimental design

The experimental design was largely consistent with that of the study 1. All participants underwent assessments to determine perception threshold, pain threshold, and pain tolerance in response to electrical stimulation applied to the skin surface of the left and right groin and knee (see the Fig. A-1). These thresholds were used to calibrate the intensities of both painful and non-painful stimulation intensity. A block design was employed to deliver the stimulation, and participants rated their perceived intensity using a VAS. Throughout the experiment, fNIRS was used to monitor concentration changes in cortical oxygenation and deoxygenation.

However, several modifications were made to accommodate the specific characteristics of the current study population. First, as the participants in this study were predominantly older adults, we preset the intensity for non-painful stimulation from 50% (midpoint between the perception and pain thresholds) to 80% of the range between the perception threshold and pain threshold, based on pilot testing. The intensity for painful stimulation was preset at 80% of the range between the pain threshold and pain tolerance. To ensure the suitability of the stimulation intensity, participants rated each stimulus using the VAS rating. As in Study 1, the VAS scale was presented as a 600-pixel (16.2 cm) vertical line, with “No sensation” at the bottom, “Pain sensation” in the middle, and “Extreme pain” at the top. A VAS rating above 50% was classified as painful stimulation, whereas a rating below 50% was considered non-painful stimulation. Both painful and non-painful stimulation modalities were applied to each body site. Each stimulation modality consisted of six stimulation blocks, each lasting 5 seconds. To minimize participants’ anticipation of the stimuli and reduce the potential influence of pain expectation on the recorded signals, six rest blocks of pseudo-random duration (25-29 seconds) were interleaved between stimulation blocks. Compared to the previous study, participants in this study were asked to rate the perceived stimulation using a VAS rating after the third and sixth stimulation blocks. The order of stimulation patterns was counterbalanced across participants. Prior to the

first stimulation block, a 25-second baseline period was recorded to capture neuro-metabolic activity, during which participants were instructed to relax and fixate on a cross displayed on the screen. Throughout the experiment, participants kept their eyes open and maintained visual focus on the screen, which displayed task-related instructions and served as a fixation point during stimulation.

2.2.3 FNIRS data recording

Cerebral hemodynamic activity was recorded using a non-invasive, multichannel functional near-infrared spectrometer (NIRScout 24×24, NIRx Medical Technologies, Berlin, Germany) operating at wavelengths of 760 and 850 nm. Data acquisition was conducted using NIRStar software at a sampling rate of 5.21 Hz. Building upon the first study, we utilized a MATLAB-based toolbox (fOLD - fNIRS Optode Location Decider) to identify the functional brain regions of interest for optode-based neurometabolic measurements. As in Study 1, we identified Brodmann areas 1, 2, 3, 9, 10, 11, and 46 as the main study areas in this study. To ensure comprehensive coverage of the target brain areas, in this study we adjusted the specificity threshold to 5% to include channels that received at least 5% of the total photon flux in the specific study area. Channel selection and spatial localization were further refined and visualized using NIRSite software. Based on previous findings (Bolognini et al., 2013; Gallace & Bellan, 2018; Horing et al., 2019), five additional channels were included in the parietal lobe. The optode configuration consisted of 22 sources and 19 detectors, forming a total of 64 channels with an inter-optode distance of up to 3 cm. The placement of optodes and channels is illustrated in Figure B-1, and detailed information on individual channels is provided in Supplementary Table B-S1. Optodes were embedded in EEG caps, with cap sizes selected according to the participant's head circumference (54 cm, 56 cm, 58 cm, or 60 cm).

Figure B-1 (a-b)

FNIRS optode and channel placement.

(a)

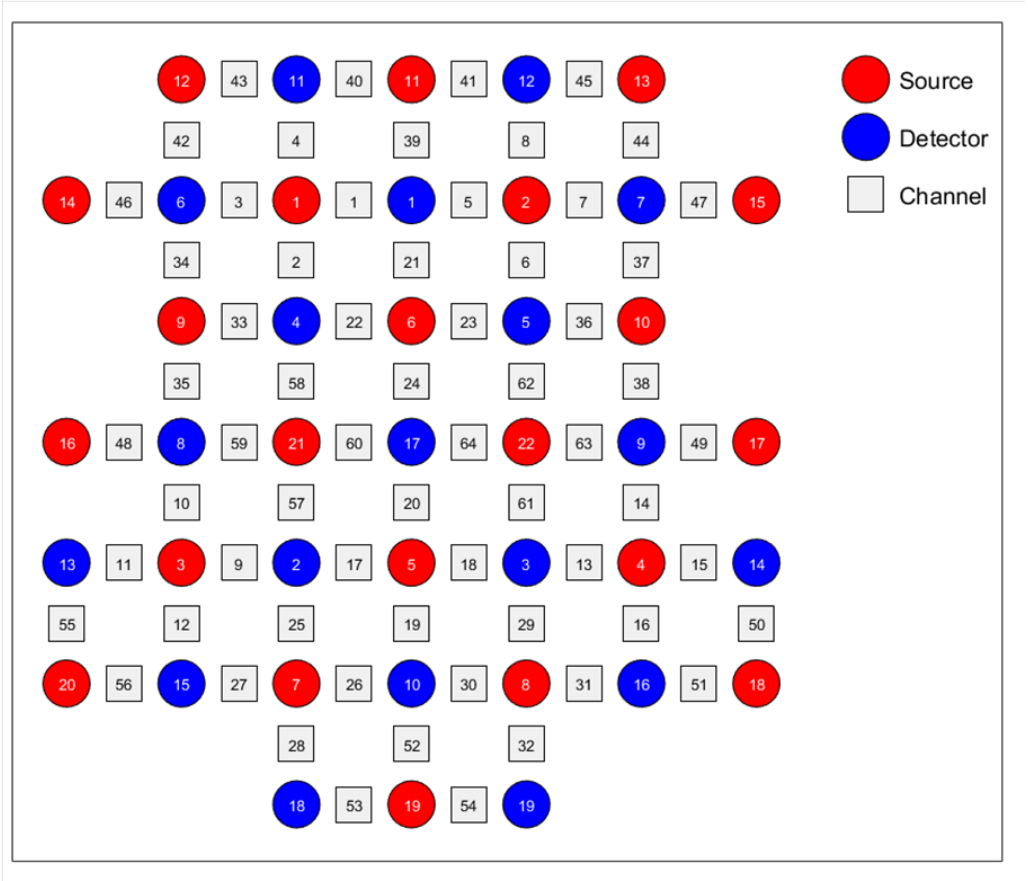

(b)

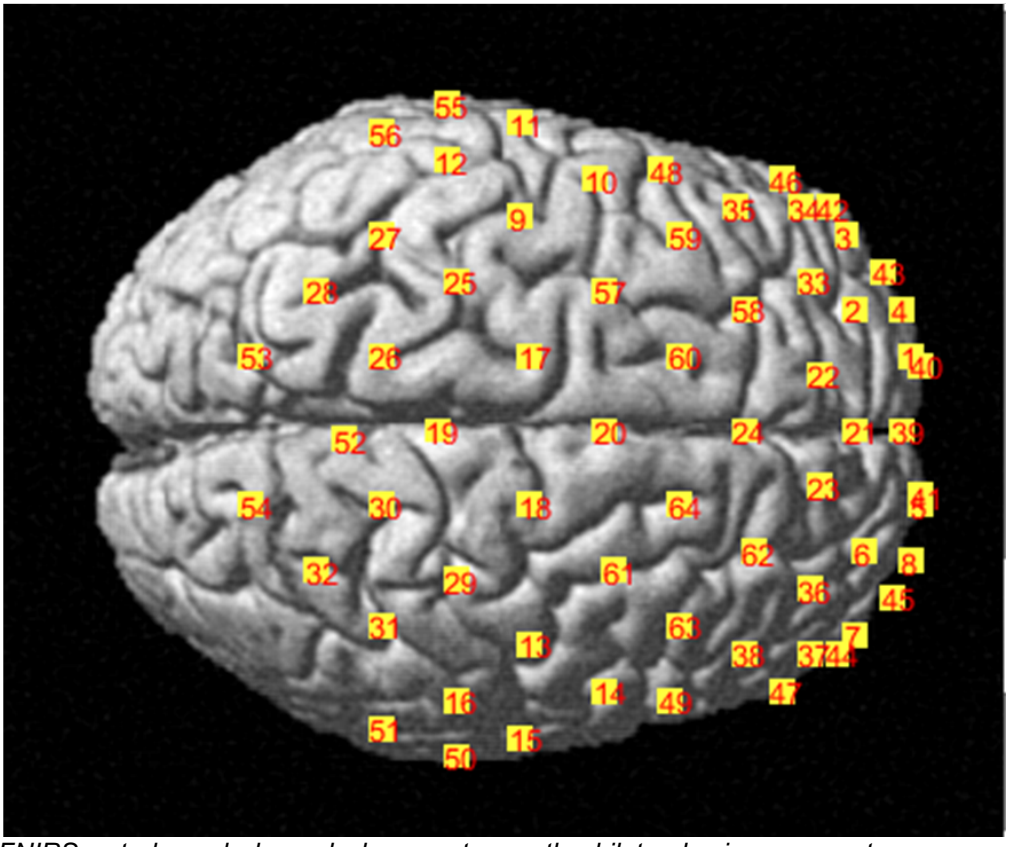

Notes: (a) FNIRS optode and channel placement over the bilateral primary somatosensory cortex, prefrontal cortex and parietal cortex within the international 10–10 standard system. The red and blue dots represent the location of light sources and detectors, respectively. The white squares represent the

location of the channels. Sources 03, 04, and 06 represent C3, C4, and Fz, respectively; (b) The co-registration of the 64 channels on a standard human brain template.

2.2.4 Data processing, analysis and statistics

Based on visual inspection of the recorded data, segments containing apparent signal spikes were removed, and channels exhibiting severe baseline drifts were also excluded entirely (Bizzego et al., 2022; Hocke et al., 2018). Furthermore, channels in which cardiac-related oscillations were not observed in the power spectral density were also discarded from further analysis, as the lack of cardiac-related oscillations in a channel often indicates abnormal signals or poor probe contact (Aarabi & Huppert, 2016). In the healthy control group, brain data from one participant were excluded due to poor signal quality, resulting in a total of nine healthy participants included in the subsequent analyses. In the patient group, due to varying health conditions prior to amputation, some patients were unable to complete measurements for all body sites. Additionally, one left-handed patient was excluded to avoid potential confounding effects of hemispheric lateralization on the experimental results. Consequently, the number of patients included in each condition was as follows: 19 patients for the non-painful stimulation and 17 for the painful stimulation of the left groin, respectively; 16 patients for the non-painful stimulation and 15 for the painful stimulation of the right groin, respectively; 14 patients for the non-painful stimulation and 13 for the painful stimulation of the left knee, respectively; 14 patients for the non-painful stimulation and 16 for the painful stimulation of the right knee, respectively. For the percentage of data retained for the further analysis, see the Figure B-S1. Subsequent preprocessing of the retained data was performed using the Homer2 toolbox (Huppert et al., 2009b). Raw intensity signals were first converted to optical density using the 'hmrIntensity2OD' function. Motion artifacts were detected and corrected via the 'hmrMotionCorrectWavelet' function (*iqr*=1.5). Next, a bandpass filter ('hmrBandpassFilt') was applied to remove physiological noise outside the range of 0.01-0.2 Hz. The optical density signals were then converted into changes in hemoglobin concentrations using the 'hmrOD2Conc' function. Finally, the hemodynamic response function (HRF) was estimated using block averaging through the 'hmrBlockAvg' function with the time range from -5s to 15s. According to the montage designed for this study, the 64 channels were grouped into 17 regions based on 10-10 EEG systems and the detailed location information for each channel (Table B-S1). These regions include the fronto-polar (PF; channel 40 and 41), anterior frontal

(AF; channel 1, 5 and 39), left anterior frontal (LAF; channel 2, 4 and 43), right anterior frontal (RAF; channel 6, 8 and 45), frontal (F; channel 21, 22 and 23), left frontal (LF; channel 3, 33, 34, 42 and 46), right frontal (RF; channel 7, 36, 37, 44 and 47), fronto-central (FC; channel 24, 60 and 64), left fronto-central (LFC; channel 35, 48, 57, 58 and 59), right fronto-central (RFC; 38, 49, 61, 62 and 63), central (C; channel 17, 18 and 20), left central (LC; channel 9, 10, 11 and 25), right central (RC; channel 13, 14, 15 and 29), centro-parietal (CP; channel 19, 26 and 30), left centro-parietal (LCP; channel 12, 27, 28, 55 and 56), right centro-parietal (RCP; channel 16, 31, 32, 50 and 51), and parietal (P; channel 52, 53 and 54) areas. For the analysis comparing patients with and without phantom limb pain (PLP) to healthy controls, patients were regrouped based on the side of amputation, and the corresponding data from healthy participants were reclassified accordingly. To eliminate the confounding effects of the side of amputation on the results, the brain imaging data were flipped along the left–right axis according to the amputated side (J. Zhang et al., 2018). A total of nine healthy controls were included in the analysis. The number of patients included under each condition was as follows: for non-painful stimulation of the groin on the amputated side, 5 patients with PLP and 9 without PLP; for painful stimulation of the groin on the amputated side, 5 with PLP and 8 without PLP. For non-painful stimulation of the groin on the non-amputated side, 7 with PLP and 8 without PLP; for painful stimulation of the groin on the non-amputated side, 6 with PLP and 8 without PLP. For non-painful stimulation of the knee on the amputated side, 4 with PLP and 7 without PLP; for painful stimulation of the knee on the amputated side, 6 with PLP and 7 without PLP. For non-painful stimulation of the knee on the non-amputated side, 4 with PLP and 7 without PLP; and for painful stimulation of the knee on the non-amputated side, 5 with PLP and 5 without PLP. For statistical analysis of the preprocessed brain data, the average hemodynamic response was calculated as the mean signal value within the time window from -5 to 15 seconds. For each brain region, the baseline mean (i.e., the average signal from -5 to 0 seconds) was subtracted to compute the baseline-corrected response (Zhou et al., 2020). The resulting value was considered stimulus-related: values greater than zero were interpreted as an increase of the oxygenated hemoglobin (i.e. activation), while values less than zero were interpreted as a decrease of the oxygenated hemoglobin (i.e. deactivation).

Data analysis was conducted using MATLAB R2020a. The Shapiro-Wilk test was used to assess the normality of all continuous variables. For normally distributed variables,

independent-samples t-tests were employed to compare groups. For variables that did not meet the assumption of normality, non-parametric test (Mann - Whitney U test) were applied. Categorical variables were analyzed using the chi-square test. A three-way ANOVA was conducted to analyze stimulation thresholds with three factors: group (2 levels: patients group and healthy controls), threshold (3 levels: perception and pain thresholds, pain tolerance) and body site (4 levels: left and right groin, left and right knee). The three-way ANOVA was conducted to analyze stimulation intensities and global average hemodynamic responses with three factors: group (2 levels: patients group and healthy controls), modality (2 levels: painful and non-painful stimulation) and body site (4 levels: left and right groin, left and right knee). Repeated-measures ANOVA was applied to assess VAS ratings. For comparisons of regional average hemodynamic responses, independent-samples t-tests were used to compare the patient group and healthy controls, while one-way ANOVA was conducted to compare the non-PLP patient group, the PLP patient group, and healthy controls. Prior to ANOVA, tests for normality and homogeneity of variance were performed. For datasets violating these assumptions, corresponding non-parametric analyses were conducted. As the results of non-parametric analyses were consistent with those of ANOVA, the ANOVA results were retained and reported in this study. Post-hoc comparisons for the three-way ANOVA results were conducted using the Tukey - Kramer test to correct for multiple pairwise comparisons. The false discovery rate (FDR) method was applied to control for multiple testing of independent-samples t-tests and one-way ANOVA. A significance threshold of 0.05 was used for all statistical tests. Note that the main objective of this study was to investigate intergroup differences. In the exploratory analysis of the PLP subgroup, particular emphasis was placed on comparisons between the PLP group and the other two groups.

3 RESULTS

3.1 Study 1

3.1.1 Stimulation intensity

Descriptive statistics of stimulus intensities over the two stimulation modalities and the four different body sites are presented in Fig. A-4 and Table A-S1. The two-way ANOVA with stimulation intensities as a dependent variable, based on a total of 16 observations, revealed significant main effects of body site and stimulation modality (painful vs. non- painful) on the stimulation intensities (body site: F_3 = 6.6, p < 0.001, η^2 = 0.142; stimulation modality: F_1 = 6.2, p = 0.014, η^2 = 0.049), but no significant interaction between these two factors (F_3 = 1.2, p = 0.330, η^2 = 0.028). Post-hoc Tukey test revealed that the stimulation intensities at both knees were significantly smaller than those assessed at the left groin (left groin vs. left knee: p < 0.001; left groin vs. right knee: p < 0.05), see Supplementary Table A-2 for details.

Figure A-4

Stimulation intensity (mA) of each body site under the two stimulation modalities.

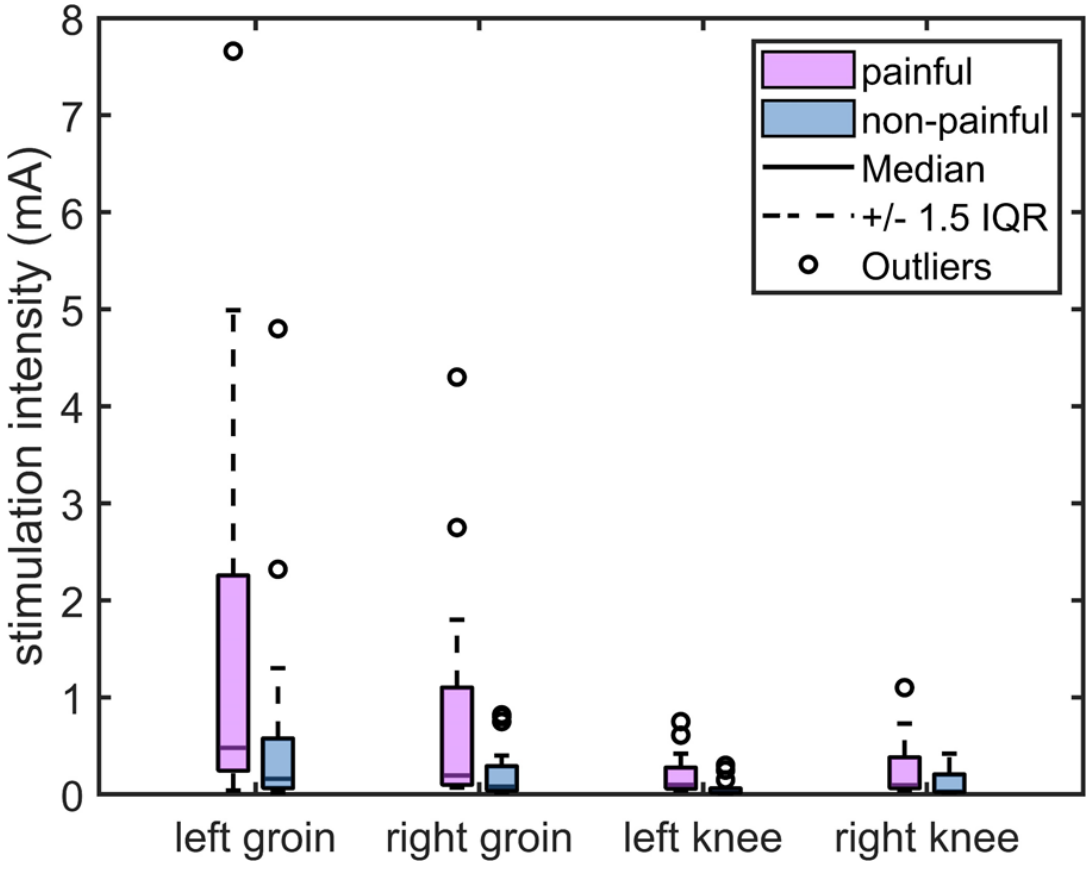

Note: Boxplots are used to display the painful stimulus values (represented by pink boxes) and non-painful stimulus values (represented by blue boxes) at each of the four locations. The central line within each box represents the median. The edges of the box correspond to the 25th and 75th percentiles, defining the interquartile range (IQR). Whiskers extend to the most extreme data points within 1.5 times the IQR from the first and third quartiles. Outliers are depicted as circles outside the boxes.

3.1.2 Visual Analogue Scale rating

Descriptive statistics of the VAS ratings over the two stimulation modalities and the four body sites are represented in Fig. A-5 and Table A-S3. The repeated-measures ANOVA of the VAS rating, with a total of 16 observations, showed a significant main effect of body site and a significant main effect of stimulation modality (painful vs. non-painful), but no significant main effect of time (before the stimulation modality vs. after the stimulation modality) (body site: F_3 = 3.6, p = 0.022, η^2 = 0.191; stimulation modality: F_1 = 413.4, p < 0.001, η^2 = 0.965; time: F_1 = 0.1, p = 0.720, η^2= 0.009) (see Table A-1). The post-hoc Tukey test depicted in Fig. A-6 revealed no significant differences after multiple comparisons correction among the body sites. However, the VAS rating for the right groin was lower than that for the left knee, showing a trend, as indicated by a p-value of 0.05; see Supplementary Table A-4 for details.

Figure A-5 (a-b)

The visual analogue scale (VAS) ratings of each body site under the two stimulation modalities.

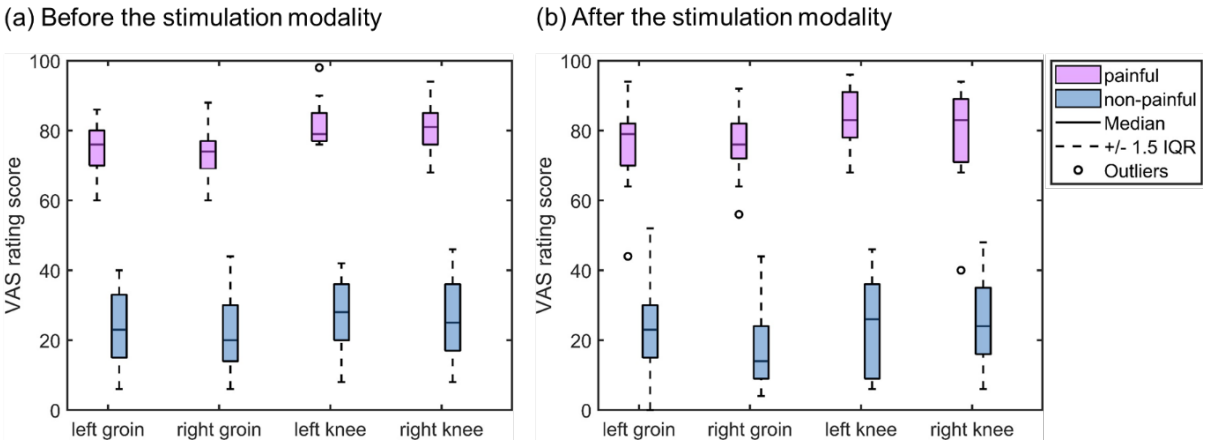

Notes: Boxplots are used to display the VAS ratings under the painful stimulation (represented by pink boxes) and non-painful stimulation (represented by blue boxes) at each of the four locations. The central line within each box represents the median. The edges of the box correspond to the 25th and 75th percentiles, defining the interquartile range (IQR). Whiskers extend to the most extreme data points within 1.5 times the IQR from the first and third quartiles. Outliers are depicted as circles outside the boxes. The (a, b) show the different rating times (a before the stimulation modality; b after the stimulation modality).

Table A-1

Repeated-measures analysis of variance (ANOVA) results for visual analogue scale (VAS) rating.

Source	Df	F	*p*	η^2
Body sites	3	3.6	0.022	0.191
Stimulation modality	1	413	<0.001	0.965
Time	1	0.1	0.720	0.009
Body sites*time	3	0.04	0.989	0.003
Body sites*stimulation modality	3	0.9	0.437	0.058
Stimulation modality*time	1	3.3	0.090	0.179
Body sites*stimulation modality*time	3	2.1	0.114	<0.001

Notes: Stimulation modality: painful and non-painful stimulation; Time: before the stimulation modality and after the stimulation modality; Df: degree of freedom; F: F-statistic; p: p-value; η^2: partial eta-squared.

Figure A-6

Bar plots showing the mean visual analogue scale (VAS) rating across body sites.

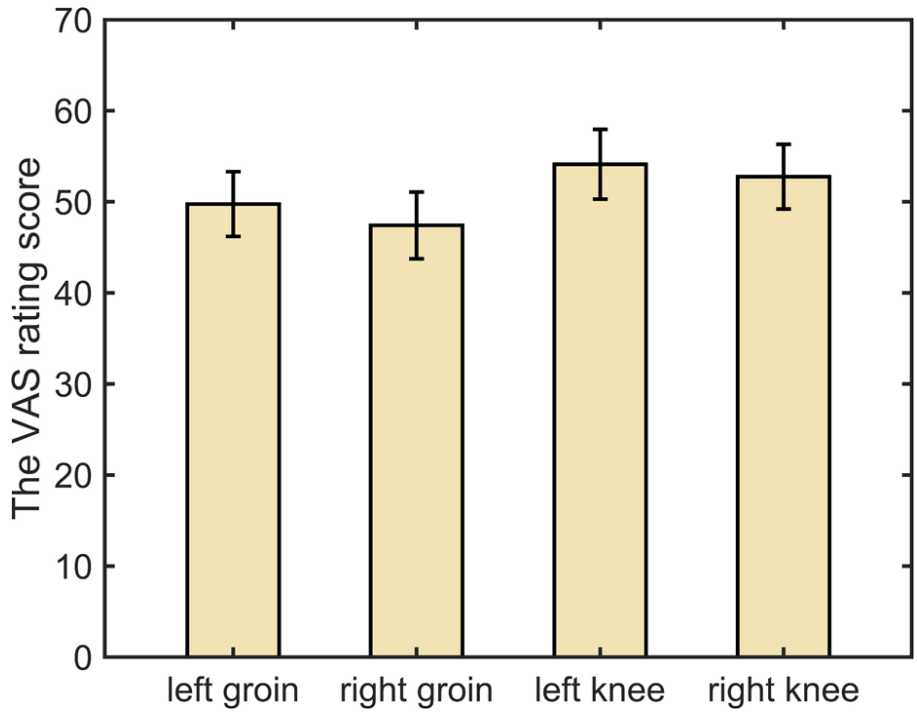

Notes: Error bars represent the standard error of the mean (SE).

3.1.3 Analysis of brain activation

We utilized the general linear model to generate interpolated topographical maps for the different body sites exposed to painful and non-painful stimuli. This enabled us to examine how various brain regions were activated or deactivated in response to these stimuli. As described in the method section, a positive β value reflects the activation of regional neuro-metabolic activity during stimulation compared to non-stimulation intervals, while a negative β value indicates its deactivation. The repeated-measures ANOVA of the β values, with a total of 12 observations, showed a significant main effect of brain region (F_2 = 9.2, p = 0.001, η^2 = 0.455), but no significant main effect of body site and stimulation modality (painful and non-painful) (Body site: F_3 = 0.2, p = 0.921, η^2 = 0.014; Stimulation modality: F_2 = 0.10, p = 0.761, η^2 = 0.009). The interaction between body site, stimulation modality, and brain region was significant (F_6 = 3.1, p = 0.009, η^2 = 0.221), indicating that the combined effects of these factors significantly influenced the β values. See the Supplementary Table A-6 for the detailed information. The results of the post-hoc multiple comparisons between the β values for each brain region can be found in Supplementary Table A-7. Figure A-7 showed the results of post-hoc multiple comparisons of the β value of each brain region under different stimulation modalities (painful and non-painful) for each body site. We observed the activation of bilateral S1 and PFC areas in response to a non-painful stimulation on the left groin. During painful stimulation of the left groin, we noted deactivation in the ipsilateral S1 cortex and PFC. Figure A-7 (b) clearly indicated a significant increase in oxyhemoglobin levels in bilateral S1 cortex and PFC during non-painful stimulation compared to painful stimulation of left groin. When we applied electrical stimulation to the right groin, we observed activation in the bilateral S1 cortex and deactivation in the PFC, independent of the stimulation modality. However, the ipsilateral S1 cortex exhibited greater activation in response to non-painful stimuli compared to painful stimuli, as shown in Fig. A-7 (b). When we stimulated the left knee, we observed activation in the bilateral S1 cortex and deactivation in the PFC. There is no statistical significance observed in the alterations within these three distinct brain regions when comparing activity patterns of the cerebral cortex under painful and non-painful stimulation, as depicted in Fig. A-7 (b). As can be seen in Fig. A-7 (a), we saw activation in the bilateral S1 cortex and deactivation in the PFC when the painful stimulation were provided on the right knee. We observed activation in the ipsilateral S1 cortex and deactivation in the contralateral S1 cortex, the PFC, during non-painful

stimulation of right knee. We found a significant increase in oxyhemoglobin levels in these three brain regions during the painful stimulation when compared to non-painful stimulation; see Fig. A-7 (b). See the Supplementary Table A-8 for the statistical results of Fig. A-7 (b).

Figure A-7 (a-b)

Topographic brain activity and group-averaged β value comparisons across body site Stimulations.

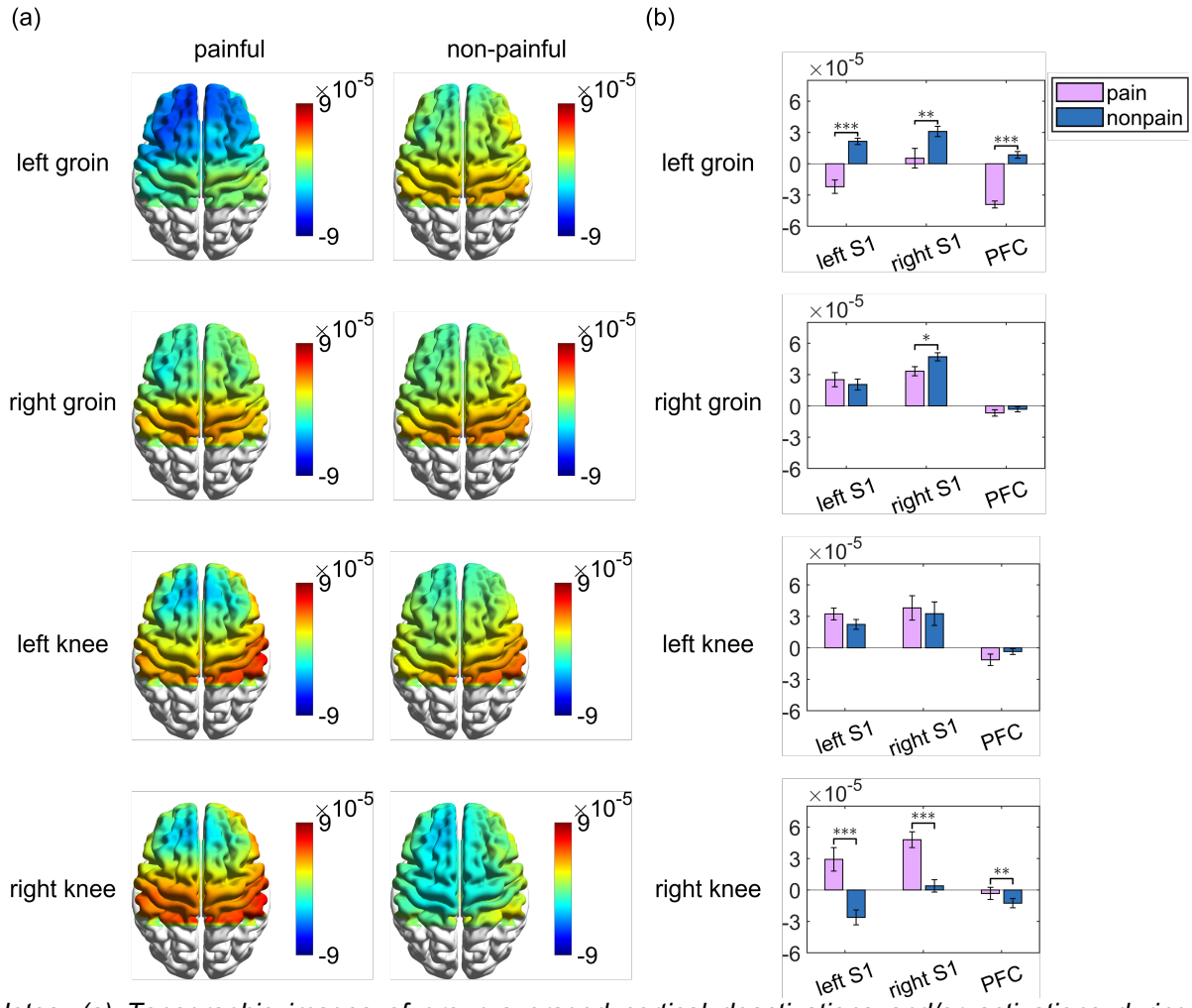

Notes: (a) Topographic images of group-averaged cortical deactivations and/or activations during painful (left) and non-painful (right) stimulation modalities given on each body site (left groin, right groin, left knee and right knee). (b) Comparisons of the group-averaged β values of different brain regions when stimulating different body sites. The pink bar represents the painful stimuli, and the blue bar represents the non-painful stimuli. Left S1 means left primary somatosensory area, right S1 means right primary somatosensory area, and PFC means prefrontal area. Error bars represent the standard error of the mean. (=p<0.05, **=p<0.01, ***=p<0.001).*

3.2 Study 2

3.2.1 Demographic and clinical characteristics of patient group and healthy controls group

In this study, the majority of the 21 patients scheduled to undergo lower limb amputation were male (76.2%). The amputations were primarily due to occlusive arterial disease, either associated with diabetes (66.7%) or not associated with diabetes (33.3%). The levels of amputation varied: 38.1% underwent above-knee amputations, 28.6% below-knee, 14.3% forefoot, and 23.8% toe amputations. Follow-up assessments were conducted three to eight months post-amputation (mean: 5.1 ± 1.8 months), during which 16 patients participated. Among them, 7 reported experiencing phantom limb pain, accounting for 43.8% of the follow-up group. A comparison between the patient group (N = 18) and the healthy control group (N = 10) revealed significantly higher pain severity in the patient group ($p < 0.001$). There were no significant differences between the patient group (N = 21) and the healthy control group (N = 10) in terms of age (p = 0.482), sex (p = 0.353), BMI (p = 0.364), or handedness (p = 0.483). See the table B-1 for the details.

Table B-1

Demographic, clinical data of patient group and healthy control group.

Characteristic	Patient group (N = 21)	HC group (N = 10)	*t* or *chi²*	*p*
Age	71.0 ± 10.2	68.4 ± 7.7	0.712	0.482
Gender(female / male)	5 / 16	4 / 6	0.862	0.353
BMI	26.9 ± 6.0	24.9 ± 3.9	0.990	0.364
Handedness	20 Right-handed (95%) 1 Left- handed (5%)	100% Right-handed	0.492	0.483
Amputation reason	66.7% occlusive arterial disease with diabetes mellitus (N=14) 33.3% occlusive arterial disease without diabetes mellitus (N=7)	-	-	-
Pain severity (MPI: N(P)=18)	3.5 ± 1.4	0.7 ± 1.1	5.770	<0.001*
After the amputation (5.1 ± 1.8 months)				
Amputation site (left / right)	9 / 12	-	-	-
Amputation level	38.1% above knee (N=8) 28.6% below knee (N=6) 14.3% forefoot (N=2) 23.8% Toes (N=5)	-	-	-
Phantom limb pain (N(P)=16)	43.8% (N=7)	-	-	-

Note: HC: healthy controls; N: number; BMI: body mass index; P: patient group; t: t-statistic; chi2: chi-square statistic; p: p-value.

3.2.2 Stimulation thresholds

Descriptive statistics of stimulus values over the three stimulation thresholds, four different body sites and the two groups are presented in Table B-S2. The three-way ANOVA with stimulation values as a dependent variable, based on a total of 31 observations, revealed significant main effects of stimulation threshold (perception, pain and pain tolerance) and group (patient group vs. healthy control group) on the stimulus value (threshold: $F_2 = 14.8$, $p < 0.001$; group: $F_1 = 26.0$, $p < 0.001$), and the significant interaction effect between these two factors ($F_2 = 3.6$, $p = 0.029$). See the Table B-2 for the details. Post-hoc Tukey test revealed that the stimulation values of pain tolerance threshold in patient group were significantly higher than those in the healthy control group. In the patient group, the stimulus values of pain tolerance threshold were significantly higher than the stimulus values of perception and pain thresholds, and the stimulus values of pain threshold were significantly higher than the stimulus values of perception threshold. See the figure B-1. See the table B-S3 for the detailed information.

Table B-2

Table for stimulation thresholds. Three-way analysis of variance (ANOVA) with factors threshold, body site, group.

Source	df	SS	MS	F	*p*
Threshold	2	727.9	363.9	14.8	<0.001*
Body site	3	174.4	58.1	2.4	0.071
Group	1	637.8	637.8	26.0	<0.001*
Threshold x body site	6	166.4	27.7	1.1	0.345
Threshold x group	2	176.4	88.2	3.6	0.029*
Body site x group	3	26.1	8.7	0.4	0.786
Error	306	7511.7	24.5		

*Note: Threshold: perception threshold, pain threshold and pain tolerance; Body site: left and right groin, left and right knee; df: degree of freedom; SS: Sum of Squares; MS: Mean Square; F: F-statistic; p: p-value; *=p<0.05.*

Figure B-1

Bar plots showing the mean stimulation value across thresholds.

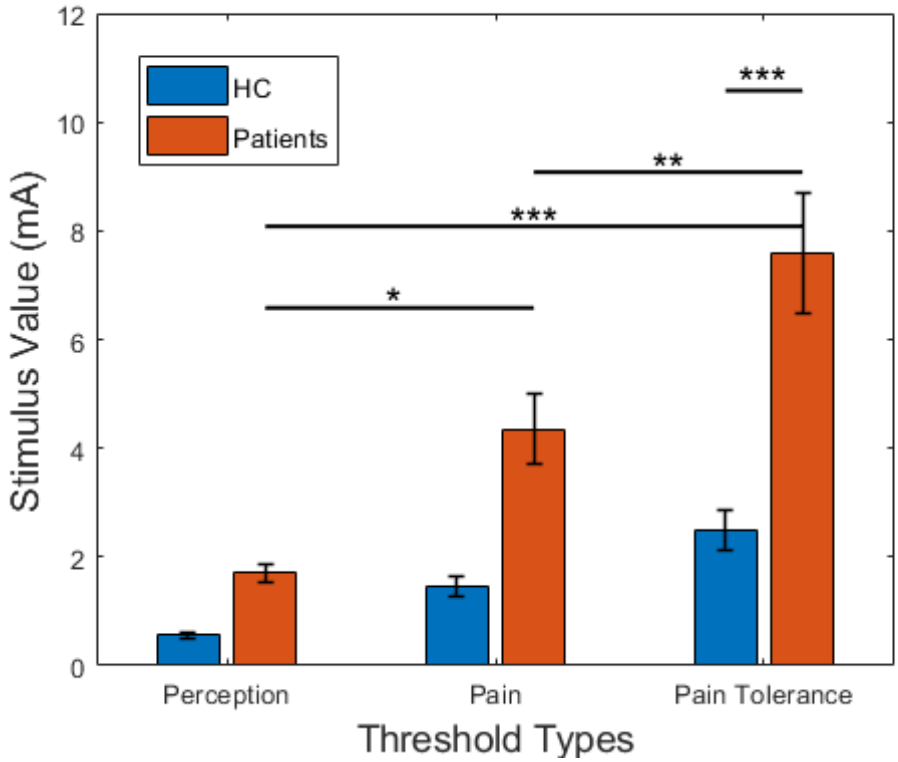

*Note: Error bars represent the standard error of the mean (SE). (HC: healthy control group; *=p<0.05, **=p<0.01 and ***=p<0.001).*

3.2.3 Stimulation intensities

Descriptive statistics of stimulus intensities over the four body sites, two stimulation modalities and the two groups are presented in Table B-S4. The three-way ANOVA with stimulation intensities as a dependent variable, based on a total of 31 observations, revealed significant main effects of body site (left groin, right groin, left knee and right knee), stimulation modality (painful vs. non- painful) and group (patient group vs. healthy control group) on the stimulation intensities (body site: $F_3 = 2.8$, $p = 0.043$; stimulation modality: $F_1 = 10.8$, $p = 0.001$; group: $F_1 = 22.8$, $p < 0.001$), but no significant interaction effect among the three factors. See the Table B-3. Post-hoc Tukey test revealed that the painful stimulation intensities in patient group were significantly higher than those in the healthy control group ($p < 0.001$). In the patient group, the painful stimulation intensities were higher than the non-painful stimulation intensities ($p < 0.001$). See the figure B-2. Although a main effect of stimulation intensity was observed across different body sites, no significant group differences were found within the same body site after the post-hoc Tukey test correction. See the figure B-3. See the table B-S5 and B-S6 for the details of Post-hoc Tukey test.

Table B-3

Table for stimulation intensities. Three-way analysis of variance (ANOVA) with factors body site, stimulation modality, group.

Source	df	SS	MS	F	*p*
Body site	3	212.3	70.8	2.8	0.043*
Modality	1	276.0	276.0	10.8	0.001*
Group	1	583.8	583.8	22.8	<0.001*
Body site x modality	3	72.3	24.1	0.9	0.422
Body site x group	3	19.1	6.4	0.2	0.862
Modality x group	1	65.0	65.0	2.5	0.113
Error	203	5193.9	25.6		

*Note: Body site: left and right groin, left and right knee; Modality: painful and non-painful stimulation; Group: patient group and healthy control group; df: degree of freedom; SS: Sum of Squares; MS: Mean Square; F: F-statistic; p: p-value; *=p<0.05.*

Figure B-2

Bar plots showing the mean stimulation value across stimulation modalities.

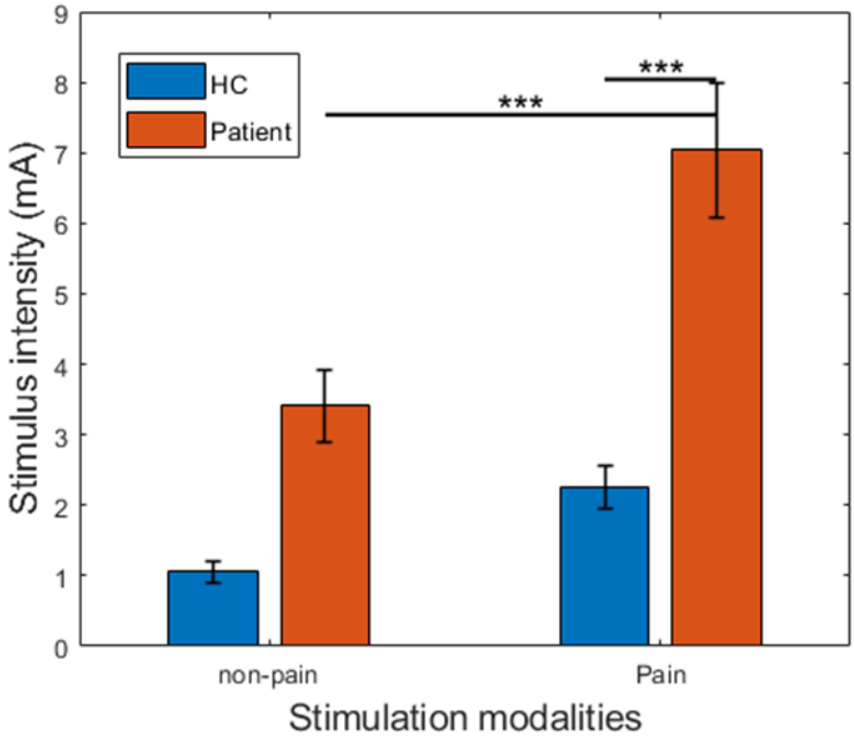

*Note: Error bars represent the standard error of the mean (SE). (*** = p < 0.001).*

Figure B-3

Bar plots showing the mean stimulation value across body sites.

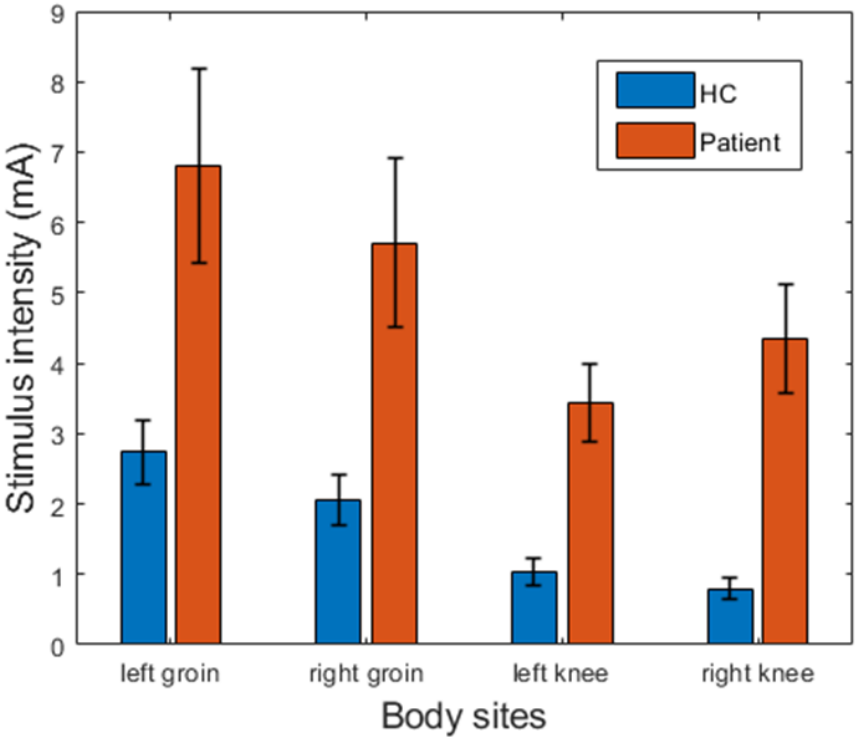

Note: Error bars represent the standard error of the mean (SE).

3.2.4 Visual Analogue Scale rating

Descriptive statistics of the VAS ratings over the two groups, the two stimulation modalities, the four body sites and the three time points are represented in Table B-S7. The repeated-measures ANOVA of the VAS rating, with a total of 31 observations, showed a significant main effect of stimulation modality (painful vs. non-painful), but neither significant main effect of group (patient group vs. healthy control group) nor body site (left groin, right groin, left knee and right knee) and time point (before the stimulation modality, after 3rd block and after 6th block) (group: F_1 = 0.2, p = 0.651; body site: F_3 < 0.1, p = 0.992; stimulation modality: F_1 = 23.3, p < 0.001; time point: F_2 = 0.6, p = 0.520) (see Table B-4). Figure B-4 illustrates that there were no statistically significant differences in VAS rating over different time points and between groups.

Table B-4

Table for VAS ratings. Repeated-measure analysis of variance (ANOVA) with factors body site, modality, group, time point.

Source	df	SS	MS	F	*p*
Group	1	166.7	166.7	0.2	0.651
Body site	3	13.3	4.4	0.0	0.992
Group x Body site	3	274.3	91.4	0.3	0.753
Modality	1	13585.6	13585.6	23.3	<0.001*
Group x Modality	1	190.5	190.5	0.3	0.574
Time point	2	137.8	68.9	0.6	0.520
Group x Time point	2	122.5	61.3	0.6	0.556
Body site x Modality	3	244.8	81.6	0.4	0.757
Group x Body site x Modality	3	372.3	124.1	0.6	0.619
Body site x Timepoint	6	279.6	46.6	0.8	0.505
Group x Body site x Time point	6	248.7	41.4	0.7	0.564
Modality x Time point	2	398.9	199.4	3.1	0.069
Group x Modality x Time point	2	413.8	206.9	3.2	0.063
Body site x Modality x Time point	6	513.4	85.6	1.7	0.168
Group x Body site x Modality x Time point	6	752.4	125.4	2.5	0.057

*Notes: Body site: left and right groin, left and right knee; Modality: painful and non-painful stimulation; Group: patient group and healthy control group; Time point: before the modality, after the 3rd and 6th blocks; df: degree of freedom; SS: Sum of Squares; MS: Mean Square; F: F-statistic; p: p-value; *=p<0.05.*

Figure B-4

Line plots showing the mean VAS rating across different time points.

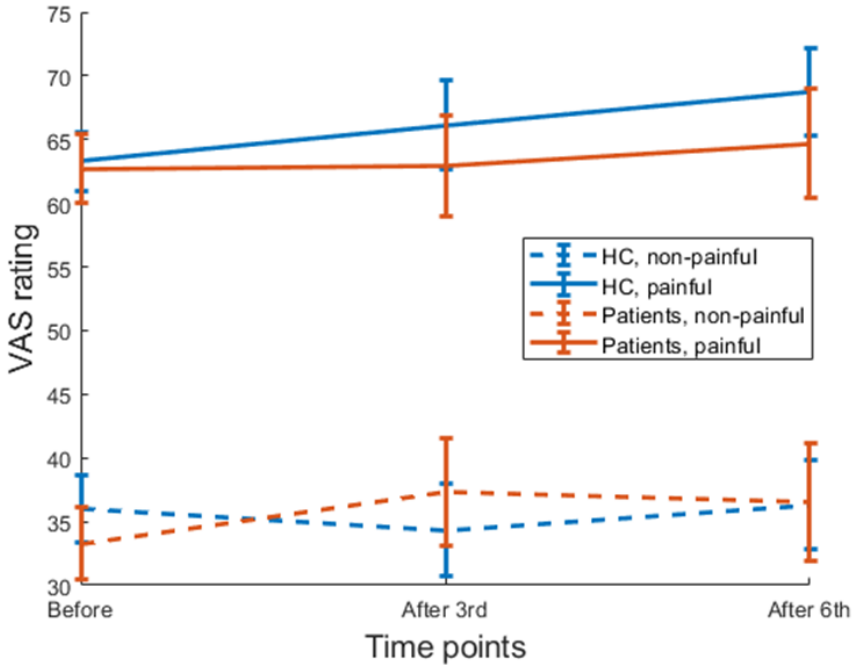

Note: Error bars represent the standard error of the mean (SE). (Time points: before the modality, after the 3rd and 6th blocks; HC: healthy controls)

3.2.5 Global cortical hemodynamic response

Descriptive statistics of the mean change in HbO2 and HbR concentration over the two groups, the two stimulation modalities and the four body sites are represented in Tables B-S8 and B-S11. The three-way ANOVA of the mean change in HbO2 concentration, with a total of 28 observations, showed a significant main effect of body site (left groin, right groin, left knee and right knee), a significant main effect of stimulation modality (painful vs. non-painful) and significant main effect of group (patient group vs. healthy control group), (group: $F_1 = 60.3$, $p < 0.001$; body site: $F_3 = 2.8$, $p = 0.042$; stimulation modality: $F_1 = 8.5$, $p = 0.004$). There was a significant interaction effect between the stimulation modality and group ($F_1 = 11.7$, $p < 0.001$), see Table B-5. Post-hoc Tukey test showed that the mean change of HbO2 concentration in the patient group was significantly higher than that in the healthy control group, regardless of whether painful stimulation ($p < 0.05$) or non-painful stimulation ($p < 0.001$) was given. In the patient group, the mean change in HbO2 concentration was significantly smaller during painful stimulation compared to non-painful stimulation ($p < 0.001$). See the figure B-5. In addition, the mean change of HbO2 concentration in the patient group was significantly higher than that in the healthy control group when given the stimulation on the right groin ($p < 0.001$) and the right knee ($p < 0.001$). See the figure B-6. See the table B-S9 and B-S10 for the detailed information.

The three way ANOVA of the mean change in HbR concentration, with a total of 28 observations, showed a significant main effect of group (patient group vs. healthy control group) (group: $F_1 = 116.3$, $p < 0.001$). There was a significant interaction effect among the three factors, body site, stimulation modality and group ($F_3 = 2.9$, $p = 0.035$), see Table B-S6. Post-hoc Tukey test revealed that, for stimulation at the left groin, left knee, and right knee, the patient group showed significantly greater mean changes in HbR concentration compared to the healthy control group, regardless of whether the stimulation was painful or non-painful. For stimulation at the right groin, the patient group showed significantly higher mean changes in HbR concentration under painful stimulation compared to the healthy control group, while the healthy control group showed significantly lower HbR concentration changes under painful stimulation compared to non-painful stimulation. See the figure B-7. See the table B-S12 for the detailed information.

Table B-5

Table for the mean change in oxyhemoglobin concentration. Three-way analysis of variance (ANOVA) with factors body site, stimulation modality, group.

Source	df	SS	MS	F	*p*
Body site	3	0.04	0.01	2.8	0.042*
Modality	1	0.04	0.04	8.5	0.004*
Group	1	0.27	0.27	60.3	<0.001*
Body site x modality	3	0.05	0.02	3.7	0.011*
Body site x group	3	0.02	0.01	1.8	0.154
Modality x group	1	0.05	0.05	11.7	<0.001*
Body site x modality x group	3	0.03	0.01	2.2	0.083
Error	3218	14.29	<0.01		

*Notes: Body sites: left and right groin, left and right knee; Modalities: painful and non-painful stimulation; Groups: patient group and healthy control group; df: degree of freedom; SS: Sum of Squares; MS: Mean Square; F: F-statistic; p: p-value; *=p<0.05.*

Figure B-5

Bar plots showing the mean change in oxyhemoglobin concentration across stimulation modalities and groups.

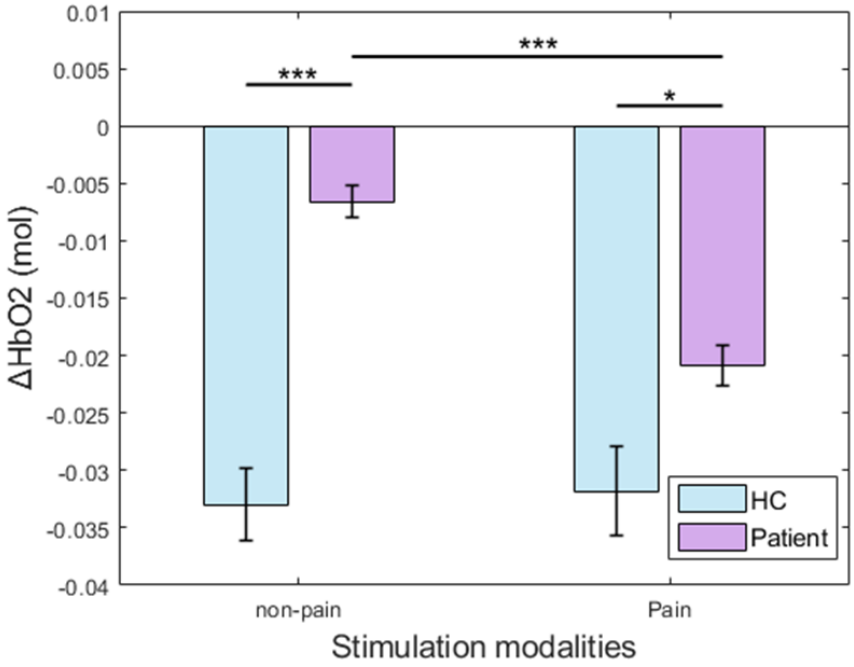

Notes: Error bars represent the standard error of the mean (SE). (=p<0.05, ***=p<0.001, HC: healthy controls).*

Figure B-6

Bar plots showing the mean change in oxyhemoglobin concentration of across groups and body sites.

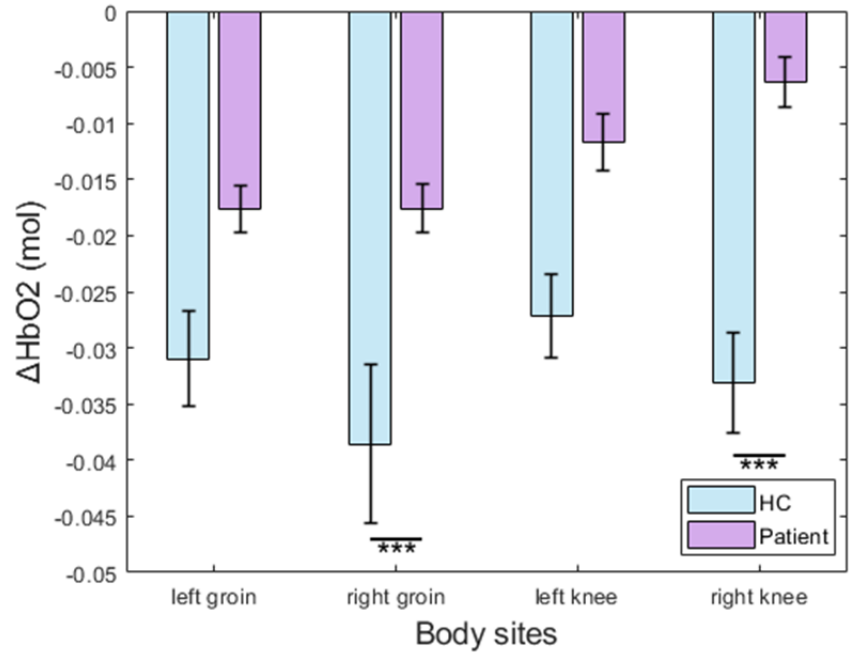

*Notes: Error bars represent the standard error of the mean (SE). (***=p<0.001).*

Table B-6

Table for the mean change in deoxyhemoglobin concentration. Three-way analysis of variance (ANOVA) with factors body site, stimulation modality, group.

Source	df	SS	MS	F	*p*
Body site	3	<0.01	<0.01	1.7	0.174
Modality	1	<0.01	<0.01	3.8	0.053
Group	1	0.05	0.05	116.3	<0.001*
Body site x modality	3	0.01	<0.01	5.2	0.001*
Body site x group	3	<0.01	<0.01	0.7	0.578
Modality x group	1	<0.01	<0.01	4.0	0.046*
Body site x modality x group	3	<0.01	<0.01	2.9	0.035*
Error	3218	1.42	<0.01		

*Notes: Body site: left and right groin, left and right knee; Modality: painful and non-painful stimulation; Group: patient group and healthy control group; df: degree of freedom; SS: Sum of Squares; MS: Mean Square; F: F-statistic; p: p-value; *=p<0.05.*

Figure B-7

Bar plots showing the mean change in deoxyhemoglobin concentration of across groups, body sites and stimulation modalities.

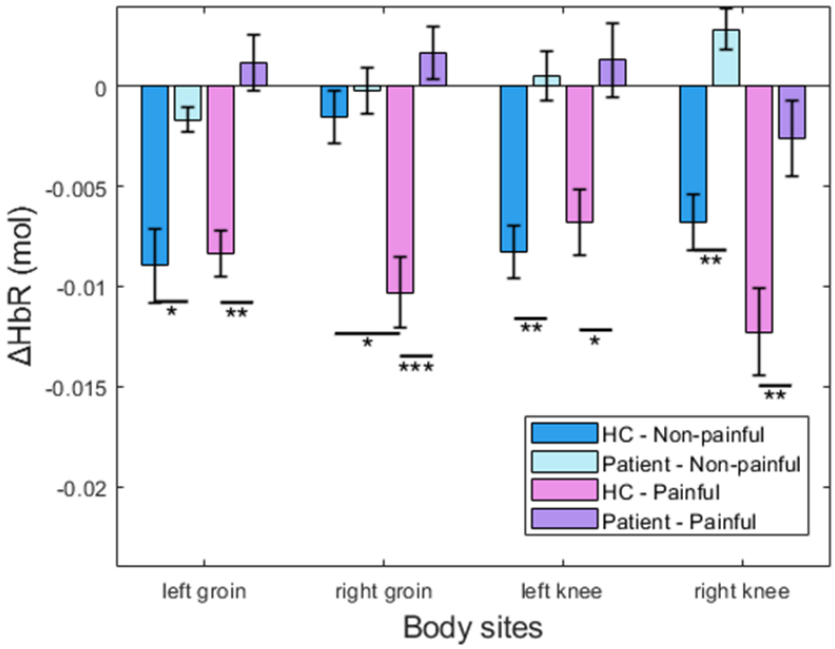

Notes: Error bars represent the standard error of the mean (SE). (=p<0.05; **=p<0.01; ***=p<0.001; HC: healthy controls).*

3.2.6 Regional cortical hemodynamic response

Following FDR correction, independent-samples t-tests revealed significant regional differences in cortical hemodynamic responses between groups. Under right groin pain stimulation, the patient group showed significantly greater mean changes in HbR concentration in the left central cortex (LC; p = 0.004) and right frontal cortex (RF; p = 0.002) compared to healthy controls. See the figure B-8. Under non-painful stimulation of the right knee, significantly increased HbR changes were also observed in the right centro-parietal cortex (RCP; p = 0.002) in patients. See the figure B-9. These results are detailed in Tables B-S13 and B-S14. No other significant group differences were found across remaining brain regions or stimulation conditions (see Supplementary Tables B-15 – B-20 and Figure B-2 – B-7).

Figure B-8

Between-group comparisons of hemoglobin concentration changes across cortical regions under right groin painful stimulation.

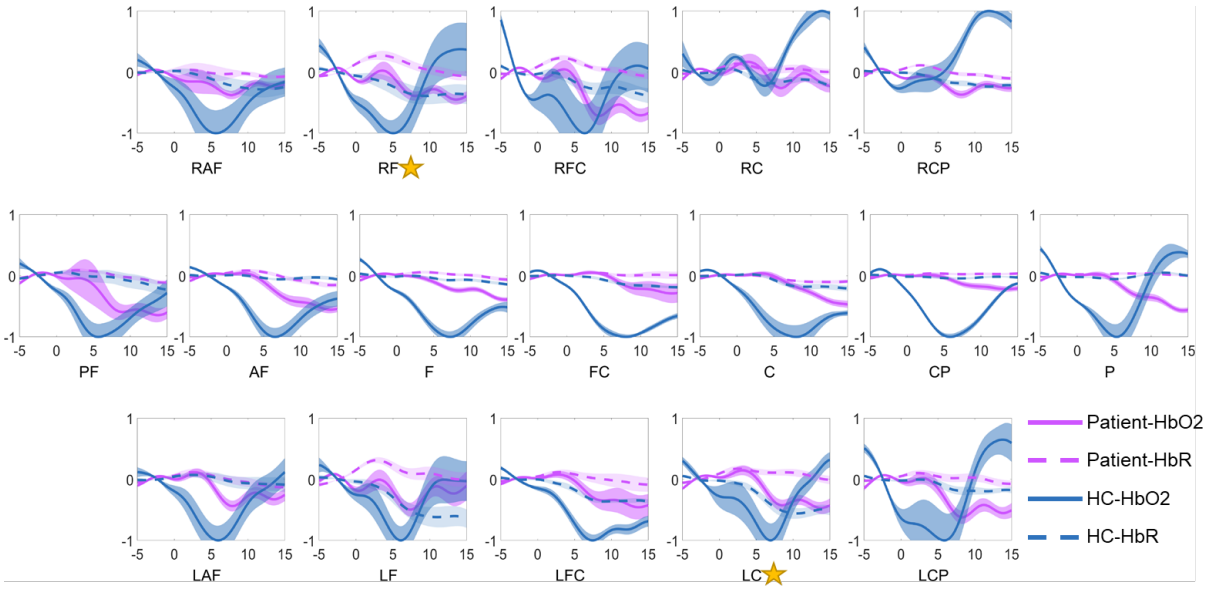

Notes: PF: fronto-polar area; AF: anterior frontal area; LAF: left anterior frontal area; RAF: right anterior frontal area; F: frontal area; LF: left frontal area; RF: right frontal area; FC: fronto-central area; LFC: left fronto-central area; RFC: right fronto-central area; C: central area; LC: left central area; RC: right central area; CP: centro-parietal area; LCP: left centro-parietal area; RCP: right centro-parietal area; P: parietal area; HC: healthy control group; Patient: patient group; HbO2: oxyhemoglobin; HbR: deoxyhemoglobin. The x-axis represents time (in seconds), and the y-axis represents normalized changes in hemoglobin concentration (range: -1 to 1). Yellow stars indicate significant between-group differences in HbR concentration after FDR correction.

Figure B-9

Between-group comparisons of hemoglobin concentration changes across cortical regions under right knee non-painful stimulation.

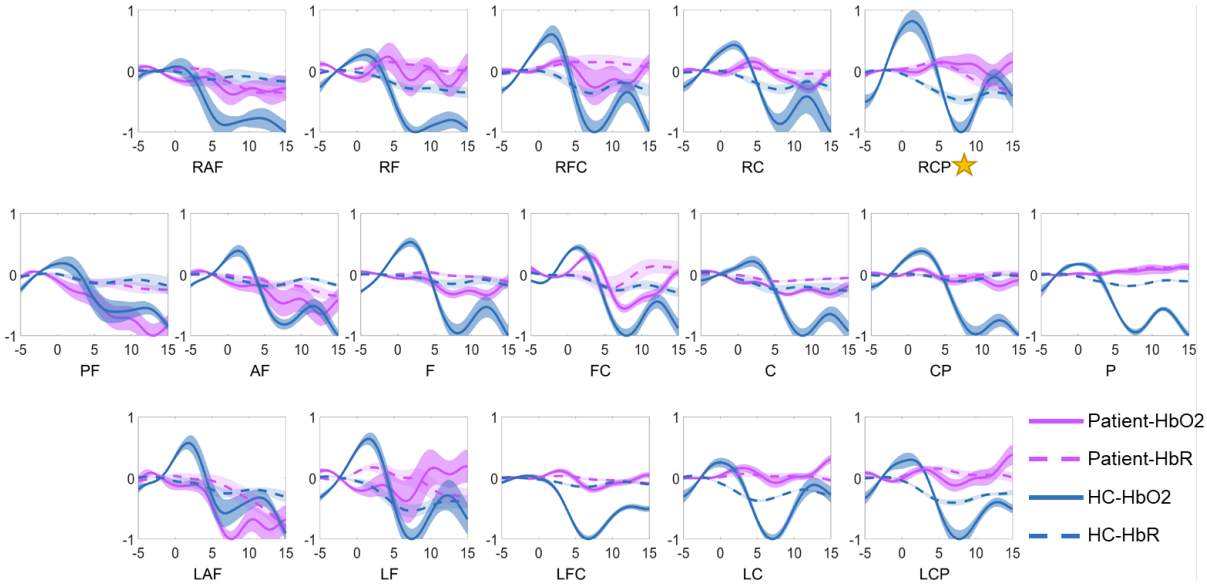

Notes: PF: fronto-polar area; AF: anterior frontal area; LAF: left anterior frontal area; RAF: right anterior frontal area; F: frontal area; LF: left frontal area; RF: right frontal area; FC: fronto-central area; LFC: left fronto-central area; RFC: right fronto-central area; C: central area; LC: left central area; RC: right central area; CP: centro-parietal area; LCP: left centro-parietal area; RCP: right centro-parietal area; P: parietal area; HC: healthy control group; Patient: patient group; HbO_2: oxyhemoglobin; HbR: deoxyhemoglobin. The x-axis represents time (in seconds), and the y-axis represents normalized changes in hemoglobin concentration (range: -1 to 1). Yellow stars indicate significant between-group differences in HbR concentration after FDR correction.

3.2.7 Comparison between PLP and Non-PLP patient subgroups and healthy controls

(1) Demographic and clinical characteristics

The demographic and clinical characteristics of the PLP, non-PLP patient subgroups, and healthy controls are summarized in Table B-7. All participants were right-handed, and there were no significant differences among the three groups in terms of age (p = 0.649), gender (p = 0.132), or BMI (p = 0.450). Additionally, there were no significant differences between the PLP and non-PLP groups in terms of amputation level (p = 0.484), residual limb pain (p = 0.377), or phantom sensation (p = 0.949). However, a significant group difference was observed in pain severity scores assessed by the MPI (p <0.001). Post-hoc Tukey test showed that the pain severity scores of non-PLP group were significantly higher than the scores of PLP group and healthy control group. In addition, the pain severity scores of PLP group were notably higher than the scores of healthy control group. See the figure B-10. See the table B-S21 for the detailed information.

Table B-7

Demographic and clinical characteristics of PLP and Non-PLP patient subgroups and healthy controls group.

Characteristic	PLP group (N = 7)	Non-PLP group (N = 9)	HC group (N = 9)	*F* or *chi²*	*p*-value
Age	67.0 ± 12.8	71.0 ± 9.8	67.2 ± 7.1	0.4	0.649
Gender (female / male)	4 / 3	1/ 8	4 / 5	4.1	0.132
BMI	28.6 ± 6.8	25.9 ± 6.8	24.8 ± 4.1	0.8	0.450
Handedness	all Right-handed	all Right-handed	all Right-handed	-	-
Amputation reason	occlusive arterial disease with diabetes mellitus (N=3) occlusive arterial disease without diabetes mellitus (N=4)	occlusive arterial disease with diabetes mellitus (N=7) occlusive arterial disease without diabetes mellitus (N=2)	-	2.0	0.152
Pain severity (MPI: $N_{(plp)}$=6; $N_{(nplp)}$=7)	3.0 ± 0.6	4.3 ± 0.7	0.7 ± 1.1	34.4	<0.001*
Amputation site (left / right)	4 / 3	5 / 4	4 / 5	0.3	0.850
Amputation level	above knee (N=2) below knee (N=4) toes (N=1)	above knee (N=4) below knee (N=2) forefoot (N=1) toes (N=2)	-	2.5	0.484
Residual limb pain	3 / 4	2 / 7	-	0.8	0.377
Phantom limb sensation	4 / 3	5 / 4	-	<0.1	0.949

Note: HC: healthy controls; N: number; BMI: body mass index; PLP: the phantom limb pain patient group; NPLP: the non-phantom limb pain group.

Figure B-10

Bar plots showing the mean pain severity value across groups.

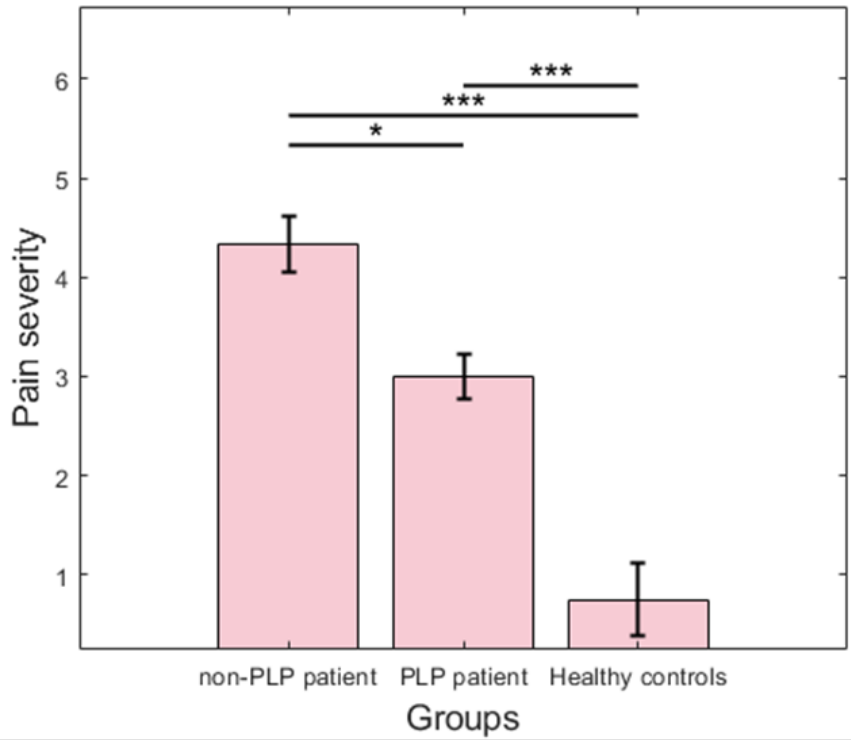

Note: Error bars represent the standard error of the mean (SE). (=p<0.05, ***=p<0.001).*

(2) Stimulation thresholds

Descriptive statistics of stimulus values over the three stimulation thresholds, four different body sites and the three groups are presented in Table B-S22. The three-way ANOVA with stimulation values as a dependent variable, based on a total of 25 observations, revealed significant main effects of stimulation threshold (perception, pain and pain tolerance) and group (PLP patient group, non-PLP patient group and healthy control group) on the stimulus value (threshold: $F_2 = 21.1$, $p < 0.001$; group: $F_2 = 15.2$, $p < 0.001$), and there was no significant interaction effect among the three factors. See the table B-8 for the details. Post-hoc Tukey test revealed that the stimulation values of pain tolerance thresholds in healthy control group were significantly smaller than those in the non-PLP patient and PLP patient group. The stimulation values of pain thresholds in non-PLP patient group were significantly higher than those in the healthy control group. See the figure B-11. See the table B-S23 for the detailed information.

Table B-8

Table for stimulation thresholds. Three-way analysis of variance (ANOVA) with factors threshold, body site, group.

Source	df	SS	MS	F	*p*
Threshold	2	1081.2	540.6	21.1	<0.001*
Body site	3	134.4	44.8	1.7	0.158
Group	2	779.8	389.9	15.2	<0.001*
Threshold x body site	6	131.8	22.0	0.9	0.528
Threshold x group	4	241.8	60.4	2.4	0.054
Body site x group	6	250.2	41.7	1.6	0.141
Error	249	6331.5	25.7		

*Notes: Threshold: perception threshold, pain threshold and pain tolerance; Body site: groin on the amputated side, groin on the non-amputation side, knee on the amputated side, knee on the non-amputation side; df: degree of freedom; SS: Sum of Squares; MS: Mean Square; F: F-statistic; p: p-value; *=p<0.05.*

Figure B-11

Bar plots showing the mean stimulation value across thresholds.

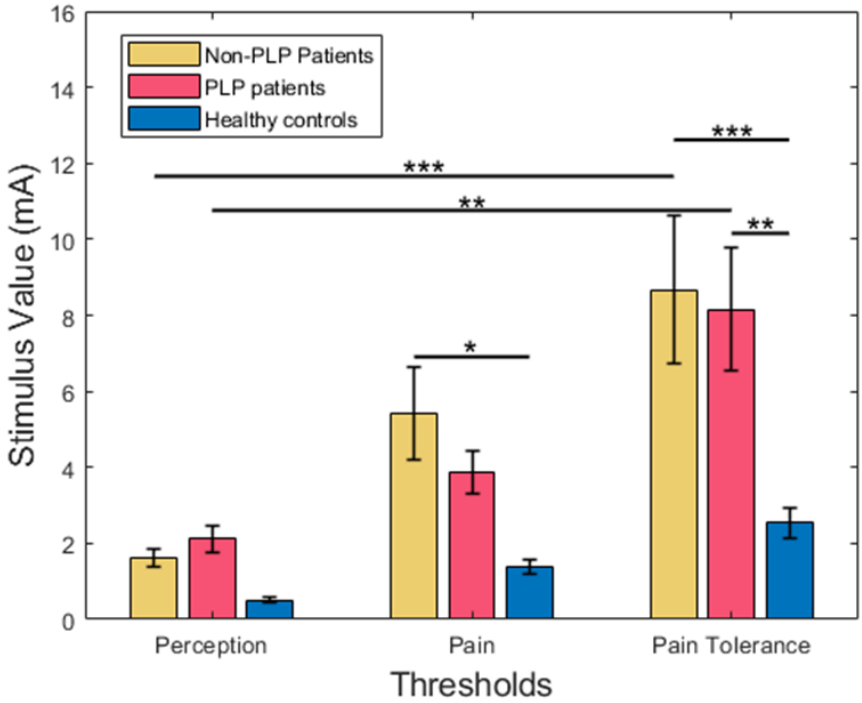

Notes: Error bars represent the standard error of the mean (SE). (=p<0.05, **=p<0.01 and ***=p<0.001).*

(2) Stimulation intensities

Descriptive statistics of stimulus values over the three stimulation thresholds, four different body sites and the three groups are presented in Table B-S24. The three-way ANOVA with stimulation intensities as a dependent variable, based on a total of 25 observations, revealed significant main effects of stimulation modality (non-painful vs.

painful) and group (the non-PLP, PLP patient group and the healthy control group) (stimulation modality: $F_1 = 14.6$, $p < 0.001$; group: $F_2 = 13.9$, $p < 0.001$), and there was no significant interaction effect among the three factors. See the table B-9 for the details. Post-hoc Tukey test revealed that the painful stimulation intensities in the healthy control group were significantly smaller than those in the non-PLP patient and PLP patient group. The painful stimulation intensities were significantly higher than the non-painful stimulation intensities in non-PLP patient group. See the figure B-12. See the table B-S25 for the detailed information.

Table B-9

Table for stimulation intensities. Three-way analysis of variance (ANOVA) with factors body site, modality, group.

Source	df	SS	MS	F	*p*
Modality	1	389.4	389.4	14.6	<0.001*
Body site	3	148.5	49.5	1.9	0.138
Group	2	741.2	370.6	13.9	<0.001*
Body site x modality	3	50.6	16.9	0.6	0.594
Modality x group	2	77.0	38.5	1.4	0.238
Body site x group	6	209.1	34.8	1.3	0.255
Error	164	4362.2	26.6		

*Notes: Body site: groin on the amputated side, groin on the non-amputation side, knee on the amputated side, knee on the non-amputation side; Modality: painful and non-painful stimulation; Group: non-PLP patient group, PLP patient group and healthy control group; df: degree of freedom; SS: Sum of Squares; MS: Mean Square; F: F-statistic; p: p-value; *=p<0.05.*

Figure B-12

Bar plots showing the mean stimulation value across stimulation modalities.

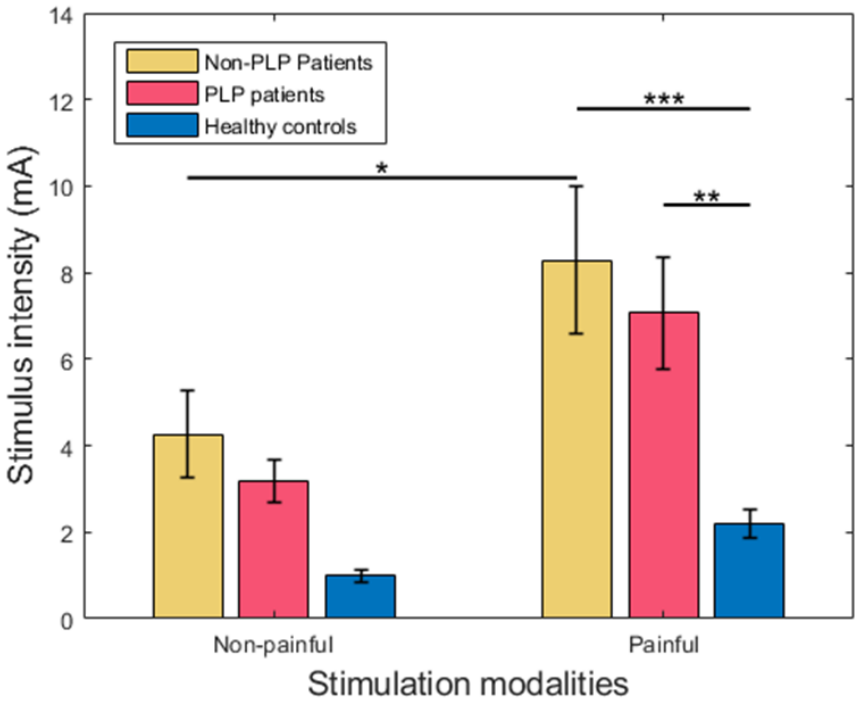

Notes: Error bars represent the standard error of the mean (SE). (=p<0.05, **=p<0.01 and ***=p<0.001).*

(4) Global cortical hemodynamic response

Descriptive statistics of the mean change in HbO2 and HbR concentration over the two groups, the two stimulation modalities and the four body sites are represented in Table B-S26 and S28. The three way ANOVA of the mean change in HbO2 concentration, with a total of 25 observations, showed a significant main effect of body site (groin on the amputation side, groin on the non-amputation site, knee on the amputation side and knee on the non-amputation side), a significantly main effect of stimulation modality (painful vs. non-painful) and significantly main effect of group (the PLP patient group, the non-PLP patient group, the healthy control group), (body site: $F_3 = 4.6$, $p = 0.003$; stimulation modality: $F_1 = 9.0$, $p = 0.003$; group: $F_2 = 40.4$, $p < 0.001$) (see Table B-10). There was a significant interaction effect among these three factors ($F_6 = 4.5$, $p < 0.001$). Post-hoc Tukey test revealed that, under non-painful stimulation applied to the groin on the amputation side, the mean changes in HbO2 concentration were significantly lower in both the non-PLP patient group and the healthy control group compared to the PLP patient group. See the figure B-13. See the table B-S27 for the detailed information.

The three way ANOVA of the mean change in HbR concentration, with a total of 25 observations, showed a significant main effect of group (the PLP patient group, the non-PLP patient group, the healthy control group), (group: $F_2 = 67.3$, $p < 0.001$) (see

Table B-11). There was a significant interaction effect among these three factors (F_6 = 3.3, p = 0.003). Post-hoc Tukey test showed that, under painful stimulation applied to the groin and knee on the amputation side, the mean changes in HbR concentration were significantly lower in the non-PLP patient group and the healthy control group compared to the PLP patient group. See the figure B-14. See the table B-S29 for the detailed information.

Table B-10

Table for the mean change in oxyhemoglobin concentration. Three-way analysis of variance (ANOVA) with factors body site, stimulation modality, group.

Source	df	SS	MS	F	*P*
Body site	3	0.06	0.02	4.6	0.003*
Modality	1	0.03	0.03	9.0	0.003*
Group	2	0.35	0.18	40.4	<0.001*
Body site x modality	3	0.02	0.01	2.1	0.101
Body site x group	6	0.24	0.04	9.3	<0.001*
Modality x group	2	0.03	0.02	4.0	0.020*
Body site x modality x group	6	0.11	0.02	4.5	<0.001*
Error	2831	12.40	0.00		

*Notes: Body site: groin on the amputated side, groin on the non-amputation side, knee on the amputated side, knee on the non-amputation side; Modality: painful and non-painful stimulation; Group: non-PLP patient group, PLP patient group and healthy control group; df: degree of freedom; SS: Sum of Squares; MS: Mean Square; F: F-statistic; p: p-value; *=p<0.05.*

Figure B-13

Bar plots showing the mean change in oxyhemoglobin concentration of across group, stimulation modality and body site.

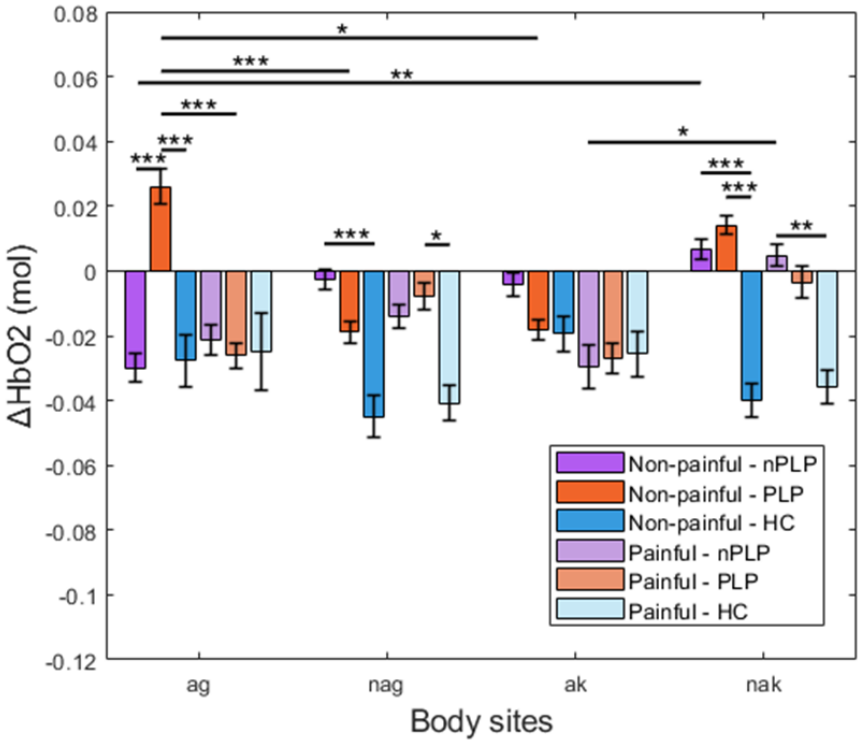

*Notes: Error bars represent the standard error of the mean (SE). (ag: groin on the amputated side; nag: groin on the non-amputation side; ak: knee on the amputated side; nak: knee on the non-amputation side; nPLP: non-phantom limb pain patient group; PLP: phantom limb pain patient group; HC: healthy control group; *=p<0.05, **=p<0.01, ***=p<0.001).*

Table B-11

Table for the mean change in deoxyhemoglobin concentration. Three-way analysis of variance (ANOVA) with factors body site, stimulation modality, group.

Source	df	SS	MS	F	*P*
Body site	3	<0.01	<0.01	0.4	0.775
Modality	1	<0.01	<0.01	0.9	0.347
Group	2	0.05	0.02	67.3	<0.001*
Body site x modality	3	0.02	0.01	16.8	<0.001*
Body site x group	6	0.02	<0.01	11.9	<0.001*
Modality x group	2	<0.01	<0.01	3.1	0.044*
Body site x modality x group	6	0.01	<0.01	3.3	0.003*
Error	2831	0.97	<0.01		

*Notes: Body site: groin on the amputated side, groin on the non-amputation side, knee on the amputated side, knee on the non-amputation side; Modality: painful and non-painful stimulation; Group: non-PLP patient group, PLP patient group and healthy control group; df: degree of freedom; SS: Sum of Squares; MS: Mean Square; F: F-statistic; p: p-value; *=p<0.05.*

Figure B-14

Bar plots showing the mean change in deoxyhemoglobin concentration of across group, stimulation modality and body site.

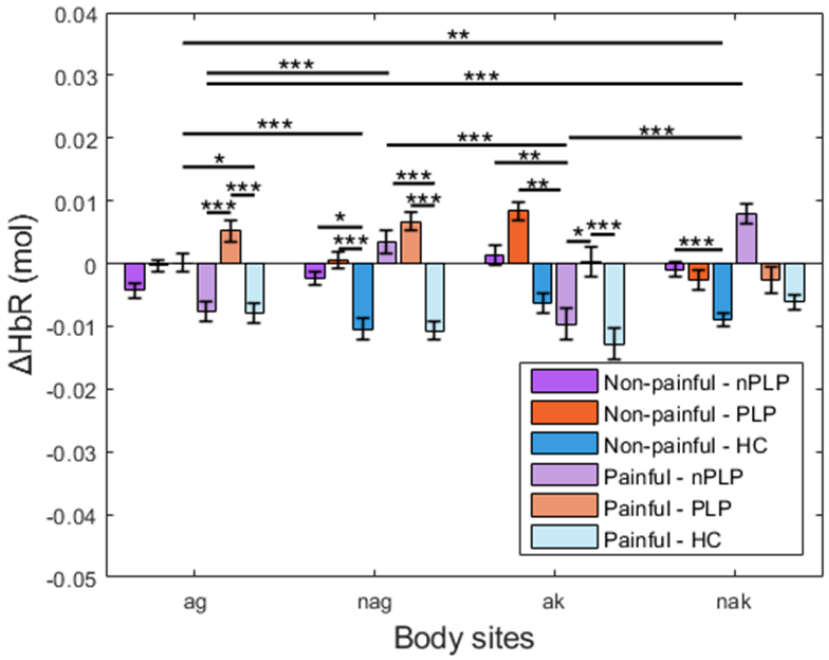

*Notes: Error bars represent the standard error of the mean (SE). (ag: groin on the amputated side; nag: groin on the non-amputation side; ak: knee on the amputated side; nak: knee on the non-amputation side; nPLP: non-phantom limb pain patient group; PLP: phantom limb pain patient group; HC: healthy control group; *=p<0.05, **=p<0.01, ***=p<0.001).*

(5) Regional cortical hemodynamic response

After FDR correction, one-way ANOVA revealed that, under painful stimulation of the non-amputated side knee, the non-PLP patient group showed significantly greater mean changes in HbR concentration in the ipsilateral frontal cortex (IF; p = 0.004) and contralateral fronto-central cortex (CFC; p = 0.002) compared to both the PLP group and healthy controls (see Figure B-15). These results are detailed in Table B-S30. No other significant between-group differences were observed across brain regions or stimulation conditions (see Supplementary Tables B-31 to B-37 and Figure B-8 – B-14).

Figure B-15

Between-group comparisons of hemoglobin concentration changes across cortical regions under non-amputation side knee painful stimulation.

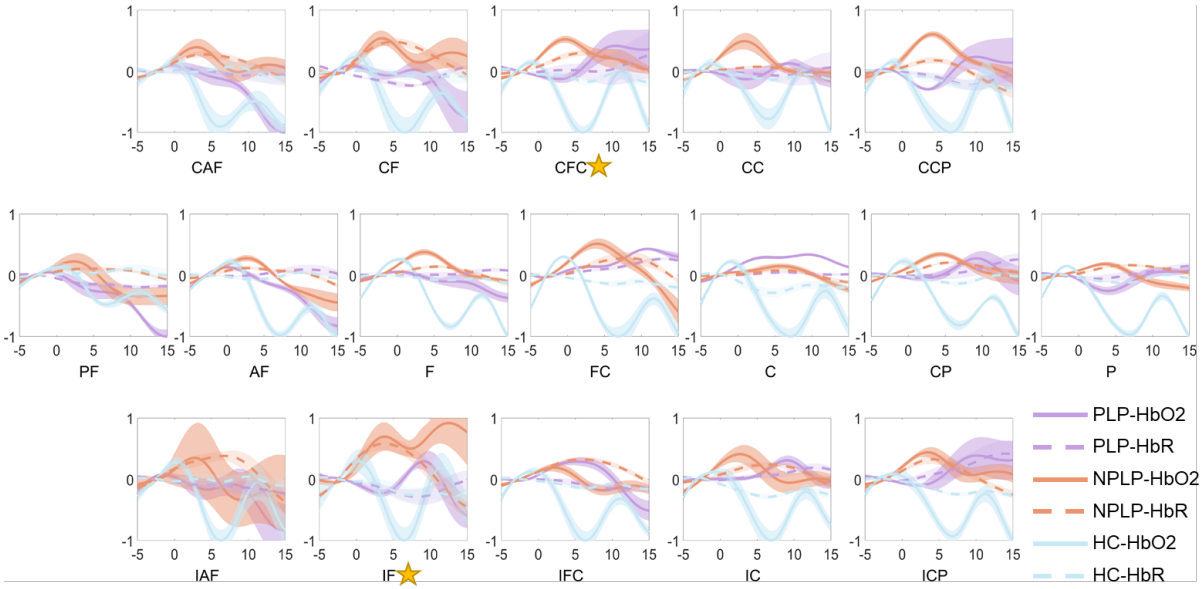

Notes: PF: fronto-polar area; AF: anterior frontal area; IAF: ipsilateral anterior frontal area; CAF: contralateral anterior frontal area; F: frontal area; IF: ipsilateral frontal area; CF: contralateral frontal area; FC: fronto-central area; IFC: ipsilateral fronto-central area; CFC: contralateral fronto-central area; C: central area; IC: ipsilateral central area; CC: contralateral central area; CP: centro-parietal area; ICP: ipsilateral centro-parietal area; CCP: contralateral centro-parietal area; P: parietal area; HC: healthy control group; NPLP: non-phantom limb pain patient group; PLP: phantom limb pain patient group; HbO2: oxyhemoglobin; HbR: deoxyhemoglobin. The x-axis represents time (in seconds), and the y-axis represents normalized changes in hemoglobin concentration (range: -1 to 1). Yellow stars indicate significant between-group differences in HbR concentration after FDR correction.

4 DISCUSSION

4.1 Study 1

This study examined changes in oxyhemoglobin levels in the cerebral cortex when healthy persons were subjected to painful and non-painful stimuli administered at four lower extremity sites using fNIRS. We found that there was no significant main effect of body sites and stimulation modalities on oxyhemoglobin activity. However, brain regions and the interaction between body sites, stimulation modalities, and brain regions significantly influenced oxyhemoglobin activity. Specifically, painful stimulation of the left groin resulted in deactivation of the PFC and the bilateral S1 compared to non-painful stimulation. In contrast, painful stimulation of the right knee induced activation of these regions compared to non-painful stimulation. Additionally, we also observed differences in perception of electrical stimulation across four different body sites.

The repeated-measures ANOVA of the β values revealed that there was no significant main effect of stimulation across different body sites on oxyhemoglobin activity, aligning with our hypothesis. This result may be attributed to the adjacency of cortical projections for the bilateral groin and knees within S1, as well as the relatively small cortical representation of these lower limb regions (Penfield, 1937). Due to the spatial limitations of fNIRS, it is possible that the method was unable to detect significant differences in sensory cortical activation associated with stimulation of distinct lower limb regions. Additionally, we also found that the different levels of stimulation modality (painful and non-painful) did not significantly affect oxygenated hemodynamic activity, while the pattern of the oxygenated hemodynamic activity significantly depended on observed brain regions. From the supplement Table A-S7, it is evident that the β values of right S1 were higher than the β values of PFC. This phenomenon may be attributed to the specialization of the right hemisphere in the regulation of emotional and pain processing (Duerden & Albanese, 2013), as well as the complexity of the PFC in interpreting sensory stimuli. These aspects will be clarified in the following discussion. Interestingly, the interaction between body sites, stimulation modalities, and brain regions significantly influenced oxygenated hemodynamic responses. This suggests that the combination of these factors exerts a complex modulatory effect on oxyhemoglobin activity, with the impact of different body sites potentially varying

depending on the brain region and stimulation intensity. Consistent with the objectives of this study, the primary focus was on the differences in regional brain activation under painful and non-painful stimulation intensities. From the post-hoc tests, we observed that the PFC exhibited deactivation during painful stimulation compared to non-painful stimulation when electrical stimulation was applied to the left groin. This finding is in line with previous brain imaging studies. For instance, In an fMRI study, Kong et al. (2010). reported that high thermal pain stimulation applied to the right forearm of healthy persons induced bilateral deactivation of the medial prefrontal cortex. In an fNIRS study, Yücel et al. (2015) found that both acute electrical noxious and innocuous stimuli applied to the left thumb of healthy participants led to a significant decrease in HbO2 concentration in the superior and middle frontal gyrus. The deactivation was stronger in response to noxious stimuli, although this difference did not reach statistical significance. Similarly, our study observed deactivation in the PFC under painful stimulation, with significantly greater deactivation compared to non-painful stimulation. Notably, we also observed activation in the PFC under non-painful stimulation when the left groin was stimulated, this activation was not statistically significant. This observation may be related to the lack of subdivision of the PFC, a point we discuss in more detail later. Regarding the deactivation of this region, we can attribute it to the default mode network (DMN). The DMN comprises interactive brain areas that tend to show reduced activity when individuals are engaged in external tasks that require attention (M. E. Raichle et al., 2001). This network primarily involves the following three areas: ventromedial PFC (vmPFC), dorsomedial PFC (dmPFC), the posterior cingulate cortex (PCC), adjacent precuneus and angular gyrus (M. E. Raichle, 2015). One study demonstrated that pain-induced DMN deactivation is less pronounced when individuals shift their thoughts away from pain (Kucyi, Salomons & Davis, 2013). Another study exploring the analgesic effect of cold therapy noted that the group with negative experiences reported less pain under cold compression conditions compared to the group with positive experiences. This difference may be attributed to participants in the positive experience group directing more attention to their pain, resulting in the deactivation of the inferior parietal lobule (Choi et al., 2022). Based on these observations, it is plausible to infer that as subjects receive different levels of electrical stimulation, higher stimulation intensities may lead to increased attention to pain, consequently resulting in more pronounced prefrontal cortex deactivation in the central region. Although no statistically significant differences were observed for the right groin

and left knee, a consistent pattern is evident in Fig. A-6 (b), which aligns with the significant findings from the left groin. Surprisingly, the results of stimulating the right knee in this study contradicted the hypothesis, revealing that prefrontal deactivation was more pronounced during non-painful stimulation. However, as shown in Fig. A-6 (a), deactivation appeared to be focused more in the central part of the PFC, while activation appeared to be more lateralized in the PFC during painful stimulation compared to the non-stimulation periods at this site. This observation would suggest that a finer subdivision of the PFC cortical surface in more targeted regions of interest. In an fMRI study, similar results were observed, indicating that individual differences in PFC activation during thermal stimulation of the lower leg in healthy individuals were localized near the lateral aspect of the superior frontal gyrus (Coghill et al., 2003). We can attribute this result to the regulation of the salience network (SN). The SN is a large-scale network in the human brain involved in detecting and filtering significant stimuli, as well as engaging related functional networks. It integrates sensory, emotional, and cognitive information for various complex functions, including communication and self-awareness (Menon & Uddin, 2010; Peters et al., 2016). Consequently, when exposed to painful stimulation, the SN potentially establishes a functional pathway for interaction between the lateral PFC and the “somatosensory network”, enabling their participation in sensory detection, as well as higher-level integration and regulatory processes (Peng et al., 2018). The outcomes of this study underscore the pivotal role of the prefrontal lobe in pain processing, suggesting that distinct regions within the prefrontal lobe exert varying regulatory influences on pain and sensory stimulation.

Interestingly, compared to non-painful stimulation, different lower limb regions revealed contrasting activation patterns in the bilateral S1 cortex under the painful stimulation. In detail, when right knee painful stimulation was administered, the neuro-metabolic activity of this brain region was significantly higher than that observed during non-painful stimulation. In contrast, the neuro-metabolic activity of the bilateral S1cortex was significantly lower during painful stimulation of the left groin compared to non-painful stimulation. The same activity pattern was observed in right S1 when painful stimulation was applied to the right groin. A prior meta-analytic study highlighted the activation of the sensory cortex in response to painful stimuli, employing various imaging modalities (Apkarian et al., 2005). Furthermore, it was observed that the S1 cortex predominantly processes signals of pain (Vierck et al., 2013). These could

explain the observations when stimulating the right knee, but the results for the groin contradict these results. Although research on this specific site is limited, our further discussion of stimulation intensities across various body sites suggests that anatomical distinctions between the groin and knee may contribute to this outcome. Another study involving 15 healthy participants suggested that experimental groin pain may encompass the lower abdomen (Drew et al., 2017). Consequently, we can hypothesize that the distribution and conduction of pain in response to painful stimuli differ between the groin and the knee, leading to reduced sensory cortex activation during painful stimulation. Additionally, it is important to note that the observed differences in activity patterns do not directly reflect the effect of stimulation at different body sites globally, instead they reflect the specific interaction effect. Therefore, further research is needed to elucidate the underlying mechanism.

In this study, it is evident that the stimulation intensity applied to the left groin was significantly higher than the one applied to the bilateral knees, indicating lower sensitivity to electrical stimulation at this body site. In the process of determining appropriate intensities for both painful and non-painful stimuli, we aimed to adjust stimulation intensities to elicit comparable perceived intensities across body sites. However, owing to the variability inherent in VAS ratings, our results revealed significant differences in the main effect across stimulated body sites when perception was assessed before and after the stimulation modality using the same VAS scale. Nevertheless, in the outcomes after multiple comparisons correction, no significant differences were observed among the four distinct body sites. Noteworthy, we observed a trend towards significance for higher ratings for the left knee in comparison to the right groin. One plausible explanation for these observations is that the knees exhibit a higher sensitivity compared to the groins. We assume that these differences may be attributed to variations in the related physiological and anatomical structures. The knee area contains a high concentration of nerve endings and a denser population of sensory neurons, rendering it more susceptible to irritation (Horner & Dellon, 1994). Additionally, nerves such as the femoral nerve, carry both sensory and motor signals and innervates the groin, front of the thigh, and knee regions. Specifically, the anterior branch of the femoral nerve, responsible for sensory innervation, supplies the anterior medial skin regions of the distal thigh and the knee, may play a role in this sensitivity (Kampitak et al., 2021). Therefore, we hypothesize that when stimulating the knee, due to the broader distribution of nerves in the knee area, including some passing through

the groin region, we observe increased sensitivity in the knee. However, this increased sensitivity does not imply a difference in pain perception between the left and right knee. Additionally, in our study, we did not specifically hypothesize a lateral difference in sensitivity, and the absence of such a difference in reported stimulation perception may be attributed to the balanced experimental design, which randomized the order of stimulation.

This study has several limitations that should be acknowledged: (1) Limited age group: the participants recruited for this study were predominantly young individuals, averaging around 24 years of age. As a result, caution should be exercised when generalizing the findings of this study to different age groups. Additionally, we did not conduct a power calculation prior to recruitment. However, an a posteriori analysis indicated that our sample size of 16 participants provided approximately 80% power to detect large effect sizes (Cohen's d=0.8) and around 50% power to detect medium effect sizes (Cohen's d=0.5) at a significance level of 0.05. Future studies should conduct a power calculation prior to recruitment to ensure sufficient sample sizes. (2) Simplified analysis of fNIRS data: The analysis of our fNIRS data primarily relied on statistical analysis centered on beta values, focusing on spatial activation patterns. While this approach provides valuable insights, future research could benefit from incorporating time domain analysis techniques to delve deeper into cortical activation patterns and potential habituation effects when stimulating various lower limb regions. (3) Low spatial resolution: Given the spatial resolution limitations of fNIRS, the regional division method employed in this study and the use of average beta values may dilute localized effects and potentially reduce the overall effect. Future studies could address this issue by adopting finer regional divisions based on the framework established in this study or by focusing on representative individual channels for analysis. On the other hand, a channel-wise analysis of the hemodynamic responses would require additional measures to mitigate the risk of type I errors. (4) HbR concentration changes: The results obtained using the changes in concentration of HbR were not entirely consistent with those obtained with HbO2. The differences appear to rely on the biophysical modelling of the hemodynamic response of the two measures, which captures the two interconnected neuro-metabolic phenomena with different levels of sensitivity. Although an optimization of the HbR hemodynamic response would be required, this type of sensitivity analysis would entail additional investigations which are out of the scope of the present study. Nonetheless, this does not limit the validity

of the statistical inference carried out using HbO2 data. (5) Exclusion of scalp hemodynamics: given the scarcity of prior studies focusing on lower limb regions and the limitations of fNIRS monitoring depth, this study aimed to capture hemodynamics across the entire cortex of interest. Therefore, we did not employ short separation channels to monitor scalp hemodynamics. In future experiments, incorporating this technique could help mitigate the potential impact of painful stimulation on hemodynamics in the target cortex. These limitations provide valuable insights into areas for potential refinement and expansion in future research endeavors.

In summary, our study demonstrates that stimulation at different lower limb regions does not significantly affect brain oxygen hemodynamic activity in healthy subjects subjected to acute electrical stimulation. However, the interaction of various factors, including stimulation site and intensity, plays a role in modulating brain activity, resulting in different activity patterns under specific stimulation modalities. This could be related to the brain activity of distinct regions within the PFC in response to painful stimulation, as well as the differential distribution and conduction of pain to the groin and knee. Additionally, our findings suggest that the knee exhibits greater sensitivity to sensory stimulation than the left groin. Consequently, our study contributes valuable evidence regarding the modulation of pain perception at the cortical level. Furthermore, it underscores the potential and feasibility of employing fNIRS to investigate pain mechanisms across diverse lower limb areas.

4.2 Study 2

Similarly to Study 1, this study aimed at comparing cortical hemodynamic response between pre-amputation patients and healthy controls in response to painful and non-painful electrical stimulation applied to different lower limb sites. In addition, perception threshold, pain threshold, and pain tolerance were assessed and compared between the two groups. Furthermore, based on postoperative outcomes, patients were subdivided into those who developed PLP and those who did not. By comparing these subgroups with healthy controls, the study sought to identify potential neural predictors of PLP prior to amputation.

The three-way ANOVA of the mean changes in HbO2 concentration revealed significant main effects of stimulation body sites, stimulation modalities, and groups. Regarding the interaction between groups and stimulation modalities, both painful and

non-painful electrical stimulation elicited an overall deactivation pattern, as reflected by decreased HbO2 levels. However, this decrease was less pronounced in the patient group compared to the healthy controls. Additionally, the ANOVA results for HbR showed that, under both painful and non-painful stimulation, the patient group exhibited significantly greater changes in HbR concentration than the control group. Notably, a significant three-way interaction was observed, with the most significant difference occurring under painful stimulation, with the patient group showing significantly higher HbR changes compared with the healthy control group, regardless of which lower limb site was stimulated. These findings, combined with the hemodynamic responses in each brain region (Figures B-8, B-9, B-S2-B-S7), may indicate that, prior to amputation, patients exhibited impaired neurovascular coupling (NVC) in response to external stimuli, as reflected by the reduced hemodynamic responses in the cortex and the increased oxygen demand during painful stimulation compared to healthy controls. Indeed, the patients in this study underwent amputation due to occlusive arterial disease, with 66.7% also diagnosed with diabetes mellitus. Existing studies have shown that NVC is impaired to varying degrees in both diabetic patients and those with peripheral arterial disease (PAD). For example, a cross-sectional study using fMRI to measure blood oxygen level-dependent responses to visuomotor stimulation in patients with early-stage diabetes found alterations in the hemodynamic response function, indicating impaired neurovascular coupling in the brain of diabetic patients (Duarte et al., 2015). In another study involving 11 PAD patients and 11 age- and sex-matched healthy controls, fNIRS was used to assess NVC responses during a cognitive task (Owens et al., 2022). The results revealed a positive correlation between participants' microvascular endothelial function, neurovascular endothelial responses, and cognitive performance. Furthermore, PAD patients exhibited significantly impaired neurovascular endothelial responses and peripheral microvascular endothelial function compared to healthy controls. Diabetes mellitus can induce widespread structural and functional abnormalities in the cerebral microvasculature, including endothelial dysfunction, increased capillary permeability, impaired integrity of the blood–brain barrier, and reduced capacity for cerebral autoregulation (Feng & Gao, 2024; Starr et al., 2003; Yang et al., 2024). Lower extremity occlusive arterial disease is also associated with reduced blood flow and impaired tissue perfusion (Normahani et al., 2021). Therefore, considering the long-term effects of these two diseases on both systemic and cerebral vascular systems, patients may already exhibit underlying

impairments in neural regulation and cerebral blood flow even before amputation. These alterations interfere with neurovascular responses to neuronal activity, thereby attenuating the magnitude of stimulus-evoked changes in HbO2 concentrations. Moreover, an animal study demonstrated that, compared to the neocortex, the hippocampus exhibits lower blood flow, reduced oxygen saturation, and diminished neurovascular coupling. Oxygen diffusion modeling further indicated that these structural and functional characteristics limit oxygen availability, rendering the hippocampus highly susceptible to hypoxic conditions. Under insufficient oxygen supply, increased metabolic demand leads to enhanced oxygen extraction, reflected by a relative increase in HbR concentration (Shaw et al., 2021). Consistent with these findings, our study observed a more pronounced HbR increase in patients during non-painful stimulation, suggesting that even under low-demand conditions, cortical regions fail to generate an adequate vascular response. This further supports the notion of impaired vascular reactivity and disrupted neurovascular coupling in these patients.

In this study, during painful stimulation of the right groin, patients exhibited significantly higher HbR concentrations of in the right frontal (RF) and left central (LC) regions compared to healthy controls. According to the location information of the fNIRS channels (Table B-S1), the RF region primarily corresponds to the right dorsolateral prefrontal cortex (DLPFC), while the LC region mainly covers the left primary somatosensory cortex (S1) and left motor cortex, particularly Brodmann areas 4 (BA 4) and 6 (BA 6). In neuroimaging studies, DLPFC is thought to be involved in the processing of noxious stimuli and the modulation of pain (Seminowicz & Moayedi, 2017). Although its precise role remains unclear, existing studies suggest that the DLPFC may contribute to the cognitive and emotional regulation of pain and may also be associated with pain sensitization processes (Lorenz et al., 2002, 2003; Petrovic et al., 2010). Furthermore, an fMRI study employing thermal stimulation on the dorsum of the foot revealed, through dynamic causal modeling, that the influence of the right DLPFC increased during painful stimulation, suggesting that the right DLPFC may play a more critical modulatory role in pain processing (Sevel et al., 2016). In addition, as discussed in study 1, the S1 cortex plays an important role in pain processing. BA 4 and 6 are traditionally known for their involvement in voluntary motor execution and the planning and coordination of complex movements (Donoghue & Sanes, 1994; Manthey et al., 2003; Sharma et al., 2008). However, many studies suggest that these

motor cortices are also closely linked to pain processing. For example, a quantitative EEG study on focused muscle contraction therapy found abnormal baseline activity in BA 4 and 9, after six months of treatment, none of the participants exhibited clinically significant activity in these areas, suggesting a potential association between BA 4 and chronic pain (N. Cohen et al., 2022). Furthermore, another study have shown that BA 6 is activated by various noxious stimuli, and in most experimental paradigms, the BA 6 responds to pain bilaterally (Casey, 1999). Moreover, previous studies have indicated that pain processing involves a widely distributed and bilaterally engaged neural network, including bilateral regions such as the cerebellum, thalamus, insula, anterior cingulate cortex, and secondary somatosensory cortex, as well as the contralateral S1 and supplementary motor area (SMA) (Coghill et al., 1999). However, in the present study, during painful stimulation of the right groin, a significant increase in HbR concentration was observed only in the left sensorimotor cortex of patients compared to healthy controls, with no significant changes detected on the right side. Additionally, during non-painful stimulation of the right knee, patients showed a higher mean HbR concentration in the right centro-parietal region, which primarily includes the S1 cortex, compared to healthy controls. These findings suggest that although pain processing generally involves integration across multiple brain regions, the DLPFC and S1 cortex may play a more prominent role in pain modulation in patients awaiting lower limb amputation. It is noteworthy that no corresponding significant findings were observed at the HbO2 level in this study. This may be attributable to impaired neurovascular coupling in these patients. The pain stimulation increases the brain's oxygen demand; however, reduced cerebral blood flow in patients may compromise compensatory mechanisms, leading to elevated HbR concentrations without corresponding changes in HbO2 signals (Hoshi et al., 2001b). Interestingly, this study did not observe significant differences across brain regions during stimulation of the left groin and left knee. This finding is inconsistent with previous studies, particularly considering that all participants included in the statistical analysis were right-handed. Prior research, by applying different levels of sensory stimulation on/near the left and right hands, found that for right-handed people, subjective pain perception and brain activation to painful stimuli were more easily detected when the non-dominant hand of the body (left side) was stimulated compared to the dominant hand (right side) (H. Zhang et al., 2021). However, studies specifically investigating pain in the groin and knee regions remain limited. Notably, the patients in the present study were unique in

that they reported pain corresponding to their planned amputation sites. Therefore, the cortical mechanisms underlying pain processing in patients awaiting amputation still need further investigation.

According to the demographic information, patients exhibited significantly higher scores in pain severity on the MPI scale compared to healthy controls. Most patients reported pain predominantly localized to the limb or region scheduled for amputation, which is likely related to their underlying condition. Severe PAD can present as critical limb ischemia, typically characterized by rest pain and/or ischemic skin lesions such as gangrene or ulcers (Behroozian & Beckman, 2020). Rest pain often occurs at night or when lying down, manifesting as persistent pain in the foot, indicating severe tissue hypoxia due to inadequate blood supply (Ouriel, 2001b). In patients with diabetes, ischemic pain caused by arterial insufficiency is often accompanied by peripheral neuropathy, which can further intensify pain perception or lead to sensory disturbances (Ram et al., 1991). Studies have shown that PAD in individuals with diabetes is more likely to progress to severe ischemia, chronic ulcers, and infections, significantly increasing the risk of amputation (Barnes et al., 2020; Lang et al., 2006). Interestingly, the results from both stimulation thresholds and stimulation intensity assessments showed that patients exhibited a notably higher pain tolerance compared to healthy controls. The painful stimulation intensities used in fNIRS measurements were also significantly higher for the patient group. A similar study employing electrical stimulation found that diabetic patients, especially those with neuropathy, demonstrated significantly higher pain thresholds and tolerance in both upper and lower limbs, suggesting a blunted response to painful stimuli (Telli & Cavlak, 2006). This aligns broadly with our findings; although no statistically significant difference was observed between groups in our study, the average pain threshold in patients was still higher than that in healthy controls. This may be related to structural, metabolic, and functional abnormalities in peripheral nerves and/or limited statistical power due to the small sample size. PAD can lead to chronic ischemia of the lower limbs, resulting in prolonged insufficient blood supply to nerve tissue, which in turn causes nerve fiber degeneration, demyelination, and axonal damage (McDermott et al., 2006). Clinically, this manifests as sensory loss, pain, numbness, and other symptoms of peripheral neuropathy. Diabetic neuropathy often coexists with PAD, further reducing pain sensitivity and leading patients to overlook early ischemic symptoms (Petropoulos et al., 2010). As a result, medical attention is often only sought after severe complications

have developed, ultimately increasing the risk of amputation. In addition, diabetic peripheral neuropathy is frequently characterized by reduced nerve conduction velocity, sensory abnormalities, and either painful or painless ulcers (P. Sun et al., 2015). Chronic hyperglycemia in diabetes can also trigger microvascular complications, impairing blood supply to nerves and causing further nerve tissue damage (Di Carli et al., 2003; Jonas et al., 1999). Additionally, this study did not reveal any significant differences in VAS scores across different time points during the experiment, suggesting that the participants did not exhibit habituation to the stimuli.

In this study, we further explored the differences among the PLP group, the non-PLP group, and healthy controls in terms of basic characteristics, stimulation thresholds, stimulation intensities used during the experiment, and cortical responses to painful and non-painful stimuli applied to different lower limb regions prior to amputation. Consistent with previous findings, the primary differences in stimulation thresholds and stimulus intensities were observed between patients and healthy controls. There is no difference between the PLP groups and the non-PLP group. However, it is noteworthy that even before amputation, the PLP group showed significantly different cortical responses to both painful and non-painful stimuli compared to the non-PLP group and healthy controls. In detail, during non-painful stimulation of the groin on the side to be amputated, HbO2 levels in the PLP group were significantly higher than those in the other two groups. Moreover, during painful stimulation of both the groin and the knee on the amputation side, HbR levels in the PLP group were markedly increased. These findings indicate that patients who later developed PLP may have exhibited enhanced cortical activation prior to amputation. Based on previous research into the mechanisms underlying PLP, we hypothesize that the phenomena observed in this study may be associated with preoperative central excitability in patients who later developed PLP. A systematic review has indicated that PLP patients often exhibit hyperexcitability in the cerebral cortex, particularly in the sensorimotor areas, and such cortical excitability changes are considered one of the key central mechanisms contributing to the development of PLP (Garcia-Pallero et al., 2022). PLP is associated with maladaptive reorganization of the sensorimotor cortex, reflected in impaired intracortical inhibition and an altered balance of inhibitory and excitatory neurotransmitters such as gamma-aminobutyric acid and glutamate, resulting in heightened corticospinal excitability (Akhlaghdoust *et al*., 2023). Additionally, another systematic review focusing on the use of repetitive transcranial magnetic stimulation

for the treatment of PLP suggests that repetitive transcranial magnetic stimulation can alleviate both painful and non-painful phantom phenomena by affecting cortical excitability, with stimulation of the contralateral parietal or motor cortex showing significant clinical improvement in PLP symptoms (Nardone et al., 2019b). However, these studies have been conducted exclusively in post-amputation populations, and there is currently a lack of sufficient pre-amputation neuroimaging evidence to support the findings of the present study. Therefore, our hypothesis remains preliminary and requires further investigation. Moreover, in our exploratory analysis of different cortical regions, we found that only during painful stimulation of the knee of the non-amputated side did the non-PLP group show significantly greater average HbR changes in the ipsilateral frontal and contralateral fronto-central regions compared to both the PLP and healthy control groups. No significant differences were observed in response to stimulation on the amputated side, making it difficult to further interpret the findings observed at the global level. This may be partly attributable to the small sample size and large inter-individual variability in our study. Future studies with larger sample sizes and prospective neuroimaging designs are warranted to further explore whether patients with PLP already have altered cortical function prior to amputation.

Despite the preliminary findings of this study in revealing differences between lower limb amputees and healthy controls, as well as providing initial evidence for a potential association between pre-amputation cortical activity and the subsequent development of PLP, several limitations should be acknowledged and addressed in future research. First, the relatively small sample size in this study, particularly in subgroup analyses between PLP and non-PLP patients, may have limited the statistical power and increased susceptibility to individual variability. In addition, due to the specific nature of the patient population, recruitment and experimental procedures posed practical challenges, and some participants were unable to complete measurements at all designated body sites. Future studies could refine the experimental design based on these findings to improve data completeness and comparability. Second, this study employed a cross-sectional design, assessing only pre-amputation neuroimaging features; thus, causal inferences between cortical changes and PLP onset cannot be drawn. Longitudinal studies with postoperative follow-ups are warranted to validate the proposed mechanisms. Moreover, detailed medical information regarding patients' underlying conditions (e.g., diabetes, arteriosclerosis) was not included in this study, making it difficult to assess whether the severity of these comorbidities or vascular

status contributed to the observed cortical responses. From a technical perspective, while fNIRS offers the advantages of being non-invasive and portable, it has limited spatial resolution and insufficient penetration depth, which may restrict its ability to capture activity in deeper brain structures involved in pain processing. Future studies can build on this study and combine fMRI or other brain imaging equipment to explore the brain activity of lower limb amputees before amputation. Finally, due to the generally poor physical condition of the patients before amputation and the limited time to participate in the experiment, most patients were unable to participate in psychological assessments during the experimental phase. Therefore, this study did not systematically evaluate or control for psychological variables such as anxiety and depression, although these factors may influence pain perception, cortical activation and occurrence of PLP. Future research should aim to expand the sample size, optimize the study design, and incorporate comprehensive clinical, behavioral, and psychological assessments to more fully elucidate the central mechanisms of PLP and identify potential preoperative predictors.

In summary, this study investigated pain perception and cortical functional characteristics in lower limb amputees prior to surgery, and further analyzed their potential association with the development of post-amputation PLP. The results showed that amputees exhibited higher pain tolerance and painful stimulation intensity before the amputation, which may be related to peripheral nerve damage caused by the underlying disease. Meanwhile, cortical functional alterations suggested that neurovascular coupling might be impaired in the patient group. The DLPFC and sensorimotor cortex may play a more prominent role in pain modulation in patients awaiting lower limb amputation. Further subgroup analysis indicated that the occurrence of PLP might be associated with preoperative central excitability; however, the underlying mechanisms require further elucidation. This study provides preliminary clues for predicting the relationship between cerebral cortical changes and PLP formation in patients with lower limb amputation before amputation. At the same time, the results also provide new evidence for the possible reduced cerebral blood flow and abnormal neurovascular coupling function in patients with occlusive vascular disease. In addition, this study further verifies the potential application of fNIRS in exploring the mechanism of lower limb amputation and PLP.

4.3 Conclusion

These two studies employed fNIRS to systematically investigate cortical responses to electrical stimulation applied to the lower limbs, extending the scope from healthy individuals to lower limb amputees. The primary aim was to explore the preoperative cortical functional characteristics and their potential association with the development of PLP after amputation.

In healthy participants, although electrical stimulation at different lower limb sites did not elicit significant differences in cortical hemodynamic responses, the significant interactions were observed among stimulation site, stimulation modality, and brain region. Additionally, the perceived stimulation intensity at the knees was significantly lower than that at the groin. These findings suggest that pain processing in the brain is modulated by multiple factors. Specifically, compared to non-painful stimulation, neuro-metabolic activity in the prefrontal and bilateral primary somatosensory cortices decreased with painful stimulation of the left groin, whereas neuro-metabolic activity increased with painful stimulation of the right knee. These findings highlight the potential and feasibility of using fNIRS to study pain mechanisms associated with stimulation of different lower limb regions. Therefore, these results lay an important foundation for subsequent clinical investigations.

In the clinical cohort, amputees exhibited higher pain tolerance and higher painful intensity prior to surgery, likely due to peripheral neuropathic damage caused by underlying diseases. Cortical hemodynamic responses indicated neurovascular coupling might be impaired and declined cerebral blood flow in the patient group, with the dorsolateral prefrontal cortex and sensorimotor cortex playing prominent roles during pain processing. Further subgroup analysis suggested that the abnormal increase in central excitability observed before amputation in patients who later developed PLP may have contributed to its onset. These findings offer preliminary insights for future studies aimed at preoperative prediction of PLP.

In conclusion, these two studies involving healthy individuals and lower limb amputees demonstrate the feasibility and potential of fNIRS in investigating the neural mechanisms underlying lower limb pain. Moreover, the findings provide new insights into the development of PLP, suggesting that alterations in cortical activity may already be present prior to amputation in patients who later develop PLP.

5 SUMMARY

The pathogenesis of phantom limb pain (PLP) remains a key focus in current pain research. However, investigations into cortical activity prior to amputation are still limited. The present research employed functional near-infrared spectroscopy (fNIRS) to examine cortical responses to painful and non-painful stimulation at different lower limb sites in both healthy individuals and pre-amputation patients.

Study 1 assessed 16 healthy participants and observe brain changes in oxyhemoglobin levels (HbO2) during painful and non-painful electrical stimulation of various lower limb sites. The results indicated no significant main effect of stimulation site on cortical HbO2 activity. However, significant interactions were observed among stimulation site, stimulation modality, and brain region. Specifically, painful stimulation to the left groin led to reduced neuro-metabolic activity in the prefrontal cortex and bilateral primary somatosensory cortex compared to non-painful stimulation, whereas painful stimulation to the right knee resulted in increased activity. These findings highlight the feasibility and potential of fNIRS in investigating pain mechanisms associated with stimulation of distinct lower limb regions.

Study 2 included 21 lower limb amputees and 10 healthy controls and explored differences between two groups in sensory thresholds and cortical activation patterns. Pre-amputation patients exhibited significantly higher pain tolerance thresholds, potentially due to peripheral nerve damage associated with underlying pathologies. Furthermore, compared to healthy controls, altered global hemodynamic responses in the patient group suggested impaired neurovascular coupling and reduced cerebral blood flow, with the dorsolateral prefrontal cortex and sensorimotor cortex being implicated in pain processing. Subgroup analyses revealed that patients who later developed PLP showed significantly elevated hemodynamic responses to the painful stimulation on the amputated side preoperatively, suggesting increased central excitability may contribute to PLP onset. However, the precise mechanisms remain to be fully elucidated.

Taken together, both studies emphasize the key role of cortical activity in lower limb pain processing and the impact of the interaction between different factors on hemodynamic response. These findings also demonstrate the feasibility and potential of fNIRS in investigating the neural mechanisms underlying lower limb pain.

6 REFERENCES

Aarabi, A., & Huppert, T. J. (2016). Characterization of the relative contributions from systemic physiological noise to whole-brain resting-state functional near-infrared spectroscopy data using single-channel independent component analysis. *Neurophotonics*, *3*(2), 025004. https://doi.org/10.1117/1.nph.3.2.025004

Aasted, C. M., Yücel, M. A., Steele, S. C., Peng, K., Boas, D. A., Becerra, L., & Borsook, D. (2016). Frontal lobe hemodynamic responses to painful stimulation: A potential brain marker of nociception. *PLoS ONE*, *11*(11), 1–12. https://doi.org/10.1371/journal.pone.0165226

Abbott, C. A., Malik, R. A., Van Ross, E. R. E., Kulkarni, J., & Boulton, A. J. M. (2011). Prevalence and characteristics of painful diabetic neuropathy in a large community-based diabetic population in the U.K. *Diabetes Care*, *34*(10), 2220–2224. https://doi.org/10.2337/dc11-1108

Aboud, T., Deep, A., Pryweller, J., Pasquina, P., & Tsao, J. (2018). Time Course of Onset of Phantom Pain in Male and Female Amputees (P5.334). *Neurology*, *90*(15_supplement), P5.334. https://doi.org/10.1212/WNL.90.15_supplement.P5.334

Afrasiabi, M., & Noroozian, N. (2015). Advantages and limitations of functional magnetic resonance imaging (fMRI) of the human visual brain. *Horizons in Neuroscience Research Series*, *17*, 65–72.

Ahmed, A., Bhatnagar, S., Mishra, S., Khurana, D., Joshi, S., & Ahmad, S. (2017). Prevalence of phantom limb pain, stump pain, and phantom limb sensation among the amputated cancer patients in India: A prospective, observational study. *Indian Journal of Palliative Care*, *23*(1), 24–35. https://doi.org/10.4103/0973-1075.197944

Andoh, J., Milde, C., Diers, M., Bekrater-Bodmann, R., Trojan, J., Fuchs, X., Becker, S., Desch, S., & Flor, H. (2020). Assessment of cortical reorganization and preserved function in phantom limb pain: a methodological perspective. *Scientific Reports*, *10*(1), 1–15. https://doi.org/10.1038/s41598-020-68206-9

Apkarian, A. V., Bushnell, M. C., Treede, R. D., & Zubieta, J. K. (2005). Human brain mechanisms of pain perception and regulation in health and disease. *European Journal of Pain*, *9*(4), 463. https://doi.org/10.1016/j.ejpain.2004.11.001

Arena, J. G., Sherman, R. A., Bruno, G. M., & Smith, J. D. (1990). The relationship between situational stress and phantom limb pain: cross-lagged correlational data from six month pain logs. *Journal of Psychosomatic Research*, *34*(1), 71–77.

Barnes, J. A., Eid, M. A., Creager, M. A., & Goodney, P. P. (2020). Epidemiology and risk of amputation in patients with diabetes mellitus and peripheral artery disease. *Arteriosclerosis, Thrombosis, and Vascular Biology*, *40*(8), 1808–1817. https://doi.org/10.1161/ATVBAHA.120.314595

Becerra, L., Harris, W., Joseph, D., Huppert, T., Boas, D. A., & Borsook, D. (2008). Diffuse optical tomography of pain and tactile stimulation: Activation in cortical sensory and emotional systems. *NeuroImage*, *41*(2), 252–259. https://doi.org/10.1016/j.neuroimage.2008.01.047

Behrendt, C.-A., Sigvant, B., Szeberin, Z., Beiles, B., Eldrup, N., Thomson, I. A., Venermo, M., Altreuther, M., Menyhei, G., Nordanstig, J., Clarke, M., Rieß, H. C., Björck, M., & Debus, E. S. (2018). International Variations in Amputation Practice: A VASCUNET Report. *European Journal of Vascular and Endovascular Surgery*, *56*(3), 391–399. https://doi.org/https://doi.org/10.1016/j.ejvs.2018.04.017

Behroozian, A., & Beckman, J. A. (2020). Microvascular Disease Increases Amputation in Patients With Peripheral Artery Disease. *Arteriosclerosis, Thrombosis, and Vascular Biology*, *40*(3), 534–540. https://doi.org/10.1161/ATVBAHA.119.312859

Berliner, J. A., Navab, M., Fogelman, A. M., Frank, J. S., Demer, L. L., Edwards, P. A., Watson, A. D., & Lusis, A. J. (1995). Atherosclerosis: Basic Mechanisms. *Circulation*, *91*(9), 2488–2496. https://doi.org/10.1161/01.CIR.91.9.2488

Bizzego, A., Neoh, M., Gabrieli, G., & Esposito, G. (2022). A Machine Learning Perspective on fNIRS Signal Quality Control Approaches. *IEEE Transactions on Neural Systems and Rehabilitation Engineering*, *30*, 2292–2300. https://doi.org/10.1109/TNSRE.2022.3198110

Boccia, M., Di Vita, A., Palermo, L., Nemmi, F., Traballesi, M., Brunelli, S., De Giorgi, R., Galati, G., & Guariglia, C. (2020). Neural modifications in lower limb amputation: an fMRI study on action and non-action oriented body representations. *Brain Imaging and Behavior*, *14*(2), 416–425. https://doi.org/10.1007/s11682-019-00142-3

Bolognini, N., Olgiati, E., Maravita, A., Ferraro, F., & Fregni, F. (2013). Motor and parietal cortex stimulation for phantom limb pain and sensations. *PAIN*, *154*(8). https://journals.lww.com/pain/fulltext/2013/08000/motor_and_parietal_cortex_stimulation_for_phantom.15.aspx

Bornhövd, K., Quante, M., Glauche, V., Bromm, B., Weiller, C., & Büchel, C. (2002). Painful stimuli evoke different stimulus–response functions in the amygdala, prefrontal, insula and somatosensory cortex: a single-trial fMRI study. *Brain*, *125*(6), 1326–1336. https://doi.org/10.1093/brain/awf137

Boulton, A. J. M., Malik, R. A., Arezzo, J. C., & Sosenko, J. M. (2004). *Diabetic Somatic Neuropathies*. http://diabetesjournals.org/care/article-pdf/27/6/1458/646055/zdc00604001458.pdf

Bramati, I. E., Rodrigues, E. C., Simões, E. L., Melo, B., Höfle, S., Moll, J., Lent, R., & Tovar-Moll, F. (2019). Lower limb amputees undergo long-distance plasticity in sensorimotor functional connectivity. *Scientific Reports*, *9*(1), 2518.

Buch, N. S., Qerama, E., Finnerup, N. B., & Nikolajsen, L. (2020). Neuromas and postamputation pain. *Pain*, *161*(1), 147–155.

Bushnell, M. C., Ceko, M., & Low, L. A. (2013). Cognitive and emotional control of pain and its disruption in chronic pain. *Nature Reviews. Neuroscience*, *14*(7), 502–511. https://doi.org/10.1038/nrn3516

Callaghan, B. C., Cheng, H. T., Stables, C. L., Smith, A. L., & Feldman, E. L. (2012). Review Diabetic neuropathy: clinical manifestations and current treatments. In *www.thelancet.com/neurology* (Vol. 11). www.thelancet.com/neurology

Canbolat Seyman, Cigdem, & Uzar Ozcetin, Yeter Sinem. (2021). “I Wish I Could Have My Leg”: A Qualitative Study on the Experiences of Individuals With Lower

Limb Amputation. *Clinical Nursing Research*, *31*(3), 509–518. https://doi.org/10.1177/10547738211047711

Casey, K. L. (1999). Forebrain mechanisms of nociception and pain: analysis through imaging. *Proceedings of the National Academy of Sciences*, *96*(14), 7668–7674.

Chaudhary, U., Hall, M., DeCerce, J., Rey, G., & Godavarty, A. (2011). Frontal activation and connectivity using near-infrared spectroscopy: Verbal fluency language study. *Brain Research Bulletin*, *84*(3), 197–205. https://doi.org/10.1016/j.brainresbull.2011.01.002

Chaudhary, U., Hall, M., Gonzalez, J., Elbaum, L., Bloyer, M., & Godavarty, A. (2014). Motor response investigation in individuals with cerebral palsy using near infrared spectroscopy: pilot study. *Appl. Opt.*, *53*(3), 503–510. https://doi.org/10.1364/AO.53.000503

Chen, R., Cohen, L. G., & Hallett, M. (2002). Nervous system reorganization following injury. *Neuroscience*, *111*(4), 761–773.

Chen, T. L., Babiloni, C., Ferretti, A., Perrucci, M. G., Romani, G. L., Rossini, P. M., Tartaro, A., & Del Gratta, C. (2008). Human secondary somatosensory cortex is involved in the processing of somatosensory rare stimuli: An fMRI study. *NeuroImage*, *40*(4), 1765–1771. https://doi.org/10.1016/j.neuroimage.2008.01.020

Chern, R., Corwell, B., Yaseen, Z., Hallett, M., & Cohen, L. G. (1998). Mechanisms of cortical reorganization in lower-limb amputees. *Journal of Neuroscience*, *18*(9), 3443–3450. https://doi.org/10.1523/jneurosci.18-09-03443.1998

Choi, J. C., Park, H.-J., Park, J. A., Kang, D. R., Choi, Y.-S., Choi, S., Lee, H. G., Choi, J.-H., Choi, I.-H., Yoon, M. W., Lee, J.-M., & Kim, J. (2022). The increased analgesic efficacy of cold therapy after an unsuccessful analgesic experience is associated with inferior parietal lobule activation. *Scientific Reports*, *12*(1), 14687. https://doi.org/10.1038/s41598-022-18181-0

Clarke, C., Lindsay, D. R., Pyati, S., & Buchheit, T. (2013). *Residual Limb Pain Is Not a Diagnosis A Proposed Algorithm to Classify Postamputation Pain*. www.clinicalpain.com

Coghill, R. C., McHaffie, J. G., & Yen, Y. F. (2003). Neural correlates of interindividual differences in the subjective experience of pain. *Proceedings of the National Academy of Sciences of the United States of America*, *100*(14), 8538–8542. https://doi.org/10.1073/pnas.1430684100

Coghill, R. C., Sang, C. N., Maisog, J. M., & Iadarola, M. J. (1999). *Pain Intensity Processing Within the Human Brain: A Bilateral, Distributed Mechanism*.

Cohen, J. (1988). *Statistical Power Analysis for the Behavioral Sciences (2nd ed.)*. Routledge. https://doi.org/https://doi.org/10.4324/9780203771587

Cohen, N., Hachaj, G., Rubio, J., Kastelz, A., Hachaj, M., Zierfuss, D., Osman, M., Tsiampas, P., Fernhall, B., Velis, E. V., Benedetti, E., & Bartholomew, A. (2022). *The effect of focused muscle contraction therapy on chronic pain and Brodmann Area activity in former National Football League players*. https://doi.org/10.1101/2022.03.09.22272106

Collins, K. L., Russell, H. G., Schumacher, P. J., Robinson-Freeman, K. E., O'Conor, E. C., Gibney, K. D., Yambem, O., Dykes, R. W., Waters, R. S., & Tsao, J. W. (2018). A review of current theories and treatments for phantom limb pain. *The Journal of Clinical Investigation*, *128*(6), 2168–2176.

Cui, X., Bray, S., Bryant, D. M., Glover, G. H., & Reiss, A. L. (2011a). A quantitative comparison of NIRS and fMRI across multiple cognitive tasks. *Neuroimage*, *54*(4), 2808–2821.

Cui, X., Bray, S., Bryant, D. M., Glover, G. H., & Reiss, A. L. (2011b). A quantitative comparison of NIRS and fMRI across multiple cognitive tasks. *NeuroImage*, *54*(4), 2808–2821. https://doi.org/10.1016/j.neuroimage.2010.10.069

Curtin, A., Tong, S., Sun, J., Wang, J., Onaral, B., & Ayaz, H. (2019). A systematic review of integrated functional near-infrared spectroscopy (fNIRS) and

transcranial magnetic stimulation (TMS) studies. *Frontiers in Neuroscience*, *13*, 84.

Davies, M. G. (2012). *Methodist DeBakey Cardiovascular Journal Vol. 8, No. 4*.

Demet, K., Martinet, N., Guillemin, F., Paysant, J., & André, J.-M. (2003). Health related quality of life and related factors in 539 persons with amputation of upper and lower limb. *Disability and Rehabilitation*, *25*(9), 480–486.

Di Carli, M. F., Janisse, J., Ager, J., & Grunberger, G. (2003). Role of chronic hyperglycemia in the pathogenesis of coronary microvascular dysfunction in diabetes. *Journal of the American College of Cardiology*, *41*(8), 1387–1393.

Dickinson, B. D., Head, C. A., Gitlow, S., & Osbahr III, A. J. (2010). Maldynia: Pathophysiology and Management of Neuropathic and Maladaptive Pain—A Report of the AMA Council on Science and Public Health. *Pain Medicine*, *11*(11), 1635–1653. https://doi.org/10.1111/j.1526-4637.2010.00986.x

Dillingham, T. R., Pezzin, L. E., & Shore, A. D. (2005). Reamputation, mortality, and health care costs among persons with dysvascular lower-limb amputations. *Archives of Physical Medicine and Rehabilitation*, *86*(3), 480–486. https://doi.org/https://doi.org/10.1016/j.apmr.2004.06.072

Donadel, D. G., Zortea, M., Torres, I. L. S., Fregni, F., & Caumo, W. (2021). The mapping of cortical activation by near-infrared spectroscopy might be a biomarker related to the severity of fibromyalgia symptoms. *Scientific Reports*, *11*(1), 15754.

Donoghue, J. P., & Sanes, J. N. (1994). Motor areas of the cerebral cortex. *Journal of Clinical Neurophysiology*, *11*(4), 382–396.

Drew, M. K., Palsson, T. S., Hirata, R. P., Izumi, M., Lovell, G., Welvaert, M., Chiarelli, P., Osmotherly, P. G., & Graven-Nielsen, T. (2017). Experimental pain in the groin may refer into the lower abdomen: Implications to clinical assessments. *Journal of Science and Medicine in Sport*, *20*(10), 904–909. https://doi.org/10.1016/j.jsams.2017.04.007

Duarte, J. V., Pereira, J. M. S., Quendera, B., Raimundo, M., Moreno, C., Gomes, L., Carrilho, F., & Castelo-Branco, M. (2015). Early disrupted neurovascular coupling

and changed event level hemodynamic response function in type 2 diabetes: An fMRI study. *Journal of Cerebral Blood Flow and Metabolism*, *35*(10), 1671–1680. https://doi.org/10.1038/jcbfm.2015.106

Duerden, E. G., & Albanese, M.-C. (2013). Localization of pain-related brain activation: a meta-analysis of neuroimaging data. *Human Brain Mapping*, *34*(1), 109–149. https://doi.org/10.1002/hbm.21416

Dunn, J., Yeo, E., Moghaddampour, P., Chau, B., & Humbert, S. (2017). Virtual and augmented reality in the treatment of phantom limb pain: A literature review. *NeuroRehabilitation*, *40*(4), 595–601.

Eggebrecht, A. T., Ferradal, S. L., Robichaux-Viehoever, A., Hassanpour, M. S., Dehghani, H., Snyder, A. Z., Hershey, T., & Culver, J. P. (2014). Mapping distributed brain function and networks with diffuse optical tomography. *Nature Photonics*, *8*(6), 448–454. https://doi.org/10.1038/nphoton.2014.107

Ehlis, A.-C., Schneider, S., Dresler, T., & Fallgatter, A. J. (2014). Application of functional near-infrared spectroscopy in psychiatry. *NeuroImage*, *85*, 478–488. https://doi.org/https://doi.org/10.1016/j.neuroimage.2013.03.067

Ellis, A., & Bennett, D. L. H. (2013). Neuroinflammation and the generation of neuropathic pain. *British Journal of Anaesthesia*, *111*(1), 26–37.

Espinoza, S., & Habas, C. (2018). Neuroimaging of Pain. In C. Habas (Ed.), *The Neuroimaging of Brain Diseases: Structural and Functional Advances* (pp. 323–337). Springer International Publishing. https://doi.org/10.1007/978-3-319-78926-2_14

Evans, Adam G, Chaker, Sara C, Curran, Gabrielle E, Downer, Mauricio A, Assi, Patrick E, Joseph, Jeremy T, Kassis, S. Al, & Thayer, Wesley P. (2021). Postamputation Residual Limb Pain Severity and Prevalence: A Systematic Review and Meta-Analysis. *Plastic Surgery*, *30*(3), 254–268. https://doi.org/10.1177/22925503211019646

Feng, L., & Gao, L. (2024). The role of neurovascular coupling dysfunction in cognitive decline of diabetes patients. In *Frontiers in Neuroscience* (Vol. 18). Frontiers Media SA. https://doi.org/10.3389/fnins.2024.1375908

Ferrari, M., & Quaresima, V. (2012). A brief review on the history of human functional near-infrared spectroscopy (fNIRS) development and fields of application. *NeuroImage*, *63*(2), 921–935. https://doi.org/https://doi.org/10.1016/j.neuroimage.2012.03.049

Flor, H. (2002a). Phantom-limb pain: Characteristics, causes, and treatment. *Lancet Neurology*, *1*(3), 182–189. https://doi.org/10.1016/S1474-4422(02)00074-1

Flor, H. (2002b). *Review Phantom-limb pain : characteristics , causes , and treatment*. *1*(July), 182–189.

Flor, H. (2008). Maladaptive plasticity, memory for pain and phantom limb pain: review and suggestions for new therapies. *Expert Review of Neurotherapeutics*, *8*(5), 809–818.

Flor, H., Elbert, T., Knecht, S., Wienbruch, C., Pantev, C., Birbaumers, N., Larbig, W., & Taub, E. (1995). Phantom-limb pain as a perceptual correlate of cortical reorganization following arm amputation. *Nature*, *375*(6531), 482–484. https://doi.org/10.1038/375482a0

Flor, H., Elbert, T., Mühlnickel, W., Pantev, C., Wienbruch, C., & Taub, E. (1998). Cortical reorganization and phantom phenomena in congenital and traumatic upper-extremity amputees. *Experimental Brain Research*, *119*(2), 205–212. https://doi.org/10.1007/s002210050334

Flor, H., Nikolajsen, L., & Staehelin Jensen, T. (2006). Phantom limb pain: a case of maladaptive CNS plasticity? *Nature Reviews Neuroscience*, *7*(11), 873–881. https://doi.org/10.1038/nrn1991

Flor, H., Rudy, T. E., Birbaumer, N., Streit, B., & Schugens, M. M. (1990). *Zur Anwendbarkeit des West Haven-Yale Multidimensional Pain Inventory im deutschen Sprachraum Daten zur Reliabilitfit und Validit/it des MPI-D * The*

applicability of the West Haven-Yale multidimensional pain inventory in German-speaking countries. Data on the reliability and validity of the MPI-D.

Fowkes, F. G. R., Rudan, D., Rudan, I., Aboyans, V., Denenberg, J. O., McDermott, M. M., Norman, P. E., Sampson, U. K. A., Williams, L. J., Mensah, G. A., & Criqui, M. H. (2013). Comparison of global estimates of prevalence and risk factors for peripheral artery disease in 2000 and 2010: A systematic review and analysis. *The Lancet*, *382*(9901), 1329–1340. https://doi.org/10.1016/S0140-6736(13)61249-0

Freund, W., Klug, R., Weber, F., Stuber, G., Schmitz, B., & Wunderlich, A. P. (2009). Perception and suppression of thermally induced pain: A fMRI study. *Somatosensory and Motor Research*, *26*(1), 1–10. https://doi.org/10.1080/08990220902738243

Friston, K. J., Holmes, A. P., Poline, J. B., Grasby, P. J., Williams, S. C. R., Frackowiak, R. S. J., & Turner, R. (1995). Analysis of fMRI time-series revisited. In *Neuroimage* (Vol. 2, Issue 1, pp. 45–53). https://doi.org/10.1006/nimg.1995.1007

Fuchs, X., Flor, H., & Bekrater-Bodmann, R. (2018a). Psychological Factors Associated with Phantom Limb Pain: A Review of Recent Findings. *Pain Research and Management*, *2018*(1), 5080123. https://doi.org/https://doi.org/10.1155/2018/5080123

Fuchs, X., Flor, H., & Bekrater-Bodmann, R. (2018b). Psychological factors associated with phantom limb pain: a review of recent findings. *Pain Research and Management*, *2018*(1), 5080123.

Furtado, S., Grimer, R. J., Cool, P., Murray, S. A., Briggs, T., Fulton, J., Grant, K., & Gerrand, C. H. (2015). Physical functioning, pain and quality of life after amputation for musculoskeletal tumours. *The Bone & Joint Journal*, *97-B*(9), 1284–1290. https://doi.org/doi:10.1302/0301-620X.97B9.35192

Gallace, A., & Bellan, V. (2018). Chapter 5 - The parietal cortex and pain perception: a body protection system. In G. Vallar & H. B. Coslett (Eds.), *Handbook of Clinical Neurology* (Vol. 151, pp. 103–117). Elsevier. https://doi.org/https://doi.org/10.1016/B978-0-444-63622-5.00005-X

Garcia-Pallero, M. Á., Cardona, D., Rueda-Ruzafa, L., Rodriguez-Arrastia, M., & Roman, P. (2022). Central nervous system stimulation therapies in phantom limb pain: a systematic review of clinical trials. In *Neural Regeneration Research* (Vol. 17, Issue 1, pp. 59–64). Wolters Kluwer Medknow Publications. https://doi.org/10.4103/1673-5374.314288

Giacometti, P., & Diamond, S. G. (2013). Diffuse optical tomography for brain imaging: continuous wave instrumentation and linear analysis methods. *Optical Methods and Instrumentation in Brain Imaging and Therapy*, 57–85.

Ginanneschi, F., Padua, L., Hede Yan, I., Lu, H., Abdullah Ezzi, H. S., Abdulla Hasan Abdulla, H. M., Copyright, fneur, Abdullah Ezzi, H., Abdulla Hasan Abdulla, H., Yang, H., Dong, Y., Wang, Z., Lai, J., Yao, C., Zhou, H., Alhaskawi, A., Hasan Abdullah Ezzi, S., Goutham Kota, V., & Hasan Abdulla Hasan Abdulla, M. (2023). *Traumatic neuromas of peripheral nerves: Diagnosis, management and future perspectives*.

Hanley, M. A., Jensen, M. P., Smith, D. G., Ehde, D. M., Edwards, W. T., & Robinson, L. R. (2007). Preamputation Pain and Acute Pain Predict Chronic Pain After Lower Extremity Amputation. *Journal of Pain*, *8*(2), 102–109. https://doi.org/10.1016/j.jpain.2006.06.004

Hernández-Román, J., Montero-Hernández, S., Vega, R., Orihuela-Espina, F., & Soto, E. (2023). Galvanic vestibular stimulation activates the parietal and temporal cortex in humans: A functional near-infrared spectroscopy (fNIRS) study. *European Journal of Neuroscience*, *58*(1), 2267–2277.

Hill, A., Niven, A. C., & Knussen, C. (1996). Pain memories in phantom limbs: a case study. *Pain*, *66*(2), 381–384.

Hocke, L. M., Oni, I. K., Duszynski, C. C., Corrigan, A. V., Frederick, B. de B., & Dunn, J. F. (2018). Automated processing of fNIRS data-A visual guide to the pitfalls and consequences. *Algorithms*, *11*(5). https://doi.org/10.3390/a11050067

Holmes, M., Aalto, D., & Cummine, J. (2024). Opening the dialogue: A preliminary exploration of hair color, hair cleanliness, light, and motion effects on fNIRS signal quality. *PLoS ONE*, *19*(5 May). https://doi.org/10.1371/journal.pone.0304356

Homan, R. W., Herman, J., & Purdy, P. (1987). Cerebral location of international 10–20 system electrode placement. *Electroencephalography and Clinical Neurophysiology*, *66*(4), 376–382.

Horgan, O., & MacLachlan, M. (2004). Psychosocial adjustment to lower-limb amputation: A review. In *Disability and Rehabilitation* (Vol. 26, Issues 14–15, pp. 837–850). https://doi.org/10.1080/09638280410001708869

Horing, B., Sprenger, C., & Büchel, C. (2019). The parietal operculum preferentially encodes heat pain and not salience. *PLoS Biology*, *17*(8). https://doi.org/10.1371/journal.pbio.3000205

Horner, G., & Dellon, A. L. (1994). Innervation of the human knee joint and implications for surgery. *Clinical Orthopaedics and Related Research*, *301*(301), 221–226. https://doi.org/10.1097/00003086-199404000-00034

Hoshi, Y. (2005). Functional Near-Infrared Spectroscopy: Potential and Limitations in Neuroimaging Studies. In *International Review of Neurobiology* (Vol. 66, pp. 237–266). https://doi.org/10.1016/S0074-7742(05)66008-4

Hoshi, Y. (2016). Chapter 7 - Hemodynamic signals in fNIRS. In K. Masamoto, H. Hirase, & K. Yamada (Eds.), *Progress in Brain Research* (Vol. 225, pp. 153–179). Elsevier. https://doi.org/https://doi.org/10.1016/bs.pbr.2016.03.004

Hoshi, Y., Kobayashi, N., & Tamura, M. (2001a). Interpretation of near-infrared spectroscopy signals: A study with a newly developed perfused rat brain model. *Journal of Applied Physiology*, *90*(5), 1657–1662. https://doi.org/10.1152/jappl.2001.90.5.1657

Hoshi, Y., Kobayashi, N., & Tamura, M. (2001b). *Interpretation of near-infrared spectroscopy signals: a study with a newly developed perfused rat brain model*. http://www.jap.org

Hsu, E., & and Cohen, S. P. (2013). Postamputation pain: epidemiology, mechanisms, and treatment. *Journal of Pain Research*, *6*(null), 121–136. https://doi.org/10.2147/JPR.S32299

Hu, X.-S., Nascimento, T. D., & DaSilva, A. F. (2021). Shedding light on pain for the clinic: a comprehensive review of using functional near-infrared spectroscopy to monitor its process in the brain. *Pain*, *162*(12), 2805–2820. https://doi.org/10.1097/j.pain.0000000000002293

Huang, T., Gu, Q., Deng, Z., Tsai, C., Xue, Y., Zhang, J., Zou, L., Chen, Z., & Wang, K. (2019). Executive function performance in young adults when cycling at an active workstation: an fNIRS study. *International Journal of Environmental Research and Public Health*, *16*(7), 1119.

Huppert, T. J., Diamond, S. G., Franceschini, M. A., & Boas, D. A. (2009a). HomER: a review of time-series analysis methods for near-infrared spectroscopy of the brain. *Applied Optics*, *48*(10), D280–D298.

Huppert, T. J., Diamond, S. G., Franceschini, M. A., & Boas, D. A. (2009b). HomER: a review of time-series analysis methods for near-infrared spectroscopy of the brain. *Applied Optics*, *48*(10), D280–D298. https://doi.org/10.1364/AO.48.00D280

Husain, S. F., Tang, T.-B., Tam, W. W., Tran, B. X., Ho, C. S., & Ho, R. C. (2021). Cortical haemodynamic response during the verbal fluency task in patients with bipolar disorder and borderline personality disorder: a preliminary functional near-infrared spectroscopy study. *BMC Psychiatry*, *21*(1), 201. https://doi.org/10.1186/s12888-021-03195-1

Iso, N., Moriuchi, T., Fujiwara, K., Matsuo, M., Mitsunaga, W., Hasegawa, T., Iso, F., Cho, K., Suzuki, M., & Higashi, T. (2021). Hemodynamic Signal Changes During Motor Imagery Task Performance Are Associated With the Degree of Motor Task Learning. *Frontiers in Human Neuroscience*, *15*(April), 1–14. https://doi.org/10.3389/fnhum.2021.603069

Jensen, T. S., Krebs, B., Nielsen, J., & Rasmussen, P. (1985a). Immediate and long-term phantom limb pain in amputees: Incidence, clinical characteristics and relationship to pre-amputation limb pain. *PAIN*, *21*(3). https://journals.lww.com/pain/fulltext/1985/03000/immediate_and_long_term_phantom_limb_pain_in.5.aspx

Jensen, T. S., Krebs, B., Nielsen, J., & Rasmussen, P. (1985b). Immediate and long-term phantom limb pain in amputees: Incidence, clinical characteristics and relationship to pre-amputation limb pain. *Pain*, *21*(3), 267–278. https://doi.org/https://doi.org/10.1016/0304-3959(85)90090-9

Jensen, T. S., Krebs, B., Nielsen, J., & Rasmussen, P. (1985c). Immediate and long-term phantom limb pain in amputees: Incidence, clinical characteristics and relationship to pre-amputation limb pain. *Pain*, *21*(3), 267–278. https://doi.org/10.1016/0304-3959(85)90090-9

Jeon, S., Chien, J., Song, C., & Hong, J. (2018). A preliminary study on precision image guidance for electrode placement in an EEG study. *Brain Topography*, *31*, 174–185.

Jöbsis, F. F. (1977). Noninvasive, infrared monitoring of cerebral and myocardial oxygen sufficiency and circulatory parameters. *Science*, *198*(4323), 1264–1267.

Jonas, J.-C., Sharma, A., Hasenkamp, W., Ilkova, H., Patane, G., Laybutt, R., Bonner-Weir, S., & Weir, G. C. (1999). Chronic hyperglycemia triggers loss of pancreatic β cell differentiation in an animal model of diabetes. *Journal of Biological Chemistry*, *274*(20), 14112–14121.

Jones, L., Verriotis, M., Cooper, R. J., Laudiano-Dray, M. P., Rupawala, M., Meek, J., Fabrizi, L., & Fitzgerald, M. (2022). Widespread nociceptive maps in the human neonatal somatosensory cortex. *Elife*, *11*, e71655.

Journal, C., Alejandra, M., Angarita, M., Carrillo Villa, S., Fernando, O., Ribero, G., García, R. G., Arturo, F., & Sieger, S. (2013). *Revista Colombiana de Anestesiología Pathophysiology and treatment of phantom limb pain*.

Kajander, K. C., Wakisaka, S., & Bennett, G. J. (1992). Spontaneous discharge originates in the dorsal root ganglion at the onset of a painful peripheral neuropathy in the rat. *Neuroscience Letters*, *138*(2), 225–228.

Kampitak, W., Tanavalee, A., Tansatit, T., Ngarmukos, S., Songborassamee, N., & Vichainarong, C. (2021). The analgesic efficacy of anterior femoral cutaneous nerve block in combination with femoral triangle block in total knee arthroplasty: a

randomized controlled trial. *Korean Journal of Anesthesiology*, *74*(6), 496–505. https://doi.org/10.4097/kja.21120

Karunakaran, K. D., Peng, K., Berry, D., Green, S., Labadie, R., Kussman, B., & Borsook, D. (2021). NIRS measures in pain and analgesia: Fundamentals, features, and function. *Neuroscience and Biobehavioral Reviews*, *120*, 335–353. https://doi.org/10.1016/j.neubiorev.2020.10.023

Katayama, Y., Yamamoto, T., Kobayashi, K., Kasai, M., Oshima, H., & Fukaya, C. (2002). Motor cortex stimulation for phantom limb pain: comprehensive therapy with spinal cord and thalamic stimulation. *Stereotactic and Functional Neurosurgery*, *77*(1–4), 159–162.

Katz, J., & Melzack, R. (1990). Pain 'memories' in phantom limbs: review and clinical observations. *PAIN*, *43*(3). https://journals.lww.com/pain/fulltext/1990/12000/pain__memories__in_phantom_limbs__review_and.7.aspx

Katz, J., & Melzack, R. (1991). Auricular transcutaneous electrical nerve stimulation (TENS) reduces phantom limb pain. *Journal of Pain and Symptom Management*, *6*(2), 73–83. https://doi.org/https://doi.org/10.1016/0885-3924(91)90521-5

Kaur, A., & Guan, Y. (2018). Phantom limb pain: A literature review. *Chinese Journal of Traumatology*, *21*(06), 366–368.

Khan, M. A. B., Hashim, M. J., King, J. K., Govender, R. D., Mustafa, H., & Kaabi, J. Al. (2020). Epidemiology of Type 2 diabetes - Global burden of disease and forecasted trends. *Journal of Epidemiology and Global Health*, *10*(1), 107–111. https://doi.org/10.2991/JEGH.K.191028.001

Kocsis, L., Herman, P., & Eke, A. (2006). The modified Beer–Lambert law revisited. *Physics in Medicine & Biology*, *51*(5), N91.

Kong, J., Loggia, M. L., Zyloney, C., Tu, P., LaViolette, P., & Gollub, R. L. (2010). Exploring the brain in pain: Activations, deactivations and their relation. *Pain*, *148*(2), 257–267. https://doi.org/10.1016/j.pain.2009.11.008

Kozel, F. A., Tian, F., Dhamne, S., Croarkin, P. E., McClintock, S. M., Elliott, A., Mapes, K. S., Husain, M. M., & Liu, H. (2009). Using simultaneous repetitive transcranial magnetic stimulation/functional near infrared spectroscopy (rTMS/fNIRS) to measure brain activation and connectivity. *Neuroimage*, *47*(4), 1177–1184.

Kröger, K., Berg, C., Santosa, F., Malyar, N., & Reinecke, H. (2017). Lower Limb Amputation in Germany. *Deutsches Ärzteblatt International*, 2–9. https://doi.org/10.3238/arztebl.2017.0130

Kucyi, A., Salomons, T. V., & Davis, K. D. (2013). Mind wandering away from pain dynamically engages antinociceptive and default mode brain networks. *Proceedings of the National Academy of Sciences of the United States of America*, *110*(46), 18692–18697. https://doi.org/10.1073/pnas.1312902110

Kuffler, D. P. (2018). Origins of Phantom Limb Pain. *Molecular Neurobiology*, *55*(1), 60–69. https://doi.org/10.1007/s12035-017-0717-x

Kulkarni, B., Bentley, D. E., Elliott, R., Youell, P., Watson, A., Derbyshire, S. W. G., Frackowiak, R. S. J., Friston, K. J., & Jones, A. K. P. (2005). Attention to pain localization and unpleasantness discriminates the functions of the medial and lateral pain systems. *The European Journal of Neuroscience*, *21*(11), 3133–3142. https://doi.org/10.1111/j.1460-9568.2005.04098.x

Kuner, R., & Flor, H. (2017). Structural plasticity and reorganisation in chronic pain. *Nature Reviews Neuroscience*, *18*(1), 20–30. https://doi.org/10.1038/nrn.2016.162

Lafuente, F. (2002). *Phantom limb: from Paré to Moby Dick*.

Lang, P. M., Schober, G. M., Rolke, R., Wagner, S., Hilge, R., Offenbächer, M., Treede, R.-D., Hoffmann, U., & Irnich, D. (2006). Sensory neuropathy and signs of central sensitization in patients with peripheral arterial disease. *Pain*, *124*(1–2), 190–200.

Larbig, W., Andoh, J., Huse, E., Stahl-Corino, D., Montoya, P., Seltzer, Z., & Flor, H. (2019). Pre- and postoperative predictors of phantom limb pain. *Neuroscience Letters*, *702*, 44–50. https://doi.org/10.1016/j.neulet.2018.11.044

Lee, C. H., Sugiyama, T., Kataoka, A., Kudo, A., Fujino, F., Chen, Y. W., Mitsuyama, Y., Nomura, S., & Yoshioka, T. (2013). Analysis for Distinctive Activation Patterns of Pain and Itchy in the Human Brain Cortex Measured Using Near Infrared Spectroscopy (NIRS). *PLoS ONE*, *8*(10). https://doi.org/10.1371/journal.pone.0075360

Lee, J. H., Yoon, J. S., Lee, H. W., Won, K. C., Moon, J. S., Chung, S. M., & Lee, Y. Y. (2020). Risk factors affecting amputation in diabetic foot. *Yeungnam University Journal of Medicine*, *37*(4), 314–320. https://doi.org/10.12701/yujm.2020.00129

Li, R., Rui, G., Chen, W., Li, S., Schulz, P. E., & Zhang, Y. (2018). Early Detection of Alzheimer's Disease Using Non-invasive Near-Infrared Spectroscopy. *Frontiers in Aging Neuroscience*, *10*. https://doi.org/10.3389/fnagi.2018.00366

Li, Y., Xu, Z., Xie, H., Fu, R., Lo, W. L. A., Cheng, X., Yang, J., Ge, L., Yu, Q., & Wang, C. (2023). Changes in cortical activation during upright stance in individuals with chronic low back pain: An fNIRS study. *Frontiers in Human Neuroscience*, *17*. https://www.frontiersin.org/journals/human-neuroscience/articles/10.3389/fnhum.2023.1085831

Limakatso, K., Bedwell, G. J., Madden, V. J., & Parker, R. (2020). The prevalence and risk factors for phantom limb pain in people with amputations: A systematic review and meta-analysis. *PLOS ONE*, *15*(10), e0240431-. https://doi.org/10.1371/journal.pone.0240431

Limakatso, K., Ndhlovu, F., Usenbo, A., Rayamajhi, S., Kloppers, C., & Parker, R. (2024). The prevalence and risk factors for phantom limb pain: a cross-sectional survey. *BMC Neurology*, *24*(1), 57. https://doi.org/10.1186/s12883-024-03547-w

Lin, P., Chen, J. J., & Lin, S. (2013). The cortical control of cycling exercise in stroke patients: an fNIRS study. *Human Brain Mapping*, *34*(10), 2381–2390.

Lin, P.-Y., Chen, J.-J. J., & Lin, S.-I. (2013). The cortical control of cycling exercise in stroke patients: An fNIRS study. *Human Brain Mapping*, *34*(10), 2381–2390. https://doi.org/https://doi.org/10.1002/hbm.22072

List, E. B., Krijgh, D. D., Martin, E., & Coert, J. H. (2021). Prevalence of residual limb pain and symptomatic neuromas after lower extremity amputation: a systematic review and meta-analysis. *PAIN*, *162*(7). https://journals.lww.com/pain/fulltext/2021/07000/prevalence_of_residual_limb_pain_and_symptomatic.3.aspx

Liu, B., Yu, J., Wu, J., Qin, Y., Xiao, W., & Ren, Z. (2023). Runners with better cardiorespiratory fitness had higher prefrontal cortex activity during both single and exercise-executive function dual tasks: an fNIRS study. *Frontiers in Physiology*, *14*, 1246741.

Liu, H., Andoh, J., Lyu, Y., Milde, C., Desch, S., Zidda, F., Schmelz, M., Curio, G., & Flor, H. (2020). *Peripheral input and phantom limb pain: A somatosensory event-related potential study*. *24*(7), 1314–1329. https://doi.org/10.1002/ejp.1579

Liu, Z., Shore, J., Wang, M., Yuan, F., Buss, A., & Zhao, X. (2021). A systematic review on hybrid EEG/fNIRS in brain-computer interface. *Biomedical Signal Processing and Control*, *68*, 102595.

Livingston, K. E. (1945). The phantom limb syndrome. A discussion of the role of major peripheral nerve neuromas. *Journal of Neurosurgery*, *2*(3), 251–255.

Löffler, M., Kamping, S., Brunner, M., Bustan, S., Kleinböhl, D., Anton, F., & Flor, H. (2018). Impact of controllability on pain and suffering. *Pain Reports*, *3*(6), 1–10. https://doi.org/10.1097/PR9.0000000000000694

Lorenz, J., Cross, D. J., Minoshima, S., Morrow, T. J., Paulson, P. E., & Casey, K. L. (2002). A unique representation of heat allodynia in the human brain. *Neuron*, *35*(2), 383–393.

Lorenz, J., Minoshima, S., & Casey, K. L. (2003). Keeping pain out of mind: the role of the dorsolateral prefrontal cortex in pain modulation. *Brain*, *126*(5), 1079–1091.

Lotze, M., Flor, H., Grodd, W., Larbig, W., & Birbaumer, N. (2001). Phantom movements and pain An fMRI study in upper limb amputees. *Brain*, *124*(11), 2268–2277. https://doi.org/10.1093/brain/124.11.2268

MacIver, K., Lloyd, D. M., Kelly, S., Roberts, N., & Nurmikko, T. (2008). Phantom limb pain, cortical reorganization and the therapeutic effect of mental imagery. *Brain*, *131*(8), 2181–2191. https://doi.org/10.1093/brain/awn124

Makin, T. R., & Krakauer, J. W. (2023). Against cortical reorganisation. *ELife*, *12*, 1–43. https://doi.org/10.7554/eLife.84716

Makin, T. R., Scholz, J., Filippini, N., Henderson Slater, D., Tracey, I., & Johansen-Berg, H. (2013). Phantom pain is associated with preserved structure and function in the former hand area. *Nature Communications*, *4*(1), 1570. https://doi.org/10.1038/ncomms2571

Manthey, S., Schubotz, R. I., & Von Cramon, D. Y. (2003). Premotor cortex in observing erroneous action: an fMRI study. *Cognitive Brain Research*, *15*(3), 296–307.

Marshall, C., & Stansby, G. (2008). Amputation. *Surgery (Oxford)*, *26*(1), 21–24. https://doi.org/https://doi.org/10.1016/j.mpsur.2007.10.011

Matsuda, M., Huh, Y., & Ji, R.-R. (2019). Roles of inflammation, neurogenic inflammation, and neuroinflammation in pain. *Journal of Anesthesia*, *33*, 131–139.

McCormick, D. A. (2014). Chapter 12 - Membrane Potential and Action Potential. In J. H. Byrne, R. Heidelberger, & M. N. Waxham (Eds.), *From Molecules to Networks (Third Edition)* (pp. 351–376). Academic Press. https://doi.org/https://doi.org/10.1016/B978-0-12-397179-1.00012-9

McDermott, M. M., Sufit, R., Nishida, T., Guralnik, J. M., Ferrucci, L., Tian, L., Liu, K., Tan, J., Pearce, W. H., & Schneider, J. R. (2006). Lower extremity nerve function in patients with lower extremity ischemia. *Archives of Internal Medicine*, *166*(18), 1986–1992.

Menon, V., & Uddin, L. Q. (2010). Saliency, switching, attention and control: a network model of insula function. *Brain Structure & Function*, *214*(5–6), 655–667. https://doi.org/10.1007/s00429-010-0262-0

Meru, A. V, Mittra, S., Thyagarajan, B., & Chugh, A. (2006). Intermittent claudication: An overview. *Atherosclerosis*, *187*(2), 221–237. https://doi.org/https://doi.org/10.1016/j.atherosclerosis.2005.11.027

Monden, Y., Dan, H., Nagashima, M., Dan, I., Tsuzuki, D., Kyutoku, Y., Gunji, Y., Yamagata, T., Watanabe, E., & Momoi, M. Y. (2012). Right prefrontal activation as a neuro-functional biomarker for monitoring acute effects of methylphenidate in ADHD children: an fNIRS study. *NeuroImage: Clinical*, *1*(1), 131–140.

Monden, Y., Dan, I., Nagashima, M., Dan, H., Uga, M., Ikeda, T., Tsuzuki, D., Kyutoku, Y., Gunji, Y., & Hirano, D. (2015). Individual classification of ADHD children by right prefrontal hemodynamic responses during a go/no-go task as assessed by fNIRS. *NeuroImage: Clinical*, *9*, 1–12.

Muir, R. L. (2009). Peripheral arterial disease: Pathophysiology, risk factors, diagnosis, treatment, and prevention. *Journal of Vascular Nursing*, *27*(2), 26–30. https://doi.org/https://doi.org/10.1016/j.jvn.2009.03.001

Muthalib, M., Re, R., Zucchelli, L., Perrey, S., Contini, D., Caffini, M., Spinelli, L., Kerr, G., Quaresima, V., Ferrari, M., & Torricelli, A. (2015). Effects of Increasing Neuromuscular Electrical Stimulation Current Intensity on Cortical Sensorimotor Network Activation: A Time Domain fNIRS Study. *PLOS ONE*, *10*(7), e0131951-. https://doi.org/10.1371/journal.pone.0131951

Nardone, R., Versace, V., Sebastianelli, L., Brigo, F., Christova, M., Scarano, G. I., Saltuari, L., Trinka, E., Hauer, L., & Sellner, J. (2019a). Transcranial magnetic stimulation in subjects with phantom pain and non-painful phantom sensations: a systematic review. *Brain Research Bulletin*, *148*, 1–9.

Nardone, R., Versace, V., Sebastianelli, L., Brigo, F., Christova, M., Scarano, G. I., Saltuari, L., Trinka, E., Hauer, L., & Sellner, J. (2019b). Transcranial magnetic stimulation in subjects with phantom pain and non-painful phantom sensations: a systematic review. *Brain Research Bulletin*, *148*, 1–9.

Navarro, X., Vivó, M., & Valero-Cabré, A. (2007). Neural plasticity after peripheral nerve injury and regeneration. In *Progress in Neurobiology* (Vol. 82, Issue 4, pp. 163–201). https://doi.org/10.1016/j.pneurobio.2007.06.005

Ng, S. K., Urquhart, D. M., Fitzgerald, P. B., Cicuttini, F. M., Hussain, S. M., & Fitzgibbon, B. M. (2018). The Relationship between Structural and Functional Brain Changes and Altered Emotion and Cognition in Chronic Low Back Pain Brain Changes A Systematic Review of MRI and fMRI Studies. *Clinical Journal of Pain*, *34*(3), 237–261. https://doi.org/10.1097/AJP.0000000000000534

Nikolajsen, L., & Christensen, K. F. (2015). Phantom limb pain. *Nerves and Nerve Injuries*, 23–34.

Normahani, P., Khosravi, S., Sounderajah, V., Aslam, M., Standfield, N. J., & Jaffer, U. (2021). The Effect of Lower Limb Revascularization on Flow, Perfusion, and Systemic Endothelial Function: A Systematic Review. In *Angiology* (Vol. 72, Issue 3, pp. 210–220). SAGE Publications Inc. https://doi.org/10.1177/0003319720969543

Oliver, D., Tachtsidis, I., & Hamilton, A. F. de C. (2018). The role of parietal cortex in overimitation: a study with fNIRS. *Social Neuroscience*, *13*(2), 214–225.

Osumi, M., Inomata, K., Inoue, Y., Otake, Y., Morioka, S., & Sumitani, M. (2019). Characteristics of phantom limb pain alleviated with virtual reality rehabilitation. *Pain Medicine*, *20*(5), 1038–1046.

Ouriel, K. (2001a). Peripheral arterial disease. *The Lancet*, *358*(9289), 1257–1264. https://doi.org/10.1016/S0140-6736(01)06351-6

Ouriel, K. (2001b). Peripheral arterial disease. *The Lancet*, *358*(9289), 1257–1264.

Owens, C. D., Mukli, P., Csipo, T., Lipecz, A., Silva-Palacios, F., Dasari, T. W., Tarantini, S., Gardner, A. W., Montgomery, P. S., Waldstein, S. R., Kellawan, J. M., Nyul-Toth, A., Balasubramanian, P., Sotonyi, P., Csiszar, A., Ungvari, Z., & Yabluchanskiy, A. (2022). Microvascular dysfunction and neurovascular uncoupling are exacerbated in peripheral artery disease, increasing the risk of cognitive decline in older adults. *American Journal of Physiology - Heart and Circulatory Physiology*, *322*(6), H924–H935. https://doi.org/10.1152/ajpheart.00616.2021

Öztürk, Ö., Algun, Z. C., Bombacı, H., & Erdoğan, S. B. (2021). Changes in prefrontal cortex activation with exercise in knee osteoarthritis patients with chronic pain: An fNIRS study. *Journal of Clinical Neuroscience*, *90*, 144–151. https://doi.org/10.1016/j.jocn.2021.05.055

Pascale, B. A., & Potter, B. K. (2014). Residual limb complications and management strategies. *Current Physical Medicine and Rehabilitation Reports*, *2*, 241–249.

Peng, K., Steele, S. C., Becerra, L., & Borsook, D. (2018). Brodmann area 10: Collating, integrating and high level processing of nociception and pain. *Progress in Neurobiology*, *161*, 1–22. https://doi.org/10.1016/j.pneurobio.2017.11.004

Penpield, B. Y. W. (1937). Somatic Motor and Sensory Representation in. *Atlantic*.

Pereira, J., Direito, B., Lührs, M., Castelo-Branco, M., & Sousa, T. (2023). Multimodal assessment of the spatial correspondence between fNIRS and fMRI hemodynamic responses in motor tasks. *Scientific Reports*, *13*(1), 2244. https://doi.org/10.1038/s41598-023-29123-9

Peters, S. K., Dunlop, K., & Downar, J. (2016). Cortico-Striatal-Thalamic Loop Circuits of the Salience Network: A Central Pathway in Psychiatric Disease and Treatment. *Frontiers in Systems Neuroscience*, *10*, 104. https://doi.org/10.3389/fnsys.2016.00104

Petropoulos, I., Fadavi, H., Asghar, O., Alam, U., Ponirakis, G., Tavakoli, M., & Malik, R. (2010). Diabetic neuropathy: Review of diagnosis and management. *Diabetes & Primary Care*, *12*(3), 165–174.

Petrovic, P., Kalso, E., Petersson, K. M., Andersson, J., Fransson, P., & Ingvar, M. (2010). A prefrontal non-opioid mechanism in placebo analgesia. *Pain*, *150*(1), 59–65.

Pham, V. M., Tu, N. H., Katano, T., Matsumura, S., Saito, A., Yamada, A., Furue, H., & Ito, S. (2018). Impaired peripheral nerve regeneration in type-2 diabetic mouse model. *European Journal of Neuroscience*, *47*(2), 126–139. https://doi.org/https://doi.org/10.1111/ejn.13771

Phillips, Aaron A, Chan, Franco H N, Zheng, Mei Mu Zi, Krassioukov, A. V, & Ainslie, Philip N. (2015). Neurovascular coupling in humans: Physiology, methodological advances and clinical implications. *Journal of Cerebral Blood Flow & Metabolism*, *36*(4), 647–664. https://doi.org/10.1177/0271678X15617954

Pinti, P., Aichelburg, C., Gilbert, S., Hamilton, A., Hirsch, J., Burgess, P., & Tachtsidis, I. (2018). A review on the use of wearable functional near-infrared spectroscopy in naturalistic environments. *Japanese Psychological Research*, *60*(4), 347–373.

Pinti, P., Tachtsidis, I., Hamilton, A., Hirsch, J., Aichelburg, C., Gilbert, S., & Burgess, P. W. (2020). The present and future use of functional near-infrared spectroscopy (Fnirs) for cognitive neuroscience. *Annals of the New York Academy of Sciences*, *1464*(1), 5–29. https://doi.org/10.1111/nyas.13948

Piper, S. K., Krueger, A., Koch, S. P., Mehnert, J., Habermehl, C., Steinbrink, J., Obrig, H., & Schmitz, C. H. (2014). A wearable multi-channel fNIRS system for brain imaging in freely moving subjects. *NeuroImage*, *85*, 64–71. https://doi.org/10.1016/j.neuroimage.2013.06.062

Pomares, G., Coudane, H., Dap, F., & Dautel, G. (2020). Psychological effects of traumatic upper-limb amputations. *Orthopaedics & Traumatology: Surgery & Research*, *106*(2), 297–300. https://doi.org/https://doi.org/10.1016/j.otsr.2019.12.013

Raichle, K. A., Osborne, T. L., Jensen, M. P., Ehde, D. M., Smith, D. G., & Robinson, L. R. (2015). Preoperative State Anxiety, Acute Postoperative Pain, and Analgesic Use in Persons Undergoing Lower Limb Amputation. *Clinical Journal of Pain*, *31*(8), 699–706. https://doi.org/10.1097/AJP.0000000000000150

Raichle, M. E. (2015). The Brain's Default Mode Network. *Annual Review of Neuroscience*, *38*, 433–447. https://doi.org/10.1146/annurev-neuro-071013-014030

Raichle, M. E., MacLeod, A. M., Snyder, A. Z., Powers, W. J., Gusnard, D. A., & Shulman, G. L. (2001). A default mode of brain function. *Proceedings of the National Academy of Sciences of the United States of America*, *98*(2), 676–682. https://doi.org/10.1073/pnas.98.2.676

Ram, Z., Sadeh, M., Walden, R., & Adar, R. (1991). Vascular insufficiency quantitatively aggravates diabetic neuropathy. *Archives of Neurology*, *48*(12), 1239–1242.

Rorden, C., & Brett, M. (2000). Stereotaxic display of brain lesions. *Behavioural Neurology*, *12*(4), 191–200. https://doi.org/10.1155/2000/421719

Rüger, L. J., Irnich, D., Abahji, T. N., Crispin, A., Hoffmann, U., & Lang, P. M. (2008a). Characteristics of chronic ischemic pain in patients with peripheral arterial disease. *PAIN*, *139*(1), 201–208. https://doi.org/https://doi.org/10.1016/j.pain.2008.03.027

Rüger, L. J., Irnich, D., Abahji, T. N., Crispin, A., Hoffmann, U., & Lang, P. M. (2008b). Characteristics of chronic ischemic pain in patients with peripheral arterial disease. *PAIN*, *139*(1), 201–208. https://doi.org/https://doi.org/10.1016/j.pain.2008.03.027

Sakuma, S., Inamoto, K., Higuchi, N., Ariji, Y., Nakayama, M., & Izumi, M. (2014). Experimental pain in the gingiva and its impact on prefrontal cortical hemodynamics: A functional near-infrared spectroscopy study. *Neuroscience Letters*, *575*, 74–79. https://doi.org/https://doi.org/10.1016/j.neulet.2014.05.040

Sandström, A., Ellerbrock, I., Jensen, K. B., Martinsen, S., Altawil, R., Hakeberg, P., Fransson, P., Lampa, J., & Kosek, E. (2019). Altered cerebral pain processing of noxious stimuli from inflamed joints in rheumatoid arthritis: An event-related fMRI study. *Brain, Behavior, and Immunity*, *81*(June), 272–279. https://doi.org/10.1016/j.bbi.2019.06.024

Schone, H. R., Baker, C. I., Katz, J., Nikolajsen, L., Limakatso, K., Flor, H., & Makin, T. R. (2022a). Making sense of phantom limb pain. *Journal of Neurology, Neurosurgery &Amp; Psychiatry*, *93*(8), 833. https://doi.org/10.1136/jnnp-2021-328428

Schone, H. R., Baker, C. I., Katz, J., Nikolajsen, L., Limakatso, K., Flor, H., & Makin, T. R. (2022b). Making sense of phantom limb pain. *Journal of Neurology, Neurosurgery and Psychiatry*, *93*(8), 833–843. https://doi.org/10.1136/jnnp-2021-328428

Seminowicz, D. A., & Moayedi, M. (2017). The Dorsolateral Prefrontal Cortex in Acute and Chronic Pain. *Journal of Pain*, *18*(9), 1027–1035. https://doi.org/10.1016/j.jpain.2017.03.008

Seo, C. H., Park, C. H., Jung, M. H., Baek, S., Song, J., Cha, E., & Ohn, S. H. (2019). Increased white matter diffusivity associated with phantom limb pain. *Korean Journal of Pain*, *32*(4), 271–279. https://doi.org/10.3344/kjp.2019.32.4.271

Serda, E., Batmaz, I., Karakoc, M., Aydin, A., Bozkurt, M., ÇAĞLAYAN, M., & Kemal, N. (2015). Determining sleep quality and its associated factors in patients with lower limb amputation. *Turk J Phys Med Rehab*, *61*(3), 241–246.

Sevel, L. S., Letzen, J. E., Staud, R., & Robinson, M. E. (2016). Interhemispheric Dorsolateral Prefrontal Cortex Connectivity is Associated with Individual Differences in Pain Sensitivity in Healthy Controls. *Brain Connectivity*, *6*(5), 357–364. https://doi.org/10.1089/brain.2015.0405

Sharma, N., Jones, P. S., Carpenter, T. A., & Baron, J.-C. (2008). Mapping the involvement of BA 4a and 4p during motor imagery. *Neuroimage*, *41*(1), 92–99.

Shaw, K., Bell, L., Boyd, K., Grijseels, D. M., Clarke, D., Bonnar, O., Crombag, H. S., & Hall, C. N. (2021). Neurovascular coupling and oxygenation are decreased in hippocampus compared to neocortex because of microvascular differences. *Nature Communications*, *12*(1). https://doi.org/10.1038/s41467-021-23508-y

Shukla, G. D., Sahu, S. C., Tripathi, R. P., & Gupta, D. K. (1982). Phantom Limb: A Phenomenological Study. *British Journal of Psychiatry*, *141*(1), 54–58. https://doi.org/DOI: 10.1192/bjp.141.1.54

Shuvra, L. T., Md Rabiul Islam, S., Zaman, N., & Hasan, M. A. (2019). Identification of human pain perception using fNIRS. *1st International Conference on Robotics, Electrical and Signal Processing Techniques, ICREST 2019*, 434–439. https://doi.org/10.1109/ICREST.2019.8644087

Simis, M., Marques, L. M., Barbosa, S. P., Sugawara, A. T., Sato, J. R., Pacheco-Barrios, K., Battistella, L. R., & Fregni, F. (2024). Distinct patterns of metabolic motor cortex activity for phantom and residual limb pain in people with

amputations: A functional near-infrared spectroscopy study. *Neurophysiologie Clinique*, *54*(1), 102939.

Sloan, G., Shillo, P., Selvarajah, D., Wu, J., Wilkinson, I. D., Tracey, I., Anand, P., & Tesfaye, S. (2018). A new look at painful diabetic neuropathy. *Diabetes Research and Clinical Practice*, *144*, 177–191. https://doi.org/https://doi.org/10.1016/j.diabres.2018.08.020

Sparling, T., Iyer, L., Pasquina, P., & Petrus, E. (2024a). Cortical Reorganization after Limb Loss: Bridging the Gap between Basic Science and Clinical Recovery. *The Journal of Neuroscience*, *44*(1), e1051232024. https://doi.org/10.1523/JNEUROSCI.1051-23.2023

Sparling, T., Iyer, L., Pasquina, P., & Petrus, E. (2024b). Cortical Reorganization after Limb Loss: Bridging the Gap between Basic Science and Clinical Recovery. *Journal of Neuroscience*, *44*(1). https://doi.org/10.1523/JNEUROSCI.1051-23.2023

Srivastava, D. (2017). Chronic post-amputation pain: peri-operative management–Review. *British Journal of Pain*, *11*(4), 192–202.

Srivastava, Devjit. (2017). Chronic post-amputation pain: peri-operative management – Review. *British Journal of Pain*, *11*(4), 192–202. https://doi.org/10.1177/2049463717736492

Stankevicius, A., Wallwork, S. B., Summers, S. J., Hordacre, B., & Stanton, T. R. (2021). Prevalence and incidence of phantom limb pain, phantom limb sensations and telescoping in amputees: A systematic rapid review. *European Journal of Pain*, *25*(1), 23–38. https://doi.org/https://doi.org/10.1002/ejp.1657

Starr, J. M., Wardlaw, J., Ferguson, K., MacLullich, A., Deary, I. J., & Marshall, I. (2003). Increased blood–brain barrier permeability in type II diabetes demonstrated by gadolinium magnetic resonance imaging. *Journal of Neurology, Neurosurgery & Psychiatry*, *74*(1), 70. https://doi.org/10.1136/jnnp.74.1.70

Steinbrink, J., Villringer, A., Kempf, F., Haux, D., Boden, S., & Obrig, H. (2006). Illuminating the BOLD signal: combined fMRI–fNIRS studies. *Magnetic Resonance Imaging*, *24*(4), 495–505.

STOkVIS, Annemie. (2010). *Surgical management of painful neuromas*.

Subedi, B., & Grossberg, G. T. (2011a). Phantom Limb Pain: Mechanisms and Treatment Approaches. *Pain Research and Treatment*, *2011*(1), 864605. https://doi.org/https://doi.org/10.1155/2011/864605

Subedi, B., & Grossberg, G. T. (2011b). Phantom Limb Pain: Mechanisms and Treatment Approaches. *Pain Research and Treatment*, *2011*(1), 864605. https://doi.org/https://doi.org/10.1155/2011/864605

Sun, P., Guo, J., & Xu, N. (2015). Correlation between diabetic lower-extremity arterial disease and diabetic neuropathy in patients with type II diabetes: an exploratory study. In *Int J Clin Exp Med* (Vol. 8, Issue 1). www.ijcem.com/

Sun, Q., Wang, X., Huang, B., Sun, J. C., Li, J., Zhuang, H., & Xiong, G. (2020). Cortical Activation Patterns of Different Masking Noises and Correlation With Their Masking Efficacy, Determined by Functional Near-Infrared Spectroscopy. *Frontiers in Human Neuroscience*, *14*(April), 1–10. https://doi.org/10.3389/fnhum.2020.00149

Swinehart, D. F. (1962). The beer-lambert law. *Journal of Chemical Education*, *39*(7), 333.

Tachibana, A., Noah, J. A., Bronner, S., Ono, Y., & Onozuka, M. (2011). Parietal and temporal activity during a multimodal dance video game: an fNIRS study. *Neuroscience Letters*, *503*(2), 125–130.

Telli, O., & Cavlak, U. (2006). Measuring the pain threshold and tolerance using electrical stimulation in patients with Type II diabetes mellitus. *Journal of Diabetes and Its Complications*, *20*(5), 308–316. https://doi.org/10.1016/j.jdiacomp.2005.07.004

Trevelyan, E. G., Turner, W. A., & Robinson, N. (2016). Perceptions of phantom limb pain in lower limb amputees and its effect on quality of life: a qualitative study. *British Journal of Pain*, *10*(2), 70–77.

Tsuji, T., Arikuni, F., Sasaoka, T., Suyama, S., Akiyoshi, T., Soh, Z., Hirano, H., Nakamura, R., Saeki, N., Kawamoto, M., Yoshizumi, M., Yoshino, A., & Yamawaki, S. (2021). Peripheral arterial stiffness during electrocutaneous stimulation is positively correlated with pain-related brain activity and subjective pain intensity: an fMRI study. *Scientific Reports*, *11*(1), 4425. https://doi.org/10.1038/s41598-021-83833-6

Üçeyler, N., Zeller, J., Kewenig, S., Kittel-Schneider, S., Fallgatter, A. J., & Sommer, C. (2015). Increased cortical activation upon painful stimulation in fibromyalgia syndrome. *BMC Neurology*, *15*(1). https://doi.org/10.1186/s12883-015-0472-4

Vaso, A., Adahan, H.-M., Gjika, A., Zahaj, S., Zhurda, T., Vyshka, G., & Devor, M. (2014). Peripheral nervous system origin of phantom limb pain. *PAIN®*, *155*(7), 1384–1391.

Vierck, C. J., Whitsel, B. L., Favorov, O. V., Brown, A. W., & Tommerdahl, M. (2013). Role of primary somatosensory cortex in the coding of pain. *Pain*, *154*(3), 334–344. https://doi.org/10.1016/j.pain.2012.10.021

Vural Keleş, Ö., & Yıldırım, E. (2023). Depression affects working memory performance: A Functional Near Infrared Spectroscopy (fNIRS) Study. *Psychiatry Research: Neuroimaging*, *329*, 111581. https://doi.org/https://doi.org/10.1016/j.pscychresns.2022.111581

Walter, N., Alt, V., & Rupp, M. (2022). Lower Limb Amputation Rates in Germany. *Medicina (Lithuania)*, *58*(1). https://doi.org/10.3390/medicina58010101

Weeks, S. R., Anderson-Barnes, V. C., & Tsao, J. W. (2010). Phantom limb pain: theories and therapies. *The Neurologist*, *16*(5), 277–286.

Weigel, J. P. (2020). Amputation. In *High-Quality, High-Volume Spay and Neuter and Other Shelter Surgeries* (pp. 375–386). https://doi.org/https://doi.org/10.1002/9781119646006.ch19

WEISS, A. A. (1956). THE PHANTOM LIMB. *Annals of Internal Medicine*, *44*(4), 668–677. https://doi.org/10.7326/0003-4819-44-4-668

Wilcox, R. R. (2011). *Introduction to robust estimation and hypothesis testing*. Academic press.

Wilcox, T., & Biondi, M. (2015a). fNIRS in the developmental sciences. *Wiley Interdisciplinary Reviews: Cognitive Science*, *6*(3), 263–283.

Wilcox, T., & Biondi, M. (2015b). fNIRS in the developmental sciences. *Wiley Interdisciplinary Reviews: Cognitive Science*, *6*(3), 263–283.

Willems, R. M., & Cristia, A. (2017). Hemodynamic Methods: fMRI and fNIRS. In *Research Methods in Psycholinguistics and the Neurobiology of Language* (pp. 266–287). https://doi.org/https://doi.org/10.1002/9781394259762.ch14

Williamson, A., & Hoggart, B. (2005). Pain: A review of three commonly used pain rating scales. *Journal of Clinical Nursing*, *14*(7), 798–804. https://doi.org/10.1111/j.1365-2702.2005.01121.x

Wulf, M. J., & Tom, V. J. (2023). Consequences of spinal cord injury on the sympathetic nervous system. *Frontiers in Cellular Neuroscience*, *17*. https://www.frontiersin.org/journals/cellular-neuroscience/articles/10.3389/fncel.2023.999253

Xia, M., Wang, J., & He, Y. (2013). BrainNet Viewer: A Network Visualization Tool for Human Brain Connectomics. *PLoS ONE*, *8*(7). https://doi.org/10.1371/journal.pone.0068910

Xie, H.-M., Zhang, K.-X., Wang, S., Wang, N., Wang, N., Li, X., & Huang, L.-P. (2022). Effectiveness of mirror therapy for phantom limb pain: a systematic review and meta-analysis. *Archives of Physical Medicine and Rehabilitation*, *103*(5), 988–997.

Yan, T., Liang, M., Peng, J., Yu, Q., Li, Y., Yang, J., Zhang, S., & Wang, C. (2024). Cortical Mechanisms Underlying Effects of Repetitive Peripheral Magnetic Stimulation on Dynamic and Static Postural Control in Patients with Chronic Non-

Specific Low Back Pain: A Double-Blind Randomized Clinical Trial. *Pain and Therapy*, *13*(4), 953–970. https://doi.org/10.1007/s40122-024-00613-6

Yang, D. R., Wang, M. Y., Zhang, C. L., & Wang, Y. (2024). Endothelial dysfunction in vascular complications of diabetes: a comprehensive review of mechanisms and implications. In *Frontiers in Endocrinology* (Vol. 15). Frontiers Media SA. https://doi.org/10.3389/fendo.2024.1359255

Yarnitsky, D., Barron, S. A., & Bental, E. (1988). Disappearance of phantom pain after focal brain infarction. *PAIN*, *32*(3). https://journals.lww.com/pain/fulltext/1988/03000/disappearance_of_phantom_pain_after_focal_brain.5.aspx

Ye, J. C., Tak, S., Jang, K. E., Jung, J., & Jang, J. (2009). NIRS-SPM: Statistical parametric mapping for near-infrared spectroscopy. *NeuroImage*, *44*(2), 428–447. https://doi.org/10.1016/j.neuroimage.2008.08.036

Yildirim, M., & Kanan, N. (2016). The effect of mirror therapy on the management of phantom limb pain. *Agri*, *28*(3), 127–134.

Yin, Y., Zhang, L., Xiao, H., Wen, C.-B., Dai, Y.-E., Yang, G., Zuo, Y.-X., & Liu, J. (2017). The pre-amputation pain and the postoperative deafferentation are the risk factors of phantom limb pain: a clinical survey in a sample of Chinese population. *BMC Anesthesiology*, *17*, 1–6.

Yücel, M. A., Aasted, C. M., Petkov, M. P., Borsook, D., Boas, D. A., & Becerra, L. (2015). Specificity of Hemodynamic Brain Responses to Painful Stimuli: A functional near-infrared spectroscopy study. *Scientific Reports*, *5*, 1–9. https://doi.org/10.1038/srep09469

Zhang, H., Lu, X., Bi, Y., & Hu, L. (2021). A modality selective effect of functional laterality in pain detection sensitivity. *Scientific Reports*, *11*(1). https://doi.org/10.1038/s41598-021-85111-x

Zhang, J., Zhang, Y., Wang, L., Sang, L., Li, L., Li, P., Yin, X., & Qiu, M. (2018). Brain Functional Connectivity Plasticity Within and Beyond the Sensorimotor Network in

Lower-Limb Amputees. *Frontiers in Human Neuroscience*, *12*. https://doi.org/10.3389/fnhum.2018.00403

Zhou, X., Sobczak, G., McKay, C. M., & Litovsky, R. Y. (2020). Comparing fNIRS signal qualities between approaches with and without short channels. *PloS One*, *15*(12), e0244186.

7 APPENDIX

Supplementary Table A-1

Descriptive statistics and normality test results of stimulation intensities with a unit of milliamps (mA) over the two stimulation modalities and four different body sites.

Body sites	Stimulation modality	Number	Mean ± SD (mA)	Normality Test (*p*)
Left groin	Painful	16	1.62 ± 2.25	Not normal ($p = 0.0004$)
Left groin	Non-painful	16	0.68 ± 1.26	Not normal ($p = 0.0000$)
Right groin	Pain	16	0.81 ± 1.21	Not normal ($p = 0.0002$)
Right groin	Non-painful	16	0.22 ± 0.30	Not normal ($p = 0.0002$)
Left knee	Pain	16	0.20 ± 0.22	Not normal ($p = 0.0011$)
Left knee	Non-painful	16	0.07 ± 0.09	Not normal ($p = 0.0002$)
Right knee	Pain	16	0.26 ± 0.32	Not normal ($p = 0.0003$)
Right knee	Non-painful	16	0.12 ± 0.15	Not normal ($p = 0.0001$)

Note: Number represents sample sizes; SD means Standard deviation; Normality Test represents the result from Shapiro-Wilk normality test.

Supplementary Table A-2

Post-hoc multiple comparisons between the stimulation intensity of each body site.

(I)Body sites	(J)Body sites	Mean difference(I-J)	*p*	Cohen's *d*	95% Confidence Interval	
					Lower Bound	Upper Bound
	Right groin	0.63	0.0691	0.4326	-0.03	1.30
Left groin	Left knee	1.01	0.0007	0.7671	0.34	1.68
	Right knee	0.96	0.0015	0.7246	0.29	1.63
	Left groin	-0.63	0.0691	-0.4326	-1.30	0.03
Right groin	Left knee	0.38	0.4540	0.5734	-0.29	1.04
	Right knee	0.33	0.5789	0.4861	-0.34	0.99
	Left groin	-1.01	0.0007	-0.7671	-1.68	-0.34
Left knee	Right groin	-0.38	0.4540	-0.5734	-1.04	0.29
	Right knee	-0.05	0.9971	-0.2334	-0.72	0.62
	Left groin	-0.96	0.0015	-0.7246	-1.63	-0.29
Right knee	Right groin	-0.33	0.5789	-0.4861	-0.99	0.34
	Left knee	0.05	0.9971	0.2334	-0.62	0.72

Supplementary Table A-3

Descriptive statistics and normality test results of VAS ratings (ranging from "No sensation" to "Extreme pain," with values from 0 to 100) over the two stimulation modalities, two time points and four different body sites.

Body sites	Stimulation modality	Time	Number	Mean ± SD	Normality Test (*p*)
Left groin	Painful	Before	16	75.75 ± 7.30	Normal (p = 0.4660)
Left groin	Painful	After	16	75.88 ± 11.47	Not Normal (p = 0.0320)
Left groin	Non-painful	Before	16	23.88 ± 10.08	Normal (p = 0.6432)
Left groin	Non-painful	After	16	23.50 ± 14.30	Normal (p = 0.6355)
Right groin	Pain	Before	16	73.25 ± 8.06	Normal (p = 0.6013)
Right groin	Pain	After	16	76.25 ± 8.91	Normal (p = 0.4879)
Right groin	Non-painful	Before	16	22.00 ± 10.33	Normal (p = 0.1226)
Right groin	Non-painful	After	16	18.13 ± 11.72	Normal (p = 0.1031)
Left knee	Painful	Before	16	81.50 ± 6.35	Not Normal (p = 0.0060)
Left knee	Painful	After	16	84.13 ± 8.02	Normal (p = 0.6676)
Left knee	Non-painful	Before	16	27.00 ± 10.46	Normal (p = 0.6531)
Left knee	Non-painful	After	16	23.88 ± 14.56	Not Normal (p = 0.0332)
Right knee	Pain	Before	16	80.75 ± 6.57	Normal (p = 0.8161)
Right knee	Pain	After	16	79.38 ± 13.60	Not Normal (p = 0.0093)
Right knee	Non-painful	Before	16	25.63 ± 11.89	Normal (p = 0.5740)
Right knee	Non-painful	After	16	25.25 ± 13.80	Normal (p = 0.1927)

Note: Number represents sample sizes; SD means Standard deviation; Normality Test represents the result from Shapiro-Wilk normality test.

Supplementary Table A-4

Post-hoc multiple comparisons between the VAS ratings of each body site.

(I)Body sites	(J)Body sites	Mean difference(I-J)	*p*	Cohen's *d*	95% Confidence Interval	
					Lower Bound	Upper Bound
Left groin	Left knee	-4.38	0.2697	-1.8987	-11.02	2.27
	Right groin	2.34	0.4276	1.5627	-1.98	6.67
	Right knee	-3.00	0.6892	-1.1099	-10.79	4.79
Left knee	Left groin	4.38	0.2697	1.8987	-2.27	11.02
	Right groin	6.72	0.0507	2.8747	-0.02	13.45
	Right knee	1.38	0.8569	0.7921	-3.63	6.38
Right groin	Left groin	-2.34	0.4276	-1.5627	-6.67	1.98
	Left knee	-6.72	0.0507	-2.8747	-13.45	0.02
	Right knee	-5.34	0.2442	-1.9648	-13.18	2.50
Right knee	Left groin	3.00	0.6892	1.1099	-4.79	10.79
	Left knee	-1.38	0.8569	-0.7921	-6.38	3.63
	Right groin	5.34	0.2442	1.9648	-2.50	13.18

Supplementary Table A-5

Descriptive statistics and normality test results of β values (HbO2) over the two stimulation modalities, four different body sites and three brain regions.

Body sites	Stimulation modality	Brain region	Number	Mean ± SD ($\times 10^{-5}$)	Normality Test (p)
Left groin	Non-painful	Left S1	13	2.15 ± 0.81	Not normal (p = 0.0055)
Left groin	Non-painful	Right S1	13	3.10 ± 1.30	Not normal (p = 0.0021)
Left groin	Non-painful	PFC	13	0.85 ± 1.73	Not normal (p = 0.0031)
Left groin	Painful	Left S1	13	-2.20 ± 1.71	Not normal (p = 0.0345)
Left groin	Painful	Right S1	13	0.53 ± 2.50	Not normal (p = 0.0045)
Left groin	Painful	PFC	13	-3.91 ± 1.81	Normal (p = 0.3281)
Right groin	Non-painful	Left S1	16	2.05 ± 1.37	Normal (p = 0.8412)
Right groin	Non-painful	Right S1	16	4.70 ± 1.02	Normal (p = 0.0906)
Right groin	Non-painful	PFC	16	-0.32 ± 1.36	Normal (p = 0.8685)
Right groin	Painful	Left S1	16	2.51 ± 1.81	Not normal (p = 0.0328)
Right groin	Painful	Right S1	16	3.32 ± 1.15	Normal (p = 0.9613)
Right groin	Painful	PFC	16	-0.68 ± 1.65	Normal (p = 0.8918)
Left knee	Non-painful	Left S1	16	2.23 ± 1.25	Normal (p = 0.8633)
Left knee	Non-painful	Right S1	16	3.25 ± 2.97	Normal (p = 0.2854)
Left knee	Non-painful	PFC	16	-0.35 ± 1.49	Normal (p = 0.5882)
Left knee	Painful	Left S1	16	3.23 ± 1.49	Not normal (p = 0.0147)
Left knee	Painful	Right S1	16	3.80 ± 3.07	Not normal (p = 0.0145)
Left knee	Painful	PFC	16	-1.14 ± 2.95	Not normal (p = 0.0399)
Right knee	Non-painful	Left S1	15	-2.62 ± 1.88	Normal (p = 0.0787)
Right knee	Non-painful	Right S1	15	0.39 ± 1.57	Normal (p = 0.6343)
Right knee	Non-painful	PFC	15	-1.27 ± 2.36	Not normal (p = 0.0487)
Right knee	Painful	Left S1	15	2.92 ± 2.97	Normal (p = 0.0834)
Right knee	Painful	Right S1	15	4.79 ± 1.99	Normal (p = 0.4295)
Right knee	Painful	PFC	15	-0.33 ± 3.14	Normal (p = 0.3822)

Note: Number represents sample sizes; SD means Standard deviation; Normality Test represents the result from Shapiro-Wilk normality test.

Supplementary Table A-6

Table for β values (HbO2). Repeated-measures analysis of variance (ANOVA) with factors body sites, stimulation modality (non-painful, painful), brain groin (left S1, right S1 and PFC).

Source	Df	F	*p*	η^2
Body sites	3	0.16	0.9214	0.014
Stimulation modality	1	0.10	0.7609	0.009
Brain region	2	9.18	0.0013	0.455
Body sites*stimulation modality	3	1.23	0.3144	0.101
Body sites*brain region	6	0.69	0.6609	0.059
Stimulation modality*brain region	2	0.30	0.7460	0.026
Body sites*stimulation modality*brain region	6	3.12	0.0094	0.221

Note: Df means degree of freedom.

Supplementary Table A-7

Post-hoc multiple comparisons between the β values (HbO2) of each brain region.

(I)Brain region	(J)Brain region	Mean difference (I-J)	*p*	Cohen's d	95% confidence interval	
					Lower Bound	Upper Bound
Left S1	PFC	2.31E-05	0.0880	0.2177	-3.30E-06	4.96E-05
	Right S1	-2.09E-05	0.0851	-0.1662	-4.46E-05	2.78E-06
PFC	Left S1	-2.31E-05	0.0880	-0.2177	-4.96E-05	3.30E-06
	Right S1	-4.41E-05	0.0096	-0.4264	-7.66E-05	-1.16E-05
Right S1	Left S1	2.09E-05	0.0851	0.1662	-2.78E-06	4.46E-05
	PFC	4.41E-05	0.0096	0.4264	1.16E-05	7.66E-05

Supplementary Table A-8

Post-hoc multiple comparisons between the β values (HbO2) of different brain regions when stimulating different body sites.

Body sites	Brain regions	$Mean_{pain}$ ($\times 10^{-5}$)	$Mean_{non\text{-}pain}$ ($\times 10^{-5}$)	SD_{pain} ($\times 10^{-5}$)	$SD_{non\text{-}pain}$ ($\times 10^{-5}$)	*p*	Cohen's *d*
left groin	left S1	-2.20	2.15	1.71	0.81	**0.0002**	-3.2560
	right S1	0.53	3.10	2.50	1.30	**0.0096**	-1.2890
	PFC	-3.91	0.85	1.81	1.73	**<0.0001**	-2.6847
right groin	left S1	2.51	2.05	1.81	1.37	0.2746	0.2900
	right S1	3.32	4.70	1.15	1.02	**0.0185**	-1.2739
	PFC	-0.68	-0.32	1.65	1.36	0.1210	-0.2344
left knee	left S1	3.23	2.23	1.49	1.25	0.1559	0.7255
	right S1	3.80	3.25	3.07	2.97	0.4590	0.1816
	PFC	-1.14	-0.35	2.95	1.49	0.1537	-0.3372
right knee	left S1	2.92	-2.62	2.97	1.88	**0.0002**	2.2288
	right S1	4.79	0.39	1.99	1.57	**0.0002**	2.4612
	PFC	-0.33	-1.27	3.14	2.36	**0.0086**	0.3362

Note: SD means Standard deviation. Bold p-values indicate statistical significance after controlling for false discovery rate (FDR).

Supplementary Figure A-1

Topographic brain activity and group-averaged β value comparisons across body site Stimulations.

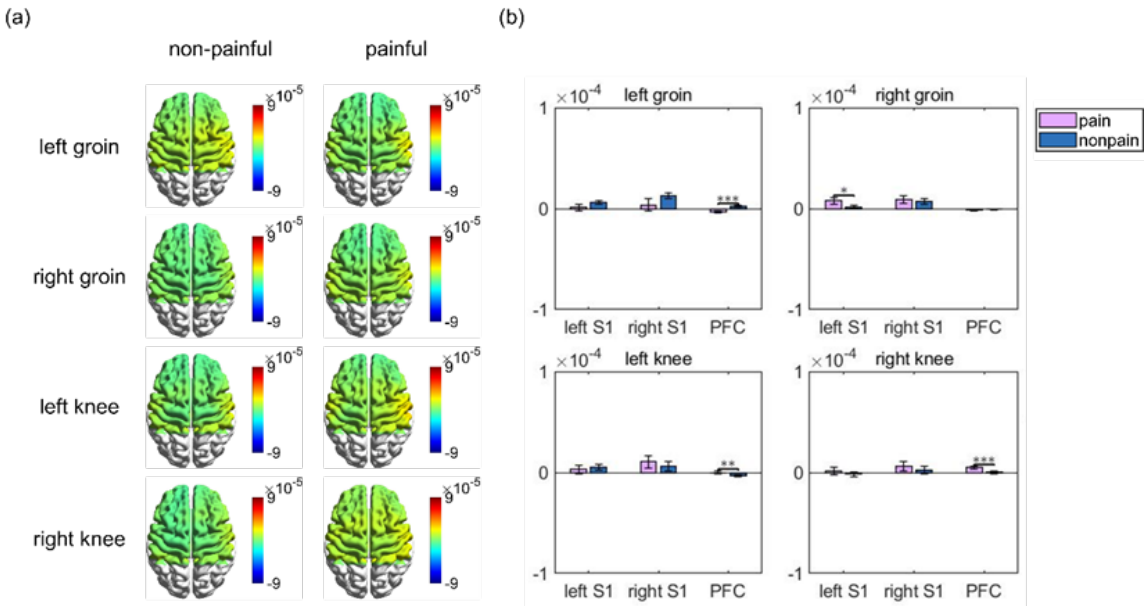

Notes: (a) Topographic images of group-averaged cortical deactivations and/or activations (HbR) during non-painful and painful stimulation modalities given on each body site. (b) Comparisons of the group-averaged β values (HbR) of different brain regions when stimulating different body sites. The pink bar represents the painful stimuli, and the blue bar represents the non-painful stimuli. Left S1 means left primary somatosensory area, right S1 means right primary somatosensory area, and PFC means prefrontal area. Error bars represent the standard error of the mean. (= p<0.05, **= p<0.01 and ***= p<0.001).*

Supplementary Table A-9

Comparisons of the group-averaged β values (HbR) of different brain regions when stimulating different body sites.

Body sites	Brain regions	$Mean_{pain}$ ($\times 10^{-5}$)	$Mean_{non\text{-}pain}$ ($\times 10^{-5}$)	SD_{pain} ($\times 10^{-5}$)	$SD_{non\text{-}pain}$ ($\times 10^{-5}$)	*p*	Cohen's *d*
left groin	left S1	0.11	0.66	0.90	0.50	0.0294	-0.7482
	right S1	0.38	1.26	1.61	0.77	0.0454	-0.6987
	PFC	-0.36	0.21	0.53	0.39	**<0.0001**	-1.2199
right groin	left S1	0.80	0.16	0.86	0.38	**0.0160**	0.9552
	right S1	0.90	0.68	0.91	0.79	0.3749	0.2596
	PFC	-0.16	-0.09	0.33	0.46	0.3795	-0.1753
left knee	left S1	0.31	0.53	1.08	0.76	0.3833	-0.2371
	right S1	1.04	0.62	1.62	1.28	0.1961	0.2909
	PFC	-0.03	-0.35	0.66	0.35	**0.0024**	0.5994
right knee	left S1	0.15	-0.15	0.95	0.61	0.2752	0.3750
	right S1	0.64	0.26	1.27	1.00	0.0892	0.3377
	PFC	0.49	0.02	0.71	0.66	**<0.0001**	0.6967

Note: SD means Standard deviation. Bold p-values indicate statistical significance after controlling for false discovery rate (FDR).

Supplementary Table A-10

Channel location and β values (HbO2) for per channel.

Channel	Source	Detector	X (mm)	Y (mm)	Z (mm)	Landmark	Left groin		Right groin		Left knee		Right knee	
							β (np)	β (p)	β (np)	β (p)	β (np)	β (p)	β (np)	β (p)
1	AF3	AFz	-12	62	23	10 9 46	-1.37E-05	-8.66E-05	-7.19E-06	-5.32E-06	-1.52E-05	-6.96E-06	-3.37E-05	-2.12E-06
2	AF3	F1	-23	52	32	9 46 10	-1.20E-05	-7.66E-05	-1.38E-05	-1.93E-05	-2.74E-05	-3.89E-05	-4.37E-05	-3.72E-05
3	AF3	F5	-39	50	17	46 45 10	1.34E-05	-4.21E-05	-9.08E-07	2.69E-06	-1.20E-05	1.98E-05	1.17E-06	2.90E-05
4	AF3	Fp1	-24	63	9	10 11 46	-1.10E-05	-6.44E-05	-2.06E-05	-1.98E-05	-2.52E-05	-6.22E-06	-2.07E-05	1.47E-05
5	AF4	AFz	13	61	24	10 9 46	-1.34E-05	-6.11E-05	-9.10E-06	5.64E-06	1.98E-06	-1.76E-06	-1.84E-05	9.42E-06
6	AF4	F2	22	52	33	9 46 10	-1.24E-05	-8.04E-05	-1.55E-05	-1.70E-05	-3.13E-06	-2.18E-05	-1.02E-05	-9.51E-06
7	AF4	F6	40	50	16	46 45 10	1.22E-05	-2.86E-05	-5.45E-07	4.59E-06	3.32E-05	3.53E-05	3.12E-05	4.37E-05
8	AF4	Fp2	25	63	9	10 11 46	-1.39E-05	-4.73E-05	-6.20E-06	-5.88E-06	1.03E-05	2.01E-05	1.80E-05	3.45E-05
9	C3	FC3	-50	-3	50	6 4 3 9	8.15E-06	-6.66E-05	1.99E-06	-5.95E-06	1.41E-05	8.28E-06	-4.40E-05	-2.40E-05
10	C3	C1	-42	-20	62	4 6 3	1.46E-05	-4.17E-05	5.18E-06	1.60E-05	2.87E-05	2.57E-05	-3.80E-05	6.19E-06
11	C3	C5	-60	-18	37	3 43 2 48 4 1	2.45E-05	-1.59E-05	2.15E-05	2.36E-05	3.83E-06	3.97E-05	-3.84E-05	4.01E-06
12	C3	CP3	-52	-34	52	40 2 3 1	3.29E-05	-2.24E-05	2.52E-05	1.74E-05	3.62E-05	3.90E-05	-1.60E-05	1.47E-05
13	C4	FC4	52	-4	48	6 4 3 9	2.56E-05	-3.65E-05	3.84E-05	1.24E-05	-1.15E-05	1.75E-07	7.82E-07	2.50E-05
14	C4	C2	42	-21	62	4 6 3	1.23E-05	-3.60E-05	4.06E-05	2.43E-05	2.45E-05	1.37E-05	-4.16E-06	9.01E-06
15	C4	C6	62	-20	37	2 3 43 1 48 4 40	1.76E-05	1.25E-05	3.92E-05	3.60E-05	-1.12E-06	2.73E-05	6.03E-06	3.94E-05
16	C4	CP4	53	-35	52	40 2 3 1	3.31E-05	-8.13E-06	6.72E-05	3.98E-05	5.56E-05	3.75E-05	1.62E-05	4.02E-05
17	Fz	AFz	2	50	39	9 10 8 32	9.72E-06	-4.26E-05	5.20E-06	-2.02E-06	3.40E-06	-2.14E-05	-2.13E-05	-3.05E-05
18	Fz	F1	-9	41	50	9 8	1.44E-05	-4.82E-05	-2.76E-06	7.51E-06	-8.97E-06	-5.37E-05	-3.30E-05	-6.87E-05
19	Fz	F2	10	41	50	9 8	1.47E-05	-4.91E-05	-4.90E-07	2.37E-06	-6.23E-06	-5.39E-05	-2.41E-05	-5.69E-05
20	Fz	FCz	1	27	58	8 6 9	3.15E-05	-3.51E-05	1.72E-05	2.65E-05	1.87E-07	-4.45E-05	-3.00E-05	-5.02E-05
21	F3	F1	-31	39	41	9 46	-1.67E-05	-5.77E-05	-1.30E-05	-2.80E-05	-7.61E-06	-3.92E-05	-3.73E-05	-5.03E-05
22	F3	F5	-46	39	26	45 46	3.19E-06	-5.01E-05	-5.21E-06	-1.68E-05	3.43E-06	-9.79E-06	-8.16E-06	-4.62E-06
23	F3	FC3	-45	25	41	9 44 45 46 6	-4.77E-07	-7.17E-05	-8.16E-06	-3.91E-05	-7.41E-06	-2.87E-05	-3.36E-05	-3.34E-05
24	F4	F2	30	40	41	9 46 8	9.20E-06	-6.04E-05	-5.99E-06	3.06E-06	-3.99E-06	-4.05E-05	-1.89E-05	-1.82E-05
25	F4	F6	46	38	24	45 46	1.54E-05	-4.06E-05	-3.32E-06	3.62E-06	8.05E-06	1.02E-05	1.06E-05	2.23E-05
26	F4	FC4	44	25	40	9 44 46 45 6	3.69E-05	-4.63E-05	2.13E-05	8.01E-07	1.90E-05	-1.53E-05	-4.24E-06	-1.10E-05

Table A-10. Channel location and β values (HbO2) for per channel (continued).

Channel	Source	Detector	X (mm)	Y (mm)	Z (mm)	Landmark	Left groin		Right groin		Left knee		Right knee	
							β (np)	β (p)	β (np)	β (p)	β (np)	β (p)	β (np)	β (p)
27	Fpz	AFz	1	64	14	10 9	-2.66E-05	-6.05E-05	-1.13E-05	-5.42E-06	-1.59E-05	-4.93E-06	-1.95E-05	-4.22E-06
28	Fpz	Fp1	-12	67	0	10 11	-3.74E-05	-6.51E-05	-2.54E-05	-3.47E-05	-2.90E-05	-1.40E-05	-3.47E-05	-1.85E-05
29	Fpz	Fp2	13	67	0	10 11	-2.31E-05	-5.82E-05	-3.59E-05	-2.40E-05	-3.37E-05	-3.06E-07	-1.42E-05	1.33E-05
30	AF7	F5	-47	46	6	45 46	2.26E-05	-2.51E-05	4.81E-06	-3.73E-06	4.52E-06	3.16E-05	1.27E-05	1.24E-05
31	AF7	Fp1	-33	59	-2	11 46 10 47	2.13E-06	-3.10E-05	-4.62E-07	-1.42E-06	-1.21E-05	1.90E-05	-1.07E-05	3.36E-06
32	AF8	F6	48	46	5	45 46 47	3.31E-05	9.52E-06	2.66E-05	2.92E-05	1.18E-05	4.76E-05	3.65E-05	4.96E-05
33	AF8	Fp2	34	59	-2	10 11 46 47	-1.61E-05	-4.14E-06	1.13E-05	7.04E-06	-4.03E-07	3.62E-05	3.42E-05	2.60E-05
34	CP1	C1	-27	-36	71	4 3 6 7 1 2 5	3.22E-05	7.59E-06	2.89E-05	4.30E-05	1.09E-05	2.54E-05	-2.17E-05	4.81E-05
35	CP1	CP3	-39	-48	60	40 7 2 3	2.89E-05	-1.17E-05	4.17E-05	4.48E-05	3.33E-05	3.16E-05	-1.72E-05	3.62E-05
36	CP2	C2	28	-36	71	4 3 6 7 1 2 5	3.76E-05	1.92E-05	4.35E-05	4.67E-05	3.89E-05	3.13E-05	-1.30E-05	2.44E-05
37	CP2	CP4	39	-49	60	40 7 2 3	3.80E-05	8.12E-06	4.92E-05	4.01E-05	5.85E-05	6.64E-05	2.47E-05	3.37E-05
38	CP5	C5	-63	-32	23	48 22 42 2 40	3.09E-05	-1.05E-05	1.89E-05	3.69E-05	2.89E-05	5.62E-05	1.16E-05	5.81E-05
39	CP5	CP3	-57	-48	38	40 39 48 22	3.75E-05	-1.45E-05	3.86E-05	1.64E-05	2.59E-05	4.41E-05	1.28E-05	3.91E-05
40	CP6	C6	65	-33	23	22 48 2 40 42	2.67E-05	1.81E-05	5.11E-05	3.32E-05	6.28E-05	8.97E-05	2.99E-05	8.22E-05
41	CP6	CP4	58	-48	38	40 39 48 22	4.88E-05	1.16E-05	4.89E-05	2.89E-05	6.96E-05	6.92E-05	4.19E-05	6.72E-05
42	FC2	F2	24	26	55	8 9 6	1.05E-05	-4.86E-05	7.15E-06	-8.17E-07	4.42E-07	-4.12E-05	-6.39E-06	-3.37E-05
43	FC2	FC4	39	12	54	6 9 8	1.42E-05	-4.04E-05	1.54E-05	-1.21E-05	1.03E-05	-2.18E-05	1.65E-05	-5.08E-06
44	FC2	C2	27	-4	68	6 8	7.85E-06	-3.65E-05	1.17E-05	6.64E-06	1.71E-05	-6.57E-07	-1.26E-05	-3.45E-06
45	FC2	FCZ	14	13	66	6 8	1.37E-05	-1.99E-05	1.91E-05	1.69E-05	1.49E-05	-1.56E-05	-1.38E-05	-2.55E-05
46	FC1	F1	-23	26	56	8 9 6	-6.37E-06	-6.75E-05	-8.07E-06	-2.17E-05	-1.18E-05	-5.52E-05	-3.86E-05	-5.69E-05
47	FC1	FC3	-38	12	55	6 9 8	-2.10E-05	-6.33E-05	-8.05E-06	-3.17E-05	1.09E-05	-3.07E-05	-1.81E-05	-2.78E-05
48	FC1	C1	-26	-5	68	6 8 4	2.89E-06	-5.22E-05	-5.10E-07	-1.38E-05	1.13E-05	-6.72E-06	-2.11E-05	5.10E-06
49	FC1	FCZ	-13	12	67	6 8	9.39E-06	-3.47E-05	1.86E-05	1.78E-05	-6.91E-07	-4.56E-05	-3.72E-05	-3.43E-05

Note: X, Y, Z coordinates refer to the spatial locations in the brain based on the MNI coordinate system. Landmark represents the Brodmann area (1, 2, 3 - Primary Somatosensory Cortex; 4 - Primary Motor Cortex; 5, 7 - Somatosensory Association Cortex; 6 - Pre-Motor and Supplementary Motor Cortex; 8 - Includes Frontal eye fields; 9 - Dorsolateral prefrontal cortex; 10 - Frontopolar area; 11 - Orbitofrontal area; 22 - Superior Temporal Gyrus; 32 - Dorsal anterior cingulate cortex; 40 - Supramarginal gyrus part

of Wernicke's area; 42 - Primary and Auditory Association Cortex; 43 - Subcentral area; 44 - pars opercularis, part of Broca's area; 45 - pars triangularis Broca's area; 46 - Dorsolateral prefrontal cortex; 47 - Inferior prefrontal gyrus; 48 - Retrosubicular area). β values (np) means the β values for the non-painful stimulation modality; β values (p) means the β values for the painful stimulation modality.

Supplementary Table B-1

The detailed information for each channel.

Channel	Source	Detector	X (mm)	Y (mm)	Z (mm)	Landmark	Specificity (%)
1	AF3	Afz	-12	62	23	10 - Frontopolar area	75.76
						9 - Dorsolateral prefrontal cortex	14.55
						46 - Dorsolateral prefrontal cortex	8.05
2	AF3	F1	-23	52	32	9 - Dorsolateral prefrontal cortex	48.44
						46 - Dorsolateral prefrontal cortex	32.04
						10 - Frontopolar area	16.89
3	AF3	F5	-39	50	17	46 - Dorsolateral prefrontal cortex	49.34
						45 - pars triangularis Broca's area	32.12
						10 - Frontopolar area	16.04
4	AF3	Fp1	-24	63	9	10 - Frontopolar area	69.63
						11 - Orbitofrontal area	20.12
						46 - Dorsolateral prefrontal cortex	8.79
5	AF4	Afz	13	61	24	10 - Frontopolar area	72.47
						9 - Dorsolateral prefrontal cortex	16.97
						46 - Dorsolateral prefrontal cortex	7.98
6	AF4	F2	22	52	33	9 - Dorsolateral prefrontal cortex	51.52
						46 - Dorsolateral prefrontal cortex	26.42
						10 - Frontopolar area	18.41
7	AF4	F6	40	50	16	46 - Dorsolateral prefrontal cortex	47.36
						45 - pars triangularis Broca's area	30.60
						10 - Frontopolar area	18.97
8	AF4	Fp2	25	63	9	10 - Frontopolar area	68.78
						11 - Orbitofrontal area	21.57
						46 - Dorsolateral prefrontal cortex	6.61
9	C3	C1	-42	-20	62	4 - Primary Motor Cortex	34.98
						6 - Pre-Motor and Supplementary Motor Cortex	34.57
						3 - Primary Somatosensory Cortex	24.55
10	C3	FC3	-50	-3	50	6 - Pre-Motor and Supplementary Motor Cortex	61.71
						4 - Primary Motor Cortex	17.58
						3 - Primary Somatosensory Cortex	9.24
						9 - Dorsolateral prefrontal cortex	6.95
11	C3	C5	-60	-18	37	3 - Primary Somatosensory Cortex	23.83
						43 - Subcentral area	21.28
						2 - Primary Somatosensory Cortex	17.78
						48 - Retrosubicular area	12.95
						4 - Primary Motor Cortex	10.46
						1 - Primary Somatosensory Cortex	6.86
12	C3	CP3	-52	-34	52	40 - Supramarginal gyrus part of Wernicke's area	43.32
						2 - Primary Somatosensory Cortex	22.52
						3 - Primary Somatosensory Cortex	21.18
						1 - Primary Somatosensory Cortex	6.96
13	C4	C2	42	-21	62	4 - Primary Motor Cortex	36.77
						6 - Pre-Motor and Supplementary Motor Cortex	29.48
						3 - Primary Somatosensory Cortex	25.60
14	C4	FC4	52	-4	48	6 - Pre-Motor and Supplementary Motor Cortex	56.87
						4 - Primary Motor Cortex	19.48
						3 - Primary Somatosensory Cortex	11.41
						9 - Dorsolateral prefrontal cortex	6.12
15	C4	C6	62	-20	37	2 - Primary Somatosensory Cortex	27.65
						3 - Primary Somatosensory Cortex	19.92
						43 - Subcentral area	16.21
						1 - Primary Somatosensory Cortex	12.30
						48 - Retrosubicular area	7.94
						4 - Primary Motor Cortex	6.47
						40 - Supramarginal gyrus part of Wernicke's area	5.22
16	C4	CP4	53	-35	52	40 - Supramarginal gyrus part of Wernicke's area	50.04
						2 - Primary Somatosensory Cortex	18.86
						3 - Primary Somatosensory Cortex	17.66
						1 - Primary Somatosensory Cortex	8.36
17	Cz	C1	-17	-20	74	6 - Pre-Motor and Supplementary Motor Cortex	56.45
						4 - Primary Motor Cortex	39.76
18	Cz	C2	17	-21	75	6 - Pre-Motor and Supplementary Motor Cortex	55.39
						4 - Primary Motor Cortex	39.92
19	Cz	Cpz	1	-35	75	4 - Primary Motor Cortex	47.13
						5 - Somatosensory Association Cortex	29.14
						6 - Pre-Motor and Supplementary Motor Cortex	10.54
						3 - Primary Somatosensory Cortex	5.31
20	Cz	FCz	-1	-4	72	6 - Pre-Motor and Supplementary Motor Cortex	83.77
						4 - Primary Motor Cortex	11.38
21	Fz	Afz	2	50	39	9 - Dorsolateral prefrontal cortex	61.77
						10 - Frontopolar area	20.26
						8 - Includes Frontal eye fields	12.15
						32 - Dorsal anterior cingulate cortex	5.08
22	Fz	F1	-9	41	50	9 - Dorsolateral prefrontal cortex	63.16
						8 - Includes Frontal eye fields	34.73
23	Fz	F2	10	41	50	9 - Dorsolateral prefrontal cortex	68.93
						8 - Includes Frontal eye fields	28.89
24	Fz	FCz	1	27	58	8 - Includes Frontal eye fields	60.02
						6 - Pre-Motor and Supplementary Motor Cortex	24.18
						9 - Dorsolateral prefrontal cortex	12.94

Table B-S1: The detailed information for each channel (continued)

Channel	Source	Detector	X (mm)	Y (mm)	Z (mm)	Landmark	Specificity (%)
25	Cp1	C1	-27	-36	71	4 - Primary Motor Cortex	31.56
						3 - Primary Somatosensory Cortex	19.10
						6 - Pre-Motor and Supplementary Motor Cortex	14.37
						7 - Somatosensory Association Cortex	12.31
						1 - Primary Somatosensory Cortex	8.91
						2 - Primary Somatosensory Cortex	6.85
						5 - Somatosensory Association Cortex	5.28
26	Cp1	Cpz	-16	-50	72	5 - Somatosensory Association Cortex	52.42
						7 - Somatosensory Association Cortex	24.93
						1 - Primary Somatosensory Cortex	8.79
27	Cp1	Cp3	-39	-48	60	40 - Supramarginal gyrus part of Wernicke's area	41.82
						7 - Somatosensory Association Cortex	27.06
						2 - Primary Somatosensory Cortex	16.43
						3 - Primary Somatosensory Cortex	5.57
28	Cp1	P1	-24	-62	62	7 - Somatosensory Association Cortex	82.72
						5 - Somatosensory Association Cortex	9.60
29	Cp2	C2	28	-36	71	4 - Primary Motor Cortex	24.07
						3 - Primary Somatosensory Cortex	24.04
						6 - Pre-Motor and Supplementary Motor Cortex	18.02
						7 - Somatosensory Association Cortex	11.62
						1 - Primary Somatosensory Cortex	7.95
						2 - Primary Somatosensory Cortex	6.91
						5 - Somatosensory Association Cortex	5.23
30	Cp2	Cpz	17	-50	73	5 - Somatosensory Association Cortex	47.39
						7 - Somatosensory Association Cortex	30.46
						3 - Primary Somatosensory Cortex	7.00
						1 - Primary Somatosensory Cortex	6.80
31	Cp2	Cp4	39	-49	60	40 - Supramarginal gyrus part of Wernicke's area	45.11
						7 - Somatosensory Association Cortex	25.25
						2 - Primary Somatosensory Cortex	13.53
						3 - Primary Somatosensory Cortex	5.76
32	Cp2	P2	25	-62	63	7 - Somatosensory Association Cortex	86.02
						5 - Somatosensory Association Cortex	6.62
33	F3	F1	-31	39	41	9 - Dorsolateral prefrontal cortex	66.61
						46 - Dorsolateral prefrontal cortex	24.85
34	F3	F5	-46	39	26	45 - pars triangularis Broca's area	72.56
						46 - Dorsolateral prefrontal cortex	21.84
35	F3	FC3	-45	25	41	9 - Dorsolateral prefrontal cortex	36.92
						44 - pars opercularis, part of Broca's area	26.54
						45 - pars triangularis Broca's area	14.70
						46 - Dorsolateral prefrontal cortex	12.25
						6 - Pre-Motor and Supplementary Motor Cortex	6.84
36	F4	F2	30	40	41	9 - Dorsolateral prefrontal cortex	68.37
						46 - Dorsolateral prefrontal cortex	22.40
						8 - Includes Frontal eye fields	5.57
37	F4	F6	46	38	24	45 - pars triangularis Broca's area	70.67
						46 - Dorsolateral prefrontal cortex	23.45
38	F4	FC4	44	25	40	9 - Dorsolateral prefrontal cortex	30.71
						44 - pars opercularis, part of Broca's area	27.47
						46 - Dorsolateral prefrontal cortex	16.39
						45 - pars triangularis Broca's area	14.61
						6 - Pre-Motor and Supplementary Motor Cortex	7.63
39	Fpz	AFz	1	64	14	10 - Frontopolar area	87.48
						9 - Dorsolateral prefrontal cortex	5.08
40	Fpz	Fp1	-12	67	0	10 - Frontopolar area	54.50
						11 - Orbitofrontal area	44.90
41	Fpz	Fp2	13	67	0	10 - Frontopolar area	54.46
						11 - Orbitofrontal area	44.85
42	AF7	F5	-47	46	6	45 - pars triangularis Broca's area	48.79
						46 - Dorsolateral prefrontal cortex	43.20
43	AF7	Fp1	-33	59	-2	11 - Orbitofrontal area	32.71
						46 - Dorsolateral prefrontal cortex	25.27
						10 - Frontopolar area	25.13
						47 - Inferior prefrontal gyrus	13.10
44	AF8	F6	48	46	5	45 - pars triangularis Broca's area	43.88
						46 - Dorsolateral prefrontal cortex	43.18
						47 - Inferior prefrontal gyrus	5.07
45	AF8	Fp2	34	59	-2	10 - Frontopolar area	31.08
						11 - Orbitofrontal area	30.47
						46 - Dorsolateral prefrontal cortex	20.40
						47 - Inferior prefrontal gyrus	12.45
						Brain_Outside	5.11
46	F7	F5	-53	37	6	45 - pars triangularis Broca's area	79.84
						Brain_Outside	8.73
						46 - Dorsolateral prefrontal cortex	5.76
47	F8	F6	55	36	5	45 - pars triangularis Broca's area	65.82
						Brain_Outside	24.81
						46 - Dorsolateral prefrontal cortex	5.15

Table B-S1: The detailed information for each channel (continued)

Channel	Source	Detector	X (mm)	Y (mm)	Z (mm)	Landmark	Specificity (%)
48	FC5	FC3	-55	12	34	44 - pars opercularis, part of Broca's area	47.81
						6 - Pre-Motor and Supplementary Motor Cortex	35.96
						9 - Dorsolateral prefrontal cortex	8.63
49	FC6	FC4	56	12	33	44 - pars opercularis, part of Broca's area	41.45
						6 - Pre-Motor and Supplementary Motor Cortex	40.06
						9 - Dorsolateral prefrontal cortex	8.75
50	CP6	C6	65	-33	23	22 - Superior Temporal Gyrus	31.60
						48 - Retrosubicular area	26.83
						2 - Primary Somatosensory Cortex	18.95
						40 - Supramarginal gyrus part of Wernicke's area	11.48
						42 - Primary and Auditory Association Cortex	7.78
51	CP6	CP4	58	-48	38	40 - Supramarginal gyrus part of Wernicke's area	68.98
						39 - Angular gyrus, part of Wernicke's area	12.80
						48 - Retrosubicular area	7.47
						22 - Superior Temporal Gyrus	6.94
52	Pz	Cpz	2	-61	66	7 - Somatosensory Association Cortex	58.83
						5 - Somatosensory Association Cortex	37.60
53	Pz	P1	-13	-73	56	7 - Somatosensory Association Cortex	91.59
						19 - V3	5.26
54	Pz	P2	15	-73	57	7 - Somatosensory Association Cortex	93.86
55	CP5	C5	-63	-32	23	48 - Retrosubicular area	36.01
						22 - Superior Temporal Gyrus	22.25
						42 - Primary and Auditory Association Cortex	14.79
						2 - Primary Somatosensory Cortex	13.97
						40 - Supramarginal gyrus part of Wernicke's area	8.27
56	CP5	CP3	-57	-48	38	40 - Supramarginal gyrus part of Wernicke's area	65.46
						39 - Angular gyrus, part of Wernicke's area	14.35
						48 - Retrosubicular area	9.28
						22 - Superior Temporal Gyrus	5.91
57	FC1	C1	-26	-5	68	6 - Pre-Motor and Supplementary Motor Cortex	81.78
						8 - Includes Frontal eye fields	10.37
						4 - Primary Motor Cortex	6.00
58	FC1	F1	-23	26	56	8 - Includes Frontal eye fields	63.72
						9 - Dorsolateral prefrontal cortex	26.04
						6 - Pre-Motor and Supplementary Motor Cortex	8.30
59	FC1	FC3	-38	12	55	6 - Pre-Motor and Supplementary Motor Cortex	37.52
						9 - Dorsolateral prefrontal cortex	35.13
						8 - Includes Frontal eye fields	23.49
60	FC1	FCz	-13	12	67	6 - Pre-Motor and Supplementary Motor Cortex	73.21
						8 - Includes Frontal eye fields	25.88
61	FC2	C2	27	-4	68	6 - Pre-Motor and Supplementary Motor Cortex	82.46
						8 - Includes Frontal eye fields	11.24
62	FC2	F2	24	26	55	8 - Includes Frontal eye fields	58.07
						9 - Dorsolateral prefrontal cortex	33.14
						6 - Pre-Motor and Supplementary Motor Cortex	7.12
63	FC2	FC4	39	12	54	6 - Pre-Motor and Supplementary Motor Cortex	38.21
						9 - Dorsolateral prefrontal cortex	35.79
						8 - Includes Frontal eye fields	21.49
64	FC2	FCz	14	13	66	6 - Pre-Motor and Supplementary Motor Cortex	62.95
						8 - Includes Frontal eye fields	35.34

Note: X, Y, Z coordinates refer to the spatial locations in the brain based on the MNI coordinate system.

Supplementary Figure B-1

Percentage of data retained for analysis across experimental conditions.

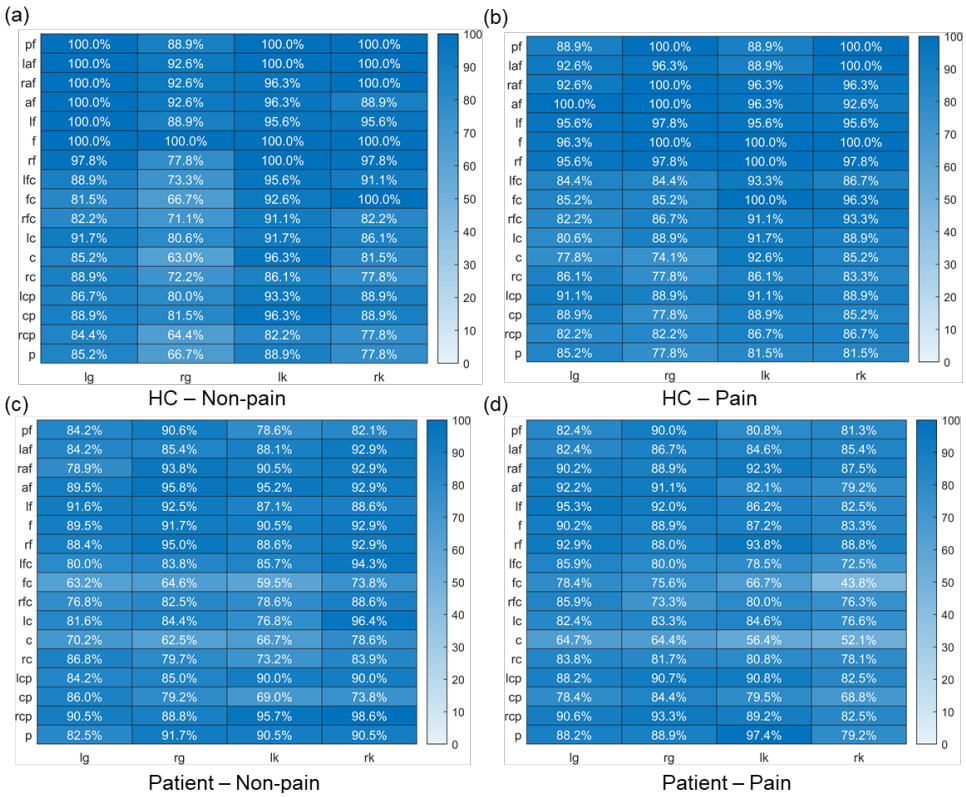

Note: The figure shows the proportion of channels that met the quality criteria and were included in the final statistical analysis (HC: healthy control group; Patient: patients group; lg: left groin; rg: right groin; lk: left knee; rk: right knee).

Supplementary Table B-2

Descriptive statistics and normality test results of stimulation values with a unit of milliamps (mA) over the three stimulation thresholds, two groups and four different body sites.

Groups	Body sites	Stimulation thresholds	Number	Mean ± SD (mA)	Normality Test (*p*)
Patients	Left groin	Perception	21	1.94 ± 1.62	Not normal ($p = 0.0025$)
		Pain	21	5.16 ± 6.89	Not normal ($p = 0.0001$)
		Pain tolerance	21	10.52 ± 13.26	Not normal ($p = 0.0001$)
	Right groin	Perception	16	1.65 ± 1.14	Not normal ($p = 0.0209$)
		Pain	16	4.58 ± 6.29	Not normal ($p = 0.0000$)
		Pain tolerance	16	8.08 ± 8.74	Not normal ($p = 0.0020$)
	Left knee	Perception	15	1.52 ± 1.63	Not normal ($p = 0.0001$)
		Pain	15	3.16 ± 2.57	Not normal ($p = 0.0164$)
		Pain tolerance	15	4.82 ± 4.11	Not normal ($p = 0.0267$)
	Right knee	Perception	16	1.61 ± 1.59	Not normal ($p = 0.0006$)
		Pain	16	4.20 ± 3.36	Not normal ($p = 0.0381$)
		Pain tolerance	16	5.80 ± 5.35	Not normal ($p = 0.0132$)
HC	Left groin	Perception	10	0.63 ± 0.35	Normal ($p = 0.3404$)
		Pain	10	1.80 ± 1.08	Normal ($p = 0.6548$)
		Pain tolerance	10	3.81 ± 3.14	Normal ($p = 0.0602$)
	Right groin	Perception	10	0.73 ± 0.47	Normal ($p = 0.2369$)
		Pain	10	2.05 ± 1.56	Not normal ($p = 0.0484$)
		Pain tolerance	10	3.18 ± 2.65	Not normal ($p = 0.0410$)
	Left knee	Perception	10	0.50 ± 0.40	Normal ($p = 0.1000$)
		Pain	10	0.97 ± 0.71	Normal ($p = 0.2124$)
		Pain tolerance	10	1.54 ± 0.92	Normal ($p = 0.1029$)
	Right knee	Perception	10	0.39 ± 0.10	Not normal ($p = 0.0426$)
		Pain	10	1.04 ± 0.48	Normal ($p = 0.6245$)
		Pain tolerance	10	1.43 ± 0.80	Normal ($p = 0.3714$)

Note: Number represents sample sizes; SD means Standard deviation; Normality Test represents the result from Shapiro-Wilk normality test.

Supplementary Table B-3

Post-hoc multiple comparisons among the stimulation value (mA) of different thresholds when stimulating different groups.

(I) Thresholds * groups	(J) Thresholds * groups	Mean difference(I-J)	*p*	95% Confidence Interval	
				Lower Bound	Upper Bound
Perception * HC	Pain * HC	-4.06	0.965	-0.91	2.25
	Pain Tolerance* HC	-5.09	0.502	-1.93	1.22
	Perception * Patient	-3.92	0.877	-1.10	1.72
Pain * HC	Pain Tolerance* HC	-4.18	0.940	-1.03	2.13
	Pain * Patient	-5.62	0.053	-2.80	0.02
Pain Tolerance* HC	Pain Tolerance* Patient	-7.66	**<0.001**	-4.84	-2.02
Perception * Patient	Pain * Patient	-5.04	**0.028**	-2.61	-0.17
	Pain Tolerance* Patient	-8.11	**<0.001**	-5.68	-3.24
Pain * Patient	Pain Tolerance* Patient	-5.51	**0.004**	-3.07	-0.64

Note: Bold p-values indicate statistical significance after controlling for Tukey - Kramer test.

Supplementary Table B-4

Descriptive statistics and normality test results of stimulation intensities with a unit of milliamps (mA) over the two stimulation modalities, two groups and four different body sites.

Groups	Body sites	Stimulation modalities	Number	Mean ± SD (mA)	Normality Test (*p*)
Patients	Left groin	Non-pain	21	4.06 ± 5.54	Not normal ($p = 0.0000$)
		Pain	21	9.55 ± 10.89	Not normal ($p = 0.0002$)
	Right groin	Non-pain	16	3.82 ± 5.06	Not normal ($p = 0.0001$)
		Pain	16	7.59 ± 7.93	Not normal ($p = 0.0039$)
	Left knee	Non-pain	15	2.42 ± 2.14	Normal ($p = 0.0506$)
		Pain	15	4.45 ± 3.51	Not normal ($p = 0.0325$)
	Right knee	Non-pain	16	3.07 ± 3.03	Not normal ($p = 0.0127$)
		Pain	16	5.62 ± 5.09	Not normal ($p = 0.0234$)
HC	Left groin	Non-pain	10	1.55 ± 0.93	Normal ($p = 0.4289$)
		Pain	10	3.93 ± 2.22	Normal ($p = 0.9190$)
	Right groin	Non-pain	10	1.36 ± 1.03	Normal ($p = 0.2921$)
		Pain	10	2.76 ± 1.79	Normal ($p = 0.8692$)
	Left knee	Non-pain	10	0.80 ± 0.75	Normal ($p = 0.1192$)
		Pain	10	1.29 ± 0.89	Normal ($p = 0.1543$)
	Right knee	Non-pain	10	0.51 ± 0.45	Not normal ($p = 0.0065$)
		Pain	10	1.08 ± 0.73	Normal ($p = 0.4500$)

Note: Number represents sample sizes; SD means Standard deviation; Normality Test represents the result from Shapiro-Wilk normality test.

Supplementary Table B-5.

Post-hoc multiple comparisons among the stimulation intensity (mA) of different modalities when stimulating different groups.

(I) Modalities * groups	(J) Modalities * groups	Mean difference(I-J)	*p*	95% Confidence Interval	
				Lower Bound	Upper Bound
Non-pain * HC	Pain * HC	-4.11	0.709	-1.21	1.70
	Non-pain * Patient	-4.87	0.109	-2.28	0.32
Pain * HC	Pain * Patient	-7.15	**<0.001**	-4.55	-1.96
Non-pain * Patient	Pain * Patient	-5.72	**<0.001**	-3.48	-1.24

Note: Bold p-values indicate statistical significance after controlling for Tukey - Kramer test.

Supplementary Table B-6

Post-hoc multiple comparisons among the stimulation intensity (mA) of different body sites when stimulating different groups.

(I) Body sites * groups	(J) Body sites * groups	Mean difference(I-J)	*p*	95% Confidence Interval	
				Lower Bound	Upper Bound
Left groin * HC	Right groin * HC	-4.17	1.000	0.68	5.53
	Left knee * HC	-3.15	0.965	1.70	6.55
	Right knee * HC	-2.90	0.927	1.95	6.80
	Left groin* Patient	-8.23	0.062	-4.06	0.10
Right groin * HC	Left knee * HC	-3.83	0.998	1.02	5.87
	Right knee * HC	-3.58	0.994	1.27	6.12
	Right groin * Patient	-8.02	0.183	-3.65	0.72
Left knee * HC	Right knee * HC	-4.60	1.000	0.25	5.10
	Left knee * Patient	-6.82	0.726	-2.40	2.03
Right knee * HC	Right knee * Patient	-7.92	0.211	-3.55	0.82
Left groin* Patient	Right groin * Patient	-2.50	0.984	1.10	4.69
	Left knee * Patient	-0.30	0.099	3.37	7.03
	Right knee * Patient	-1.14	0.433	2.46	6.06
Right groin * Patient	Left knee * Patient	-1.62	0.642	2.27	6.17
	Right knee * Patient	-2.47	0.961	1.36	5.20
Left knee * Patient	Right knee * Patient	-4.81	0.997	-0.91	2.99

Supplementary Table B-7

Descriptive statistics and normality test results of VAS rating over the two stimulation modalities, two groups, four different body sites and three time points.

Groups	Body sites	Stimulation modalities	Time point	Number	Mean ± SD (mA)	Normality Test (*p*)
Patients	Left groin	Non-pain	Before	21	33.95 ± 9.65	Normal (p = 0.4372)
		Non-pain	After the 3rd block	21	31.71 ± 15.25	Normal (p = 0.9845)
		Non-pain	After the 6th block	21	30.48 ± 18.97	Normal (p = 0.4050)
		Pain	Before	21	59.52 ± 8.65	Normal (p = 0.0512)
		Pain	After the 3rd block	21	58.10 ± 11.81	Normal (p = 0.5792)
		Pain	After the 6th block	21	61.90 ± 9.07	Normal (p = 0.4763)
	Right groin	Non-pain	Before	16	34.13 ± 8.44	Normal (p = 0.6798)
		Non-pain	After the 3rd block	16	40.75 ± 10.66	Normal (p = 0.3627)
		Non-pain	After the 6th block	16	38.63 ± 12.15	Normal (p = 0.9616)
		Pain	Before	16	64.00 ± 10.35	Normal (p = 0.2469)
		Pain	After the 3rd block	16	62.00 ± 9.55	Normal (p = 0.2933)
		Pain	After the 6th block	16	62.38 ± 12.57	Normal (p = 0.9760)
	Left knee	Non-pain	Before	15	35.00 ± 10.02	Normal (p = 0.0767)
		Non-pain	After the 3rd block	15	39.73 ± 16.77	Not normal (p = 0.0188)
		Non-pain	After the 6th block	15	37.73 ± 15.71	Not normal (p = 0.0137)
		Pain	Before	15	62.93 ± 8.68	Normal (p = 0.4406)
		Pain	After the 3rd block	15	67.60 ± 16.16	Normal (p = 0.3166)
		Pain	After the 6th block	15	71.87 ± 17.08	Normal (p = 0.8097)
	Right knee	Non-pain	Before	16	30.00 ± 10.98	Normal (p = 0.3387)
		Non-pain	After the 3rd block	16	39.00 ± 15.06	Normal (p = 0.6554)
		Non-pain	After the 6th block	16	41.25 ± 14.86	Normal (p = 0.8086)
		Pain	Before	16	65.38 ± 10.22	Normal (p = 0.1775)
		Pain	After the 3rd block	16	65.88 ± 15.84	Not normal (p = 0.0096)
		Pain	After the 6th block	16	64.00 ± 19.22	Not normal (p = 0.0234)
HC	Left groin	Non-pain	Before	10	32.80 ± 10.21	Normal (p = 0.1116)
		Non-pain	After the 3rd block	10	27.60 ± 15.60	Normal (p = 0.5327)
		Non-pain	After the 6th block	10	37.20 ± 13.31	Normal (p = 0.6242)
		Pain	Before	10	62.80 ± 4.13	Normal (p = 0.0574)
		Pain	After the 3rd block	10	62.00 ± 11.66	Normal (p = 0.9713)
		Pain	After the 6th block	10	65.80 ± 10.93	Not normal (p = 0.0287)
	Right groin	Non-pain	Before	10	35.20 ± 10.16	Normal (p = 0.3166)
		Non-pain	After the 3rd block	10	34.20 ± 12.02	Normal (p = 0.4290)
		Non-pain	After the 6th block	10	34.60 ± 13.99	Normal (p = 0.5182)
		Pain	Before	10	64.00 ± 12.07	Not normal (p = 0.0120)
		Pain	After the 3rd block	10	66.80 ± 12.80	Normal (p = 0.4465)
		Pain	After the 6th block	16	69.40 ± 12.44	Normal (p = 0.5178)
	Left knee	Non-pain	Before	15	36.20 ± 8.19	Normal (p = 0.0503)
		Non-pain	After the 3rd block	15	39.00 ± 9.49	Normal (p = 0.8283)
		Non-pain	After the 6th block	16	38.90 ± 8.25	Normal (p = 0.5903)
		Pain	Before	16	62.80 ± 6.12	Normal (p = 0.2127)
		Pain	After the 3rd block	10	68.80 ± 11.93	Normal (p = 0.4316)
		Pain	After the 6th block	10	71.60 ± 12.21	Normal (p = 0.2845)
	Right knee	Non-pain	Before	10	39.80 ± 6.76	Not normal (p = 0.0018)
		Non-pain	After the 3rd block	10	36.60 ± 10.42	Normal (p = 0.2400)
		Non-pain	After the 6th block	10	34.60 ± 13.89	Normal (p = 0.6946)
		Pain	Before	10	63.60 ± 8.93	Normal (p = 0.1817)
		Pain	After the 3rd block	10	67.00 ± 12.73	Normal (p = 0.4018)
		Pain	After the 6th block	10	68.00 ± 12.54	Normal (p = 0.2080)

Note: Number represents sample sizes; SD means Standard deviation; Normality Test represents the result from Shapiro-Wilk normality test.

Supplementary Table B-8

Descriptive statistics and normality test results of the mean change in oxyhemoglobin concentration (mol) over over the two groups, the two stimulation modalities and the four body sites.

Groups	Body sites	Stimulation Modalities	Number	Mean ± SD (mol)	Normality Test (*p*)
Patients	Left groin	Non-painful	19	0.01 ± 0.05	Not normal ($p < 0.0001$)
		Painful	17	-0.02 ± 0.06	Not normal ($p < 0.0001$)
	Right groin	Non-painful	16	-0.02 ± 0.05	Not normal ($p = 0.0002$)
		Painful	15	-0.02 ± 0.04	Not normal ($p < 0.0001$)
	Left knee	Non-painful	14	0.01 ± 0.04	Not normal ($p < 0.0001$)
		Painful	13	-0.03 ± 0.06	Not normal ($p < 0.0001$)
	Right knee	Non-painful	14	-0.00 ± 0.04	Normal ($p = 0.1869$)
		Painful	16	-0.01 ± 0.06	Not normal ($p < 0.0001$)
HC	Left groin	Non-painful	9	-0.04 ± 0.08	Not normal ($p < 0.0001$)
		Painful	9	-0.03 ± 0.07	Not normal ($p < 0.0001$)
	Right groin	Non-painful	9	-0.04 ± 0.10	Not normal ($p < 0.0001$)
		Painful	9	-0.04 ± 0.15	Not normal ($p < 0.0001$)
	Left knee	Non-painful	9	-0.02 ± 0.06	Not normal ($p < 0.0001$)
		Painful	9	-0.03 ± 0.07	Not normal ($p < 0.0001$)
	Right knee	Non-painful	9	-0.03 ± 0.07	Not normal ($p < 0.0001$)
		Painful	9	-0.03 ± 0.09	Not normal ($p < 0.0001$)

Note: Number represents sample sizes; SD means Standard deviation; Normality Test represents the result from Shapiro-Wilk normality test.

Supplementary Table B-9

Post-hoc multiple comparisons among the mean change in oxyhemoglobin concentration (mol) of different stimulation modalities when stimulating different groups.

(I) Modalities * groups	(J) Modalities * groups	Mean difference(I-J)	*p*	95% Confidence Interval	
				Lower Bound	Upper Bound
Non-pain * HC	Pain * HC	<0.01	0.070	<0.01	0.01
	Non-pain * Patient	-0.01	**<0.001**	-0.01	<0.01
Pain * HC	Pain * Patient	-0.01	**<0.001**	-0.01	-0.01
Non-pain * Patient	Pain * Patient	<0.01	1.000	<0.01	<0.01

Note: Bold p-values indicate statistical significance after controlling for Tukey - Kramer test.

Supplementary Table B-10

Post-hoc multiple comparisons among the mean change in oxyhemoglobin concentration (mol) of different body sites when stimulating different groups.

(I) Body sites * groups	(J) Body sites * groups	Mean difference(I-J)	*p*	95% Confidence Interval	
				Lower Bound	Upper Bound
Left groin * HC	Right groin * HC	-0.01	0.862	0.01	0.02
	Left knee * HC	-0.02	0.997	0.00	0.01
	Right knee * HC	-0.01	1.000	0.00	0.02
	Left groin* Patient	-0.03	0.102	-0.01	0.00
Right groin * HC	Left knee * HC	-0.03	0.413	-0.01	0.01
	Right knee * HC	-0.02	0.973	-0.01	0.01
	Right groin * Patient	-0.04	**<0.001**	-0.02	-0.01
Left knee * HC	Right knee * HC	-0.01	0.957	0.01	0.02
	Left knee * Patient	-0.03	0.064	-0.01	0.00
Right knee * HC	Right knee * Patient	-0.04	**<0.001**	-0.03	-0.01
Left groin* Patient	Right groin * Patient	-0.01	1.000	0.00	0.01
	Left knee * Patient	-0.02	0.904	-0.01	0.01
	Right knee * Patient	-0.02	0.069	-0.01	0.00
Right groin * Patient	Left knee * Patient	-0.02	0.929	-0.01	0.01
	Right knee * Patient	-0.02	0.099	-0.01	0.00
Left knee * Patient	Right knee * Patient	-0.02	0.820	-0.01	0.01

Note: Bold p-values indicate statistical significance after controlling for Tukey - Kramer test.

Supplementary Table B-11

Descriptive statistics and normality test results of the mean change in deoxyhemoglobin concentration (mol) over over the two groups, the two stimulation modalities and the four body sites.

Groups	Body sites	Stimulation Modalities	Number	Mean ± SD (mol)	Normality Test (*p*)
Patients	Left groin	Non-painful	19	-0.01 ± 0.02	Not normal ($p < 0.0001$)
		Painful	17	-0.01 ± 0.01	Not normal ($p = 0.0041$)
	Right groin	Non-painful	16	-0.00 ± 0.02	Not normal ($p < 0.0001$)
		Painful	15	-0.01 ± 0.02	Not normal ($p < 0.0001$)
	Left knee	Non-painful	14	-0.01 ± 0.02	Not normal ($p < 0.0001$)
		Painful	13	-0.01 ± 0.02	Not normal ($p < 0.0001$)
	Right knee	Non-painful	14	-0.01 ± 0.02	Not normal ($p < 0.0001$)
		Painful	16	-0.01 ± 0.03	Not normal ($p < 0.0001$)
HC	Left groin	Non-painful	9	-0.00 ± 0.01	Not normal ($p = 0.0002$)
		Painful	9	0.00 ± 0.02	Not normal ($p < 0.0001$)
	Right groin	Non-painful	9	-0.00 ± 0.02	Not normal ($p < 0.0001$)
		Painful	9	0.00 ± 0.02	Not normal ($p < 0.0001$)
	Left knee	Non-painful	9	0.00 ± 0.02	Not normal ($p < 0.0001$)
		Painful	9	0.00 ± 0.03	Not normal ($p < 0.0001$)
	Right knee	Non-painful	9	0.00 ± 0.02	Not normal ($p < 0.0001$)
		Painful	9	-0.00 ± 0.03	Not normal ($p < 0.0001$)

Note: Number represents sample sizes; SD means Standard deviation; Normality Test represents the result from Shapiro-Wilk normality test.

Supplementary Table B-12

Post–hoc multiple comparisons of mean changes in deoxyhemoglobin concentration (mol) across different stimulation modalities, body sites, and groups.

(I) Body sites * modalities * groups	(J) Body sites * modalities * groups	Mean difference(I-J)	*p*	95% Confidence Interval	
				Lower Bound	Upper Bound
left groin * non-painful * HC	right groin * non-painful * HC	-0.016	0.163	-0.007	0.001
	left knee * non-painful * HC	-0.009	1.000	-0.001	0.008
	right knee * non-painful * HC	-0.010	1.000	-0.002	0.006
	left groin * painful * HC	-0.009	1.000	-0.001	0.008
	left groin * non-painful * Patient	-0.014	**0.044**	-0.007	0.000
right groin * non-painful * HC	left knee * non-painful * HC	-0.002	0.296	0.007	0.015
	right knee * non-painful * HC	-0.003	0.729	0.005	0.014
	right groin * painful * HC	0.000	**0.033**	0.009	0.017
	right groin * non-painful * Patient	-0.009	1.000	-0.001	0.006
left knee * non-painful * HC	right knee * non-painful * HC	-0.010	1.000	-0.001	0.007
	left knee * painful * HC	-0.010	1.000	-0.002	0.007
	left knee * non-painful * Patient	-0.016	**0.007**	-0.009	-0.001
right knee * non-painful * HC	right knee * painful * HC	-0.003	0.659	0.005	0.014
	right knee * non-painful * Patient	-0.017	**0.001**	-0.010	-0.002
left groin * painful * HC	right groin * painful * HC	-0.006	1.000	0.002	0.010
	left knee * painful * HC	-0.010	1.000	-0.002	0.007
	right knee * painful * HC	-0.004	0.966	0.004	0.012
	left groin * painful * Patient	-0.017	**0.001**	-0.010	-0.002
right groin * painful * HC	left knee * painful * HC	-0.012	0.987	-0.004	0.005
	right knee * painful * HC	-0.006	1.000	0.002	0.010
	right groin * painful * Patient	-0.019	**<0.001**	-0.012	-0.004
left knee * painful * HC	right knee * painful * HC	-0.003	0.640	0.006	0.014
	left knee * painful * Patient	-0.016	**0.029**	-0.008	0.000
right knee * painful * HC	right knee * painful * Patient	-0.017	**0.001**	-0.010	-0.002
left groin * painful * Patient	right groin * painful * Patient	-0.007	1.000	-0.001	0.005
	left knee * painful * Patient	-0.008	0.999	-0.002	0.004
	right knee * painful * Patient	-0.011	0.477	-0.005	0.002
right groin * painful * Patient	left knee * painful * Patient	-0.009	0.960	-0.003	0.003
	right knee * painful * Patient	-0.008	1.000	-0.002	0.004
left knee * painful * Patient	right knee * painful * Patient	-0.009	0.998	-0.002	0.004

Note: Bold p-values indicate statistical significance after controlling for Tukey - Kramer test.

Supplementary Table B-13

Between-group comparisons of HbR concentration changes across cortical regions under right groin stimulation.

	Pain				Non-pain			
	HC	Patient	*t*	*p*	HC	Patient	*t*	*p*
AF	-0.0033±0.0026	-0.0027±0.0057	-0.08	0.938	0.003±0.0031	0.00041±0.0046	0.39	0.702
C	-0.012±0.0032	-0.0061±0.0041	-0.87	0.395	-0.0021±0.0035	0.0017±0.0036	-0.61	0.548
CP	-0.0047±0.0026	0.0048±0.004	-1.51	0.147	-0.0059±0.0043	0.004±0.0037	-1.58	0.131
F	-0.0065±0.006	0.0014±0.0049	-1.01	0.325	-0.0017±0.0024	-0.0027±0.0043	0.16	0.873
FC	-0.012±0.0039	0.0023±0.0051	-1.91	0.070	-0.0061±0.0027	-0.0035±0.0072	-0.23	0.819
LAF	-0.0012±0.0086	-0.00042±0.0071	-0.07	0.946	0.0032±0.0068	5.4e-05±0.0059	0.33	0.745
LC	-0.022±0.0043	0.0061±0.006	-3.27	**0.004**	-0.006±0.0037	-0.0025±0.0033	-0.67	0.509
LCP	-0.007±0.009	0.0013±0.0054	-0.84	0.409	-0.0089±0.0047	0.0028±0.0048	-1.58	0.127
LF	-0.017±0.0081	0.0053±0.0048	-2.52	0.020	0.0016±0.0056	-0.0066±0.0049	1.06	0.301
LFC	-0.022±0.013	0.0017±0.0071	-1.76	0.093	-0.0029±0.002	-0.0055±0.0033	0.51	0.613
P	-0.00063±0.0032	0.0025±0.0052	-0.41	0.685	-0.0093±0.0075	0.00072±0.0031	-1.39	0.180
PF	-0.0055±0.0099	0.00043±0.0064	-0.53	0.603	0.008±0.005	0.0042±0.0047	0.52	0.608
RAF	-0.015±0.0099	-0.0021±0.0074	-1.03	0.314	0.0027±0.012	-0.0018±0.0061	0.38	0.709
RC	-0.0067±0.0093	0.0036±0.0058	-0.95	0.353	0.00072±0.0067	0.0042±0.0044	-0.42	0.678
RCP	-0.014±0.01	-0.00021±0.0042	-1.40	0.176	-0.0095±0.0041	-0.0014±0.005	-1.10	0.281
RF	-0.015±0.0053	0.0057±0.0032	-3.45	**0.002**	0.0018±0.0068	5.3e-05±0.0044	0.22	0.827
RFC	-0.0095±0.0034	0.004±0.0051	-1.88	0.074	0.0023±0.0055	0.002±0.0048	0.04	0.971

Notes: PF: fronto-polar area; AF: anterior frontal area; LAF: left anterior frontal area; RAF: right anterior frontal area; F: frontal area; LF: left frontal area; RF: right frontal area; FC: fronto-central area; LFC: left fronto-central area; RFC: right fronto-central area; C: central area; LC: left central area; RC: right central area; CP: centro-parietal area; LCP: left centro-parietal area; RCP: right centro-parietal area; P: parietal area; HC: healthy control group; Patient: patient group. Bolded p-values indicate significance after FDR correction.

Supplementary Table B-14

Between-group comparisons of HbR concentration changes across cortical regions under right knee stimulation.

	Pain				Non-pain			
	HC	Patient	*t*	*p*	HC	Patient	*t*	*p*
AF	-0.0081±0.0082	-0.011±0.0081	0.22	0.831	-0.0037±0.0035	-0.0008±0.0032	-0.60	0.553
C	-0.016±0.013	-0.006±0.0064	-0.77	0.449	-0.002±0.0076	0.0045±0.0042	-0.81	0.429
CP	-0.0041±0.0085	-0.00063±0.0054	-0.36	0.721	-0.0061±0.0053	0.0075±0.0028	-2.35	0.030
F	-0.0071±0.0072	-0.0014±0.0066	-0.55	0.588	-0.0021±0.0032	0.0028±0.0039	-0.89	0.385
FC	-0.0086±0.0068	-0.00087±0.01	-0.52	0.612	-0.0082±0.0066	0.0078±0.0065	-1.64	0.116
LAF	-0.0095±0.0073	-0.013±0.0094	0.27	0.792	-0.0084±0.0066	-0.0019±0.0064	-0.68	0.506
LC	-0.02±0.012	0.0023±0.0068	-1.83	0.080	-0.0067±0.0053	0.0064±0.0029	-2.34	0.029
LCP	-0.02±0.0084	0.0058±0.0073	-2.25	0.034	0.00041±0.0031	0.0013±0.0046	-0.15	0.886
LF	-0.016±0.0069	-0.0025±0.0047	-1.62	0.118	-0.013±0.0046	0.0025±0.0036	-2.67	0.014
LFC	-0.01±0.007	-0.0022±0.0062	-0.80	0.433	-0.011±0.0065	0.004±0.0029	-2.33	0.030
P	-0.014±0.01	0.0082±0.0067	-1.84	0.080	-0.0055±0.0071	0.0042±0.0031	-1.39	0.181
PF	-0.011±0.017	-0.017±0.0078	0.33	0.748	-0.0067±0.0046	-0.0084±0.008	0.16	0.878
RAF	-0.0087±0.0087	-0.014±0.015	0.25	0.804	-0.0069±0.0056	-0.0013±0.0048	-0.75	0.465
RC	-0.014±0.0087	1.1e-05±0.007	-1.20	0.244	-0.0058±0.009	0.011±0.0026	-2.13	0.046
RCP	-0.017±0.0071	-0.0028±0.0056	-1.58	0.128	-0.015±0.0058	0.0059±0.003	-3.58	**0.002**
RF	-0.013±0.0085	0.004±0.0078	-1.37	0.185	-0.0058±0.0051	-0.0027±0.0035	-0.52	0.606
RFC	-0.011±0.0093	0.0057±0.0069	-1.44	0.163	-0.009±0.0077	0.0048±0.0029	-1.94	0.066

Notes: PF: fronto-polar area; AF: anterior frontal area; LAF: left anterior frontal area; RAF: right anterior frontal area; F: frontal area; LF: left frontal area; RF: right frontal area; FC: fronto-central area; LFC: left fronto-central area; RFC: right fronto-central area; C: central area; LC: left central area; RC: right central

area; CP: centro-parietal area; LCP: left centro-parietal area; RCP: right centro-parietal area; P: parietal area; HC: healthy control group; Patient: patient group. Bolded p-values indicate significance after FDR correction.

Supplementary Table B-15

Between-group comparisons of HbR concentration changes across cortical regions under left groin stimulation.

	Pain				Non-pain			
	HC	Patient	*t*	*p*	HC	Patient	*t*	*p*
AF	-0.0072±0.0043	0.0026±0.0064	-1.04	0.311	-0.0039±0.0044	-0.0013±0.0025	-0.54	0.591
C	-0.016±0.0057	-0.00095±0.0041	-1.98	0.061	-0.017±0.011	0.00046±0.0026	-2.06	0.050
CP	-0.011±0.0054	0.0023±0.0051	-1.66	0.111	-0.012±0.012	0.0019±0.0021	-1.55	0.133
F	-0.007±0.0049	0.00095±0.005	-1.02	0.317	-0.0021±0.0037	-0.0013±0.002	-0.23	0.824
FC	-0.0078±0.0034	0.0012±0.0043	-1.33	0.199	-0.0068±0.0059	0.00092±0.0024	-1.29	0.212
LAF	-0.0032±0.0049	0.00024±0.0062	-0.37	0.713	-0.0065±0.0057	-0.0038±0.0041	-0.38	0.709
LC	-0.012±0.0068	-0.00083±0.0042	-1.42	0.170	-0.0088±0.0098	-0.0029±0.0017	-0.83	0.416
LCP	-0.011±0.0032	0.0068±0.0056	-2.19	0.039	-0.014±0.01	-0.0014±0.0019	-1.67	0.106
LF	-0.0084±0.0032	-0.0004±0.0062	-0.90	0.378	-0.01±0.0059	-0.0021±0.0025	-1.55	0.133
LFC	-0.0093±0.0034	-0.0051±0.0064	-0.45	0.657	-0.0069±0.0064	-0.0015±0.0019	-1.05	0.302
P	-0.0076±0.0026	-0.0028±0.0044	-0.72	0.479	-0.012±0.011	-0.0018±0.0023	-1.26	0.220
PF	0.011±0.0055	0.0042±0.0074	0.62	0.542	0.0036±0.0092	-0.0062±0.0046	1.06	0.298
RAF	-0.015±0.0041	0.0051±0.0065	-2.10	0.046	-0.014±0.0062	-0.0016±0.0031	-1.91	0.068
RC	-0.0087±0.0049	0.0018±0.0063	-1.07	0.298	-0.0099±0.0094	-0.00039±0.002	-1.36	0.185
RCP	-0.0091±0.0042	-0.0012±0.005	-0.99	0.332	-0.013±0.0069	-0.0034±0.0027	-1.55	0.134
RF	-0.01±0.0031	0.0039±0.0064	-1.56	0.132	-0.011±0.0043	-0.0037±0.0029	-1.48	0.151
RFC	-0.011±0.0052	0.0016±0.0071	-1.16	0.258	-0.0081±0.0062	0.00016±0.0022	-1.57	0.128

Notes: PF: fronto-polar area; AF: anterior frontal area; LAF: left anterior frontal area; RAF: right anterior frontal area; F: frontal area; LF: left frontal area; RF: right frontal area; FC: fronto-central area; LFC: left fronto-central area; RFC: right fronto-central area; C: central area; LC: left central area; RC: right central area; CP: centro-parietal area; LCP: left centro-parietal area; RCP: right centro-parietal area; P: parietal area; HC: healthy control group; Patient: patient group.

Supplementary Table B-16

Between-group comparisons of HbR concentration changes across cortical regions under left knee stimulation.

	Pain				Non-pain			
	HC	Patient	*t*	*p*	HC	Patient	*t*	*p*
AF	-9.4e-05±0.0052	0.0089±0.0062	-1.02	0.322	0.0015±0.0039	0.0024±0.0039	-0.16	0.873
C	-0.02±0.017	-0.0045±0.0041	-1.00	0.331	-0.0078±0.0037	-0.0014±0.0025	-1.42	0.171
CP	-0.0072±0.0087	0.0046±0.008	-0.97	0.343	-0.0081±0.0071	-0.0004±0.0016	-1.20	0.245
F	-0.0062±0.0034	-0.0048±0.0052	-0.19	0.852	-0.0046±0.0038	0.00012±0.0048	-0.70	0.492
FC	-0.0082±0.0053	-0.00072±0.0076	-0.73	0.476	-0.005±0.0026	0.0058±0.0059	-1.39	0.180
LAF	8.8e-05±0.0052	0.00015±0.0061	-0.01	0.995	-0.0017±0.0057	-0.0082±0.0039	0.97	0.342
LC	-0.014±0.0066	0.0048±0.0062	-2.07	0.052	-0.013±0.0068	0.00088±0.0056	-1.53	0.141
LCP	-0.01±0.0019	-0.0032±0.0089	-0.64	0.529	-0.013±0.006	0.0016±0.0053	-1.78	0.090
LF	-0.0054±0.0049	0.0033±0.0053	-1.15	0.264	-0.013±0.0034	-0.002±0.0047	-1.78	0.089
LFC	-0.011±0.0037	0.002±0.0069	-1.44	0.166	-0.0082±0.0037	-0.00088±0.004	-1.24	0.229
P	-0.0057±0.0054	0.0008±0.011	-0.44	0.663	-0.01±0.0066	0.0052±0.0037	-2.15	0.044
PF	0.0016±0.008	0.0012±0.0097	0.03	0.977	0.0033±0.0089	-0.0064±0.0072	0.83	0.416
RAF	0.003±0.0088	0.0036±0.011	-0.04	0.972	-0.0084±0.0057	-0.0023±0.0073	-0.59	0.560
RC	-0.0043±0.0057	0.0024±0.0086	-0.56	0.584	-0.014±0.0056	0.0025±0.0051	-2.00	0.059
RCP	-0.013±0.0055	-0.006±0.0069	-0.71	0.486	-0.017±0.0055	0.0021±0.0034	-3.16	0.005
RF	-0.0076±0.0046	0.0069±0.0088	-1.27	0.217	-0.014±0.0033	0.00035±0.0066	-1.64	0.117
RFC	-0.0063±0.0035	0.0023±0.0083	-0.82	0.422	-0.0089±0.0038	0.0085±0.0069	-1.89	0.073

Note: PF: fronto-polar area; AF: anterior frontal area; LAF: left anterior frontal area; RAF: right anterior frontal area; F: frontal area; LF: left frontal area; RF: right frontal area; FC: fronto-central area; LFC: left fronto-central area; RFC: right fronto-central area; C: central area; LC: left central area; RC: right central area; CP: centro-parietal area; LCP: left centro-parietal area; RCP: right centro-parietal area; P: parietal area; HC: healthy control group; Patient: patient group.

Supplementary Table B-17

Between-group comparisons of HbO2 concentration changes across cortical regions under left groin stimulation.

	Pain				Non-pain			
	HC	Patient	*t*	*p*	HC	Patient	*t*	*p*
AF	-0.045±0.017	-0.039±0.016	-0.23	0.820	-0.029±0.0093	-0.017±0.011	-0.65	0.522
C	-0.025±0.02	-0.0087±0.01	-0.76	0.459	-0.035±0.017	-0.0028±0.0074	-1.92	0.067
CP	-0.02±0.031	-0.0028±0.01	-0.64	0.530	-0.044±0.029	-0.0071±0.01	-1.46	0.158
F	-0.047±0.023	-0.037±0.015	-0.37	0.717	-0.026±0.0085	-0.012±0.012	-0.76	0.455
FC	-0.043±0.02	-0.025±0.01	-0.85	0.405	-0.017±0.008	-0.0095±0.013	-0.36	0.723
LAF	-0.02±0.018	-0.044±0.016	0.96	0.347	-0.032±0.011	-0.013±0.01	-1.13	0.269
LC	-0.013±0.022	-0.013±0.011	-0.02	0.987	-0.027±0.022	-0.0096±0.011	-0.76	0.453
LCP	-0.011±0.028	-0.021±0.01	0.44	0.666	-0.05±0.041	-0.0092±0.012	-1.25	0.222
LF	-0.014±0.017	-0.031±0.014	0.75	0.461	-0.0068±0.011	-0.0067±0.0079	-0.01	0.995
LFC	-0.031±0.015	-0.03±0.013	-0.04	0.971	-0.022±0.011	-0.014±0.01	-0.49	0.627
P	-0.031±0.033	-0.022±0.012	-0.29	0.775	-0.087±0.068	-0.014±0.014	-1.41	0.171
PF	-0.025±0.023	-0.045±0.018	0.69	0.499	-0.033±0.016	-0.027±0.014	-0.29	0.776
RAF	-0.027±0.0092	-0.032±0.014	0.24	0.809	-0.027±0.016	-0.0076±0.011	-0.98	0.337
RC	-0.039±0.032	-0.0099±0.015	-0.95	0.352	-0.058±0.046	-0.0076±0.012	-1.39	0.175
RCP	-0.015±0.029	-0.009±0.014	-0.22	0.831	-0.054±0.042	-0.0088±0.012	-1.36	0.186
RF	-0.0096±0.0092	-0.029±0.014	0.96	0.348	-0.022±0.019	-0.011±0.0087	-0.60	0.555
RFC	-0.042±0.023	-0.021±0.015	-0.80	0.429	-0.04±0.031	-0.0069±0.011	-1.28	0.211

Note: PF: fronto-polar area; AF: anterior frontal area; LAF: left anterior frontal area; RAF: right anterior frontal area; F: frontal area; LF: left frontal area; RF: right frontal area; FC: fronto-central area; LFC: left

fronto-central area; RFC: right fronto-central area; C: central area; LC: left central area; RC: right central area; CP: centro-parietal area; LCP: left centro-parietal area; RCP: right centro-parietal area; P: parietal area; HC: healthy control group; Patient: patient group.

Supplementary Table B-18

Between-group comparisons of HbO2 concentration changes across cortical regions under right groin stimulation.

	Pain				Non-pain			
	HC	Patient	*t*	*p*	HC	Patient	*t*	*p*
AF	-0.068±0.051	-0.029±0.012	-0.90	0.377	-0.047±0.027	-0.024±0.016	-0.77	0.447
C	-0.073±0.021	-0.018±0.012	-2.26	0.035	-0.052±0.035	-0.018±0.015	-0.95	0.353
CP	-0.11±0.048	-0.019±0.0094	-2.18	0.042	-0.02±0.043	-0.0091±0.013	-0.28	0.781
F	-0.073±0.042	-0.019±0.014	-1.46	0.157	-0.038±0.032	-0.019±0.018	-0.56	0.579
FC	-0.085±0.024	-0.013±0.011	-3.02	0.007	-0.01±0.015	-0.011±0.014	0.06	0.955
LAF	-0.035±0.06	-0.013±0.0095	-0.45	0.658	-0.038±0.028	-0.031±0.013	-0.23	0.818
LC	-0.024±0.045	-0.013±0.01	-0.30	0.770	-0.037±0.036	-0.012±0.012	-0.81	0.429
LCP	-0.016±0.069	-0.019±0.01	0.07	0.949	-0.031±0.035	-0.012±0.013	-0.62	0.541
LF	-0.016±0.045	-0.0083±0.01	-0.21	0.839	-0.035±0.033	-0.021±0.012	-0.47	0.647
LFC	-0.061±0.02	-0.019±0.012	-1.96	0.062	-0.0088±0.013	-0.019±0.012	0.50	0.625
P	-0.036±0.058	-0.027±0.011	-0.20	0.845	-0.036±0.036	-0.013±0.013	-0.69	0.499
PF	-0.063±0.052	-0.036±0.013	-0.62	0.545	-0.059±0.028	-0.035±0.016	-0.80	0.431
RAF	-0.05±0.045	-0.019±0.01	-0.80	0.433	-0.042±0.033	-0.016±0.013	-0.90	0.379
RC	0.022±0.069	-0.0029±0.011	0.44	0.666	-0.064±0.044	-0.014±0.014	-1.31	0.205
RCP	0.035±0.06	-0.018±0.013	1.11	0.277	-0.046±0.044	-0.012±0.015	-0.88	0.386
RF	-0.018±0.051	-0.013±0.012	-0.11	0.910	-0.036±0.033	-0.014±0.013	-0.71	0.482
RFC	-0.019±0.056	-0.019±0.0097	-0.01	0.995	-0.041±0.036	-0.01±0.011	-1.02	0.318

Note: PF: fronto-polar area; AF: anterior frontal area; LAF: left anterior frontal area; RAF: right anterior frontal area; F: frontal area; LF: left frontal area; RF: right frontal area; FC: fronto-central area; LFC: left fronto-central area; RFC: right fronto-central area; C: central area; LC: left central area; RC: right central area; CP: centro-parietal area; LCP: left centro-parietal area; RCP: right centro-parietal area; P: parietal area; HC: healthy control group; Patient: patient group.

Supplementary Table B-19

Between-group comparisons of HbO2 concentration changes across cortical regions under left knee stimulation.

	Pain				Non-pain			
	HC	Patient	*t*	*p*	HC	Patient	*t*	*p*
AF	-0.038±0.015	-0.026±0.0063	-0.77	0.449	-0.024±0.014	0.0046±0.01	-1.69	0.106
C	-0.033±0.026	-0.015±0.016	-0.57	0.578	-0.017±0.014	-0.012±0.0053	-0.41	0.687
CP	-0.042±0.032	-0.02±0.019	-0.61	0.549	-0.03±0.02	0.0051±0.0077	-1.78	0.090
F	-0.029±0.019	-0.04±0.017	0.44	0.664	-0.02±0.016	0.015±0.012	-1.78	0.089
FC	-0.03±0.019	-0.023±0.015	-0.28	0.781	-0.013±0.012	0.011±0.0083	-1.69	0.107
LAF	-0.02±0.018	-0.047±0.019	0.96	0.351	-0.023±0.02	0.0084±0.0097	-1.56	0.133
LC	-0.012±0.03	-0.026±0.015	0.46	0.653	-0.021±0.027	-0.0016±0.0088	-0.81	0.426
LCP	-0.019±0.021	-0.038±0.017	0.70	0.494	-0.032±0.035	-0.0016±0.0084	-1.04	0.312
LF	-0.0087±0.018	-0.025±0.02	0.57	0.574	-0.0074±0.011	0.02±0.011	-1.70	0.104
LFC	-0.024±0.021	-0.024±0.017	-0.00	1.000	-0.013±0.013	0.0062±0.0094	-1.25	0.223
P	-0.058±0.023	-0.048±0.024	-0.26	0.799	-0.04±0.034	0.01±0.0095	-1.71	0.102
PF	-0.059±0.032	-0.049±0.013	-0.31	0.762	-0.039±0.019	-0.0091±0.022	-0.95	0.355
RAF	-0.042±0.023	-0.028±0.014	-0.55	0.592	-0.032±0.02	0.015±0.0083	-2.48	0.022
RC	-0.023±0.027	-0.035±0.015	0.43	0.676	-0.038±0.027	0.0024±0.0085	-1.72	0.102
RCP	-0.029±0.031	-0.033±0.021	0.10	0.922	-0.023±0.026	0.011±0.0051	-1.60	0.125
RF	-0.018±0.015	-0.026±0.016	0.37	0.719	-0.014±0.013	0.013±0.0091	-1.79	0.088
RFC	-0.019±0.024	-0.035±0.016	0.57	0.579	-0.036±0.022	0.008±0.0074	-2.27	0.034

Note: PF: fronto-polar area; AF: anterior frontal area; LAF: left anterior frontal area; RAF: right anterior frontal area; F: frontal area; LF: left frontal area; RF: right frontal area; FC: fronto-central area; LFC: left fronto-central area; RFC: right fronto-central area; C: central area; LC: left central area; RC: right central area; CP: centro-parietal area; LCP: left centro-parietal area; RCP: right centro-parietal area; P: parietal area; HC: healthy control group; Patient: patient group.

Supplementary Table B-20

Between-group comparisons of HbO2 concentration changes across cortical regions under right knee stimulation.

	Pain				Non-pain			
	HC	Patient	*t*	*p*	HC	Patient	*t*	*p*
AF	-0.028±0.016	-0.024±0.025	-0.10	0.919	-0.037±0.015	-0.0039±0.0077	-2.11	0.047
C	-0.038±0.03	-0.018±0.0098	-0.75	0.462	-0.05±0.033	-0.0024±0.0075	-1.70	0.104
CP	-0.038±0.041	-0.0058±0.016	-0.85	0.405	-0.029±0.029	0.0021±0.0087	-1.13	0.272
F	-0.027±0.024	-0.014±0.011	-0.58	0.565	-0.036±0.021	-0.0015±0.0097	-1.72	0.101
FC	-0.021±0.027	-0.0073±0.01	-0.47	0.645	-0.05±0.022	-0.0018±0.0087	-2.34	0.029
LAF	-0.012±0.021	-0.03±0.019	0.61	0.551	-0.016±0.015	-0.004±0.011	-0.64	0.533
LC	-0.031±0.035	0.0054±0.0072	-1.33	0.197	-0.025±0.026	0.011±0.0074	-1.59	0.127
LCP	-0.031±0.03	0.0037±0.011	-1.29	0.211	-0.0083±0.019	0.0089±0.0085	-0.93	0.363
LF	-0.014±0.021	-0.003±0.01	-0.52	0.611	-0.0056±0.014	-0.0022±0.012	-0.18	0.856
LFC	-0.063±0.053	-0.0039±0.01	-1.38	0.182	-0.04±0.019	0.0047±0.0074	-2.51	0.020
P	-0.062±0.04	0.0065±0.014	-1.92	0.068	-0.039±0.032	-0.0001±0.01	-1.37	0.185
PF	-0.044±0.028	-0.065±0.028	0.47	0.640	-0.041±0.023	-0.013±0.019	-0.93	0.365
RAF	-0.051±0.019	-0.02±0.016	-1.21	0.237	-0.038±0.017	-0.0056±0.011	-1.69	0.106
RC	-0.027±0.024	-0.0043±0.012	-0.90	0.377	-0.058±0.038	-0.006±0.012	-1.54	0.139
RCP	-0.0091±0.021	0.003±0.013	-0.52	0.607	-0.036±0.029	-0.0075±0.01	-1.08	0.294
RF	-0.031±0.021	-0.001±0.011	-1.43	0.165	-0.029±0.013	-0.004±0.01	-1.53	0.140
RFC	-0.019±0.026	-0.0027±0.011	-0.65	0.521	-0.049±0.033	-0.0046±0.0092	-1.56	0.134

Note: PF: fronto-polar area; AF: anterior frontal area; LAF: left anterior frontal area; RAF: right anterior frontal area; F: frontal area; LF: left frontal area; RF: right frontal area; FC: fronto-central area; LFC: left fronto-central area; RFC: right fronto-central area; C: central area; LC: left central area; RC: right central area; CP: centro-parietal area; LCP: left centro-parietal area; RCP: right centro-parietal area; P: parietal area; HC: healthy control group; Patient: patient group.

Supplementary Table B-21

Post-hoc multiple comparisons among the pain severity value of different groups.

(I) Conditions * groups	(J) Conditions * groups	Mean difference(I-J)	*p*	95% Confidence Interval	
				Lower Bound	Upper Bound
Non-PLP patient	PLP patient	0.09	**0.034**	1.33	2.57
	Healthy controls	2.47	**<0.001**	3.59	4.72
PLP patient	Healthy controls	1.08	**<0.001**	2.26	3.43

Supplementary Table B-22

Descriptive statistics and normality test results of stimulation values with a unit of milliamps (mA) over the three stimulation thresholds, three groups and four different body sites.

Groups	Body sites	Stimulation thresholds	Number	Mean ± SD (mA)	Normality Test (*p*)
Non-PLP patients	Groin on the amputation side	Perception	9	1.78 ± 1.48	Normal ($p = 0.0541$)
		Pain	9	6.33 ± 8.34	Not normal ($p = 0.0024$)
		Pain tolerance	9	10.09 ± 11.37	Not normal ($p = 0.0179$)
	Groin on the non-amputation side	Perception	8	2.16 ± 2.10	Not normal ($p = 0.0238$)
		Pain	8	7.61 ± 9.48	Not normal ($p = 0.0170$)
		Pain tolerance	8	13.41 ± 16.41	Not normal ($p = 0.0378$)
	Knee on the amputation side	Perception	7	1.46 ± 0.72	Normal ($p = 0.2380$)
		Pain	7	3.77 ± 3.21	Normal ($p = 0.2434$)
		Pain tolerance	7	5.13 ± 4.13	Normal ($p = 0.3362$)
	Knee on the non-amputation side	Perception	7	0.93 ± 0.44	Normal ($p = 0.2860$)
		Pain	7	3.34 ± 3.24	Not normal ($p = 0.0299$)
		Pain tolerance	7	4.93 ± 4.43	Normal ($p = 0.0653$)
PLP patients	Groin on the amputation side	Perception	6	2.11 ± 1.49	Normal ($p = 0.0800$)
		Pain	6	3.49 ± 2.65	Normal ($p = 0.6386$)
		Pain tolerance	6	10.02 ± 12.27	Not normal ($p = 0.0150$)
	Groin on the non-amputation side	Perception	7	1.48 ± 0.65	Normal ($p = 0.7562$)
		Pain	7	2.41 ± 1.59	Normal ($p = 0.0835$)
		Pain tolerance	7	7.52 ± 7.61	Not normal ($p = 0.0212$)
	Knee on the amputation side	Perception	6	2.75 ± 2.90	Not normal ($p = 0.0217$)
		Pain	6	5.01 ± 3.58	Normal ($p = 0.6004$)
		Pain tolerance	6	8.41 ± 7.21	Normal ($p = 0.3846$)
	Knee on the non-amputation side	Perception	5	2.28 ± 1.49	Normal ($p = 0.4425$)
		Pain	5	5.07 ± 2.51	Normal ($p = 0.8700$)
		Pain tolerance	5	6.53 ± 3.43	Normal ($p = 0.8072$)
HC	Groin on the amputation side	Perception	9	0.76 ± 0.48	Normal ($p = 0.2728$)
		Pain	9	2.23 ± 1.59	Normal ($p = 0.0749$)
		Pain tolerance	9	4.52 ± 3.57	Normal ($p = 0.0942$)
	Groin on the non-amputation side	Perception	9	0.49 ± 0.22	Not normal ($p = 0.0320$)
		Pain	9	1.41 ± 0.79	Normal ($p = 0.8131$)
		Pain tolerance	9	2.70 ± 2.08	Normal ($p = 0.3887$)
	Knee on the amputation side	Perception	9	0.40 ± 0.33	Normal ($p = 0.0669$)
		Pain	9	0.96 ± 0.75	Normal ($p = 0.1468$)
		Pain tolerance	9	1.47 ± 0.87	Normal ($p = 0.1997$)
	Knee on the non-amputation side	Perception	9	0.40 ± 0.37	Not normal ($p = 0.0295$)
		Pain	9	1.01 ± 0.74	Normal ($p = 0.3987$)
		Pain tolerance	9	1.44 ± 1.07	Normal ($p = 0.2735$)

Note: Number represents sample sizes; SD means Standard deviation; Normality Test represents the result from Shapiro-Wilk normality test.

Supplementary Table B-23

Post-hoc multiple comparisons among the stimulation value of different thresholds when stimulating different groups.

(I) Thresholds * groups	(J) Thresholds * groups	Mean difference (I-J)	*p*	95% Confidence Interval	
				Lower Bound	Upper Bound
Perception * NPLP	Pain * NPLP	-7.75	0.086	-3.76	0.24
	Pain Tolerance* NPLP	-10.89	**<0.001**	-6.89	-2.89
	Perception * PLP	-4.97	1.000	-0.68	3.60
	Perception * HC	-2.84	0.996	1.02	4.88
Pain * NPLP	Pain Tolerance* NPLP	-7.13	0.267	-3.13	0.87
	Pain * PLP	-2.95	0.989	1.34	5.62
	Pain * HC	0.03	**0.047**	3.88	7.74
Pain Tolerance* NPLP	Pain Tolerance* PLP	-3.98	1.000	0.31	4.59
	Pain Tolerance* HC	2.03	**<0.001**	5.88	9.74
Perception * PLP	Pain * PLP	-6.28	0.960	-1.74	2.81
	Pain Tolerance* PLP	-10.45	**0.002**	-5.90	-1.36
	Perception * HC	-2.45	0.940	1.70	5.85
Pain * PLP	Pain Tolerance* PLP	-8.71	0.104	-4.16	0.38
	Pain * HC	-1.60	0.612	2.55	6.70
Pain Tolerance* PLP	Pain Tolerance* HC	1.43	**0.001**	5.58	9.73
Perception * HC	Pain * HC	-4.59	0.998	-0.89	2.81
	Pain Tolerance* HC	-5.73	0.751	-2.02	1.68
Pain * HC	Pain Tolerance* HC	-4.84	0.990	-1.13	2.57

Note: Bold p-values indicate statistical significance after controlling for Tukey - Kramer test.

Supplementary Table B-24

Descriptive statistics and normality test results of stimulation intensities with a unit of milliamps (mA) over the two stimulation modalities, three groups and four different body sites.

Groups	Body sites	Stimulation modalities	Number	Mean ± SD (mA)	Normality Test (*p*)
Non-PLP patients	Groin on the amputation side	Non-painful	9	5.38 ± 6.99	Not normal (*p* = 0.0030)
		Painful	9	10.53 ± 10.87	Not normal (*p* = 0.0250)
	Groin on the non-amputation side	Non-painful	8	5.71 ± 7.34	Not normal (*p* = 0.0182)
		Painful	8	11.63 ± 13.37	Not normal (*p* = 0.0417)
	Knee on the amputation side	Non-painful	7	2.94 ± 2.57	Not normal (*p* = 0.0348)
		Painful	7	4.86 ± 3.78	Normal (*p* = 0.2194)
	Knee on the non-amputation side	Non-painful	7	2.51 ± 2.71	Normal (*p* = 0.0582)
		Painful	7	5.03 ± 4.41	Normal (*p* = 0.1040)
PLP patients	Groin on the amputation side	Non-painful	6	3.17 ± 2.39	Normal (*p* = 0.3447)
		Painful	6	8.28 ± 9.04	Not normal (*p* = 0.0362)
	Groin on the non-amputation side	Non-painful	7	2.00 ± 1.33	Normal (*p* = 0.5261)
		Painful	7	6.04 ± 6.19	Not normal (*p* = 0.0096)
	Knee on the amputation side	Non-painful	6	4.22 ± 3.52	Normal (*p* = 0.4997)
		Painful	6	7.82 ± 6.36	Normal (*p* = 0.5803)
	Knee on the non-amputation side	Non-painful	5	3.62 ± 1.81	Normal (*p* = 0.2891)
		Painful	5	6.14 ± 3.18	Normal (*p* = 0.6763)
HC	Groin on the amputation side	Non-painful	9	1.61 ± 1.00	Normal (*p* = 0.4042)
		Painful	9	3.78 ± 2.22	Normal (*p* = 0.8022)
	Groin on the non-amputation side	Non-painful	9	1.07 ± 0.72	Not normal (*p* = 0..4499)
		Painful	9	2.85 ± 2.05	Normal (*p* = 0.6801)
	Knee on the amputation side	Non-painful	9	0.55 ± 0.57	Not normal (*p* = 0.0112)
		Painful	9	1.01 ± 0.74	Normal (*p* = 0.1751)
	Knee on the non-amputation side	Non-painful	9	0.76 ± 0.73	Not normal (*p* = 0.0301)
		Painful	9	1.17 ± 0.86	Normal (*p* = 0.2025)

Note: Number represents sample sizes; SD means Standard deviation; Normality Test represents the result from Shapiro-Wilk normality test.

Supplementary Table B-25

Post-hoc multiple comparisons among the stimulation intensity of different modalities when stimulating different groups.

(I) Modalities * groups	(J) Modalities * groups	Mean difference(I-J)	*p*	95% Confidence Interval	
				Lower Bound	Upper Bound
Non-pain * NPLP	Pain * NPLP	-7.66	**0.034**	-3.92	-0.18
	Non-pain * PLP	-3.16	0.991	0.85	4.86
	Pain * PLP	-6.96	0.292	-2.94	1.07
	Non-pain * HC	-0.49	0.136	3.12	6.72
	Pain * HC	-1.70	0.658	1.91	5.52
Pain * NPLP	Non-pain * PLP	0.76	0.009	4.77	8.78
	Pain * PLP	-3.04	0.983	0.97	4.98
	Non-pain * HC	3.42	<0.001	7.03	10.64
	Pain * HC	2.22	**<0.001**	5.83	9.44
Non-pain * PLP	Pain * PLP	-8.05	0.111	-3.80	0.45
	Non-pain * HC	-1.62	0.559	2.26	6.15
	Pain * HC	-2.82	0.971	1.06	4.94
Pain * PLP	Non-pain * HC	2.18	<0.001	6.06	9.94
	Pain * HC	0.97	**0.005**	4.86	8.74
Non-pain * HC	Pain * HC	-4.67	0.921	-1.20	2.26

Note: Bold p-values indicate statistical significance after controlling for Tukey - Kramer test.

Supplementary Table B-26

Descriptive statistics and normality test results of the mean change in oxyhemoglobin concentration (mol) over the three groups, the two stimulation modalities and the four body sites.

Groups	Body sites	Stimulation modalities	Number	Mean ± SD (mol)	Normality Test (*p*)
Non-PLP patients	Groin on the amputation side	Non-painful	9	-0.03 ± 0.06	Not normal (*p* = 0.0000)
		Painful	8	-0.02 ± 0.05	Not normal (*p* = 0.0000)
	Groin on the non-amputation side	Non-painful	8	-0.00 ± 0.04	Normal (*p* = 0.3181)
		Painful	8	-0.01 ± 0.04	Not normal (*p* = 0.0000)
	Knee on the amputation side	Non-painful	7	-0.00 ± 0.04	Not normal (*p* = 0.0001)
		Painful	7	-0.03 ± 0.07	Not normal (*p* = 0.0000)
	Knee on the non-amputation side	Non-painful	7	0.01 ± 0.04	Not normal (*p* = 0.0221)
		Painful	6	0.00 ± 0.03	Not normal (*p* = 0.0092)
PLP patients	Groin on the amputation side	Non-painful	5	0.03 ± 0.05	Not normal (*p* = 0.0000)
		Painful	5	-0.03 ± 0.04	Not normal (*p* = 0.0002)
	Groin on the non-amputation side	Non-painful	7	-0.02 ± 0.04	Normal (*p* = 0.1337)
		Painful	6	-0.01 ± 0.04	Not normal (*p* = 0.0005)
	Knee on the amputation side	Non-painful	4	-0.02 ± 0.02	Not normal (*p* = 0.0196)
		Painful	6	-0.03 ± 0.05	Normal (*p* = 0.3312)
	Knee on the non-amputation side	Non-painful	4	0.01 ± 0.02	Normal (*p* = 0.3638)
		Painful	4	-0.00 ± 0.04	Normal (*p* = 0.0943)
HC	Groin on the amputation side	Non-painful	9	-0.03 ± 0.10	Not normal (*p* = 0.0000)
		Painful	9	-0.03 ± 0.15	Not normal (*p* = 0.0000)
	Groin on the non-amputation side	Non-painful	9	-0.04 ± 0.08	Not normal (*p* = 0..0000)
		Painful	9	-0.04 ± 0.07	Not normal (*p* = 0.0007)
	Knee on the amputation side	Non-painful	9	-0.02 ± 0.07	Not normal (*p* = 0.0000)
		Painful	9	-0.03 ± 0.09	Not normal (*p* = 0.0000)
	Knee on the non-amputation side	Non-painful	9	-0.04 ± 0.06	Not normal (*p* = 0.0000)
		Painful	9	-0.04 ± 0.06	Not normal (*p* = 0.0001)

Note: Number represents sample sizes; SD means Standard deviation; Normality Test represents the result from Shapiro-Wilk normality test.

Supplementary Table B-27

Post-hoc multiple comparisons of mean changes in oxyhemoglobin concentration (mol) across different stimulation modalities, body sites, and groups.

(I) Body sites * modalities * groups	(J) Body sites * modalities * groups	Mean difference(I-J)	*p*	95% Confidence Interval	
				Lower Bound	Upper Bound
ag*non-painful*nPLP	nag*non-painful*nPLP	-0.056	0.087	-0.027	0.001
	ak*non-painful*nPLP	-0.056	0.223	-0.026	0.004
	nak*non-painful*nPLP	-0.066	**0.002**	-0.037	-0.007
	ag*painful*nPLP	-0.037	1.000	-0.009	0.020
	ag*non-painful*PLP	-0.090	**<0.001**	-0.056	-0.022
	ag*non-painful*HC	-0.030	1.000	-0.002	0.026
nag*non-painful*nPLP	ak*non-painful*nPLP	-0.029	1.000	0.002	0.032
	nak*non-painful*nPLP	-0.040	1.000	-0.009	0.021
	nag*painful*nPLP	-0.018	0.999	0.012	0.041
	nag*non-painful*PLP	-0.014	0.963	0.016	0.047
	nag*non-painful*HC	0.014	**<0.001**	0.042	0.071
ak*non-painful*nPLP	nak*non-painful*nPLP	-0.043	1.000	-0.011	0.021
	ak*painful*nPLP	-0.006	0.366	0.025	0.057
	ak*non-painful*PLP	-0.023	1.000	0.014	0.051
	ak*non-painful*HC	-0.015	0.979	0.015	0.045
nak*non-painful*nPLP	nak*painful*nPLP	-0.031	1.000	0.002	0.035
	nak*non-painful*PLP	-0.044	1.000	-0.007	0.030
	nak*non-painful*HC	0.017	**<0.001**	0.047	0.076
ag*painful*nPLP	nag*painful*nPLP	-0.037	1.000	-0.007	0.022
	ak*painful*nPLP	-0.022	1.000	0.008	0.039
	nak*painful*nPLP	-0.058	0.322	-0.026	0.006
	ag*painful*PLP	-0.029	1.000	0.005	0.039
	ag*painful*HC	-0.025	1.000	0.004	0.033
nag*painful*nPLP	ak*painful*nPLP	-0.015	0.981	0.015	0.046
	nak*painful*nPLP	-0.051	0.892	-0.019	0.013
	nag*painful*PLP	-0.038	1.000	-0.006	0.025
	nag*painful*HC	-0.002	0.113	0.027	0.055
ak*painful*nPLP	nak*painful*nPLP	-0.067	**0.031**	-0.034	-0.001
	ak*painful*PLP	-0.036	1.000	-0.003	0.030
	ak*painful*HC	-0.034	1.000	-0.004	0.026
nak*painful*nPLP	nak*painful*PLP	-0.031	1.000	0.008	0.047
	nak*painful*HC	0.009	**0.001**	0.040	0.072
ag*non-painful*PLP	nag*non-painful*PLP	0.009	**0.001**	0.045	0.080
	ak*non-painful*PLP	0.004	**0.013**	0.044	0.084
	nak*non-painful*PLP	-0.028	1.000	0.012	0.052
	ag*painful*PLP	0.014	**<0.001**	0.052	0.090
	ag*non-painful*HC	0.020	**<0.001**	0.054	0.088
nag*non-painful*PLP	ak*non-painful*PLP	-0.037	1.000	-0.001	0.036
	nak*non-painful*PLP	-0.070	0.166	-0.033	0.004
	nag*painful*PLP	-0.044	1.000	-0.011	0.022
	nag*non-painful*HC	-0.004	0.193	0.026	0.056
ak*non-painful*PLP	nak*non-painful*PLP	-0.074	0.419	-0.032	0.009
	ak*painful*PLP	-0.029	1.000	0.009	0.047
	ak*non-painful*HC	-0.034	1.000	0.001	0.036
nak*non-painful*PLP	nak*painful*PLP	-0.025	0.999	0.017	0.060
	nak*non-painful*HC	0.018	**<0.001**	0.054	0.089
ag*painful*PLP	nag*painful*PLP	-0.054	0.974	-0.018	0.017
	ak*painful*PLP	-0.035	1.000	0.001	0.037
	nak*painful*PLP	-0.063	0.931	-0.023	0.018
	ag*painful*HC	-0.034	1.000	-0.001	0.032
nag*painful*PLP	ak*painful*PLP	-0.015	0.945	0.019	0.053
	nak*painful*PLP	-0.043	1.000	-0.004	0.034
	nag*painful*HC	0.002	**0.023**	0.033	0.064
ak*painful*PLP	ak*painful*HC	-0.033	1.000	-0.001	0.030
nak*painful*PLP	nak*painful*HC	-0.004	0.160	0.032	0.068
ag*non-painful*HC	nag*non-painful*HC	-0.011	0.862	0.017	0.045
	ak*non-painful*HC	-0.037	1.000	-0.008	0.020
	nak*non-painful*HC	-0.016	0.997	0.012	0.040
	ag*painful*HC	-0.031	1.000	-0.003	0.026
nag*non-painful*HC	ak*non-painful*HC	-0.047	-0.019	0.008	0.652
	nak*non-painful*HC	-0.037	-0.009	0.019	1.000
	nag*painful*HC	-0.032	1.000	-0.004	0.024
ak*non-painful*HC	ak*non-painful*HC	-0.007	0.021	0.048	0.523
	ak*painful*HC	-0.021	1.000	0.006	0.034
nak*non-painful*HC	nak*painful*HC	-0.032	1.000	-0.004	0.024
ag*painful*HC	nag*painful*HC	-0.012	0.933	0.016	0.044
	ak*painful*HC	-0.027	1.000	0.001	0.028
	nak*painful*HC	-0.017	1.000	0.011	0.039
nag*painful*HC	ak*painful*HC	-0.043	0.949	-0.015	0.013
	nak*painful*HC	-0.033	1.000	-0.005	0.023
ak*painful*HC	nak*painful*HC	-0.018	1.000	0.010	0.038

Note: Ag: groin on the amputated side; nag: groin on the non-amputation side; ak: knee on the amputated side; nak: knee on the non-amputation side; nPLP: non-phantom limb pain patient group; PLP: phantom limb pain patient group; HC: healthy control group; bold p-values indicate statistical significance after controlling for Tukey - Kramer test.

Supplementary Table B-28

Descriptive statistics and normality test results of the mean change in deoxyhemoglobin concentration (mol) over the three groups, the two stimulation modalities and the four body sites.

Groups	Body sites	Stimulation modalities	Number	Mean ± SD (mol)	Normality Test (*p*)
Non-PLP patients	Groin on the amputation side	Non-painful	9	-0.00 ± 0.01	Not normal (*p* = 0.0000)
		Painful	8	-0.01 ± 0.02	Not normal (*p* = 0.0074)
	Groin on the non-amputation side	Non-painful	8	-0.00 ± 0.01	Not normal (*p* = 0.0008)
		Painful	8	0.00 ± 0.02	Normal (*p* = 0.0626)
	Knee on the amputation side	Non-painful	7	0.00 ± 0.02	Not normal (*p* = 0.0000)
		Painful	7	-0.01 ± 0.03	Not normal (*p* = 0.0000)
	Knee on the non-amputation side	Non-painful	7	-0.00 ± 0.01	Not normal (*p* = 0.0484)
		Painful	6	0.01 ± 0.02	Not normal (*p* = 0.0047)
PLP patients	Groin on the amputation side	Non-painful	5	-0.00 ± 0.01	Normal (*p* = 0.1591)
		Painful	5	0.01 ± 0.02	Not normal (*p* = 0.0004)
	Groin on the non-amputation side	Non-painful	7	0.00 ± 0.01	Not normal (*p* = 0.0112)
		Painful	6	0.01 ± 0.02	Not normal (*p* = 0.0016)
	Knee on the amputation side	Non-painful	4	0.01 ± 0.01	Not normal (*p* = 0.0010)
		Painful	6	0.00 ± 0.02	Not normal (*p* = 0.0000)
	Knee on the non-amputation side	Non-painful	4	-0.00 ± 0.01	Not normal (*p* = 0.0000)
		Painful	4	-0.00 ± 0.02	Not normal (*p* = 0..0000)
HC	Groin on the amputation side	Non-painful	9	0.00 ± 0.02	Not normal (*p* = 0.0000)
		Painful	9	-0.01 ± 0.02	Not normal (*p* = 0.0000)
	Groin on the non-amputation side	Non-painful	9	-0.01 ± 0.02	Not normal (*p* = 0..0000)
		Painful	9	-0.01 ± 0.02	Not normal (*p* = 0.0000)
	Knee on the amputation side	Non-painful	9	-0.01 ± 0.02	Not normal (*p* = 0.0022)
		Painful	9	-0.01 ± 0.03	Not normal (*p* = 0.0000)
	Knee on the non-amputation side	Non-painful	9	-0.01 ± 0.01	Not normal (*p* = 0.0000)
		Painful	9	-0.01 ± 0.02	Not normal (*p* = 0.0000)

Note: Number represents sample sizes; SD means Standard deviation; Normality Test represents the result from Shapiro-Wilk normality test.

Supplementary Table B-29

Post-hoc multiple comparisons of mean changes in oxyhemoglobin concentration (mol) across different stimulation modalities, body sites, and groups.

(I) Body sites * modalities * groups	(J) Body sites * modalities * groups	Mean difference(I-J)	*p*	95% Confidence Interval	
				Lower Bound	Upper Bound
ag*non-painful*nPLP	nag*non-painful*nPLP	-0.010	1.000	-0.002	0.006
	ak*non-painful*nPLP	-0.014	0.688	-0.006	0.003
	nak*non-painful*nPLP	-0.012	0.999	-0.003	0.005
	ag*painful*nPLP	-0.005	0.999	0.003	0.011
	ag*non-painful*PLP	-0.013	0.998	-0.004	0.005
	ag*non-painful*HC	-0.012	0.929	-0.004	0.003
nag*non-painful*nPLP	ak*non-painful*nPLP	-0.012	0.998	-0.004	0.005
	nak*non-painful*nPLP	-0.010	1.000	-0.001	0.007
	nag*painful*nPLP	-0.014	0.657	-0.006	0.003
	nag*non-painful*PLP	-0.011	1.000	-0.003	0.006
	nag*non-painful*HC	0.000	**0.036**	0.008	0.016
ak*non-painful*nPLP	nak*non-painful*nPLP	-0.007	1.000	0.002	0.011
	ak*painful*nPLP	0.002	**0.002**	0.011	0.020
	ak*non-painful*PLP	-0.017	0.702	-0.007	0.003
	ak*non-painful*HC	-0.001	0.132	0.008	0.016
nak*non-painful*nPLP	nak*painful*nPLP	-0.018	0.082	-0.009	0.000
	nak*non-painful*PLP	-0.009	1.000	0.002	0.012
	nak*non-painful*HC	0.000	0.076	0.008	0.016
ag*painful*nPLP	nag*painful*nPLP	-0.019	**<0.001**	-0.011	-0.003
	ak*painful*nPLP	-0.007	1.000	0.002	0.011
	nak*painful*nPLP	-0.024	**<0.001**	-0.015	-0.007
	ag*painful*PLP	-0.022	**<0.001**	-0.013	-0.003
	ag*painful*HC	-0.008	1.000	0.000	0.008
nag*painful*nPLP	ak*painful*nPLP	0.005	**<0.001**	0.013	0.022
	nak*painful*nPLP	-0.013	0.981	-0.004	0.004
	nag*painful*PLP	-0.012	1.000	-0.003	0.006
	nag*painful*HC	0.006	**<0.001**	0.014	0.022
ak*painful*nPLP	nak*painful*nPLP	-0.027	**<0.001**	-0.017	-0.008
	ak*painful*PLP	-0.019	**0.017**	-0.010	-0.001
	ak*painful*HC	-0.005	0.999	0.003	0.012
nak*painful*nPLP	nak*painful*PLP	0.000	0.072	0.010	0.021
	nak*painful*HC	0.005	**<0.001**	0.014	0.023
ag*non-painful*PLP	nag*non-painful*PLP	-0.011	1.000	-0.001	0.009
	ak*non-painful*PLP	-0.020	0.419	-0.009	0.003
	nak*non-painful*PLP	-0.009	1.000	0.002	0.014
	ag*painful*PLP	-0.010	1.000	0.000	0.009
	ag*non-painful*HC	-0.018	0.463	-0.008	0.002
ak*non-painful*PLP	ak*non-painful*PLP	-0.007	1.000	0.003	0.014
	nak*non-painful*PLP	-0.015	0.711	-0.006	0.003
	nag*painful*PLP	0.003	**<0.001**	0.011	0.019
nag*non-painful*PLP	nag*non-painful*HC	-0.001	0.086	0.011	0.023
	nak*non-painful*PLP	-0.003	0.500	0.008	0.019
	ak*painful*PLP	0.005	**<0.001**	0.015	0.024
ak*non-painful*PLP	ak*non-painful*HC	-0.012	1.000	0.000	0.012
	nak*painful*PLP	-0.004	0.821	0.006	0.016
nak*non-painful*PLP	nak*non-painful*HC	-0.011	1.000	-0.002	0.008
	nag*painful*PLP	-0.005	0.989	0.005	0.015
	ak*painful*PLP	-0.003	0.646	0.008	0.019
	nak*painful*PLP	0.004	**<0.001**	0.013	0.022
ag*painful*PLP	ag*painful*HC	-0.003	0.747	0.006	0.016
	ak*painful*PLP	-0.001	0.209	0.009	0.020
	nak*painful*PLP	0.009	**<0.001**	0.017	0.026
nag*painful*PLP	nag*painful*HC	-0.008	1.000	0.003	0.014
ak*painful*PLP	ak*painful*HC	0.005	**<0.001**	0.013	0.022
nak*painful*PLP	nak*painful*HC	-0.006	1.000	0.004	0.014
	nag*non-painful*HC	0.003	**<0.001**	0.011	0.018
	ak*non-painful*HC	-0.001	0.329	0.006	0.014
	nak*non-painful*HC	0.001	**0.007**	0.009	0.017
ag*non-painful*HC	ag*painful*HC	0.000	**0.041**	0.008	0.016
	ak*non-painful*HC	-0.012	0.947	-0.004	0.003
	nak*non-painful*HC	-0.009	1.000	-0.002	0.006
nag*non-painful*HC	nag*painful*HC	-0.008	1.000	0.000	0.008
	ak*non-painful*HC	-0.005	1.000	0.003	0.010
ak*non-painful*HC	ak*painful*HC	-0.001	0.225	0.007	0.014
nak*non-painful*HC	nak*painful*HC	-0.010	1.000	-0.003	0.005
	nag*painful*HC	-0.005	1.000	0.003	0.011
	ak*painful*HC	-0.003	0.810	0.005	0.013
ag*painful*HC	nak*painful*HC	-0.010	1.000	-0.002	0.006
nag*painful*HC	ak*painful*HC	-0.006	1.000	0.002	0.010
	nak*painful*HC	-0.012	0.905	-0.005	0.003
ak*painful*HC	nak*painful*HC	-0.014	0.211	-0.007	0.001

Note: Ag: groin on the amputated side; nag: groin on the non-amputation side; ak: knee on the amputated side; nak: knee on the non-amputation side; nPLP: non-phantom limb pain patient group; PLP: phantom limb pain patient group; HC: healthy control group; bold p-values indicate statistical significance after controlling for Tukey - Kramer test.

Supplementary Table B-30

Between-group comparisons of HbR concentration changes across cortical regions under non-amputation side knee stimulation.

	Pain				Non-pain			
	NPLP	PLP	HC	p	NPLP	PLP	HC	p
AF	0.0019±0.0046	0.0052±0.0028	-0.0014±0.0026	0.52	-9.6e-05±0.0041	-0.0051±0.0038	-0.0033±0.0028	0.661
C	-9.3e-05±0.0034	0.004±0.0048	-0.016±0.01	0.267	-0.0061±0.0061	0.0056±0.0039	-0.0063±0.0052	0.376
CP	0.013±0.011	0.0087±0.0087	-0.0063±0.0074	0.276	0.0048±0.0051	-0.00044±0.0019	-0.0094±0.0068	0.273
F	0.006±0.0061	0.001±0.0018	-0.0057±0.0037	0.178	-0.002±0.0039	-0.0016±0.0043	-0.006±0.0032	0.642
FC	0.012±0.0054	-0.0056±0	-0.007±0.0028	0.0157	-0.00069±0.0022	-0.0023±0.0056	-0.0066±0.0032	0.432
IAF	0.01±0.0046	-0.0053±0.003	0.0021±0.0039	0.104	-0.0074±0.0054	-0.0093±0.0073	-0.005±0.0029	0.829
IC	0.0068±0.0053	0.0014±0.0099	-0.011±0.0059	0.174	-0.00063±0.0033	-0.0012±0.0032	-0.011±0.0067	0.379
ICP	0.00036±0.0048	-0.011±0.0065	-0.013±0.0039	0.121	0.0012±0.0047	0.0037±0.0032	-0.018±0.0064	0.0347
IF	0.014±0.0048	-0.0099±0.0025	-0.0054±0.0039	**0.00419**	-0.0065±0.0047	-0.0034±0.003	-0.0087±0.0035	0.717
IFC	0.011±0.0043	-0.0055±0.0066	-0.0071±0.0035	0.0168	-0.0042±0.0038	-0.001±0.0042	-0.0081±0.0036	0.494
P	0.0096±0.011	0.0057±0.0075	-0.0073±0.0053	0.284	0.0032±0.003	0.0064±0.0018	-0.0091±0.0062	0.119
PF	0.0074±0.0048	-0.026±0.0095	0.0066±0.0062	0.0105	-0.0047±0.01	-0.025±0.014	-0.012±0.0038	0.343
CAF	0.007±0.0094	-0.0069±0.0036	-0.0031±0.0027	0.291	-0.0018±0.0074	-0.015±0.0087	-0.0062±0.0035	0.402
CC	-0.0016±0.0074	0.009±0.015	-0.011±0.006	0.307	0.0023±0.0041	0.002±0.0084	-0.014±0.0052	0.0753
CCP	0.0066±0.0093	0.017±0.018	-0.0099±0.0042	0.127	0.0017±0.0065	-0.0022±0.0034	-0.009±0.0053	0.387
CF	0.0092±0.0093	-0.011±0.0036	-0.0049±0.0037	0.117	0.0034±0.0051	0.00023±0.0025	-0.012±0.0033	0.0328
CFC	0.02±0.0063	-0.019±0.01	-0.0057±0.0032	**0.00175**	0.003±0.0035	0.0032±0.008	-0.008±0.0036	0.127

Note: PF: fronto-polar area; AF: anterior frontal area; IAF: ipsilateral anterior frontal area; CAF: contralateral anterior frontal area; F: frontal area; IF: ipsilateral frontal area; CF: contralateral frontal area; FC: fronto-central area; IFC: ipsilateral fronto-central area; CFC: contralateral fronto-central area; C: central area; IC: ipsilateral central area; CC: contralateral central area; CP: centro-parietal area; ICP: ipsilateral centro-parietal area; CCP: contralateral centro-parietal area; P: parietal area; HC: healthy control group; NPLP: non-phantom limb pain patient group; PLP: phantom limb pain patient group; HC: healthy control. Bolded p-values indicate significance after FDR correction.

Supplementary Table B-31

Between-group comparisons of HbR concentration changes across cortical regions under amputation side groin stimulation.

	Pain				Non-pain			
	NPLP	PLP	HC	p	NPLP	PLP	HC	p
AF	-0.0077±0.0099	0.0048±0.0044	-0.0053±0.0041	0.516	-0.00097±0.0035	-0.00011±0.0033	0.0033±0.0039	0.678
C	-0.007±0.0057	0.0057±0.01	-0.011±0.0025	0.246	-0.0029±0.0034	0.0053±0.0067	-0.012±0.01	0.438
CP	-0.0035±0.0055	0.0091±0.0073	-0.0065±0.0027	0.139	-0.00082±0.0029	0.0065±0.0037	-0.0023±0.0052	0.548
F	-0.0076±0.0054	0.0091±0.0089	-0.0064±0.0047	0.17	-0.0072±0.0048	0.0021±0.0023	0.00081±0.0017	0.161
FC	-0.014±0.006	-0.001±0.0072	-0.009±0.0041	0.35	-0.016±0.01	0.011±0.0022	-0.0033±0.002	0.254
IAF	-0.015±0.0098	0.006±0.0034	-0.0048±0.0057	0.216	-0.003±0.0067	-0.0055±0.0039	0.0057±0.0063	0.454
IC	-0.0032±0.0038	0.0077±0.011	-0.0089±0.0051	0.238	-0.0064±0.004	0.00079±0.0024	0.00092±0.0051	0.437
ICP	-0.0065±0.0064	0.0064±0.0058	-0.0022±0.0077	0.516	-3.4e-05±0.0045	-0.0017±0.0022	-0.0045±0.004	0.718
IF	-0.011±0.0047	0.0063±0.0075	-0.014±0.0083	0.192	-0.0062±0.0053	-0.0094±0.0053	0.001±0.0059	0.458
IFC	-0.017±0.006	0.018±0.012	-0.019±0.013	0.0875	-0.0089±0.0028	0.0027±0.0036	-0.0013±0.0021	0.0297
P	-0.0052±0.0058	0.0012±0.0093	-0.0025±0.0037	0.779	-0.0041±0.0031	0.0012±0.0046	-0.005±0.0078	0.811
PF	-0.00088±0.011	0.0099±0.0082	0.00035±0.0069	0.722	0.0026±0.006	-0.0034±0.0018	0.011±0.0064	0.349
CAF	-0.0075±0.0079	0.0095±0.0043	-0.023±0.008	0.038	-0.0048±0.0061	-0.0043±0.0037	0.0031±0.012	0.786
CC	-0.0055±0.0066	0.0032±0.004	-0.00023±0.0085	0.767	-0.00053±0.003	0.0031±0.0028	0.0037±0.0041	0.655
CCP	-0.0088±0.0071	-0.0032±0.0048	-0.0012±0.0056	0.667	-0.0056±0.0041	0.0026±0.0029	-0.0075±0.0028	0.21
CF	-0.0053±0.0052	-0.0016±0.0065	-0.012±0.0047	0.39	-0.0048±0.0042	-0.011±0.0015	-0.00029±0.006	0.436
CFC	-0.0038±0.0068	-0.003±0.004	-0.0076±0.0033	0.791	-0.0049±0.0046	0.0034±0.002	0.0044±0.0049	0.285

Note: PF: fronto-polar area; AF: anterior frontal area; IAF: ipsilateral anterior frontal area; CAF: contralateral anterior frontal area; F: frontal area; IF: ipsilateral frontal area; CF: contralateral frontal area; FC: fronto-central area; IFC: ipsilateral fronto-central area; CFC: contralateral fronto-central area; C: central area; IC: ipsilateral central area; CC: contralateral central area; CP: centro-parietal area; ICP: ipsilateral centro-parietal area; CCP: contralateral centro-parietal area; P: parietal area; HC: healthy control group; NPLP: non-phantom limb pain patient group; PLP: phantom limb pain patient group; HC: healthy control.

Supplementary Table B-32

Between-group comparisons of HbR concentration changes across cortical regions under non-amputation side groin stimulation.

	Pain				Non-pain			
	NPLP	PLP	HC	p	NPLP	PLP	HC	p
AF	0.01±0.0058	0.0025±0.0053	-0.0053±0.0031	0.0705	-0.0025±0.0045	0.0015±0.0046	-0.0042±0.0037	0.64
C	-0.008±0.0052	-0.0012±0.0034	-0.016±0.0057	0.178	-0.0049±0.0028	0.0097±0.005	-0.0097±0.0074	0.106
CP	-0.00028±0.0091	0.0023±0.0037	-0.01±0.0058	0.443	0.0016±0.0011	0.0075±0.0062	-0.014±0.011	0.164
F	0.0067±0.0065	0.0082±0.0052	-0.0072±0.0061	0.164	-0.0021±0.0032	0.0011±0.005	-0.0046±0.0038	0.614
FC	0.012±0.005	0.00021±0.0051	-0.011±0.0032	0.0049	0.0019±0.0037	-0.00089±0.0065	-0.0093±0.006	0.344
IAF	0.0051±0.0088	0.012±0.0059	0.00036±0.008	0.635	-0.01±0.0075	-0.0019±0.0053	-0.009±0.0057	0.627
IC	0.0031±0.0091	0.0057±0.0037	-0.025±0.0054	0.00726	-0.0035±0.0035	-0.005±0.0028	-0.016±0.0081	0.272
ICP	0.0068±0.0086	0.0094±0.0078	-0.016±0.0046	0.031	-0.0014±0.0035	0.0023±0.0043	-0.018±0.01	0.117
IF	0.0033±0.011	0.013±0.0093	-0.011±0.0032	0.131	-0.0069±0.0053	-0.0051±0.0055	-0.0099±0.0057	0.827
IFC	0.00049±0.012	0.0097±0.0045	-0.012±0.0038	0.192	5.4e-05±0.0046	-0.0053±0.0052	-0.0083±0.0062	0.548
P	-0.0061±0.0093	0.0088±0.0056	-0.0058±0.0025	0.262	5.8e-05±0.002	0.0032±0.0054	-0.016±0.01	0.163
PF	0.0043±0.0085	-0.0038±0.0053	0.0051±0.0098	0.762	-0.0027±0.0073	0.0021±0.006	0.00063±0.008	0.9
CAF	0.0014±0.0075	0.012±0.01	-0.0066±0.0059	0.304	-0.00025±0.0052	-0.00018±0.0077	-0.014±0.0059	0.199
CC	0.0017±0.0066	0.0045±0.0081	-0.015±0.0051	0.0948	-0.0041±0.0023	0.0071±0.0067	-0.013±0.01	0.214
CCP	-0.0017±0.0077	0.0071±0.0045	-0.021±0.0085	0.054	-0.0021±0.0043	-0.0032±0.0065	-0.014±0.007	0.29
CF	0.0066±0.0082	0.013±0.0072	-0.013±0.0041	0.0256	-0.0012±0.0044	-0.0043±0.0035	-0.0092±0.0059	0.498
CFC	0.0091±0.0076	0.011±0.0087	-0.012±0.005	0.0393	-0.0006±0.0029	0.0014±0.0064	-0.01±0.0063	0.285

Note: PF: fronto-polar area; AF: anterior frontal area; IAF: ipsilateral anterior frontal area; CAF: contralateral anterior frontal area; F: frontal area; IF: ipsilateral frontal area; CF: contralateral frontal area; FC: fronto-central area; IFC: ipsilateral fronto-central area; CFC: contralateral fronto-central area; C: central area; IC: ipsilateral central area; CC: contralateral central area; CP: centro-parietal area; ICP: ipsilateral centro-parietal area; CCP: contralateral centro-parietal area; P: parietal area; HC: healthy control group; NPLP: non-phantom limb pain patient group; PLP: phantom limb pain patient group; HC: healthy control.

Supplementary Table B-33

Between-group comparisons of HbR concentration changes across cortical regions under amputation side knee stimulation.

	Pain				Non-pain			
	NPLP	PLP	HC	p	NPLP	PLP	HC	p
AF	-0.021±0.016	-0.0018±0.0073	-0.0068±0.0094	0.57	0.0035±0.0041	0.007±0.0064	0.0011±0.0044	0.728
C	-0.0099±0.0068	-0.014±0.013	-0.02±0.018	0.899	0.0038±0.0067	0.0075±0.004	-0.0035±0.0068	0.553
CP	-0.0036±0.0046	0.0052±0.016	-0.0051±0.0097	0.778	0.0011±0.0023	0.0088±0.0051	-0.0048±0.0056	0.266
F	-0.018±0.0071	0.005±0.0062	-0.0075±0.0071	0.142	-0.0006±0.0084	0.011±0.0063	-0.00066±0.0037	0.451
FC	-0.013±0.015	-0.0028±0.0014	-0.0097±0.0081	0.859	0.019±0.015	0.0088±0.0041	-0.0066±0.0064	0.192
IAF	-0.0086±0.0075	0.0054±0.0031	-0.011±0.0091	0.407	-0.0055±0.0056	0.011±0.0058	-0.0035±0.0076	0.359
IC	-0.0029±0.004	-0.0067±0.011	-0.018±0.0088	0.429	0.0083±0.0055	0.011±0.0056	-0.0085±0.009	0.199
ICP	-0.017±0.0067	-0.0034±0.016	-0.014±0.0065	0.61	-0.003±0.0034	0.01±0.005	-0.011±0.005	0.0346
IF	-0.0048±0.0086	0.007±0.0054	-0.013±0.009	0.287	-0.0039±0.0061	0.006±0.0028	-0.011±0.0053	0.201
IFC	0.0022±0.013	0.0061±0.0066	-0.015±0.0092	0.313	0.01±0.0069	0.011±0.0038	-0.0091±0.0078	0.116
P	-0.017±0.01	0.013±0.015	-0.013±0.011	0.204	5.3e-05±0.0025	0.0083±0.011	-0.0066±0.0075	0.414
PF	-0.007±0.022	-0.007±0.011	-0.016±0.017	0.908	-0.0062±0.0099	-0.005±0.012	0.0084±0.0081	0.498
CAF	-0.0069±0.013	-0.009±0.0071	-0.0034±0.012	0.939	-0.0021±0.0073	0.014±0.0018	-0.011±0.0079	0.156
CC	-0.0097±0.011	0.0074±0.011	-0.015±0.013	0.429	0.0026±0.004	0.0056±0.0032	-0.0056±0.0056	0.315
CCP	-0.014±0.0054	0.003±0.011	-0.023±0.0087	0.13	-0.0073±0.0044	0.011±0.0055	-0.0077±0.0055	0.0891
CF	-0.0053±0.0074	-0.0011±0.0057	-0.018±0.0069	0.195	-0.0039±0.0033	0.0055±0.0046	-0.015±0.0045	0.0189
CFC	-0.0096±0.009	-0.00064±0.0049	-0.011±0.0071	0.665	0.005±0.0047	0.011±0.0044	-0.012±0.0066	0.0491

Note: PF: fronto-polar area; AF: anterior frontal area; IAF: ipsilateral anterior frontal area; CAF: contralateral anterior frontal area; F: frontal area; IF: ipsilateral frontal area; CF: contralateral frontal area; FC: fronto-central area; IFC: ipsilateral fronto-central area; CFC: contralateral fronto-central area; C: central area; IC: ipsilateral central area; CC: contralateral central area; CP: centro-parietal area; ICP: ipsilateral centro-parietal area; CCP: contralateral centro-parietal area; P: parietal area; HC: healthy control group; NPLP: non-phantom limb pain patient group; PLP: phantom limb pain patient group; HC: healthy control.

Supplementary Table B-34

Between-group comparisons of HbO2 concentration changes across cortical regions under amputation side groin stimulation.

	Pain				Non-pain			
	NPLP	PLP	HC	p	NPLP	PLP	HC	p
AF	-0.035±0.019	-0.029±0.015	-0.038±0.05	0.988	-0.032±0.02	0.025±0.023	-0.036±0.027	0.238
C	-0.02±0.02	-0.024±0.0084	-0.057±0.029	0.525	-0.016±0.0086	0.022±0.031	-0.042±0.036	0.418
CP	-0.013±0.015	-0.015±0.025	-0.082±0.049	0.356	-0.03±0.018	0.049±0.035	-0.0024±0.046	0.476
F	-0.02±0.018	-0.035±0.029	-0.058±0.043	0.703	-0.033±0.023	0.027±0.023	-0.031±0.032	0.36
FC	-0.045±0.02	-0.024±0.012	-0.067±0.028	0.521	-0.039±0.023	0.042±0.036	0.0015±0.012	0.177
IAF	-0.02±0.018	-0.023±0.0051	-0.018±0.061	0.997	-0.032±0.02	0.013±0.019	-0.043±0.029	0.357
IC	-0.0091±0.023	-0.02±0.019	-0.0099±0.045	0.977	-0.034±0.02	0.03±0.025	-0.026±0.037	0.393
ICP	-0.016±0.018	-0.04±0.018	-0.005±0.069	0.903	-0.032±0.019	0.026±0.026	-0.019±0.035	0.434
IF	-0.017±0.011	-0.02±0.0091	-0.01±0.046	0.978	-0.016±0.014	0.02±0.016	-0.022±0.035	0.574
IFC	-0.032±0.017	-0.012±0.011	-0.046±0.023	0.559	-0.03±0.016	0.022±0.021	0.0015±0.012	0.11
P	-0.026±0.017	-0.049±0.028	-0.025±0.058	0.926	-0.034±0.023	0.024±0.032	-0.009±0.035	0.525
PF	-0.03±0.025	-0.049±0.012	-0.025±0.052	0.926	-0.059±0.025	0.032±0.016	-0.06±0.027	0.106
CAF	-0.016±0.02	-0.022±0.012	-0.023±0.044	0.988	-0.025±0.017	0.018±0.021	-0.043±0.034	0.431
CC	-0.0067±0.025	-0.021±0.02	0.019±0.068	0.881	-0.026±0.019	0.034±0.029	-0.041±0.045	0.372
CCP	-0.014±0.021	-0.021±0.026	0.028±0.062	0.723	-0.03±0.018	0.04±0.027	-0.037±0.047	0.344
CF	-0.014±0.016	-0.0037±0.017	-0.0056±0.051	0.98	-0.018±0.017	0.014±0.018	-0.023±0.034	0.648
CFC	-0.029±0.02	-0.035±0.012	-0.01±0.056	0.915	-0.021±0.02	0.022±0.019	-0.026±0.035	0.526

Note: PF: fronto-polar area; AF: anterior frontal area; IAF: ipsilateral anterior frontal area; CAF: contralateral anterior frontal area; F: frontal area; IF: ipsilateral frontal area; CF: contralateral frontal area; FC: fronto-central area; IFC: ipsilateral fronto-central area; CFC: contralateral fronto-central area; C: central area; IC: ipsilateral central area; CC: contralateral central area; CP: centro-parietal area; ICP:

ipsilateral centro-parietal area; CCP: contralateral centro-parietal area; P: parietal area; HC: healthy control group; NPLP: non-phantom limb pain patient group; PLP: phantom limb pain patient group; HC: healthy control.

Supplementary Table B-35

Between-group comparisons of HbO2 concentration changes across cortical regions under non-amputation side groin stimulation.

	Pain				Non-pain			
	NPLP	PLP	HC	p	NPLP	PLP	HC	p
AF	-0.033±0.01	-0.014±0.02	-0.075±0.018	0.053	-0.0099±0.014	-0.02±0.013	-0.039±0.0099	0.215
C	0.00088±0.0098	0.006±0.017	-0.043±0.015	0.0544	0.0049±0.016	-0.022±0.021	-0.042±0.011	0.147
CP	-0.0028±0.008	0.0085±0.017	-0.034±0.032	0.467	0.0067±0.0097	-0.0071±0.0087	-0.055±0.026	0.0645
F	-0.019±0.013	-0.017±0.012	-0.062±0.023	0.154	0.0011±0.015	-0.017±0.015	-0.033±0.0092	0.179
FC	-0.0037±0.016	-0.0079±0.0085	-0.06±0.016	0.0265	0.0053±0.017	-0.007±0.013	-0.027±0.01	0.258
IAF	-0.042±0.023	-0.019±0.024	-0.037±0.014	0.733	-0.013±0.013	-0.039±0.013	-0.026±0.0068	0.284
IC	-0.0052±0.0094	-0.0033±0.014	-0.027±0.023	0.577	-4.9e-05±0.011	-0.0088±0.015	-0.038±0.02	0.232
ICP	0.0025±0.0064	-0.018±0.012	-0.021±0.027	0.655	-0.00019±0.013	-0.011±0.014	-0.062±0.04	0.254
IF	-0.0052±0.025	-0.02±0.02	-0.02±0.016	0.835	-0.012±0.015	-0.028±0.012	-0.02±0.0095	0.677
IFC	-0.012±0.019	-0.013±0.01	-0.046±0.011	0.184	-0.015±0.016	-0.013±0.013	-0.032±0.0092	0.532
P	-0.0092±0.0052	0.0037±0.014	-0.041±0.032	0.378	0.0071±0.019	-0.014±0.0093	-0.11±0.065	0.145
PF	-0.069±0.022	-0.037±0.028	-0.062±0.023	0.656	-0.011±0.0075	-0.042±0.018	-0.033±0.016	0.343
CAF	-0.032±0.016	-0.021±0.028	-0.054±0.012	0.432	0.00016±0.0075	-0.025±0.019	-0.026±0.015	0.357
CC	0.004±0.013	0.017±0.021	-0.037±0.033	0.318	0.0039±0.017	-0.018±0.013	-0.077±0.044	0.17
CCP	0.011±0.0056	0.0085±0.016	-0.0035±0.032	0.881	0.0014±0.015	-0.011±0.017	-0.061±0.038	0.25
CF	-0.024±0.014	-0.016±0.023	-0.021±0.0096	0.939	-0.012±0.01	-0.025±0.019	-0.035±0.018	0.605
CFC	0.003±0.0081	0.0064±0.01	-0.05±0.022	0.0384	3.4e-05±0.012	-0.01±0.012	-0.055±0.03	0.173

Note: PF: fronto-polar area; AF: anterior frontal area; IAF: ipsilateral anterior frontal area; CAF: contralateral anterior frontal area; F: frontal area; IF: ipsilateral frontal area; CF: contralateral frontal area; FC: fronto-central area; IFC: ipsilateral fronto-central area; CFC: contralateral fronto-central area; C: central area; IC: ipsilateral central area; CC: contralateral central area; CP: centro-parietal area; ICP: ipsilateral centro-parietal area; CCP: contralateral centro-parietal area; P: parietal area; HC: healthy control group; NPLP: non-phantom limb pain patient group; PLP: phantom limb pain patient group; HC: healthy control.

Supplementary Table B-36

Between-group comparisons of HbO2 concentration changes across cortical regions under amputation side knee stimulation.

	Pain				Non-pain			
	NPLP	PLP	HC	p	NPLP	PLP	HC	p
AF	-0.061±0.054	-0.034±0.011	-0.025±0.015	0.718	-0.012±0.011	-0.016±0.015	-0.028±0.015	0.699
C	-0.023±0.017	-0.028±0.018	-0.026±0.031	0.993	-0.0036±0.012	-0.017±0.0079	-0.025±0.031	0.842
CP	-0.00038±0.019	-0.012±0.021	-0.031±0.04	0.783	-0.0015±0.012	-0.013±0.015	-0.015±0.027	0.928
F	-0.041±0.023	-0.03±0.018	-0.015±0.023	0.713	-0.006±0.016	-0.024±0.01	-0.02±0.014	0.707
FC	-0.027±0.014	-0.016±0.012	-0.018±0.027	0.939	-0.0048±0.015	-0.021±0.0055	-0.03±0.021	0.617
IAF	-0.036±0.028	-0.044±0.015	-0.018±0.023	0.751	-0.0054±0.012	-0.018±0.016	-0.017±0.02	0.861
IC	-0.015±0.017	-0.027±0.024	0.0059±0.027	0.619	-0.0084±0.018	-0.033±0.021	-0.026±0.034	0.851
ICP	-0.015±0.026	-0.013±0.018	0.0098±0.015	0.604	-0.018±0.015	-0.02±0.011	-0.023±0.025	0.988
IF	-0.019±0.018	-0.033±0.027	-0.012±0.023	0.812	0.016±0.014	-0.0067±0.013	-0.016±0.01	0.174
IFC	-0.0031±0.019	-0.049±0.022	-0.0099±0.027	0.427	0.0058±0.016	-0.029±0.011	-0.035±0.033	0.526
P	-0.037±0.036	0.011±0.021	-0.051±0.04	0.495	-0.011±0.013	-0.011±0.022	-0.013±0.031	0.997
PF	-0.11±0.067	-0.052±0.018	-0.067±0.036	0.737	-0.044±0.039	-0.037±0.016	-0.027±0.022	0.908
CAF	-0.041±0.019	-0.046±0.017	-0.046±0.023	0.986	0.0045±0.012	-0.023±0.014	-0.031±0.021	0.359
CC	-0.028±0.017	-0.019±0.022	-0.037±0.035	0.91	-0.0061±0.016	-0.011±0.0046	-0.0077±0.022	0.987
CCP	-0.011±0.012	-0.0003±0.017	-0.031±0.031	0.676	-0.0024±0.012	-0.00042±0.009	0.013±0.013	0.632
CF	-0.028±0.014	-0.035±0.023	-0.017±0.017	0.773	0.02±0.017	-0.021±0.0068	0.0025±0.011	0.21
CFC	-0.027±0.014	-0.028±0.013	-0.05±0.055	0.899	-0.0038±0.015	-0.0097±0.0046	-0.029±0.02	0.561

Note: PF: fronto-polar area; AF: anterior frontal area; IAF: ipsilateral anterior frontal area; CAF: contralateral anterior frontal area; F: frontal area; IF: ipsilateral frontal area; CF: contralateral frontal area; FC: fronto-central area; IFC: ipsilateral fronto-central area; CFC: contralateral fronto-central area; C: central area; IC: ipsilateral central area; CC: contralateral central area; CP: centro-parietal area; ICP: ipsilateral centro-parietal area; CCP: contralateral centro-parietal area; P: parietal area; HC: healthy control group; NPLP: non-phantom limb pain patient group; PLP: phantom limb pain patient group; HC: healthy control.

Supplementary Table B-37

Between-group comparisons of HbO2 concentration changes across cortical regions under non-amputation side knee stimulation.

	Pain				Non-pain			
	NPLP	PLP	HC	p	NPLP	PLP	HC	p
AF	-0.0072±0.011	-0.022±0.016	-0.04±0.015	0.307	-0.0013±0.015	0.015±0.013	-0.033±0.014	0.117
C	0.0091±0.0067	0.017±0.016	-0.045±0.025	0.132	-0.012±0.013	-0.005±0.01	-0.042±0.019	0.292
CP	0.015±0.013	0.0078±0.016	-0.049±0.033	0.253	0.019±0.01	0.0065±0.0069	-0.044±0.021	0.051
F	0.0093±0.0098	-0.014±0.015	-0.041±0.018	0.118	0.012±0.015	0.012±0.015	-0.037±0.022	0.144
FC	0.011±0.0099	0.0077±0	-0.033±0.019	0.268	0.011±0.01	0.017±0.015	-0.034±0.016	0.0749
IAF	-0.011±0.013	-0.012±0.022	-0.053±0.013	0.0978	0.0028±0.014	0.016±0.016	-0.043±0.016	0.0494
IC	0.0096±0.015	-0.0046±0.022	-0.047±0.025	0.201	0.0022±0.014	0.013±0.01	-0.052±0.031	0.196
ICP	-0.00039±0.019	0.0057±0.023	-0.038±0.023	0.34	0.0095±0.0081	0.027±0.013	-0.046±0.038	0.237
IF	0.012±0.0085	-0.0061±0.022	-0.028±0.016	0.204	0.001±0.008	0.022±0.012	-0.021±0.015	0.137
IFC	0.013±0.015	-0.0023±0.018	-0.033±0.019	0.207	-0.0023±0.013	0.0095±0.0031	-0.027±0.016	0.239
P	-0.016±0.023	0.012±0.014	-0.068±0.023	0.0818	0.022±0.014	0.016±0.0044	-0.066±0.031	0.0431
PF	-0.024±0.012	-0.052±0.021	-0.037±0.022	0.707	-0.016±0.03	0.0092±0.021	-0.053±0.019	0.255
CAF	0.0094±0.011	-0.021±0.03	-0.0083±0.02	0.655	0.015±0.016	0.0061±0.0094	-0.017±0.015	0.288
CC	0.0095±0.012	0.0093±0.014	-0.018±0.027	0.629	0.0087±0.0078	0.029±0.015	-0.052±0.028	0.0597
CCP	0.0065±0.015	0.039±0.021	-0.029±0.03	0.271	0.015±0.0042	0.03±0.016	-0.045±0.025	0.0472
CF	0.026±0.013	-0.014±0.023	-0.014±0.019	0.277	0.014±0.013	0.00081±0.012	-0.022±0.014	0.159
CFC	0.012±0.017	-0.0063±0.029	-0.031±0.021	0.345	0.018±0.0092	0.014±0.0067	-0.047±0.021	0.0196

Note: PF: fronto-polar area; AF: anterior frontal area; IAF: ipsilateral anterior frontal area; CAF: contralateral anterior frontal area; F: frontal area; IF: ipsilateral frontal area; CF: contralateral frontal area; FC: fronto-central area; IFC: ipsilateral fronto-central area; CFC: contralateral fronto-central area; C: central area; IC: ipsilateral central area; CC: contralateral central area; CP: centro-parietal area; ICP: ipsilateral centro-parietal area; CCP: contralateral centro-parietal area; P: parietal area; HC: healthy control group; NPLP: non-phantom limb pain patient group; PLP: phantom limb pain patient group; HC: healthy control.

Supplementary Figure B-2

Between-group comparisons of hemoglobin concentration changes across cortical regions under left groin non-painful stimulation.

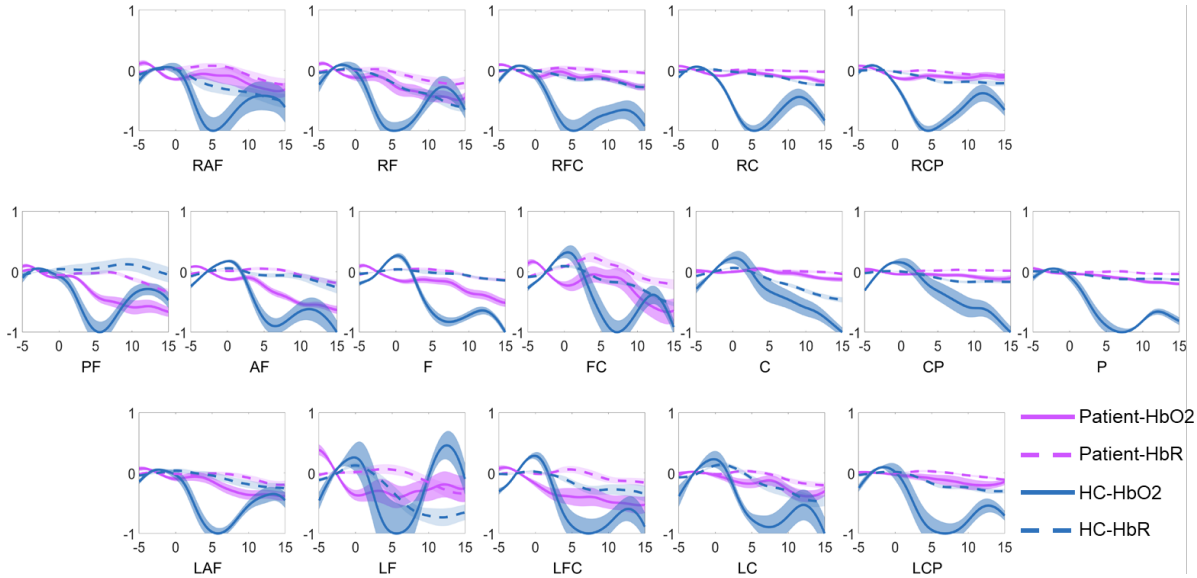

Notes: PF: fronto-polar area; AF: anterior frontal area; LAF: left anterior frontal area; RAF: right anterior frontal area; F: frontal area; LF: left frontal area; RF: right frontal area; FC: fronto-central area; LFC: left fronto-central area; RFC: right fronto-central area; C: central area; LC: left central area; RC: right central area; CP: centro-parietal area; LCP: left centro-parietal area; RCP: right centro-parietal area; P: parietal area; HC: healthy control group; Patient: patient group; HbO_2: oxyhemoglobin; HbR: deoxyhemoglobin. The x-axis represents time (in seconds), and the y-axis represents normalized changes in hemoglobin concentration (range: -1 to 1).

Supplementary Figure B-3

Between-group comparisons of hemoglobin concentration changes across cortical regions under left groin painful stimulation.

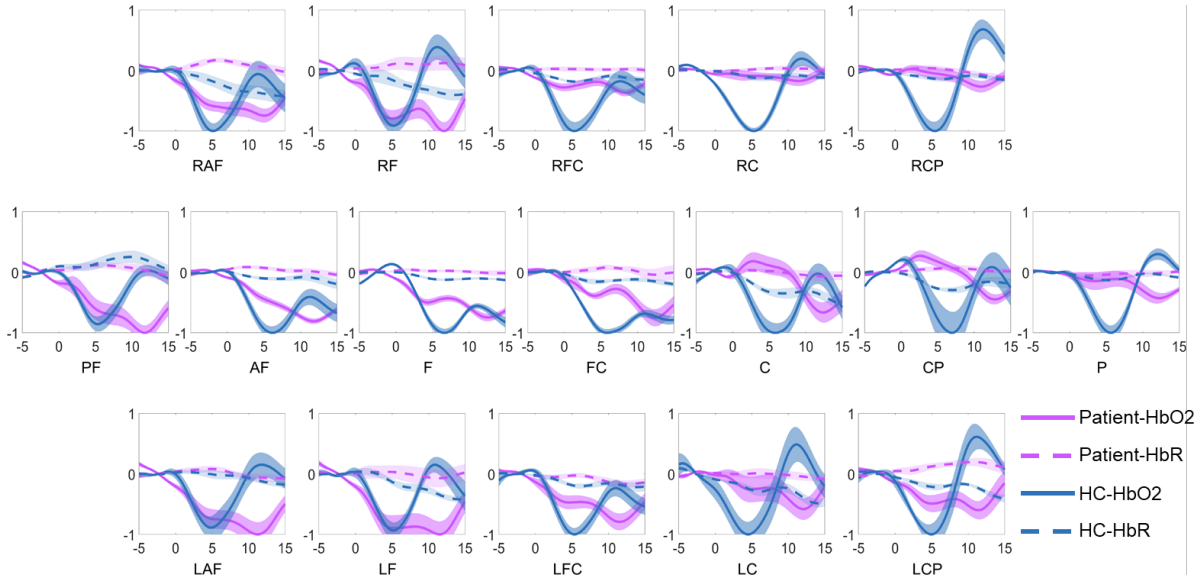

Notes: PF: fronto-polar area; AF: anterior frontal area; LAF: left anterior frontal area; RAF: right anterior frontal area; F: frontal area; LF: left frontal area; RF: right frontal area; FC: fronto-central area; LFC: left fronto-central area; RFC: right fronto-central area; C: central area; LC: left central area; RC: right central area; CP: centro-parietal area; LCP: left centro-parietal area; RCP: right centro-parietal area; P: parietal

area; HC: healthy control group; Patient: patient group; HbO_2: oxyhemoglobin; HbR: deoxyhemoglobin. The x-axis represents time (in seconds), and the y-axis represents normalized changes in hemoglobin concentration (range: -1 to 1).

Supplementary Figure B-4

Between-group comparisons of hemoglobin concentration changes across cortical regions under left knee non-painful stimulation.

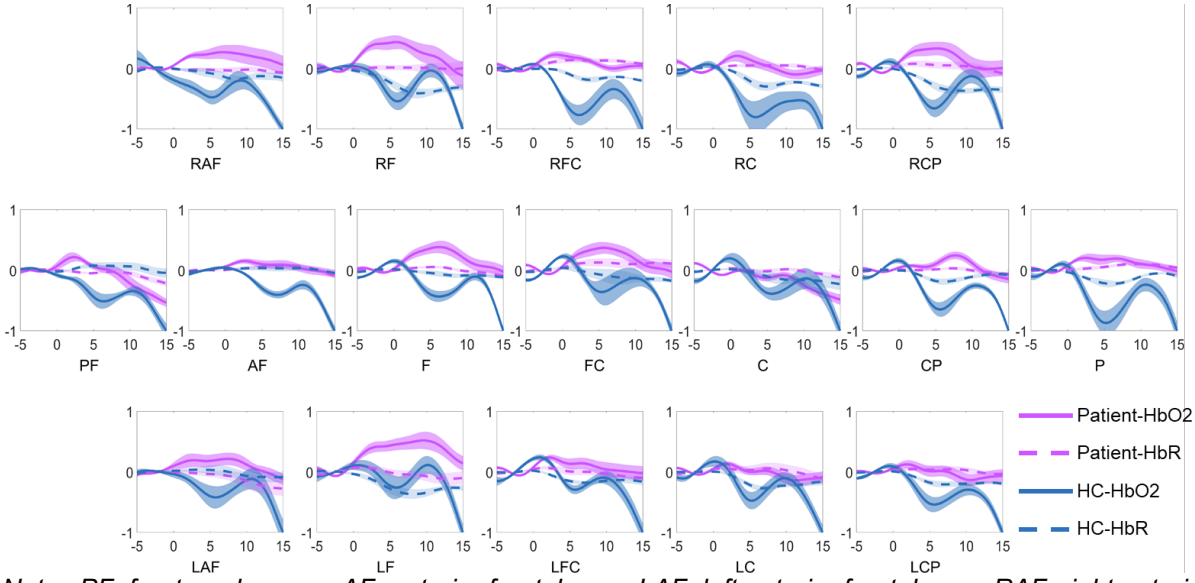

Notes:PF: fronto-polar area; AF: anterior frontal area; LAF: left anterior frontal area; RAF: right anterior frontal area; F: frontal area; LF: left frontal area; RF: right frontal area; FC: fronto-central area; LFC: left fronto-central area; RFC: right fronto-central area; C: central area; LC: left central area; RC: right central area; CP: centro-parietal area; LCP: left centro-parietal area; RCP: right centro-parietal area; P: parietal area; HC: healthy control group; Patient: patient group; HbO_2: oxyhemoglobin; HbR: deoxyhemoglobin. The x-axis represents time (in seconds), and the y-axis represents normalized changes in hemoglobin concentration (range: -1 to 1).

Supplementary Figure B-5

Between-group comparisons of hemoglobin concentration changes across cortical regions under left knee painful stimulation.

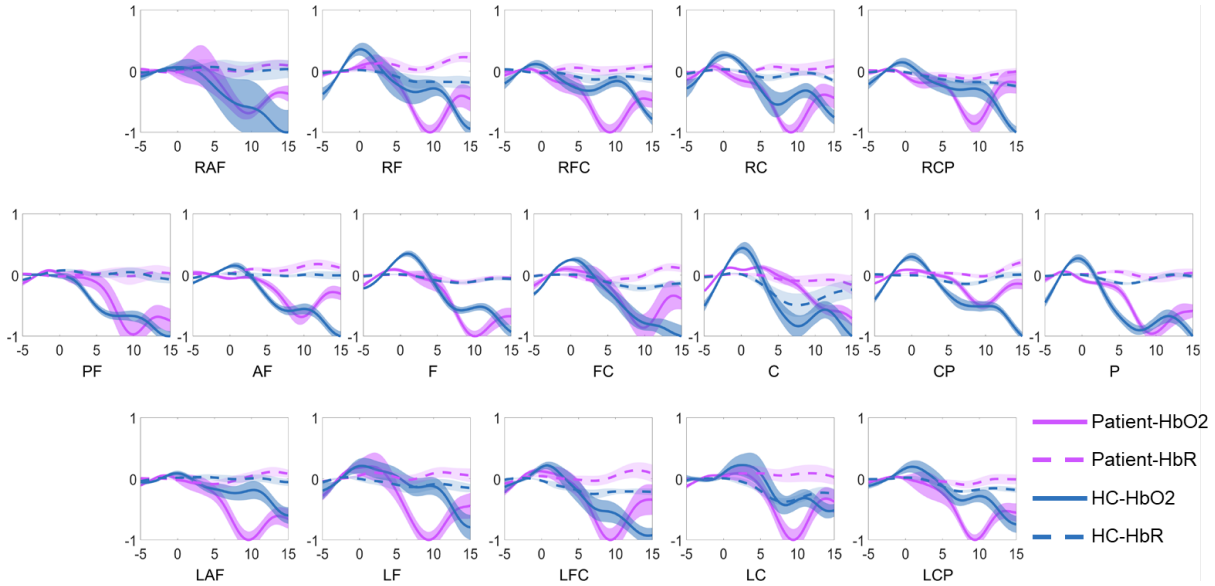

Notes: PF: fronto-polar area; AF: anterior frontal area; LAF: left anterior frontal area; RAF: right anterior frontal area; F: frontal area; LF: left frontal area; RF: right frontal area; FC: fronto-central area; LFC: left fronto-central area; RFC: right fronto-central area; C: central area; LC: left central area; RC: right central area; CP: centro-parietal area; LCP: left centro-parietal area; RCP: right centro-parietal area; P: parietal area; HC: healthy control group; Patient: patient group; HbO_2: oxyhemoglobin; HbR: deoxyhemoglobin. The x-axis represents time (in seconds), and the y-axis represents normalized changes in hemoglobin concentration (range: -1 to 1).

Supplementary Figure B-6

Between-group comparisons of hemoglobin concentration changes across cortical regions under right groin non-painful stimulation.

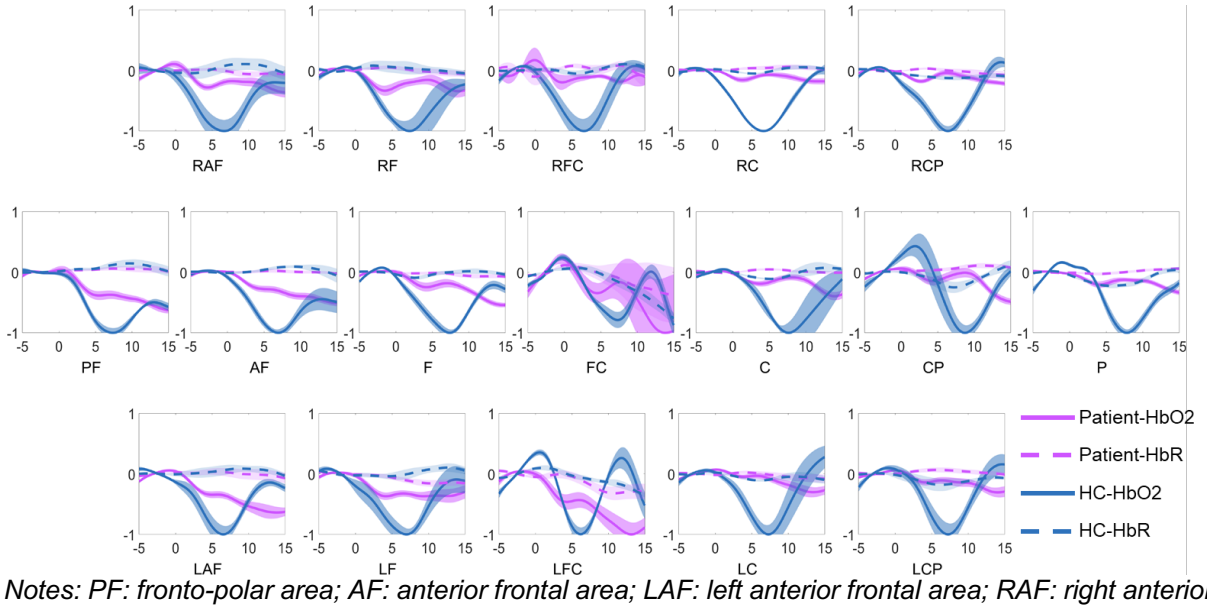

Notes: PF: fronto-polar area; AF: anterior frontal area; LAF: left anterior frontal area; RAF: right anterior frontal area; F: frontal area; LF: left frontal area; RF: right frontal area; FC: fronto-central area; LFC: left fronto-central area; RFC: right fronto-central area; C: central area; LC: left central area; RC: right central area; CP: centro-parietal area; LCP: left centro-parietal area; RCP: right centro-parietal area; P: parietal area; HC: healthy control group; Patient: patient group; HbO_2: oxyhemoglobin; HbR: deoxyhemoglobin. The x-axis represents time (in seconds), and the y-axis represents normalized changes in hemoglobin concentration (range: -1 to 1).

Supplementary Figure B-7

Between-group comparisons of hemoglobin concentration changes across cortical regions under right knee painful stimulation.

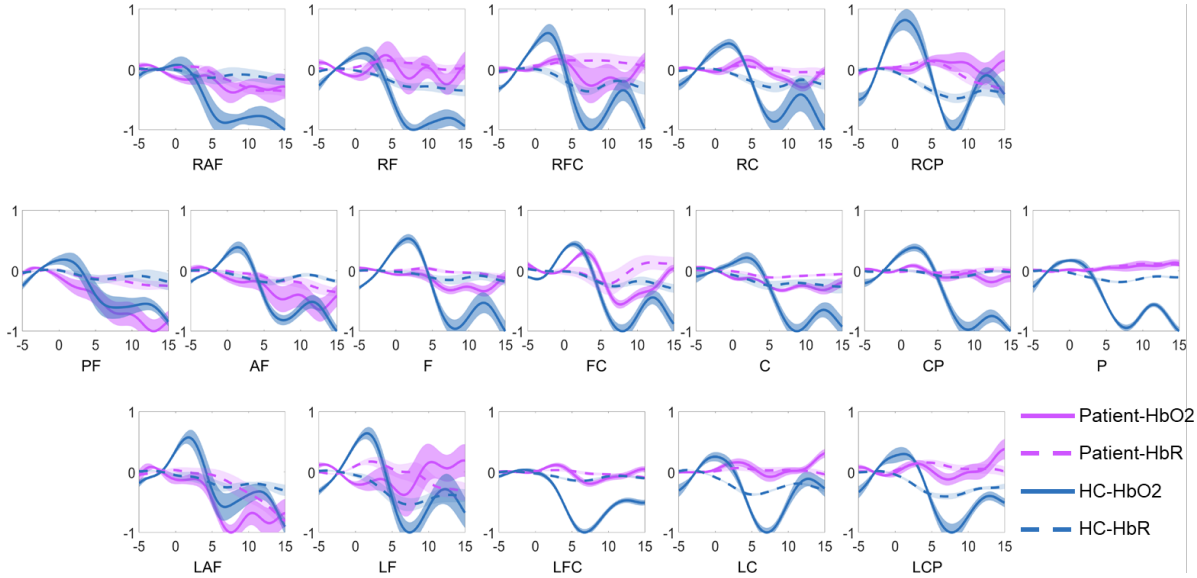

Notes: PF: fronto-polar area; AF: anterior frontal area; LAF: left anterior frontal area; RAF: right anterior frontal area; F: frontal area; LF: left frontal area; RF: right frontal area; FC: fronto-central area; LFC: left fronto-central area; RFC: right fronto-central area; C: central area; LC: left central area; RC: right central area; CP: centro-parietal area; LCP: left centro-parietal area; RCP: right centro-parietal area; P: parietal area; HC: healthy control group; Patient: patient group; HbO_2: oxyhemoglobin; HbR: deoxyhemoglobin. The x-axis represents time (in seconds), and the y-axis represents normalized changes in hemoglobin concentration (range: -1 to 1).

Supplementary Figure B-8

Between-group comparisons of hemoglobin concentration changes across cortical regions under amputation side groin non-painful stimulation.

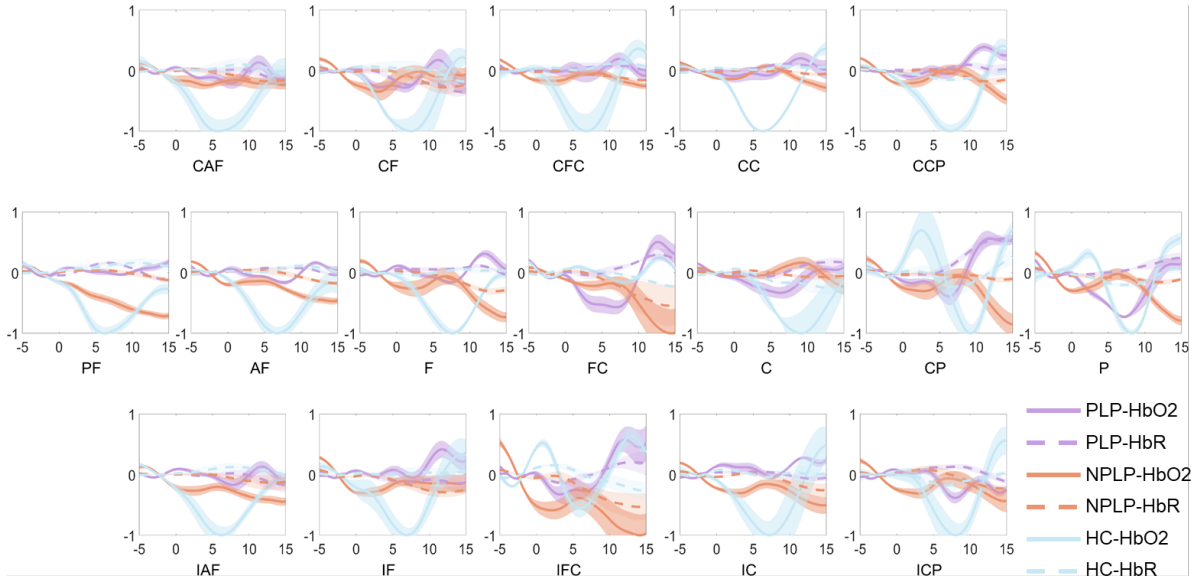

Notes: PF: fronto-polar area; AF: anterior frontal area; IAF: ipsilateral anterior frontal area; CAF: contralateral anterior frontal area; F: frontal area; IF: ipsilateral frontal area; CF: contralateral frontal area; FC: fronto-central area; IFC: ipsilateral fronto-central area; CFC: contralateral fronto-central area; C: central area; IC: ipsilateral central area; CC: contralateral central area; CP: centro-parietal area; ICP: ipsilateral centro-parietal area; CCP: contralateral centro-parietal area; P: parietal area; HC: healthy control group; NPLP: non-phantom limb pain patient group; PLP: phantom limb pain patient group; HbO2: oxyhemoglobin; HbR: deoxyhemoglobin. The x-axis represents time (in seconds), and the y-axis represents normalized changes in hemoglobin concentration (range: -1 to 1).

Supplementary Figure B-9

Between-group comparisons of hemoglobin concentration changes across cortical regions under amputation side groin painful stimulation.

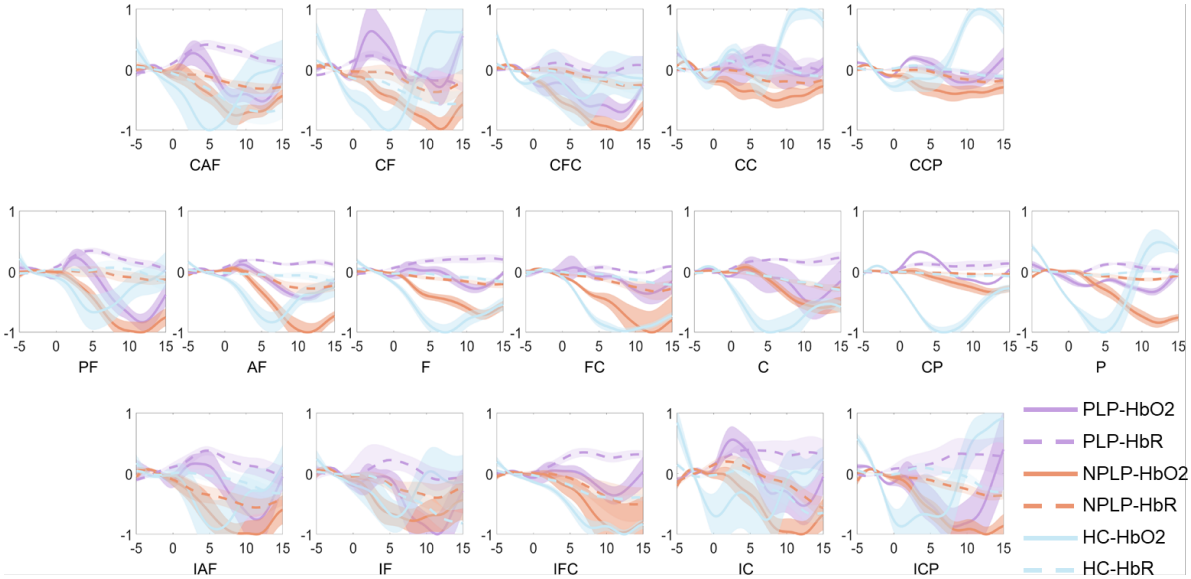

Notes: PF: fronto-polar area; AF: anterior frontal area; IAF: ipsilateral anterior frontal area; CAF: contralateral anterior frontal area; F: frontal area; IF: ipsilateral frontal area; CF: contralateral frontal area; FC: fronto-central area; IFC: ipsilateral fronto-central area; CFC: contralateral fronto-central area; C: central area; IC: ipsilateral central area; CC: contralateral central area; CP: centro-parietal area; ICP: ipsilateral centro-parietal area; CCP: contralateral centro-parietal area; P: parietal area; HC: healthy control group; NPLP: non-phantom limb pain patient group; PLP: phantom limb pain patient group; HbO2: oxyhemoglobin; HbR: deoxyhemoglobin. The x-axis represents time (in seconds), and the y-axis represents normalized changes in hemoglobin concentration (range: -1 to 1).

Supplementary Figure B-10

Between-group comparisons of hemoglobin concentration changes across cortical regions under amputation side knee non-painful stimulation.

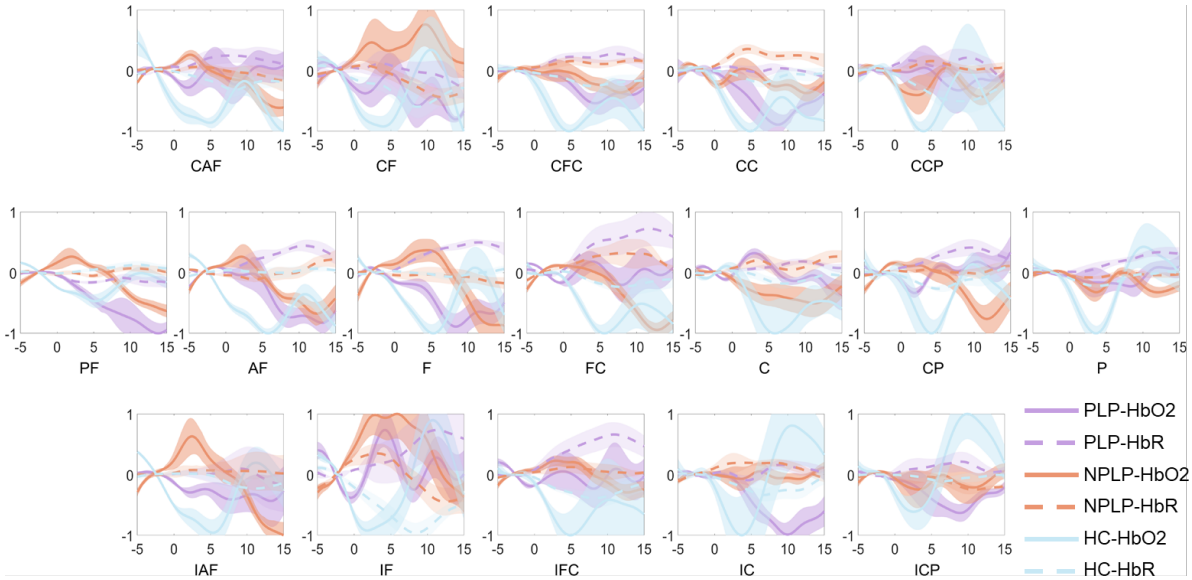

Notes: PF: fronto-polar area; AF: anterior frontal area; IAF: ipsilateral anterior frontal area; CAF: contralateral anterior frontal area; F: frontal area; IF: ipsilateral frontal area; CF: contralateral frontal area; FC: fronto-central area; IFC: ipsilateral fronto-central area; CFC: contralateral fronto-central area; C: central area; IC: ipsilateral central area; CC: contralateral central area; CP: centro-parietal area; ICP: ipsilateral centro-parietal area; CCP: contralateral centro-parietal area; P: parietal area; HC: healthy control group; NPLP: non-phantom limb pain patient group; PLP: phantom limb pain patient group; HbO2: oxyhemoglobin; HbR: deoxyhemoglobin. The x-axis represents time (in seconds), and the y-axis represents normalized changes in hemoglobin concentration (range: -1 to 1).

Supplementary Figure B-11

Between-group comparisons of hemoglobin concentration changes across cortical regions under amputation side knee painful stimulation.

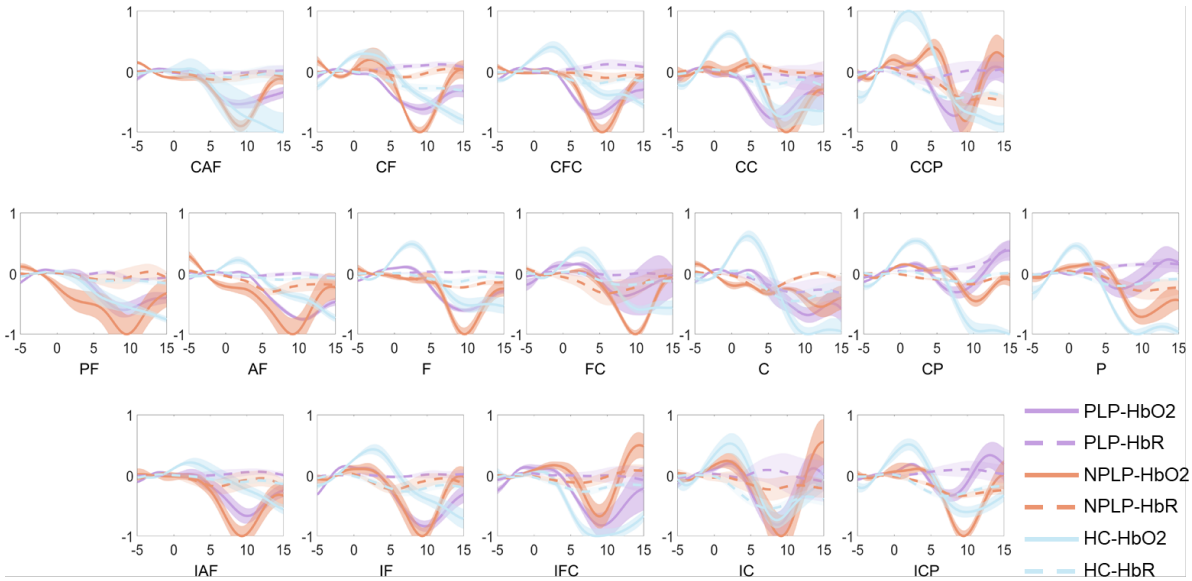

Notes: PF: fronto-polar area; AF: anterior frontal area; IAF: ipsilateral anterior frontal area; CAF: contralateral anterior frontal area; F: frontal area; IF: ipsilateral frontal area; CF: contralateral frontal area; FC: fronto-central area; IFC: ipsilateral fronto-central area; CFC: contralateral fronto-central area; C: central area; IC: ipsilateral central area; CC: contralateral central area; CP: centro-parietal area; ICP: ipsilateral centro-parietal area; CCP: contralateral centro-parietal area; P: parietal area; HC: healthy control group; NPLP: non-phantom limb pain patient group; PLP: phantom limb pain patient group;

HbO2: oxyhemoglobin; HbR: deoxyhemoglobin. The x-axis represents time (in seconds), and the y-axis represents normalized changes in hemoglobin concentration (range: -1 to 1).

Supplementary Figure B-12

Between-group comparisons of hemoglobin concentration changes across cortical regions under non-amputation side groin non-painful stimulation.

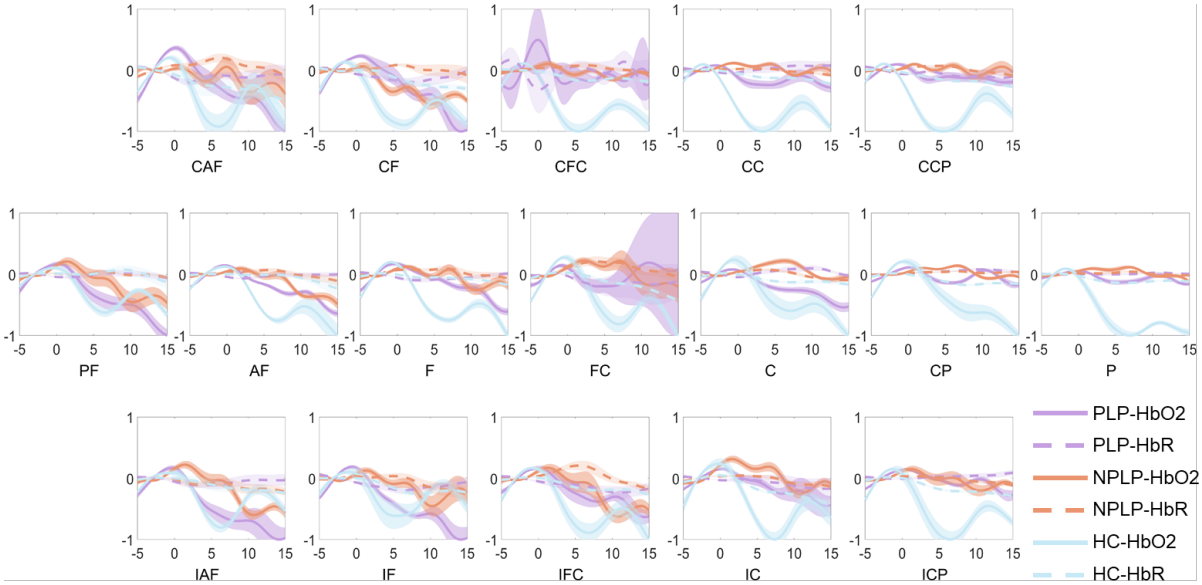

PF: fronto-polar area; AF: anterior frontal area; IAF: ipsilateral anterior frontal area; CAF: contralateral anterior frontal area; F: frontal area; IF: ipsilateral frontal area; CF: contralateral frontal area; FC: fronto-central area; IFC: ipsilateral fronto-central area; CFC: contralateral fronto-central area; C: central area; IC: ipsilateral central area; CC: contralateral central area; CP: centro-parietal area; ICP: ipsilateral centro-parietal area; CCP: contralateral centro-parietal area; P: parietal area; HC: healthy control group; NPLP: non-phantom limb pain patient group; PLP: phantom limb pain patient group; HbO2: oxyhemoglobin; HbR: deoxyhemoglobin. The x-axis represents time (in seconds), and the y-axis represents normalized changes in hemoglobin concentration (range: -1 to 1).

Supplementary Figure B-13

Between-group comparisons of hemoglobin concentration changes across cortical regions under non-amputation side groin painful stimulation.

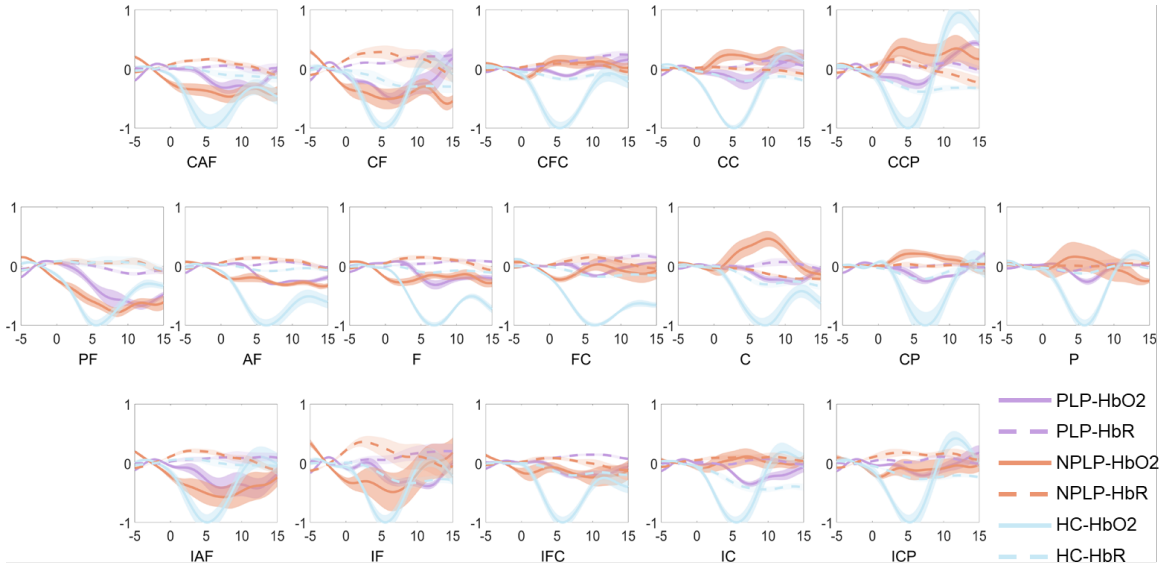

Notes: PF: fronto-polar area; AF: anterior frontal area; IAF: ipsilateral anterior frontal area; CAF: contralateral anterior frontal area; F: frontal area; IF: ipsilateral frontal area; CF: contralateral frontal area; FC: fronto-central area; IFC: ipsilateral fronto-central area; CFC: contralateral fronto-central area; C: central area; IC: ipsilateral central area; CC: contralateral central area; CP: centro-parietal area; ICP: ipsilateral centro-parietal area; CCP: contralateral centro-parietal area; P: parietal area; HC: healthy control group; NPLP: non-phantom limb pain patient group; PLP: phantom limb pain patient group; HbO2: oxyhemoglobin; HbR: deoxyhemoglobin. The x-axis represents time (in seconds), and the y-axis represents normalized changes in hemoglobin concentration (range: -1 to 1).

Supplementary Figure B-14

Between-group comparisons of hemoglobin concentration changes across cortical regions under non-amputation side knee non-painful stimulation.

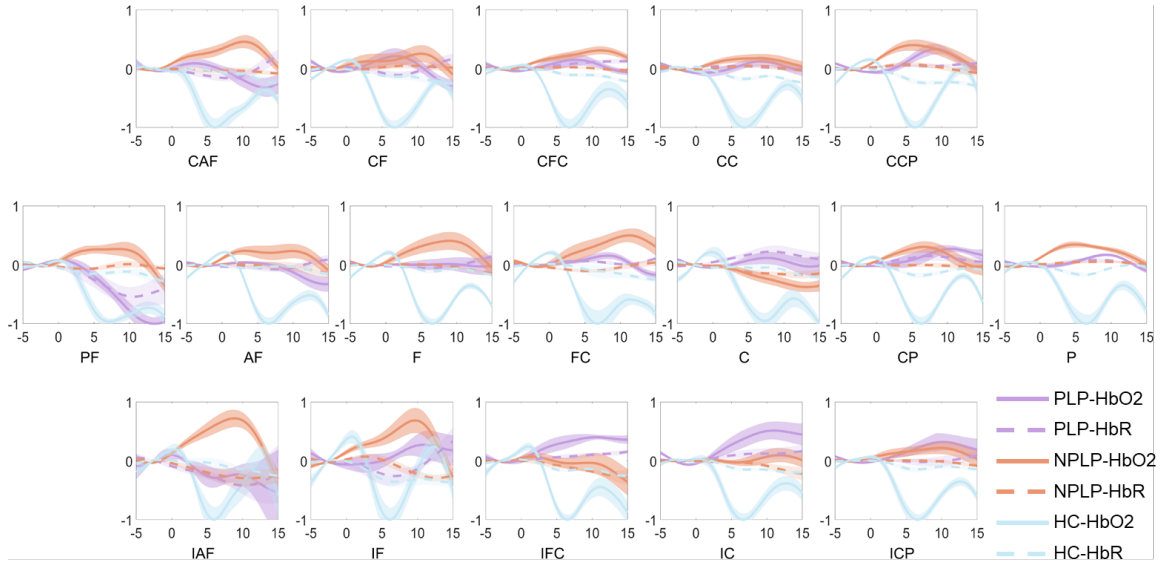

Notes: PF: fronto-polar area; AF: anterior frontal area; IAF: ipsilateral anterior frontal area; CAF: contralateral anterior frontal area; F: frontal area; IF: ipsilateral frontal area; CF: contralateral frontal area; FC: fronto-central area; IFC: ipsilateral fronto-central area; CFC: contralateral fronto-central area; C: central area; IC: ipsilateral central area; CC: contralateral central area; CP: centro-parietal area; ICP: ipsilateral centro-parietal area; CCP: contralateral centro-parietal area; P: parietal area; HC: healthy control group; NPLP: non-phantom limb pain patient group; PLP: phantom limb pain patient group; HbO2: oxyhemoglobin; HbR: deoxyhemoglobin. The x-axis represents time (in seconds), and the y-axis represents normalized changes in hemoglobin concentration (range: -1 to 1).

8 CURRICULUM VITAE

Personal Information

First name and surname:	Jiawen Liao
Date of birth:	06.11.1994
Place of birth:	Zhejiang

Higher education and Academic career

2020 - now	Doctorate candidate (Dr. sc. hum) at Central Institute of Mental Health (ZI), Medical Faculty Mannheim, Heidelberg University, Germany
2017 - 2020	Master of Clinical Medicine, Psychiatry and Mental Health, at North China University of Science and Technology, China
2012 - 2017	Bachelor of Psychiatry, at Qiqihar Medical University, China

Basic education

2009 - 2012	Anhui Tunxi No.1 Senior Middle School, China
2006 - 2009	Tunxi No.5 Middle School, China
2000 – 2006	Lotus Pond Primary School, China

9 ACKNOWLEDGMENTS

Pursuing a PhD in Germany has been a truly transformative and enriching life experience. It has not only been a journey of academic exploration, but also one of profound personal growth.

First, I would like to express my deepest gratitude to Prof. Dr. Herta Flor. I am sincerely thankful to her for giving me the opportunity to start this journey. As a successful female scientist, she has always been an inspiring role model to me. Whenever I felt exhausted and overwhelmed by the pressure and complexity of research, her unwavering research enthusiasm reignited my motivation. Whenever I felt lost or uncertain, our conversations brought clarity and helped me rediscover the direction of my work. After each meeting with her, I was struck by her vast knowledge, which has continually inspired me to remain curious and to keep expanding my knowledge. I am truly grateful to have completed my doctoral research under her guidance. This journey would not have been possible without her support and mentorship.

I am also deeply grateful to my two mentors—Dr. Stefano Silvoni and Dr. Ujwal Chaudhary. Stefano is truly one of the kindest people I have encountered in my thirty years of life. Whenever I had questions, he always answered them with great patience, explaining everything from the underlying principles to practical applications. I still remember the first time I approached him with a question. I fully thanked him for his kind and patient answer. He just told me, "Knowledge is meant to be shared. It's meaningless if only I possess it; it only gains value when I pass it on." I was very moved and inspired by his words. He has also devoted himself to helping a special group of patients. From his experience, I often think about what I could contribute to society or to my patients in the future, and how I could use my abilities to make a meaningful difference for them. Because I used the fNIRS equipment in my studies, I had the opportunity to collaborate with Ujwal. As I had no experience with this technique before, I was often worried that I might be making mistakes or questioned whether I had truly mastered it. Ujwal always provided me with reassurance and encouragement. He is an intelligent scientist who frequently provided unique insights that expanded my scientific thinking and helped me approach problems from new and diverse perspectives. I feel truly honored to have worked with these two outstanding mentors. They have each influenced me profoundly in different ways.

In addition, I am sincerely grateful to every member of the B07 project. Without their support, my doctoral research could not have progressed so smoothly. I would also like to thank Sebastian Keil, Sophia Laubel, Sina Dimmler and Angela Serian for their invaluable assistance during data collection. I am deeply thankful to Prof. Dr. Herta Flor and Dr. Jamila Andoh for their guidance and support in experimental design and manuscript preparation. I would also like to express my gratitude to the hospital in Speyer for its support in recruiting patients. I am also grateful to all the participants who took part in my experiments. Their involvement gave me a deep, firsthand understanding of the significance of scientific research and the motivation to persevere in this project.

Beyond the professional support I received, I would like to thank my parents, not only for their support in this journey, but also for their support and dedication to me over the past 30 years. Thank them for giving me life, so that I can feel this beautiful world; thank them for raising me up, so that I have a healthy body and correct values; thank them for their tolerance and understanding of me, so that I can freely choose my life; thank them for their unconditional love, which has always been my greatest source of strength whenever I felt lost or discouraged. I would also like to express my special thanks to my boyfriend. He appeared in my life like a gift during this journey. We are from the same country, even the same city, but we met, got to know each other and fell in love in a foreign country. This fate makes us cherish each other more. Sometimes he is like an experienced elder, who enlightens me when I am anxious or depressed, accepts all my negative emotions, accompanies me, encourages me, and helps me regain confidence to face life; when we share the joy of life together, he is like the cutest child in the world, with the most beautiful smile, making me forget all my troubles. He made me feel and believe in the power of love, making my entire doctoral career particularly memorable and special.

Finally, I want to thank myself deeply, thank myself for my choice, thank myself for my courage, and thank myself for my persistence. This journey of studying for a doctorate is like a journey of self-cultivation. I understood myself better than ever before, faced some shortcomings in my character, and have many new insights and thoughts on my life. With this experience, I believe I will continue to grow and become a better version of myself in the future.